

e-ISSN : 2320-0847
p-ISSN : 2320-0936



American Journal of Engineering Research (AJER)

Volume 4 Issue 10– October 2015

www.ajer.org

ajer.research@gmail.com

Editorial Board

American Journal of Engineering Research (AJER)

Dr. Moinuddin Sarker,

Qualification :PhD, MCIC, FICER,
MInstP, MRSC (P), VP of R & D
Affiliation : Head of Science / Technology
Team, Corporate Officer (CO)
Natural State Research, Inc.
37 Brown House Road (2nd Floor)
Stamford, CT-06902, USA.

Dr. June II A. Kiblasan

Qualification : Phd
Specialization: Management, applied
sciences
Country: PHILIPPINES

**Dr. Jonathan Okeke
Chimakonam**

Qualification: PHD
Affiliation: University of Calabar
Specialization: Logic, Philosophy of
Maths and African Science,
Country: Nigeria

Dr. Narendra Kumar Sharma

Qualification: PHD
Affiliation: Defence Institute of Physiology
and Allied Science, DRDO
Specialization: Proteomics, Molecular
biology, hypoxia
Country: India

Dr. ABDUL KAREEM

Qualification: MBBS, DMRD, FCIP, FAGE
Affiliation: UNIVERSITI SAINS Malaysia
Country: Malaysia

Prof. Dr. Shafique Ahmed Arain

Qualification: Postdoc fellow, Phd
Affiliation: Shah Abdul Latif University
Khairpur (Mirs),
Specialization: Polymer science
Country: Pakistan

Dr. Sukhmander Singh

Qualification: Phd
Affiliation: Indian Institute Of
Technology, Delhi
Specialization : PLASMA PHYSICS
Country: India

Dr. Alcides Chaux

Qualification: MD
Affiliation: Norte University, Paraguay,
South America
Specialization: Genitourinary Tumors
Country: Paraguay, South America

Dr. Nwachukwu Eugene Nnamdi

Qualification: Phd
Affiliation: Michael Okpara University of
Agriculture, Umudike, Nigeria
Specialization: Animal Genetics and
Breeding
Country: Nigeria

Dr. Md. Nazrul Islam Mondal

Qualification: Phd
Affiliation: Rajshahi University,
Bangladesh
Specialization: Health and Epidemiology
Country: Bangladesh

S.No.	Manuscript Title	Page No.
01.	Power Flow Control Analysis of Transmission Line Using Static VAR Compensator (SVC) J. U. Agber C. O. Onah I. G. Onate	01-07
02.	Tribological Behaviour of E-Glass /Epoxy & E-Glass /polyester Composites for Automotive Body Application Esmael Adem P.Prabhu	08-17
03.	A Generic Adaptive Method for Corruption Mitigation in Trial Monitoring System with Restful Authorization Suryanaraayan.B Subramanian.M Saikrishna.K.K Sujitha.G	18-22
04.	Estimation of Sag by the Influence of Altitude Parameter Shamim Ahmed	23-29
05.	Selection of renewable energy project using Multicriteria Method DADDA Afaf OUHBI Brahim	30-33
06.	DEVELOPMENT OF NEW DIE FOR THE FORMING OF IMPELLER VANE AND THE INVESTIGATION OF PROCESS PARAMETERS INFLUENCING ITS PART QUALITY. RAJESH.R SARAVANAN.S	34-39
07.	Analysis of Dynamic Road Traffic Congestion Control (DRTCC) Techniques Pardeep Mittal Yashpal Singh Yogesh Sharma	40-47
08.	Analysis The Electrical Properties of Co, TiO ₂ and Co/TiO ₂ Multilayer Thin Films of Different Thickness Deposited by E-Beam Technique. Md. Faruk Hossain Md. Abdullah Al Asad Md. Omar Faruk Dr. Md. Ariful Islam Nahid	48-53
09.	Investigation of the parameters on the fast pyrolysis of wheat straw for production of bio-oil Syed Kamal Zafar Syed Hassan Javed Naqvi Atif Khan	54-59
10.	A Technical Investigation of Voltage Sag Vima P. Mali R. L. Chakrasali K. S. Aprameya	60-68
11.	Electrical Energy Potential from Municipal Solid Waste in Rajshahi City Corporation, Bangladesh A.Z.A. Saifullah	69-85
12.	CMOS BASED CURRENT FEEDBACK OP-AMP WITH IMPROVED BANDWIDTH Akshay Dubey	86-91
13.	Development of Distribution Feeder Reliability Profile: A Case Study of Egbu Feeders in Imo State Nigeria	92-101

CONTENTS

	Raymond OkechukwuOpara NkwachukwuChukwuchekwa Onojo James Ondoma Joy Ulumma Chukwuchekwa	
14.	TCP-IP Model in Data Communication and Networking Pranab Bandhu Nath Md.Mofiz Uddin	102-107
15.	Drying of Chilli Pepper Using a Solar Dryer with a Back-Up Incinerator under Makurdi Humid Climate Ibrahim, J. S Barki, E Edeoja, A. O.	108-113
16.	Experimental Study of Crushed Palmyra Palm Shells As Partial Replacement For Coarse Aggregate In Concrete Osakwe C .E Nasir N Vahyala P	114-117
17.	Designing and Analysis of Microstrip Patch Antenna for Wi-Fi Communication System Using Different Dielectric Materials Raja Rashidul Hasan Md. Moidul Islam Kazi Saiful Islam Md. Mostafizur Rahman Dr. Md. Tanvir Hasan	118-126
18.	Solution of the Linear and Non-linear Partial Differential Equations Using Homotopy Perturbation Method Abaker. A. Hassaballa	127-133
19.	On Resiliency in Cyber-Road Traffic Control System using Modified Danger Theory based Optimized Artificial Immune Network Lokesh M R Dr.Y.S Kumaraswamy	134-147
20.	BIOMETRICS BASED USER AUTHENTICATION Tanuj Tiwari Tanya Tiwari Sanjay Tiwari	148-159
21.	The improvement of voltage stability and reactive power compensation in the two-area system with PSS and FACTS-devices Mohammad Niyazi AshkanBorji Siroos Hemmati	160-166
22.	Modeling and Characterization of Next Generation Network in a Developing Economy: From Data Collection to Estimation of Traffic Parameters Nathaniel S. Tarkaa Cosmas I. Ani	167-177
23.	Modal analysis of cantilever beam Structure Using Finite Element analysis and Experimental Analysis S. P. Chaphalkar Subhash. N. Khetre Arun M. Meshram	178-185
24.	Unsteady Similarity Solution of Free convective boundary layer flow over porous plate with variable properties considering viscous dissipation and Slip Effect Md.Jashim Uddin	186-191
25.	Causes of Borehole Failure in Complex Basement Terrains: ABUAD Case Study, Southwestern Nigeria Ogundana, A.K Aladesanmi A. O Okunade A., 4Olutomilola O.O	192-201

Power Flow Control Analysis of Transmission Line Using Static VAR Compensator (SVC)

J. U. Agber¹, C. O. Onah¹, I. G. Onate²

¹Department of Electrical and Electronics Engineering, University of Agriculture, Makurdi, Nigeria.

²Works Department, Kogi State University, Anyigba, Nigeria.

Abstract: Control of reactive power and voltage constitute part of the major challenge in the power system industry. Adequate absorption or injection of reactive power into electric power transmission systems solves power quality problems like voltage profile maintenance at all power transmission levels, transmission efficiency and system stability. Globally, there is increasing demand for electricity to feed the technology-driven economy, while the commensurate expansion of power generation and transmission to meet up with such demand has been severely limited due to inadequate resources and environmental factors. Flexible AC Transmission System (FACTS) controllers, such as the Static VAR Compensator (SVC), employ latest technology in the design of power electronic switching devices for electric power transmission systems to control voltage and power flow, and improve voltage regulation without the need to expand the power generation and transmission facilities. In this work, the capability of SVC in stabilizing power system's voltage through reactive power compensation was investigated. Power flow equations involving voltage drop with/without SVC were developed. Modeling equations for SVC were also developed and used to determine its parameters. The Nigeria 330kV network, 28-bus power system used for the study was modeled using MATLAB/SIMULINK software. From the simulations, the compensated and uncompensated voltages at each of the 28 buses were evaluated. It was observed from the analysis that some buses in the network had very weak voltage profile consequent to either excessive generation or absorption of the reactive power at such buses. It is therefore pertinent to note that not all the buses within the network need voltage compensation and as such, only buses with very weak voltage profile require the incorporation of SVC. Hence it can be concluded that in order to enhance the transmission system performance of the Nigerian 330kV power system, the control of the voltages at certain buses through the application of SVC is required.

Keywords: Facts, Svc, Transmission Line Analysis, Reactive Power Control, 28-bus

I. Introduction

Globally, there is increasing demand for electricity to feed the technology-driven economy, while the commensurate expansion of power generation facilities and transmission lines to meet up with such demand has been severely limited due to inadequate resources and environmental factors. In power system network voltage control, reactive power is both the challenge and the solution. It is, therefore, important that a balance of reactive power be obtained in the operation of electric power transmission systems because the control of voltage can be lost if this is not achieved. Adequate reactive power regulation of electric transmission networks can solve power quality problems by improving the power system voltage profile, transient stability improvement, increase in power transfer capacity and minimization of transmission line loss. FACTS controllers, such as the Static VAR Compensator (SVC), employ latest technology in the design of power electronic switching devices. These devices are used to control the voltage and power flow in a transmission system to improve voltage regulation without the need to expand the power generation and transmission facilities. By dynamically providing reactive power, SVC can be used for voltage regulation and compensation, transient stability improvement, power system oscillation damping improvement, increase in power transfer capacity and minimization of transmission line loss.

II. Background To The Study

The ability to control power flow in an electric power transmission system without generation rescheduling or topology changes can improve the power system performance. Using controllable components, the line flows can be changed in such a way that thermal limits are not exceeded, stability margin increased, in addition to increase in power transfer capacity and minimization of transmission line loss without violating the economic generation dispatch. FACTS technology is the ultimate tool for getting the most out of existing power system infrastructures through rapid regulation of the system's reactive power. Ali [1] investigated the performance of Static Synchronous Compensators (STATCOM) and SVC on voltage stability in power system. In the study, MATLAB/SIMULINK software simulations showed that STATCOM is more effective in midpoint voltage regulation on transmission line. Comparison between STATCOM and SVC under fault condition was also simulated and the result showed that STATCOM has the capacity to provide more reactive power for the period of a fault than SVC. The response time of STATCOM was faster than that of SVC. In the work by Murali [2], simulation and comparison of various FACTS devices using PSPICE software have been done. How to improve steady state stability by placing SVC at different places has been discussed in the study by Bhavin [3]. In the study by Akter [4], MATLAB/SIMULINK software simulation was used to demonstrate the performance of the system for each of the FACTS devices for example, Static VAR compensator (SVC), STATCOM, Thyristor controlled series capacitor (TCSC), Static synchronous series compensator (SSSC) and Unified power flow controller (UPFC) in improving the power profile and thereby voltage stability of same. Using MATLAB/SIMULINK software, performance of Fixed capacitor, shunt Thyristor Controlled Reactor (FC-TCR) and STATCOM has been discussed in the work by Das [5]. Modeling and Simulation of various FACTS devices (FC-TCR, STATCOM, TCSC and UPFC) have been done using MATLAB/SIMULINK software in the work by Dipti [6]. The research by Pardeep [7], discussed how SVC has successfully been applied to control the dynamic performance of transmission system and regulate the system voltage effectively.

III. Methodology

SVC application studies require appropriate power system models and study methods covering the particular problem to be solved by the application. The following studies are normally required for an SVC application from the early planning stage till operation [8].

- Load flow studies.
- Small and large disturbance studies.
- Harmonic studies.
- Electromagnetic transient studies and
- Fault studies.

3.1 Modeling of Static VAR Compensator for Power System Studies

The functional diagram of the SVC in fig.1 shows that one branch of the SVC is purely inductive while the other branch is purely capacitive. Therefore, the SVC consumes no active power. It either injects (capacitive) reactive power to increase the system's voltage or consumes (inductive) reactive power to reduce the system's voltage. Since the reactor consumes reactive power, the (inductive) reactor current (I_L) is positive while the capacitor which injects reactive power into the system, has negative current (I_C).

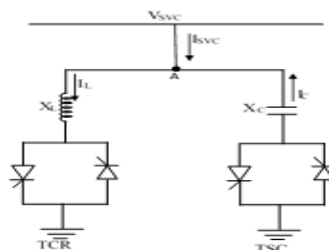


Figure1: Functional diagram of a TCR-TSC SVC

From circuit theory, it is shown that:

$$I_{SVC} + I_C - I_L = 0 \quad (1)$$

Therefore the SVC current (I_{SVC}) at maximum VAR absorption, could be expressed as follows:

Looking at point A and using Kirchoff current law (KCL), we have:

$$I_{SVC} = I_L - I_C \quad (2)$$

$$I_C = \frac{V_{SVC}}{X_C} \quad (3)$$

and

$$I_L = \frac{V_{SVC}}{X_L} \quad (4)$$

where

X_L = Inductive reactance of the SVC

X_C = Capacitive reactance of the SVC

C = Capacitance of the fixed SVC capacitor

L = Inductance of the SVC inductor

V_{SVC} = Magnitude of the bus voltage

On the assumption that no real power is consumed by the SVC (i.e. $P_{SVC} = 0$) then:

$$Q_{SVC} = I_{SVC} \times V_{SVC} \quad (5)$$

Comparing equations (1) and (5):

$$Q_{SVC} = (I_L - I_C) \times V_{SVC} \quad (6)$$

Combining equations (2), (3) and (6), yield equations (7) to (9):

$$Q_{SVC} = \left(\frac{V_{SVC}}{X_L} - \frac{V_{SVC}}{X_C} \right) \times V_{SVC} \quad (7)$$

$$Q_{SVC} = \left(\frac{1}{X_L} - \frac{1}{X_C} \right) \times V_{SVC}^2 \quad (8)$$

$$Q_{SVC} = \left(\frac{X_C - X_L}{X_L X_C} \right) V_{SVC}^2 \quad (9)$$

SVC controllers are designed in such a way that the TCR is switched on when the bus voltage becomes higher than the reference voltage and vice-versa. As a result, when the VAR absorption is at maximum, the TCR become operational and $I_C = 0$. Hence:

$$Q_{SVC}^{\max} = \frac{1}{X_L} V_{SVC}^2 \quad (10)$$

When the VAR absorption is at minimum, $I_L = 0$. Hence:

$$Q_{SVC}^{\min} = -\frac{1}{X_C} V_{SVC}^2 \quad (11)$$

Thus, the bus voltage would be regulated at or near the base voltage.

3.2 Equations for the Bus Voltage and Voltage Drop

Consider an electric power transmission line connecting two buses i and k in any given power system network as represented in Fig. 2.

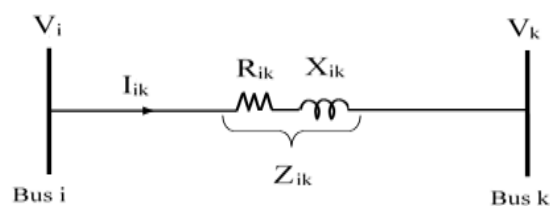


Figure 2: Transmission line model of a power system network

Definition of the symbols used in the configuration of the transmission line model in fig. 2 are as follows:

V_k = Complex voltage at bus k

V_i = complex voltage at bus i

I_{ik} = Complex current flow from bus i to k

R_{ik} = The transmission line resistance between buses i and k

Z_{ik} = The transmission line impedance between buses i and k

X_{ik} = The transmission line reactance between buses i and k

From Fig. 2, the voltage drop (V_d) between buses i and k can be expressed as:

$$V_d = V_i - V_k \quad (12)$$

By applying Ohm's law, the complex current flowing from bus i to k is expressed as:

$$I_{ik} = \frac{V_i - V_k}{Z_{ik}} \quad (13)$$

where

$$Z_{ik} = R_{ik} + jX_{ik}$$

Equation (13) is expressed in the admittance form as:

$$I_{ik} = (V_i - V_k)Y_{ik} \quad (14)$$

where

$$Y_{ik} = \frac{1}{Z_{ik}} \text{ and is defined as the admittance of the transmission line.}$$

The complex power (S_{ik}) flowing from bus i to k is given by:

$$S_{ik} = V_i I_{ik}^* \quad (15)$$

Expressing the complex power of equation (15) in real power (P) and reactive (Q) power form yields:

$$S_{ik} = P_{ik} + jQ_{ik} = V_i I_{ik}^* \quad (16)$$

Taking the conjugate of the equation (16) yields:

$$P_{ik} - jQ_{ik} = V_i^* I_{ik} \quad (17)$$

hence

$$I_{ik} = \frac{P_{ik} - jQ_{ik}}{V_i^*} \quad (18)$$

Comparison of equations (12), (13) and (18) gives equation (19) as:

$$\frac{P_{ik} - jQ_{ik}}{V_i^*} = V_d Y_{ik} \quad (19)$$

Consequently:

$$V_d = \frac{P_{ik} - jQ_{ik}}{V_i^* Y_{ik}} \quad (20)$$

Analysis of equation (20) shows that by adjusting the system's reactive power at bus k while keeping the voltage at bus i constant, the voltage between buses i and k can be controlled and the system's total voltage drop minimized.

Assuming that the SVC is installed at bus k, then equation (12) becomes:

$$V_d = V_i - V_{SVC} \quad (21)$$

Comparing equations (9) and (21) yields:

$$V_d = V_i - \sqrt{\frac{Q_{SVC} X_L X_C}{X_C - X_L}} \quad (22)$$

From equation (21), it can be seen that if the voltage at bus i is kept constant, then by regulating the voltage at bus k at or near the base voltage, the power system's voltage is stabilized and the voltage drop minimized.

IV. Results And Discussion

The test system configuration is based on the Nigerian 330kV, 28-bus power system. The Nigerian Electricity Network comprises 11,000 km transmission lines (330 and 132 kV), 24000 km of sub-transmission line (33 kV), 19,000 km of distribution line (11 kV) and 22,500 substations (National Control Centre, Power Holding Company of Nigeria, 2012). It has only one major loop system involving Benin-Ikeja West-Ayedede-Oshogbo and Benin. The absence of loops accounts mainly for the weak and unreliable power system in the country. The single line diagram of the existing 28-bus 330 kV Nigerian transmission network used as the test system is shown in figure 3. It comprises 9 generating stations, 28 buses and 52 transmission lines. Based on the MATLAB/SIMULINK configuration for this work, simulations were carried out at all the load buses within the 330kV, 28-bus Nigeria power system. Simulations of each load bus in the system without the SVC were done and the system voltage magnitude at each of the load bus were obtained. Conversely, simulations of each load bus in the system with the incorporation of SVC were carried out and the system voltage magnitude at each of the load bus were also obtained. To show the performance of the SVC, the system voltage differential at each of the load bus with/without SVC, were computed.

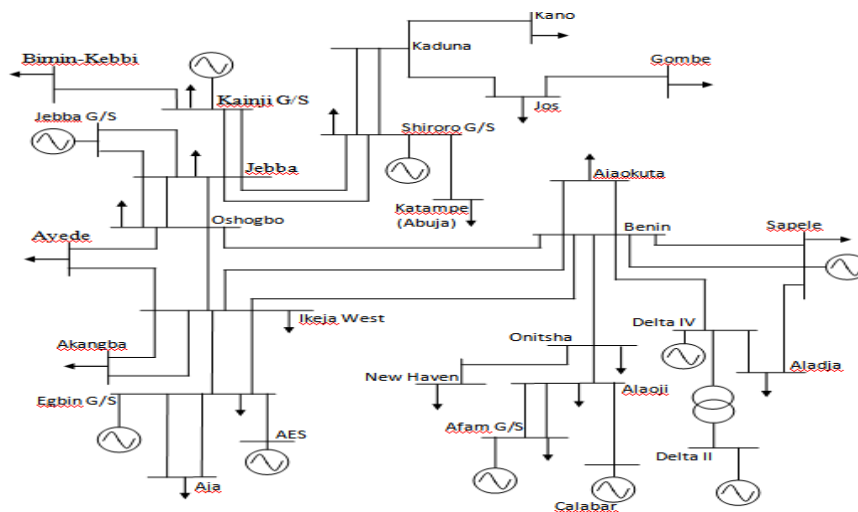


Figure 3: The 330kV, 28-bus Nigerian power system (National Control Centre, Power Holding Company of Nigeria, 2012)

Table 1: The *i*th and *k*th bus voltages of the Nigerian 28-bus power system with/without SVC.

Bus		No SVC connected		SVC connected		Performance of SVC	
<i>i</i>	<i>k</i>	$V_i(pu)$	$V_k(pu)$	$V_{i(SVC)}(pu)$	$V_{k(SVC)}(pu)$	$V_{i(SVC)} - V_i$	$V_{k(SVC)} - V_k$
1	2	0.3486	0.2548	0.3930	0.2684	0.0444	0.0136
1	3	0.3486	0.3118	0.3930	0.3388	0.0444	0.027
1	23	0.3486	0.6704	0.3930	0.6816	0.0444	0.0112
2	6	0.2548	0.2029	0.2684	0.2462	0.0136	0.0433
2	11	0.2548	0.6853	0.2684	0.6920	0.0136	0.0067
2	17	0.2548	0.6813	0.2684	0.6889	0.0136	0.0076
2	19	0.2548	0.1859	0.2684	0.2799	0.0136	0.094
3	2	0.3118	0.2548	0.3388	0.2684	0.027	0.0136
3	10	0.3118	0.6947	0.3388	0.6981	0.027	0.0034
4	1	0.02133	0.3486	0.02885	0.3930	0.00752	0.0444
4	3	0.02133	0.3118	0.02885	0.3388	0.00752	0.027
5	8	0.1911	0.08298	0.3384	0.2653	0.1473	0.18232
6	20	0.2029	0.1469	0.2462	0.2516	0.0433	0.1047
6	21	0.2029	0.6960	0.2462	0.7027	0.0433	0.0067
7	3	0.3043	0.3118	0.3400	0.3388	0.0357	0.027
10	18	0.6947	0.6686	0.6981	0.6983	0.0034	0.0297
11	15	0.6853	0.2116	0.6920	0.2262	0.0067	0.0146
17	15	0.6813	0.2116	0.6889	0.2262	0.0076	0.0146
21	22	0.6960	0.7004	0.7027	0.7071	0.0067	0.0067

23	25	0.6704	0.6974	0.6816	0.7042	0.0112	0.0068
23	27	0.6704	0.6880	0.6816	0.6947	0.0112	0.0067
25	23	0.6974	0.6704	0.7042	0.6816	0.0068	0.0112
25	26	0.6974	0.2720	0.7042	0.7581	0.0068	0.4861
27	28	0.6880	0.4674	0.6947	0.5367	0.0067	0.0693
28	5	0.4674	0.1911	0.5367	0.3384	0.0693	0.1473
28	16	0.4674	0.2216	0.5367	0.5480	0.0693	0.3264

Table 2: Identified weak buses within the network and their compensated voltage values.

Bus identification		Bus voltage without SVC installed (pu)	Bus voltage with SVC installed (pu)	Bus voltage compensation (pu)
Name	No			
Jos	5	0.1911	0.3384	0.1473
Gombe	8	0.08298	0.2653	0.18232
Kano	16	0.2216	0.5480	0.3264
Ajaokuta	19	0.1859	0.2799	0.094
N-Haven	20	0.1469	0.2516	0.1047
B-Kebbi	26	0.2720	0.7581	0.4861

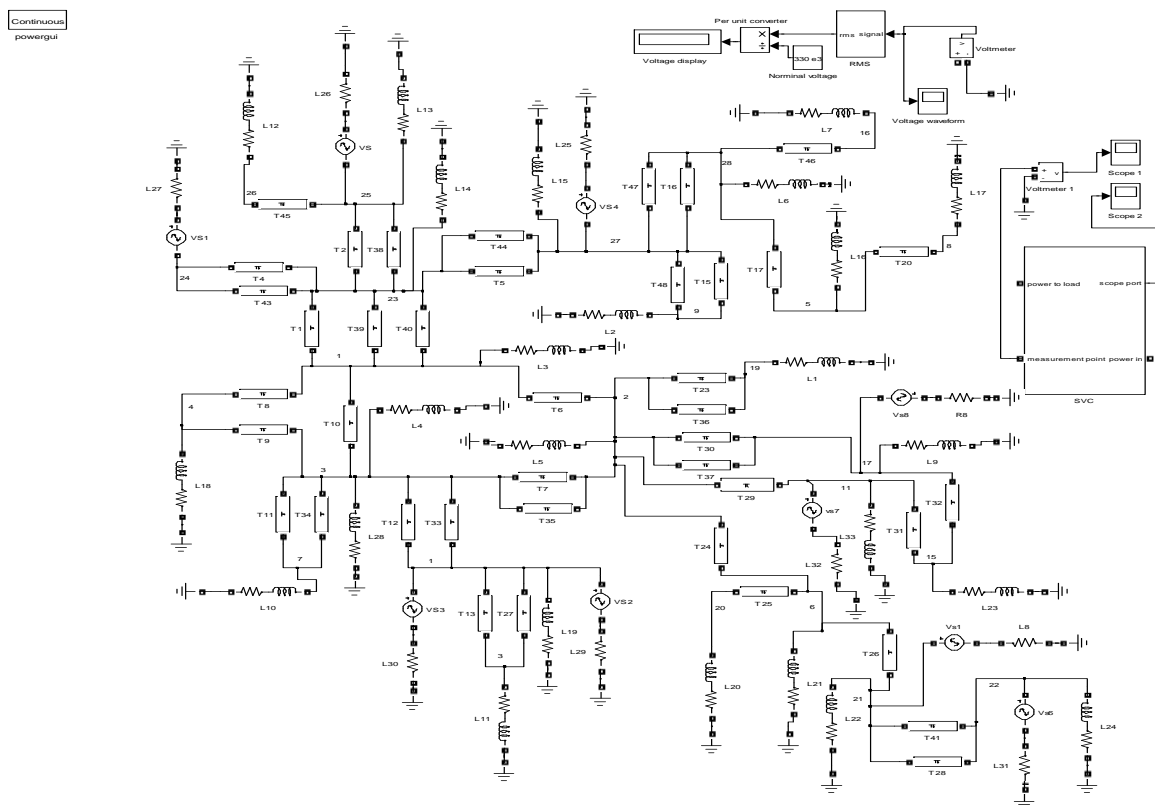


Figure 4: SIMULINK model of the Nigeria 330kV, 28-bus power system

Table 1 is a detailed analysis of the voltages at each of the load bus within the network with/without SVC compensation. It has been observed from this analysis that some buses in the network have very weak voltage profile consequent to either excessive generation or absorption of the reactive power. It is pertinent to note that not all the buses within the network need compensation and as such, only buses with very weak voltage profile require the incorporation of SVC. This information could be very valuable to the power engineers in the installation of SVC in the network. The buses, where compensation with SVC is needed, were identified and depicted in table 2. From the analysis, the overall system voltage compensation with SVC was 10.18%.

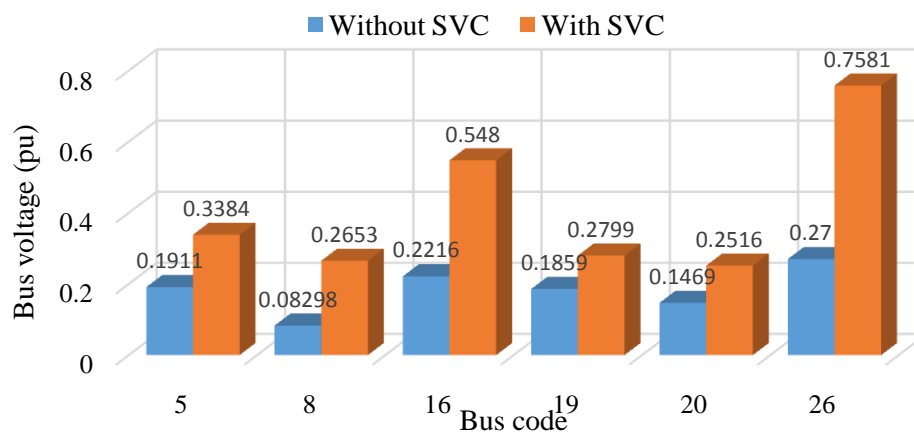


Figure 4: Weak bus voltage compensation representation

V. Conclusion

In this research work, based on the SVC and the power system parameters, SIMULINK blocks have been used to implement the Nigerian 330kV power system network, which comprises 9 generation stations, 28-buses and 52 transmission lines. The simulations were carried out in the MATLAB/ SIMULINK environment. From the simulations, the compensated and uncompensated voltages at each of the 28 buses were evaluated. It was observed from the analysis that some circuits (buses) in the network have very weak voltage profile consequent to either excessive generation or absorption of the reactive power flow at such buses. It is, therefore, pertinent to note that not all the buses within the network need voltage compensation and as such, only buses with very weak voltage profile require the incorporation of SVC. Hence, it can be concluded that in order to enhance the transmission system performance of the Nigerian 330kV power system, the control of the voltages at certain buses through the application of SVC is required. This could be practically implemented on the Nigerian power system network to improve the huge demand for power in the country, because at the moment, only synchronous reactors, which are not as effective as SVC, are being used to control the flow of reactive power in the network.

REFERENCES

- [1]. Q.W .Ali and A.U. Asar, Smart power transmission system using FACTS device, *International Journal of Applied Power Engineering (IJAPE) Vol. 2, No. 2*, August 2013, pp. 61~70 ISSN: 2252-8792,
- [2]. D. Murali, M. Rajaram, and N. Reka, Comparison of FACTS devices for power system stability enhancement. *International Journal of Computer Applications, volume 8-No4*, 2010.
- [3]. M.P. Bhavin, Enhancement of steady state voltage stability using SVC and TCSC. *National Conference on Recent Trends in Engineering and Technology*. pp 13-14, 2011.
- [4]. S. Akter, A. Saha and P. Das, Modelling, simulation and comparison of various FACTS devices in power system. *International journal of Engineering Research and Technology*, 1(8), 2012.
- [5]. A.P. Das and A.K. Chakraborty, Performance analysis and comparison of various FACTS devices in power system. *International Journal of Computer Applications*, 46(15), 2012
- [6]. M. Dipti, A. Aziz and M.A. kheen, Modeling, simulation and performance analysis of FACTS controller in transmission Line. *International Journal of Emerging Technology and Advanced Engineering*, 3(5). Pp 428-435, 2013.
- [7]. S.V. Pardeep and K.G. Vijay, Power system stability improvement of long transmission line system by using static VAR compensator (SVC). *Int. Journal of Engineering Research and Applications*. 3(5), pp. 01-03, 2013.
- [8]. E. Acha, C.R.F. Esquivel, H.A. Perez and C.A. Camacho, FACTS modelling and simulation in power system networks. 421pp. Chap 2. John Wiley & Sons Ltd, British Library, 2004.
- [9]. National Control Centre, Power Holding Company of Nigerian, 2012

Tribological Behaviour of E-Glass /Epoxy & E-Glass /polyester Composites for Automotive Body Application

Esmael Adem¹, P.Prabhu²

¹Lecturer, Department of Mechanical & Vehicle Engg., Adama Science & Technology University, Adama, Ethiopia

²Research Scholar, Department of Engg., & Technology (Mechanical), Himalayan University, Arunachal Pradesh, India

ABSTRACT: Experimental characterization of the mechanical properties of E-glass/Epoxy & E-glass/Polyester composite was conducted. The objectives of this paper is to present processing techniques of specimen preparation, conducting experiment to obtain mechanical properties and conduct experimental observation using Scanning Electron Microscopy (SEM) to know in homogeneity, porosity and fracture behavior. The effect of strain rate on E-glass/epoxy and E-glass/polyester has been investigated & experimentation was performed to determine property data for material specifications. E-glass/polyester laminates were obtained by compression moulding process and E-glass/epoxy laminate by hand lay-up vacuum assisted technique. The laminates were cut to obtain ASTM standards. This investigation deals with the testing of tensile, compression, shear and flexural strength on a universal testing machine. The graphs that are obtained from the tests were documented. This research indicates that the mechanical properties are mainly dependent on the strain rate.

Keywords - Epoxy, Fiber volume, Polyester, SE Microscope, Tensile test

I.INTRODUCTION

In order to conserve natural resources and economize energy, weight reduction has been the main focus of automobile manufacturers in the present scenario. Weight reduction can be achieved primarily by the introduction of better material, design optimization and better manufacturing processes. Even though there are several factors that influence the entire product development process to realize a lightweight vehicle, from the point of view of vehicle structural design, the main governing criteria for material selection are stiffness and strength properties that will determine the overall performance of vehicle during static and dynamic loading conditions. Due to rise in demand of lightweight vehicle and better mechanical performance of materials in automotive applications, different material combinations such as composites, plastic and light weight metals are implemented on primary and secondary structural parts of vehicles. Applications of composite materials in automotive industries already include some primary and secondary structures such as dashboard, roof, floor, front & back bumper, passenger safety cell, and rarely, A-pillar and B-pillar, [1, 2].

In order to estimate strength and stiffness, structural materials are subjected to mechanical testing such as tensile, compression, shear and flexural tests. Tests aimed at evaluating the mechanical characteristics of fibrous polymeric composites are the very foundation of technical specification of materials and for design purposes, in order to develop numerical and experimental models. The mechanical testing of composite structures to obtain parameters such as strength and stiffness is a time consuming and often difficult process. It is, however, an essential process, and can be somewhat simplified by the testing of simple structures, such as flat coupons. The data obtained from these tests can then be directly related with varying degrees of simplicity and accuracy to any structural shape, [3, 4].

George C. Jacob et.al. [5] Summarizes a detailed review of strain rate effects on the mechanical properties of polymer composite materials. An attempt was made to present and summarize much of the published work relating to the effect of strain rate studies done in the past on the tensile, shear, compressive, and flexural properties of composite materials to better understand the strain rate effects on these mechanical properties of fiber-reinforced polymer composite materials. The effect of strain rate on the tensile properties of a glass/epoxy composite was investigated by Okoli and Smith [6]. Tensile tests were performed on a glass epoxy laminate at different rates (1.7×10^{-2} -2000 mm/s). The tensile strength of the composite was found to increase with strain rate. In other studies the effects of strain rate on the tensile [7, 8], shear, and flexural properties of glass/epoxy laminate was investigated by Okoli and Smith. Tensile modulus increased by 1.82%, tensile strength increased by 9.3%, shear strength increased by 7.06%, and shear modulus increased by 11.06% per decade increase in log of strain rate. It can be inferred from this detailed review that the effect of varying loading rate on the tensile, compressive, shear, and flexural properties of fiber-reinforced composite materials has been investigated by a number of workers and a variety of contradictory observations and conclusions have resulted. Hence, more work must be done in the pursuit of eliminating all disagreements that currently exist regarding the effect of loading rate on the tensile, compressive, shear, and flexural properties of fiber-reinforced polymer composite material.

Keshavamurthy Y. C.et.al. [7] Studied tensile properties of fiber reinforced angle ply laminated composites. They conducted experiments on Glass/Epoxy laminate composite specimens with varying fiber orientation to evaluate the tensile properties i.e. three types of specimens with different stacking sequences, i.e., [00], [900], and [± 450] are generally fabricated. It is observed from the result that Glass/Epoxy with 00 fiber orientation yields high strength when compare to 300 & 450 for the same load, size & shape.

So to understand the behavior of the composite materials under different loading conditions and because composite materials are produced by different manufacturers, studying the mechanical and physical properties becomes vital. Thus, the paper tries to fill the gap which occurs on the composite manufacturer, Dejen Aviation Industry, here in Ethiopia by conducting experimental tests and presents the effect of strain rate on the mechanical behavior of E-glass/epoxy and E-glass/Polyester composite under quasi-static loading conditions by varying the strain rate in order to get the mechanical properties, this tests includes tensile, compression, flexural and shear tests.

II.MATERIALS AND EXPERIMENTAL TEST CONDITIONS

The raw materials used in this work are: E-glass fibers, Epoxy resin with its hardener, Polyester resin with its catalyst; which are obtained from Dejen Aviation Industry (DAVI), Bishoftu, Ethiopia.

E-glass: woven roving as shown in fig. 1, is a bi-directional fabric made by interweaving direct rovings and is compatible with many resin systems such as polyester, vinyl ester, epoxy and phenolic resins. These fibres are high-performance reinforcement widely used in hand lay-up and robot processes for the production of boats, vessels, plane and automotive parts, furniture and sports facilities. It is relatively low cost, the most common form of reinforcing fiber used in polymer matrix composites. "E" glass produced fibers are considered as predominant reinforcement for polymer matrix composites due to their: high electrical insulating properties, low susceptibility to moisture, high mechanical properties, and low cost. Due to this promising characteristic and is widely adopted in Dejen Aviation industry, E-glass fiber has been taken as reinforcement for this work. The type of E-glass fiber which is used in this study is woven roving's. This fiber type has good mechanical properties as compared to chopped mat and it is used when higher strength part is required.



Fig 1. E-Glass fiber

Epoxy and its hardener: The resin used for this study is Epoxy Resin with brand name of SYSTEM #2000 EPOXY RESINS, which is manufactured by Fiber Glast Development Corporation, which have low viscosity, consistent performance and doesn't contain any hazardous dilutes or extenders. In this work SYSTEM #2060 HARDNER is used; this is manufactured by Fiber Glast Development Corporation, which is characterized by low toxicity, excellent moisture resistance and excellent properties. Here, in #2060, has a one hour working time, and can be used for all sizes of parts using the contact layup method of fabrication. If the vacuum bagging

technique is being used, 2060 should only be used for smaller parts. The ratio of net epoxy resin and hardener was specified according to the manufacturer's manual, (3 part epoxy to 1 part hardener by volume or 100 part epoxy to 27 part hardener by weight).

Polyester and its Catalyst: The resin used for this study is Unsaturated Polyester with brand name of Part # - 83 manufactured by Fiber Glast Development Corporation. It is a low viscosity for fast wet-out, styrene suppressed, high thixotropic index to prevent draining on vertical surfaces. It exhibits good mechanical and electrical properties together with good chemical resistance compared to general purpose resins. The curing agent applied for the liquid resin is Hardener with brand name of #69 MEKP, Manufactured by Fiber Glast Development Corporation. The ratio of catalyst to resin is 1.25% by weight with #69 MEKP. Most of the time the ratio depends on the weather condition and it is also known that too much catalyst usually result in brittle material so care should be taken. But in this study 1.25% or 1.25g MEKP / 100g Resin was used as the ratio between catalysts to resin.

By taking technical data about E-glass fiber, epoxy and polyester resin from manufacturer's manual and taking technical measurement on mass of fiber, composite as well as equations used to determine fiber volume ratio from reference [9], the unknown values (fiber volume fraction) were evaluated and summarized in Table.

Table 1: Fiber and matrix volume contents of the composite laminate

Parameters	Value
Glass fiber volume	375.77 cc
Epoxy Matrix volume	333.33 cc
Polyester Matrix volume	574.16 cc
Fiber volume ratio for E-glass/Epoxy	53%
Fiber volume ratio for E- glass /Polyester	40%
Epoxy Matrix volume ratio	47%
Polyester Matrix volume ratio	60%
Fiber weight ratio for E-glass/Epoxy	72.5%
Epoxy Matrix weight ratio	27.5%

2.1. Composite Sample Fabrication Process

Composite laminates are formed by assembling different plies with different angles and orientations. Generally, in this work 5 plain woven plies are used for Tensile & shear specimens' preparation and 10 plies are used for compression & bending test specimens. The stacking sequence of laminate used with its respected angle is shown in fig. 2.

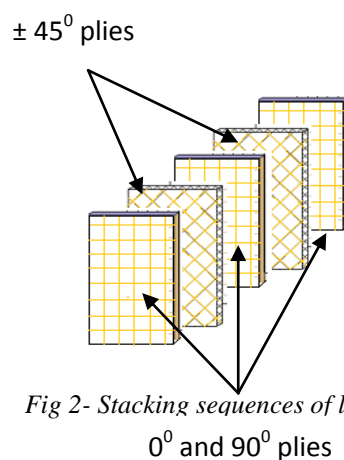


Fig 2- Stacking sequences of laminate
0° and 90° plies

Here, two types of manufacturing methods are used in order to fabricate the samples:

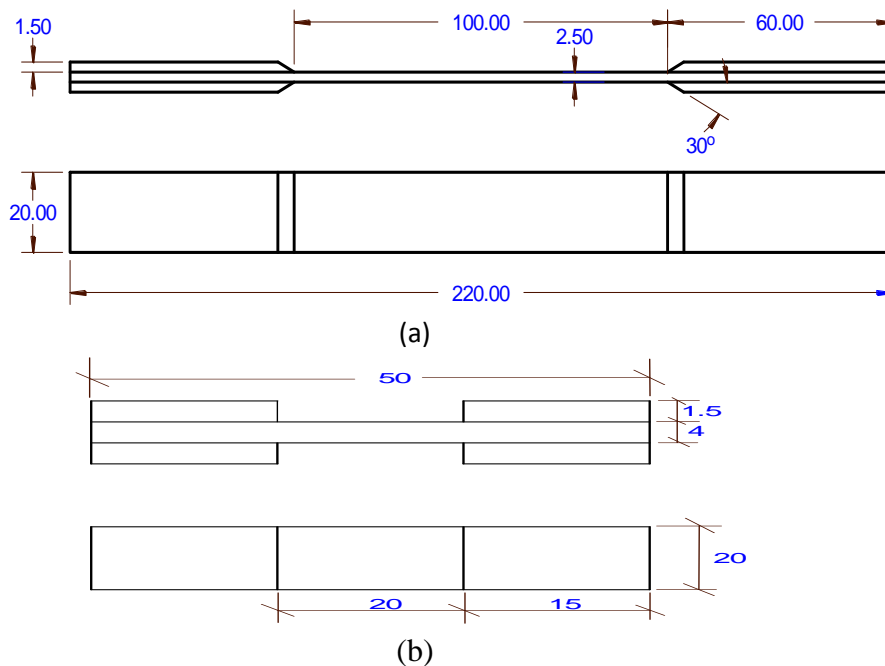
1. **Compression Molding** is used for E-glass/Polyester composite samples. This type of manufacturing method is chosen for this work due to:
 - ✓ Polyester resin has relatively high viscosity which can damage the vacuum pump when vacuum bagging is used.
 - ✓ This method is practiced and used in manufacturing of automotive components at Dejen Aviation Industry.
 - ✓ Compression molding uses fewer components than vacuum bagging technique.
2. **Hand lay-up Vacuum assisted technique (HLVA)** as shown in fig. 3, for E-glass/Epoxy composite samples. This is basically an extension of the hand lay-up process where pressure is applied to the laminate once laid-up in order to improve its consolidation. This is achieved by sealing a plastic film over the hand laid-up laminate and on to the tool. The air under the bag is extracted by a vacuum pump and thus up to one atmosphere of pressure can be applied to the laminate to consolidate it. The equipment's used are: Rotary vacuum pump, with Model No: 2TW-4C, Capacity: 8cfm, Vacuum: 6.7×10^{-2} Pa, Power: 220-240v/50Hz, Peel Ply (Release Fabric), perforated plastic film, Pressure fabric (breather), Vacuum nylon (vacuum bag), Mastic sealant (Vacuum tape), Vacuum bagging mold, Mold Release, paste wax.



Fig. 3 Techniques of composite manufacturing used in this paper
 (a) Hand lay-up technique (b) HLVA technique

2.2. Specimens Geometry and Dimensions

The geometry of each of loading configuration for E-glass/epoxy & E-glass/Polyester composite material is shown in fig. 4 below and is based on American Society of Testing & Materials (ASTM), [10-14].



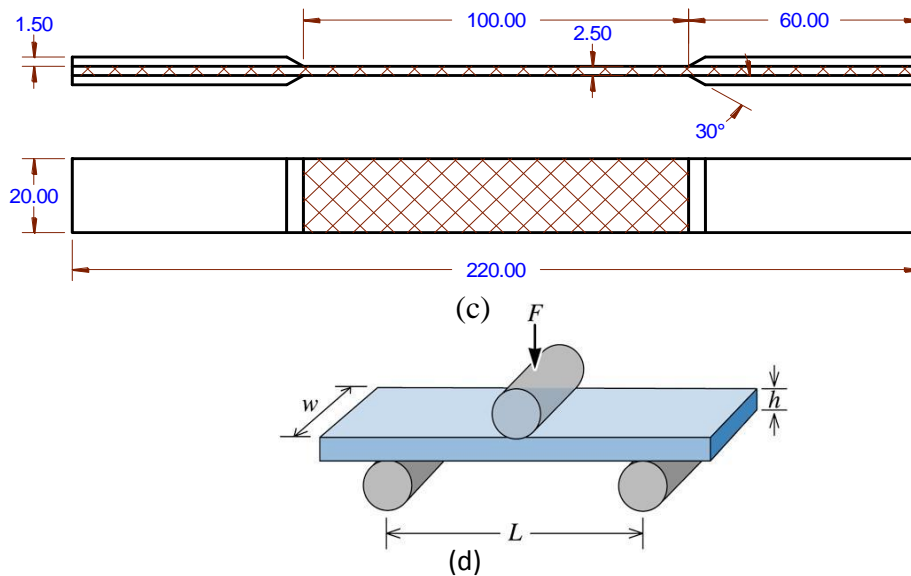


Fig. 4 Test Specimen Dimensions- (a) Tensile Test Specimen (b) Compression Test Specimen (c) In plain Shear Test Specimen (d) 3-point test

2.3. Testing Conditions

Three specimens for each test configuration were tested, in order to show the repeatability of the results through which minimizing the experimental errors, under tensile, compression, flexural and in plain shear loading with a Computer electro-hydraulic universal testing machine (model: WAW-600) with a capacity of 600 kN, precision grade is 0.5 with 0.01 - 500 mm /min test speed and manufactured in Shanghai Hualong Testing Instruments Co.LTD, China. Test world data acquisition software is used to acquire data from the machine during testing. Each specimen was clamped by means of hydraulic wedge grips. The machine was equipped with a standard load cell and a crosshead displacement measuring device. The experiment was conducted with varying strain rate values in quasi-static condition at room temperature (250C). The strain rate value, crosshead speed and repetition of specimen for these experimental tests are shown in table 2 below.

$$\text{Strain Rate} = (\text{Cross Head Speed}) / (\text{Gauge Length}) = V (\text{mm/min}) / (\text{mm})$$

Therefore, the total amount of specimen used for this study was 9 specimens for tensile, 9 specimens for shear, 9 specimens for compression and 9 specimens for flexural tests a total of 9x4 = 36 specimens were used for E-glass/Epoxy composite and the same amount was used for E-glass/Polyester composite. In general, 36x2 = 72 specimens were used for this study.

Table 2: Test Condition Parameters

Strain Rate	Tensile and shear Test		Compression Test		Flexural Test		Repetition for all tests
	Value (S-1)	Crosshead speed (mm/min)	Crosshead speed (mm/min)	Value (S-1)	Crosshead speed (mm/min)	Value (S-1)	
Strain rate 1	3.33E-5	0.2	0.2	1.66E-4	0.2	3.175E-5	3
Strain rate 2	3.33E-4	2	2	1.66E-3	2	3.175E-4	3
Strain rate 3	3.33E-3	20	20	1.66E-2	20	3.175E-3	3
Required Specimen	2x3x3=18 specimen		3x3=9specimen		3x3=9specimen		

Morphology of E-glass/Epoxy before test and the interfacial adhesion between fiber–matrix and tensile fracture after test was examined by scanning electron microscopy (SEM), Model: EM-30, serial number: CXS-3TAH-113031 with mark COXEM, which is shown in fig. 5 below.

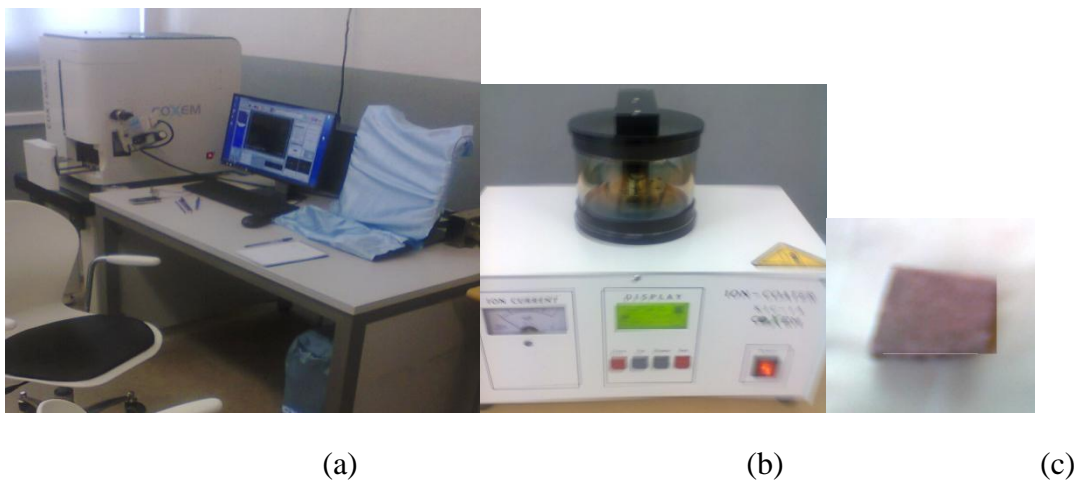
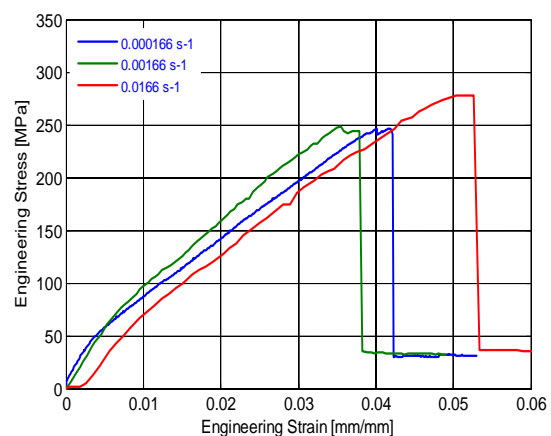
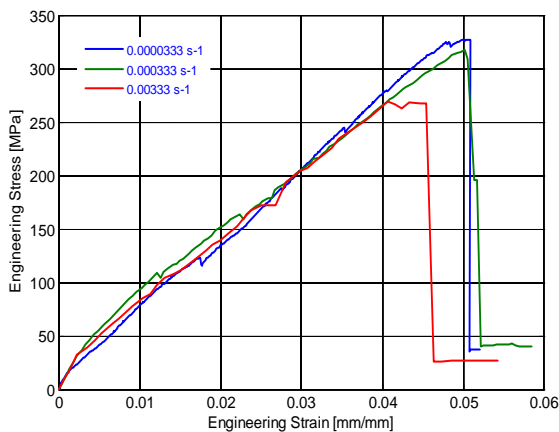


Fig. 5: (a) Scanning Electron Microscopy (b) Ion Gold Coater (c) Gold Coated Specimen

III. Experimental Results and Discussion

2.4. Tensile test

Fig. 6 (a) shows tensile strength of E-glass/Epoxy composite as a function of strain with different quasi-static strain rate. The test result shown is based on the average value of three specimens for each strain rate value. The result clearly shows when the strain rate is increased the tensile strength of the material was decreased. The percentage decrement of tensile stress is 3.06% and 15.24% for the first and second speed respectively. The effect of strain rate on tensile strength of E-glass/Polyester composite is shown in figure 6 (b). The given graph indicates the tensile strength of E-glass/Polyester composite was increased with the increase of strain rate. The percentage increment in tensile strength of the given composite is 0.514% and 11.98% for the first and second speed respectively.



(a) E-glass/Epoxy

(b) E-glass/Polyester

Fig. 6 Effect of Strain Rate on Tensile Strength of E-Glass/Epoxy and E-Glass/Polyester Composites

Regarding tensile failure mode, E-glass/Epoxy composite showed significant failure mode variation with increasing strain rate. As shown in Fig. 7 (a) limited damage within the gage length near grip area at the first speed and further strain rate increment changed the failure mode by extending the damage area to the center gage length and create fiber pullout. For example, as shown in Fig. 7 (a), at 0.000333 s-1 strain rate (TER3-02), excessive debonding between the fiber and matrix was exhibited. On the other hand, E-glass/Polyester composite showed grip area failure, as shown in Fig. 7 (b).

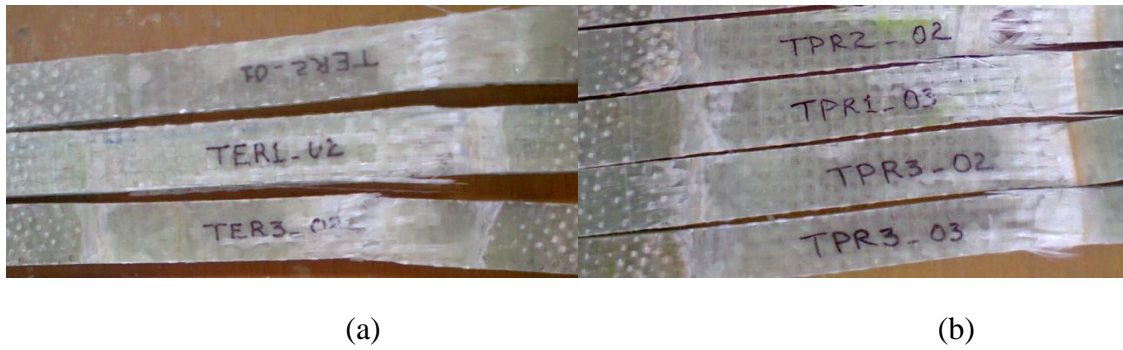


Fig. 7 Tensile Failure modes (a) E-glass/Epoxy composite (b) E-glass/Polyester Composite

2.5. In-Plane shearing Test

Fig. 8 (a) demonstrates quasi static strain rate effects on shear strength of E-glass/Epoxy composites. The test result shown is based on the average value of three specimens for each strain rate value. It can be clearly seen that the shear strength is increasing with the increase of strain rate. The percentage increment for the first two speeds are 0.44% and 19.93%. The effect of strain rate on shear strength of E-glass/Polyester is displayed in figure 8 (b) below. The result shows that the shear strength shows a decreasing trend with an increasing strain rate but, the effect of insignificant. The percentage decrement in shear strength of the given composite is 5.09% and 3.59% for the first and second speed respectively. The application of composite materials in mechanical engineering is limited by poor transverse and shear properties of unidirectional composites, which raise concern about their impact behavior [5].

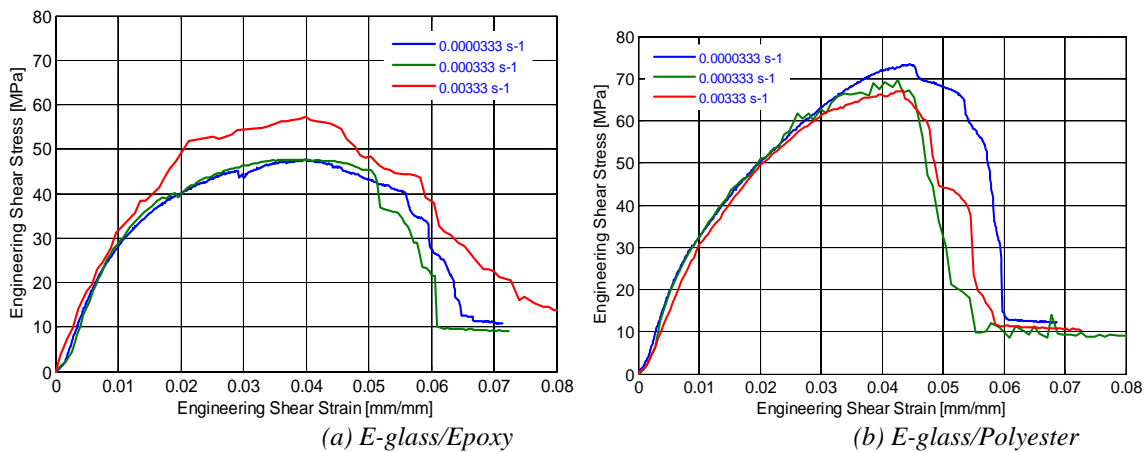


Fig. 8 In-plane shear strength of E-glass/Epoxy and E-glass/Polyester composites

Regarding in-plane shear failure mode, E-glass/Epoxy composite showed significant failure mode variation with increasing strain rate. As shown in Fig. 9 (a) limited damage within the gage length near grip area in the first strain rate and further strain rate increment changed the failure mode by extending the damage area to the center of gage length and create fiber pullout. For example, as shown in Fig. 9 (a), at 0.000333 s-1 strain rate, excessive debonding between the fiber and matrix was exhibited. On the other hand, E-glass/Polyester composite showed grip area failure, as shown in Fig. 9 (b).



Fig. 9 In-plane Shear Failure modes (a) E-glass/Epoxy composite (b) E-glass/Polyester Composite

2.6. Compression Test

The compression test results obtained from this work are not much satisfactory because the universal testing machine available in Mechanical and Industrial engineering school of Addis Ababa Institute of Technology material testing laboratory is not complete especially for this tests. For example there is no grip for compression tests. Due to this the shape of compressive stress-strain curve is unusual and the maximum value of compressive strength is lower.

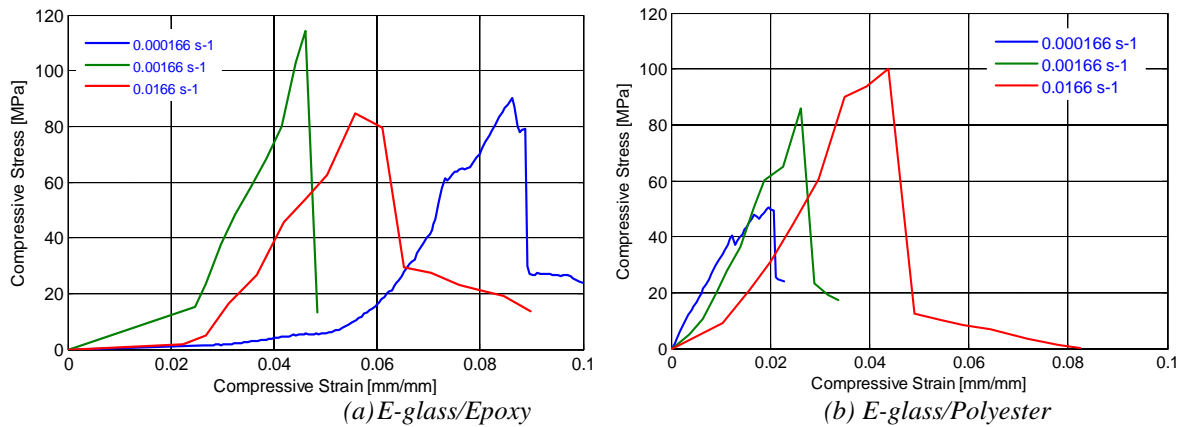


Fig. 10 Compressive strength of E-glass/Epoxy E-glass/Polyester composites

Fig. 10 (a) presents quasi-static strain rate effect on compressive strength for E-glass/epoxy composite as a function of strain rate. The test results presented are based on average values of three specimens for each strain rate value. It can be clearly seen that the compressive strength follows an increasing trend with the increase of strain rate for the first two speeds and decreases. The percentage increment and decrement for the first two strain rate values are 26.42% and 6.53% respectively. The effect of strain rate on compressive strength of E-glass/Polyester composite is shown in fig. 10 (b). The given graph indicates the compressive strength of E-glass/Polyester composite was increased with the increase of strain rate. The percentage increment in compressive strength of the given composite is 77.68% and 11.32% for the first and second strain rate values respectively.

The failure mode of compression, both E-glass/Epoxy composite and E-glass/Polyester composite shows the micro-buckling of fibers along the shear plane due to global shearing of laminate as shown in Fig. 11 (a and b).



Fig. 11 Compressive failure modes (a) E-glass/Epoxy and (b) E-glass/Polyester composites

2.7. Flexural Test

Fig. 12 (a) presents quasi-static strain rate effects on flexural strength for E-glass/epoxy composite as a function of strain rate. The test results presented are based on average values of three specimens. It can be clearly seen that the flexural strength was increasing trend with the increase of strain rate. The percentage increment for the first two strain rate values are 20.24% and 12.21%. The effect of strain rate on flexural strength of E-glass/Polyester composite is shown in figure 12 (b). The given graph indicates the flexural strength of E-glass/Polyester composite was decreased with the increase of strain rate. The percentage decrement in flexural strength of the given composite is 18.5% and 5.61% for the first and second strain rate values respectively.

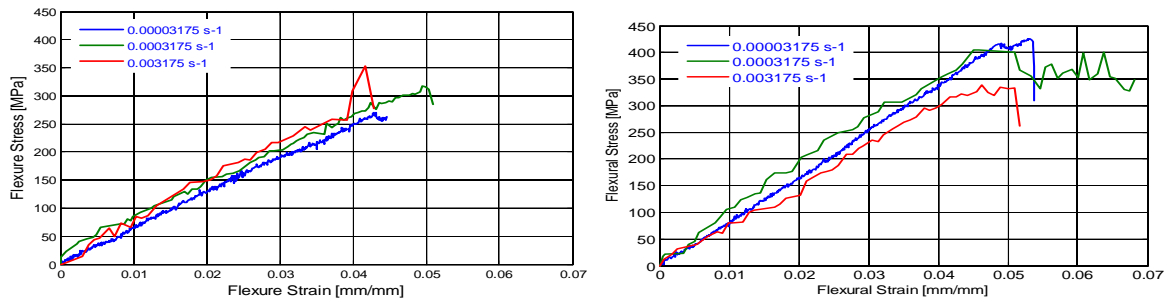


Fig. 12 Flexural strength of E-glass/Epoxy E-glass/Polyester composites

2.8. Scanning Electron Microscopy Observations

Scanning electron microscope (SEM) pictures of E-glass/epoxy composite surfaces before tensile test were obtained with different magnification scale as shown in Fig. 13a-13d. Fiber bonding and adhesion between the fiber and the matrix are clearly figured out from morphological studies. The interaction between matrix and glass fibers is good as it is seen from scanning electron microscope pictures. Fig. 13a-13b shows a small pores area. This is due to imperfect pump suction during manufacturing process. This area is a crack initiation during the application of load on tests leads pre-mature failure. The other area on this picture shows good, which clearly reveals strong adhesion and good interface attraction between glass fibers and matrix material. Figure (13c-13e) showed a rough surface and the strongly bonded fiber-matrix interface.

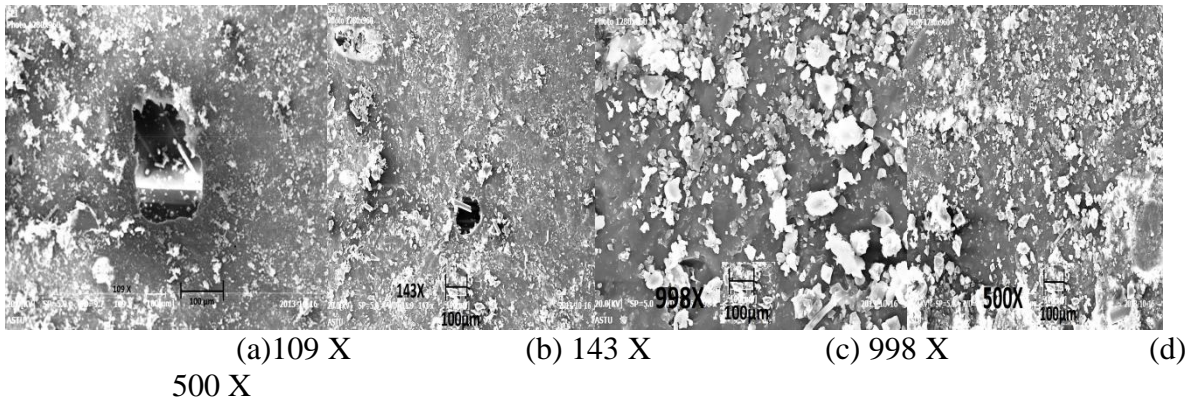


Fig. 13 SEM picture at different magnification scales before test

Fig. 14(a-c) shows SEM picture when the surface is observed after tensile test was conducted. Fig. 14 (a) indicates that some fibers are pulled out of the matrix as a result of mechanical fracturing done in tensile test. In Figure 14 (b-c), some glass fiber experience fiber pull out and delamination, which are the key features that are associated with the composites but very little fiber pull out was observed in the case of the thermoplastic modified epoxy matrix and GFRP composites, which reveals the efficiency of the modified matrix to hold the fibers. Strong interaction between thermoplastic and epoxy resin in matrix material leads to efficient stress transfer from the matrix to reinforcing glass fibers that reduce the crack growth rate, leading to good mechanical strength of the composites.[5]

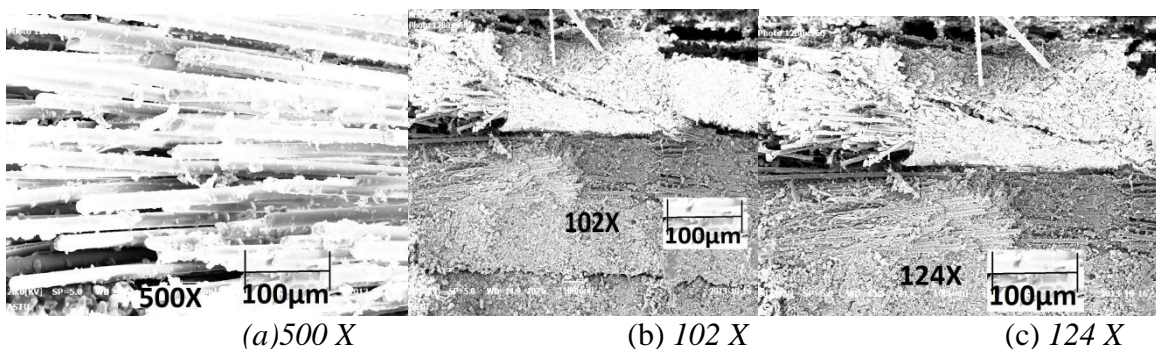


Fig. 14 SEM pictures after tensile test

IV. Conclusion

The tensile, compression, flexural and in-plane shear properties of plain woven E-glass/Epoxy & E-glass/Polyester composite are presented under quasi-static strain rate and the following conclusions are obtained.

- ▲ The compressive, shear and flexural properties of E-glass/Epoxy composite have an increasing trend when the strain rate is increasing; whereas the tensile strength decreases as the strain rate increases.
- ▲ In case of E-glass/Polyester composite, the tensile strength and compressive strength increases as the strain rate increases and the in-plane shear and flexural strength show a decreasing trend as the strain rate increases.
- ▲ SEM observation indicates the main problem of E-glass reinforced with epoxy and polyester is that fiber pull-out and delamination.

V. REFERENCES

- [1] Giovanni Belingardi, Ermias Gebrekidan Koricho, 'developing composite engine support sub-frame to achieve lightweight vehicles', 16th International Conference on Composite Structures ICCS 16, 2011 Porto.
- [2] Ermias Gebrekidan Koricho, 'implementation of composite and plastics materials for vehicle light weight', PH.D Thesis, 2012, p 44-74.
- [3] A. F. Hamed, M. M. Hamdan, B. B. Sahari and S. M. Sapuan, 'experimental characterization of filament wound glass/epoxy and carbon/epoxy composite materials', ARPN Journal of Engineering and Applied Sciences, vol.3, no.4, august 2008.
- [4] Barbero, E. J. 1998. 'Introduction to Composite Materials Design', Taylor & Francis, Philadelphia
- [5] Rafael Celeghini Santiago, Ricardo Lessa Azevedo, Antônio F. Ávila, Marclio Alves, George C. Jacob, J. Michael Starbuck, John F. Fellers, Srdan Simunovic, Raymond G. Boeman 'Mechanical characterization of glass/epoxy composite material with nanoclays' Received 4 November 2003; accepted 16 March 2004, DOI 10.1002/app.20901, Published online in Wiley InterScience (www.interscience.wiley.com).
- [6] Okoli, O. I.; Smith, G. F. In Proceedings of Society of Plastics Engineers Annual Technical Conference (ANTEC), Advanced Polymer Composites Division, 1995, Vol.2, p. 2998 –3002.
- [7] Keshavamurthy Y C, Dr. Nanjundaradhya N V, Dr. Ramesh S Sharma, Dr. R S Kulkarni, 'Investigation of Tensile Properties of Fiber Reinforced Angle Ply laminated composites', International Journal of Emerging Technology and Advanced Engineering Website: www.ijetae.com (ISSN 2250-2459, Volume 2, Issue 4, April 2012), p 700-703
- [8] Angelo G. Facc, Mark T. Kortschot, and, Ning Yan, 'Predicting the Tensile Strength of Natural Fiber Reinforced Thermoplastics', Composites Science and Technology 67 (2007) 2454 –2466.
- [9] Daniel Gay, Suong V. Hoa and Stephen W. Tsai, 'Composite materials design and applications', © 2003 by CRC Press LLC
- [10] Donald F. Adams, Leif A. Carlsson, and R. Byron Pipes, "Experimental Characterization of Advanced Composite Materials," CRC Press.
- [11] ASTM D3039. 1995. 'Standard Test Method for Tensile Properties of Polymer Matrix Composite Materials'. Annual Book of ASTM Standards, American Society for Testing and Materials, Philadelphia. 14 (2): 99-109.
- [12] ASTM D3518. 1994. 'In-plane Shear Response of Polymer Matrix Composite Materials by Tensile Test at ±45° Laminate'. Annual Book of ASTM Standards, Vol. 14.01, American Society for Testing and Materials, Philadelphia. pp. 139-145.
- [13] ASTM D 3410 'Compressive properties of unidirectional or crossply fiber-resin composites', ASTM Committee of Standards, Philadelphia, (1982).
- [14] D 790 – 03 'Standard Test Methods for Flexural Properties of Unreinforced and Reinforced Plastics and Electrical Insulating Materials'. Annual Book of ASTM Standards, 2003.

A Generic Adaptive Method for Corruption Mitigation in Trial Monitoring System with Restful Authorization

Suryanaraayan.B¹, Subramanian.M², Saikrishna.K.K³, Sujitha.G⁴

^{1,2,3,4}(Department of Computer Science and Engineering, Rajalakshmi Engineering College/Anna University, India)

Abstract: The purpose of a Trial Monitoring System is to provide a comprehensive suite where cases are created. Trial proceedings are monitored progressively to make informed decisions that include assignment of investigating entities and requesting advisors for opinions to take over the prosecution of the case. It provides a platform for applying counter petitions against an allegation's disposal and integrate proceedings in different levels of scrutiny and across tribunal entities. The outcome is the aggregation of such a data, to classify cases for statistical information and relaying the information in presentable format.

Keywords – Caching, Object Relational Mapping, RESTful Web Service

I. Introduction

A Tribunal Entity, admit about thousand cases in average every year. The accumulated data is very difficult to maintain. The existing system maintains records which either doesn't confirm to relational normalization which leads to a poor database implementation and give raise to various inconsistencies like a case of not able to track disposals, or the evolving case proceedings.

The system's scope is limited to entering data. Because of this disadvantage, the organizational entity cannot get any meaningful information or use the system productively for truly monitoring. Most of the today systems are loosely integrated, so functionalities away from the domain of operation of the system can utilize features, as a service from a remote external entity, rather than itself implementing it. Such a design allows for broader purpose of use and a better scalability as the information can be pulled instantly only when a request is processed.

Since the system naively uses such architecture, the possibility of expansion or integration is close to null. Mishaps in exercising of duties of investigating entities are unmanageable and thus may raise corruption within a tribunal entity. The workflow, is only utilized based on the traditional customary and relies on managing based on physical copies of documents, either completely duplicated or partially persisted. In such a situation, the possibility of data getting lost amidst the others is highly likely, leading to irregularity whose identification and rectification is a very time consuming and costly operation. Also the classification of records based on different criterion is time consuming as the query needs to eliminate duplicates and validate referential integrity.

Though, the existing system has some of few advantages which are like less hardware and software required, cheap in comparison of computerized system. Migration from the existing system to a new better system, calls for utilizing a rather robust requirement for the new automated system.

II. Proposed model

The Objective of designing a new system is to improve the monitoring capabilities over that of the conventional system. The proposed system suggests an adaptive method in Trial Monitoring System using RESTful Web Services and Authorization. The system provides a comprehensive suite where cases are created and the trial proceedings are monitored progressively to make informed decisions that includes assignment of investigating entities, requesting advisors for opinions to take over the prosecution of the case and applying counter petitions against an allegation's disposal by providing a platform to integrate proceedings in different levels of scrutiny and across tribunal entities, and aggregation of such a data, to classify cases for statistical information and relaying the information in presentable format.

2.1 System as RESTful Web Service

Considering REST as a design pattern is primarily to utilize the system architectural styles consisting of guidelines and best practices for creating scalable web services. It is by far optimal and supports readability of data with respect to conventional dynamic web services over HTTP. The logic of the controller is interfaced through a REST Handler, which maps the sanitized URI to one of the corresponding REST API Methods, which handle the service request.

2.1.1 REST Framework

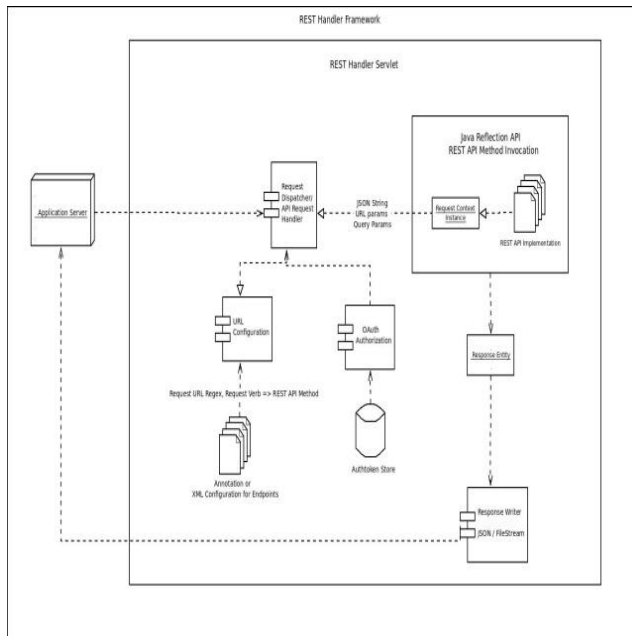


Figure 1: REST Framework

The Trial Monitoring System is proposed with a customized REST Handling Framework optimized to provide coherence with Role Based Authorization. It has been modelled to be development friendly and at the same time provide faster lookup.

2.1.2 Initiating REST Service

The framework is written with a start point of a Servlet which accepts all requests within the API context, and invokes (Java Reflection) a corresponding API method passing the context parameters, query parameters in case of GET request and additional parameter of JSON String that comes as the request payload in case of POST, PUT and DELETE requests.

The returned object from the method is an instance of either an entity in which case, it is converted to JSON or a File Stream which is written as raw bytes to the response body with content disposition of attachment. Exceptions in API, are specially handled by throwing custom exception instance and corresponding error message is written to the response.

2.1.3 Registering an Endpoint

The framework provides an elegant way to register an endpoint (map URL pattern with corresponding API method). Endpoints are registered by adding a custom annotation to each of the API methods providing the Request Method, URLRegex, and a name (that uniquely identifies an endpoint) or providing the mapping in XML files corresponding to each Request Method.

2.1.4 Optimization:

A URL Configuration singleton is instantiated, which reads the annotated methods and configuration XMLs for the endpoints. An in-memory mapping is constructed eliminating duplications. The URL Regex is compiled for once and saved in memory so that subsequent matching time is reduced. Each of the endpoints are stored in the database as an Activity and indexed using an integer key. The optimization with respect to Role Based Authorization is achieved by using this key of each endpoint for comparison, eliminating a costly operation of comparison of strings, thus making it faster.

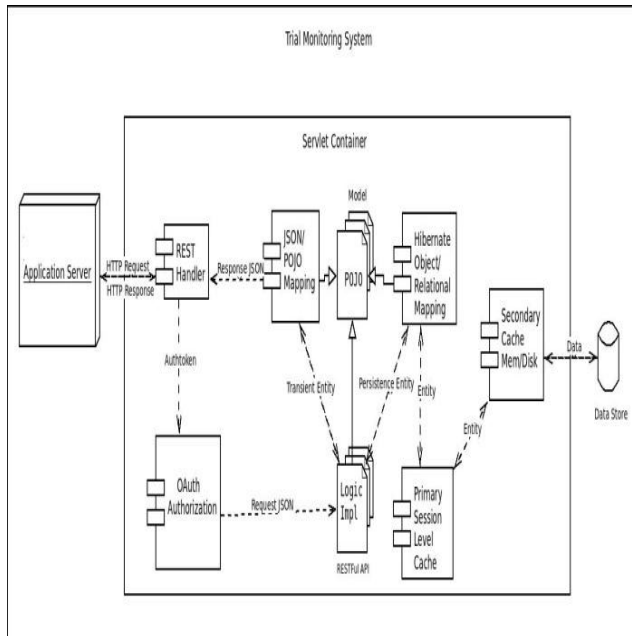


Figure 2: Proposed Trial Monitoring System

The proposed REST Handler Framework consists of a Servlet, which accepts all the requests from the context of the API. Statelessness is achieved by authorization from accepting the "Authorization Token" which is passed as with Request Header. This token is passed to the Authorization Service, which authorizes the given request to access the REST APIs, on validation against a list of services the user possessing the authtoken is eligible to exercise. The token is primarily obtained from a trusted entity, which is a RESTful service of Identity Access Management, by requesting for a token, providing the required identity information. A user may obtain more than one token and thus use the token as a grant towards executing the listed services.

Upon Authorization, the request entity is State Transferred from conventional JSON to a Java instance which is passed to the corresponding REST API corresponding the Request URI and the Request Verb (GET, POST, PUT, DELETE) used. The Response from the REST API is either one of (1) Response Entity corresponding to the given request. (2) A file or stream of content, whose content disposition is of an attachment. (3) An Error explaining any or all of exceptions with the request Entity.

Each response is associated with a status code explaining the status of the response. Conventionally, the status code corresponds to the HTTP status codes. The framework is customized in a way that allows for a clearer API implementation. It uses the context parameters reference as a single point message passing between the REST API and the REST Handler, which takes care of the Representational State Transfer. This is unlike the existing REST Frameworks that uses annotations for mapping requests and constructing separate Response object for each request, and that forces the developer to declare method arguments for each input from the request which leads to more redundancy.

2.2 Role Based Authorization

An important component of the proposed system is to exercise Role Base Authorization. Every user is associated with a predefined Role, which allows the minimum level of services accessibility of the system for that role. The system allows for customization of role permissions and overriding the access constraints to any particular user. This allows reusability and complete customization of actions and corresponding events.

2.3 Productivity and Collaboration

The system opens scope for enhanced productivity and seamless integration between other systems through reverse API, also known as WebHooks. Basically, the system incorporates a event driven approach, which allows logging of event actions remotely through an access point that connects the system's Internal API to the external API. This is done by registering a HTTP URL endpoint for selected actions within the system. The system triggers a HTTP Request to these selected endpoints in the event of selected action, passing the event data JSON as URL Parameter.

Examples of integration include integration with remote Email Server, or SMS Server, which can be used for notification of the event and ease of monitoring. More sophisticated integrations include, integration of the system with another system that runs independently and sinks services with a different level of scrutiny, which requires the data in this system, for preliminary processing.

The system offers reporting as a service, which helps classify the cases based on different criterion and relay the information in a presentable manner. The system offers collaboration of different entities by allowing every participating entity to comment and discuss on a case for making informed decision.

2.4 Platform Independence

The system operates externally using JSON standard representation, which provides a consistent data format for interoperability. Further the system suggests usage of Java as a platform, as the executable modules are platform independent and thus can run across multitude of operating systems and usage of Object Relational Mapper as an interface of accessing the database, eliminating the dependency on schema implementation across different database management systems.

2.5 Performance Evaluation

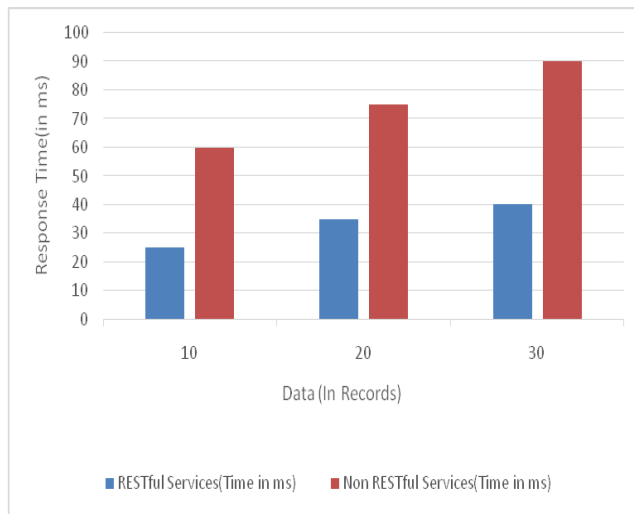


Figure 3: Performance Measure: Service Architecture

RESTful Service implementation using JSON provides better semantics and data representation, hence the added payload of other HTML, CSS or other resources for constructing the web page are loaded once. Raw JSON is used to populate the data in the webpage, thus reducing the response time for each request.

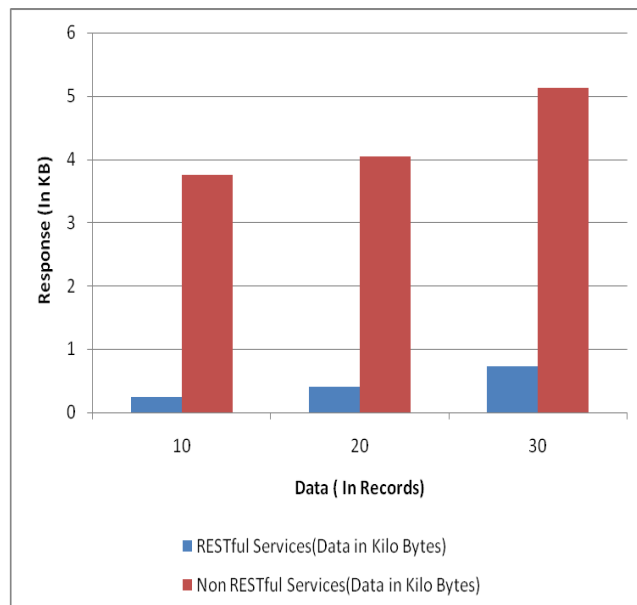


Figure 4: Performance Measure: Data Size

Conventional dynamic web apps mix HTML code with raw data, thereby adding overhead each time to the response message. On the contrary, in the RESTful implementation, Raw JSON is used to populate the data in the webpage, thus reducing the data size for each response.

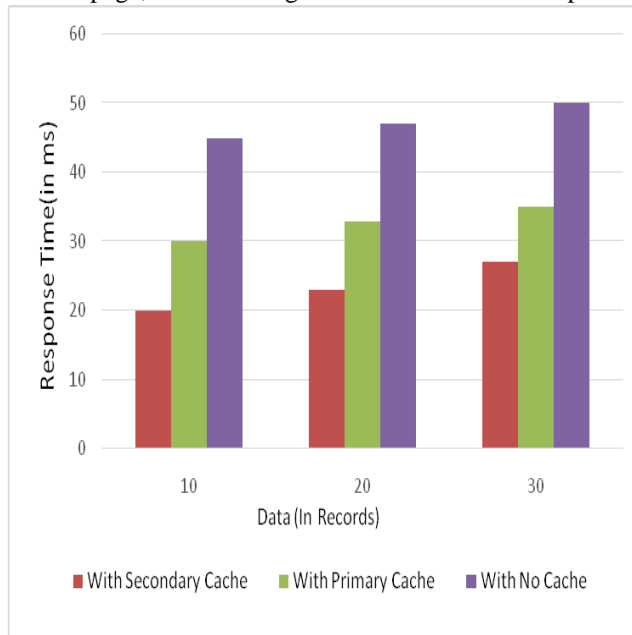


Figure 5: Performance Measure: Caching

Since the system has been modeled as entities, the query overhead and database lookup overheads can be optimized by introducing caching of entities. It has since been observed that the performance of system can still be optimized by introducing a secondary level of caching, with extended time to live, thus eliminating the buffering in the primary cache thereby lowering the response time.

III. Conclusions

The proposed Trial Monitoring System provides an adaptive method for monitoring case entities. Assuming that all the requirements are intact, the system is scalable to better levels and secure. RESTful implementation in Trial Monitoring System is the first of its kind in serving large data based on the user roles. Data access is authorized at varied levels based on the role of the user. Future work in this system, include integration of the system to higher levels of the tribunal entity and provide varied notification such as SMS and Email as a service from an external provider.

REFERENCES

- [1] Leonard Richardson, Sam Ruby, David Heinemeier Hansson, *RESTful Web Services* (Sebastopol, O'Reilly Media, 2007)
- [2] Bill Burke, *RESTful Java with JAX-RS* (Sebastopol, O'Reilly Media, 2009)
- [3] Subbu Allamaraju, *RESTful Web Services Cookbook: Solutions for Improving Scalability and Simplicity* (Sebastopol, O'Reilly Media / Yahoo Press, 2010)
- [4] Gavin King, Christian Bauer, *Java Persistence with Hibernate* (Greenwich, Manning Publications, 2006)
- [5] David Heffelfinger, *JasperReports 3.5 for Java Developers* (Birmingham, Packt Publishing Ltd, 2009)
- [6] Charbonneau. N, Newman. B, Pecelli. D, Security Incident Origin Discovery (SIOD) IP Transaction Tracking for Centralized Cyber Defense, Proc. *Military Communications Conference (MILCOM) IEEE, Baltimore, MD, 2014, 30-39.*
- [7] Rouached. M, Sallay. H, RESTful Web Services for High Speed Intrusion Detection Systems, Proc. *Web Services (ICWS), IEEE 20th International Conference, Santa Clara, CA, 2013, 62-622.*

Estimation of Sag by the Influence of Altitude Parameter

Shamim Ahmed

Medizinische Fakultät, Martin-Luther-Universität Halle-Wittenberg, 06120 Halle, Germany

ABSTRACT: In this paper, transmission line sag is studied by direct effect of altitude parameter. More precise result is achieved when the measurement is performed considering the height of the overhead transmission lines from ground. Barometrical data from American standard atmosphere is used to carry this study. The complete form of mathematical sag expression is considered here, in presence of ice coating and wind pressure. Study is performed for both cases, when the supports are equal and unequal levels. Numerical calculations are performed in Matlab®.

Keywords -Transmission lines, Sag, Quintic polynomial, Quartic polynomial, Altitude function, Matlab.

I. INTRODUCTION

In a simple definition, the vertical distance between the points of supports and the lowest point of the transmission line is referred as dip or sag. It is not possible to install the electric cables without any sag even though we wish to do so because of its acting downward weight. This sag is in practice, allowed to form to prevent the conductors from break due to the excessive tension.

Thus the sag has become a frequently handled parameter in power systems. The conventional mathematical expressions of sag are involved with the ice coating and the wind pressure [1]. This pressure again varies by the altitude or height. Some useful barometric formulae are available with different variables including the altitude. These equations are generally used to find out the barometric pressure and hence the sag of the overhead power transmission lines. But in this paper, the sag is studied considering the altitude directly.

II. CONVENTIONAL MEASUREMENT OF SAG

It is considered that the supports are at unequal levels (Fig. 1). The transmission lines are assumed with ice coating and influenced by wind pressure. Then the mathematical form [1] of sag at the support of lower level, can be expressed by (1)

$$S_l = \frac{W_r}{2T} \left(\frac{l}{2} - \frac{Th}{W_r l} \right)^2 \quad (1)$$

Expression of sag at the support of upper level, is given by (2).

$$S_u = \frac{W_r}{2T} \left(\frac{l}{2} + \frac{Th}{W_r l} \right)^2 \quad (2)$$

Where, T is the tension in the conductor. The span length is l . Difference between the two supports is h . Resultant weight per unit length of the conductor is denoted by W_r .

The resultant weight is occurred because of the weight of conductor itself, ice coating and the wind flow. Thus W_r is given by (3).

$$W_r = [(W_c + W_i)^2 + W_w^2]^{1/2} \quad (3)$$

W_c , W_i and W_w in Eq. (3) denote the weight per unit length of the conductor, weight of ice for unit length and wind force per unit length respectively.

Weight of ice per unit length can again be written as:

$$W_i = \pi t \rho_i (D + t) \quad (4)$$

ρ_i is the density of ice. Diameter of the conductor is D and t for the thickness of ice coating. Finally wind force per unit length is calculated using (5), where P is the wind pressure [1].

$$W_w = P(D + 2t) \quad (5)$$

If the supports are exactly at equal level ($h = 0$) or almost at equal level ($h \approx 0$) then Eq. (1) and Eq. (2) are reduced in a single formula. In that case the sag S becomes [1]:

$$S = \frac{W_r l^2}{8T} \quad (6)$$

A schematic diagram is shown in Fig. 1 to illustrate the involved parameters of sag formation.

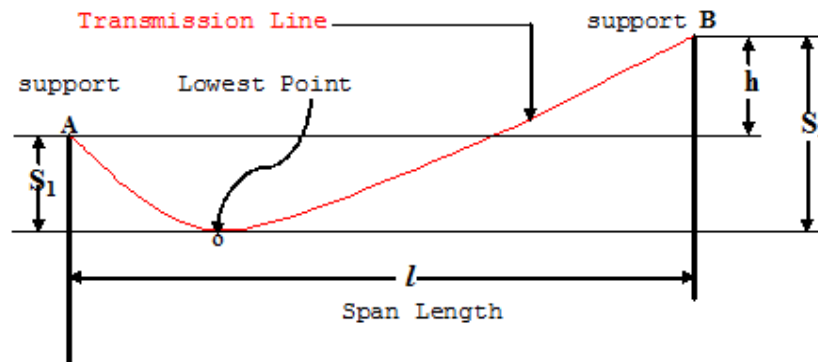


Fig.1. Formation of sag at unequal supports

These mathematical expressions [Eq. (1), Eq. (2) and Eq. (6)] are generally used for the conventional measurement of sag. The wind pressure P is in practice, calculated by some sort of barometric formulae.

This is of course a correct process but the problem is that those barometric formulae may have many variables [2]. So it would be better if the sag expressions can have only the altitude parameter, for the barometric estimation. This altitude is the height of the overhead power transmission lines. In the next section, sag is studied in this direction.

III. MEASUREMENT USING THE ALTITUDE PARAMETER

Many theoretical and experimental works have been done on sag calculation and later sag was calculated from GPS measurements [3]. But up to this time no research had been conducted to calculate the sag directly by altitude measurement system. Let us consider the variation of wind pressure with respect to the height. According to the information provided by American Standard Atmosphere [2], this variation follows the Height (H) and Pressure vector (P), as below.

$$H = [0 \ 11 \ 20 \ 32 \ 47 \ 51 \ 71] \text{ in Km}$$

$$P = [101.33 \ 22.63 \ 5.48 \ 0.87 \ 0.11 \ 0.07 \ 0.004] \text{ in KPa}$$

This data set is widely used to get the overview of the wind pressure for certain altitude levels. The variation of wind pressure with altitude and the standard deviation of wind pressure are observed in Matlab. For this purpose, the corresponding code is written in Matlab, which is shown below.

Code for wind pressure variation and standard deviation calculation

```

% observe barometric data and find standard deviation of wind pressure
%
% P and H are row vectors
%
H = [0 11 20 32 47 51 71]; % height in Km
P = [101.33 22.63 5.48 0.87 0.11 0.07 0.004]; % wind pressure in KPa
%
figure;
axis('normal')
box 'on'
grid 'off'
zoom 'off'
barh(H,P,1.5) % horizontal bar diagram
xlabel('Wind Pressure (in KPa)')
ylabel('Height (in Km)')
xlim([0 110])
text(50,5,'Pressure at Sea Level')
legend('Wind Pressure','Location','NorthEast');
%
% find standard deviation of wind pressure
%
M = mean(P); % mean of wind pressure
%
N1=P(:,1); s1=round(abs(N1-M)); % standard deviation of P at zero level
N2=P(:,2); s2=round(abs(N2-M));
N3=P(:,3); s3=round(abs(N3-M));
N4=P(:,4); s4=round(abs(N4-M));
N5=P(:,5); s5=round(abs(N5-M));
N6=P(:,6); s6=round(abs(N6-M));
N7=P(:,7); s7=round(abs(N7-M)); % standard deviation of P at 71 Km
%
S = [s1 s2 s3 s4 s5 s6 s7] % standard deviation for seven altitude levels
%
figure;
bar(S)
ylabel('Standard deviation of wind pressure')
%
str1=['at H = 0; std = ',num2str(s1)];
str2=['at H = 11 Km; std = ',num2str(s2)];
str3=['at H = 20 Km; std = ',num2str(s3)];
str4=['at H = 32 Km; std = ',num2str(s4)];
str5=['at H = 47 Km; std = ',num2str(s5)];
str6=['at H = 51 Km; std = ',num2str(s6)];
str7=['at H = 71 Km; std = ',num2str(s7)];
%
text(0.6,86,str1);
text(2,25,str2,'rotation',90);
text(3,25,str3,'rotation',90);
text(4,25,str4,'rotation',90);
text(5,25,str5,'rotation',90);
text(6,25,str6,'rotation',90);
text(7,25,str7,'rotation',90);
%

```

Wind pressure at different altitude levels and standard deviation of wind pressure are illustrated on bar diagrams in Fig. 2 and Fig. 3 respectively.

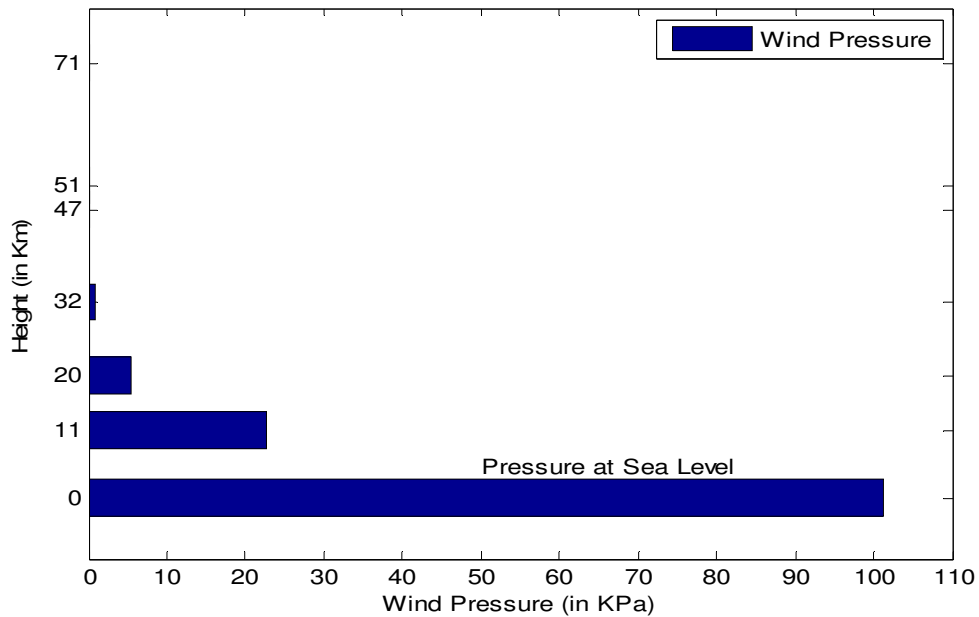


Fig. 2. Wind pressure variation with altitude

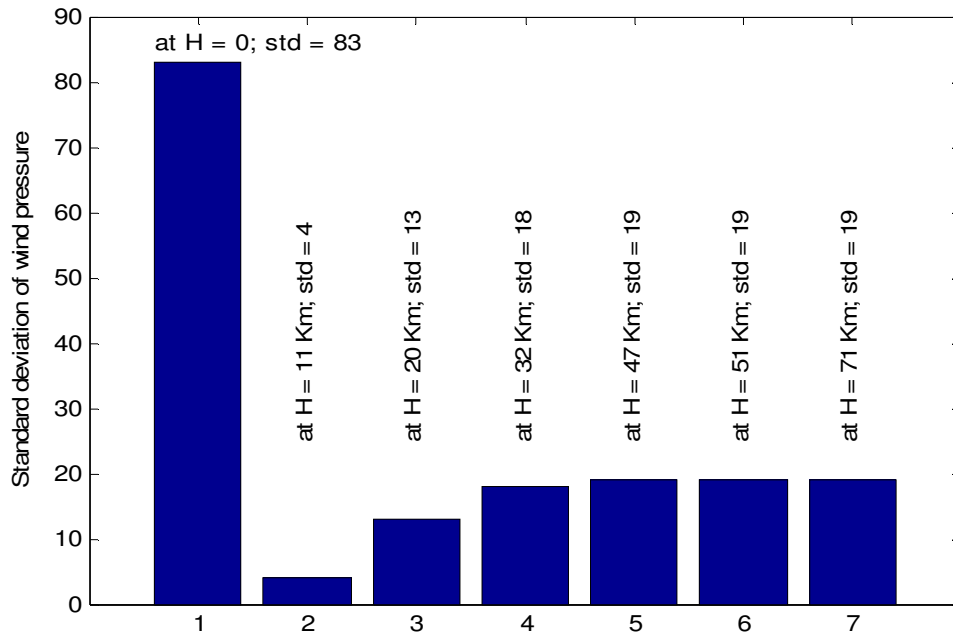


Fig. 3. Standard deviation of wind pressure for seven altitude levels

From figure 3, it is obvious that almost every cases, the standard deviations are too high. So it is not a good idea to consider the average of wind pressure at the desired level, where the overhead transmission lines are installed. This problem could be solved with a quintic polynomial, which is established by curve fitting method in Matlab.

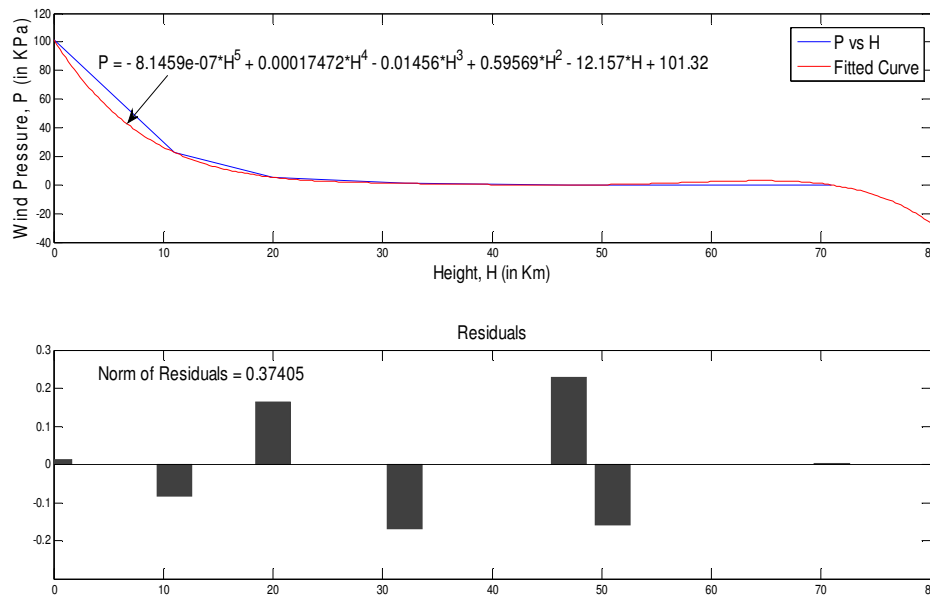


Fig. 4. Fitted wind pressure for fifth degree

The residuals are found as below.

$$\text{Residuals} = [0.013 \ -0.084 \ 0.164 \ -0.169 \ 0.230 \ -0.157 \ 0.004]$$

Hence the curve fitting leads to achieve (7).

$$\alpha(H) \approx 100.32 - 12.16 H + 0.60 H^2 - 0.015 H^3 + 0.0002H^4 - 0.0000008 H^5 \tag{7}$$

Thus $\alpha(H)$ forms a quintic polynomial, where the leading coefficient is -0.0000008 and the leading term is $-0.0000008 H^5$. This polynomial implies that higher the power of altitude, its coefficient becomes smaller.

This Altitude function $\alpha(H)$ can directly be used to measure the wind pressure P , only using the height from the ground to the overhead power transmission lines.

Eq. (5) can now be given in terms of $\alpha(H)$ as:

$$W_w = (D + 2t) * \alpha(H) \tag{8}$$

The resultant weight, using Eq. (8) stands as:

$$W_r = [(W_c + W_i)^2 + \{(D + 2t) * \alpha(H)\}^2]^{1/2} \tag{9}$$

Finally the mathematical expression of sag in Eq. (6) becomes:

$$S = \frac{l^2}{8T} [(W_c + W_i)^2 + \{(D + 2t) * \alpha(H)\}^2]^{1/2} \tag{10}$$

Eq. (10) allows to express Eq. (1) and Eq. (2) as below.

$$S_1 = \frac{[(W_c + W_i)^2 + \{(D + 2t) * \alpha(H)\}^2]^{1/2}}{2T} \left(\frac{l}{2} - \frac{Th}{l * [(W_c + W_i)^2 + \{(D + 2t) * \alpha(H)\}^2]^{1/2}} \right)^2 \tag{11}$$

$$S_2 = \frac{[(W_c+W_i)^2+\{(D+2t)*\alpha(H)\}^2]^{1/2}}{2T} \left(\frac{l}{2} + \frac{Th}{l*[(W_c+W_i)^2+\{(D+2t)*\alpha(H)\}^2]^{1/2}} \right)^2 \quad (12)$$

Eq. (11) and Eq. (12) are the desired expressions of sag. Where S_1 the sag at support of is lower level and S_2 is the sag at support of upper level. These equations are perfectly able to calculate sag by the direct effect of altitude function $\alpha(H)$.

IV. ESPECIAL CONDITION

For the minimum height that is at the sea level, $\alpha(H)$ is reduced as:

$$\alpha(H) = \lim_{H \rightarrow 0} \alpha(H) \approx 100.32 \text{ KPa} \quad (13)$$

But it is important to note that wind pressure does not follow the conventional barometric formulae above 32 Km from the sea level [3]. This is true both for the case of standard temperature lapse rate as zero or nonzero. As a result, the study of measurement is limited up to this level. But in practice, it is not a problem at all. Because the installed transmission lines are much lower than that level, even in the hilly places.

However, the rate of change of wind pressure with respect to height becomes:

$$\frac{d\alpha(H)}{dH} = -12.16 + 1.2 H - 0.05 H^2 + 0.0008 H^3 - 0.000004 H^4 \quad (14)$$

Thus Eq. (14) is a quartic polynomial when the rate of change of wind pressure with respect to the height of the transmission line is considered. It is observed from Fig. 5.

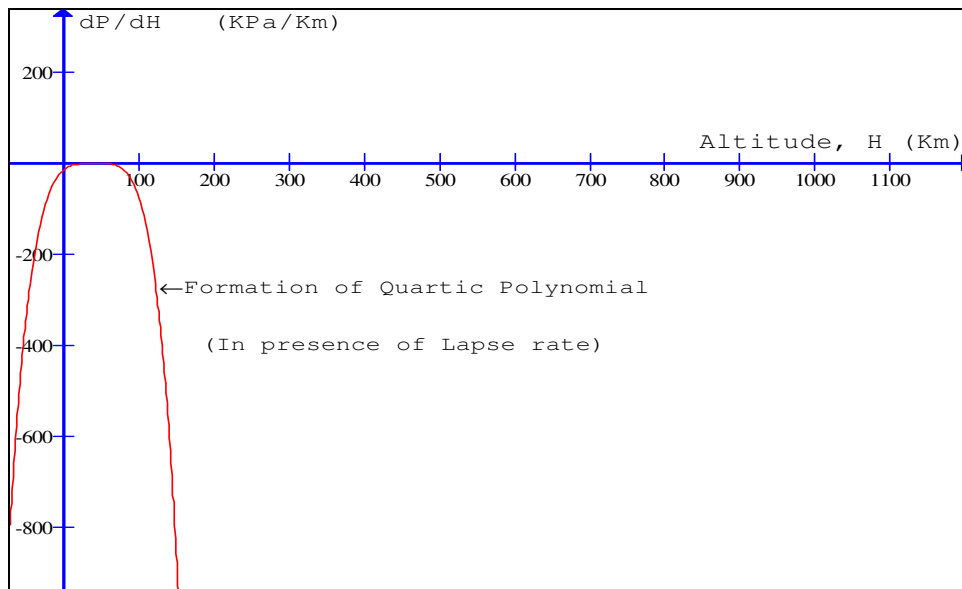


Fig. 5. Formation of quartic polynomial from quintic form

From Eq. (7), it is obvious that when we consider the height of the transmission lines at the sea level then H is to be considered zero. Thus $\alpha(H)$ becomes:

$$\alpha(H = 0) \approx 100.32 \text{ KPa}$$

$$\alpha(H = 11 \text{ Km}) = 22 \text{ KPa}; \text{ Almost same as in vector P}$$

As a same manner, for desired level (where the transmission line is installed), the corresponding wind pressure can be obtained, for the altitude range $0 \leq H < 32$.

V. CONCLUSION

Conventional sag has been studied by influence of the height of overhead transmission lines. This study is more convenient for sag calculation for any types of sag formation. In special case, the quintic polynomial has been reduced on its limiting value same as the wind pressure at sea level. This allows to have a single constant of the altitude function. The quintic polynomial was turned into a quartic polynomial when the rate of change of wind pressure near to the overhead transmission lines is considered. This approach can be used when the altitude is below 32 kilometers. The measurement is valid for both conditions when the supports are at equal and unequal levels.

REFERENCES

- [1] V. K. Mehta and R. Mehta, Principles of power system, (New Delhi: S. Chand & Company Ltd. 2003), 151-174.
- [2] U.S. standard atmosphere: http://en.wikipedia.org/wiki/U.S._Standard_Atmosphere
- [3] K. Sangeeta, R. Dahiya and P. K. Chaturvedi, A method of getting sag of power transmission line from DSP of GPS measurements, *International Journal of Engineering Science and Technology*, 2(8), 2010, 3743-3752.

Selection of renewable energy project using Multicriteria Method

DADDA Afaf¹, OUHBI Brahim¹

¹Department of Industrial and Production Engineering, ENSAM University MY ISMAIL, Morocco

ABSTRACT: Nowadays, many investors are interesting on implementing new renewable energy project around the world. The success of the decision making process regarding the selection of this projects, depends a lot on the effectiveness of the feasibility stage. During last decades, it is observed that many researches had used the Multicriteria Decision Making Methods to assist decision makers. Therefore, this paper proposes a comparative study of a three decision making process, applied in different countries. This study compares the related process in different levels. A new process is also proposed to validate a local renewable energy project.

Keywords: Renewable Energy Projects, Multicriteria Method, AHP Method, PROMETHEE Method, VIKOR Method, ELECTRE Method.

I. INTRODUCTION

The selection of Renewable Energy (RE) project is a multi-dimensional process, since it has to consider technological, financial, environmental, and social factors. Multi-criteria Decision Analysis (MCDA) appears to be the most appropriate approach to understand the different perspectives and to support the evaluation of RE project. During this last decade, the MCDA methods have attracted the attention of decision makers due to its ability of providing solutions to increasing complex energy management problems. These methods are based on one of the three approaches:

- The top-down approach, seeks to aggregate the “n” criteria into a single criterion, it supposed that the judgment are transitive (ex: $a > b$ $b > c$ so $a > c$). It includes the AHP and ANP Method.
- The Bottom-up approach, tries to compare potential alternatives to each other and set up relationships between themes. It includes the ELECTRE and the PROMETHEE Method.
- The local aggregation which tries to find an ideal solution in the first step, then, proceeds to an iterative search to find a better solution. It includes the VIKOR and the TOPSIS Method.

This article first present the results of the comparative analyze. Second explain the new proposed multicriteria process. Finally an experiment simulation is conducted to demonstrate its effectiveness and feasibility of the real cases.

II. THE PROPOSED COMPARATIVE STUDY

This section includes three international and published studies that deal with the problem of selection of an optimal renewable energy project in various countries.

First Study was published on 2009 [2] and it covers the selection of a suitable wind farm in southern China. The proposed process is using the analytic hierarchy process (AHP) associated with benefits, opportunities, costs and risks (BOCR). The example treated in their paper was based on a set of 5 power plant namely A–E. To model the selection process, they have considered a set of 29 criteria based on technical, economic, financial and political risks. The scheme proposes the installation of 500 wind turbines, each with a generating capacity of 2.5MW, a hub height of 80 m and a blade diameter of 120 m (total height 140 m). **Second Study** was published on 2011 [3] and it considers the selecting of the best electrical generation technology based on the renewable energy sources in Spain. This study had used the VIKOR method to resolve the problem of selection. The decision making matrix process includes 7 criteria and a set of 13 evaluated projects. The designed systems will be evaluated according to the considered criteria: Power (P), Investment Ratio (IR), Implementation Period (IP), Operating Hours (OH), Useful Life (UL), Operation and Maintenance

Costs (O&M) and tons of emissions of CO₂ avoided per year (tCO₂/y).

Third Study was published on 2011 [4] and it considers the selecting of the best photovoltaic plant projects in Corsica Island of France. This study had used the ELECTRE IS method to resolve the problem of selection. The decision making matrix process includes 8 criteria and a set of 16 evaluated projects. The designed systems will be evaluated according to the considered criteria: Net production in (Gwh/yr), Rent area unoccupied by the installation (RA-EA/RA in ha), the potential of ecological degradation, the observer–plant minimum distance in (meter), Use conflicts risks , Economic activity and financial benefits to inhabitants from RES facilities, Financial income at the communal level (£/yr/inhab).

Table 1: The Criteria comparative list

Criteria Type	First Study criteria	Second Study Criteria	Third Study Criteria
Technical	<ul style="list-style-type: none"> – Energy availability: power, speed or irradiation, density. – Site advantage: height of installation... – Connection to Grid – Foundation: Peripheral construction... – Technical risk 	<ul style="list-style-type: none"> – Pr owe (P) – Operating Hours (OH) – Implementation Period (IP) 	<ul style="list-style-type: none"> – Net production – Rent area unoccupied by the installation
Technological	<ul style="list-style-type: none"> – Technical functions: power, capacity, technical availability... – Advanced technologies – Material design and manufacturing 	<ul style="list-style-type: none"> – Useful Life (UL) 	
Financial	<ul style="list-style-type: none"> – Financial scheme: switchable tariff, discount... 	<ul style="list-style-type: none"> – Operation and Maintenance Costs (O&M) – Investment Ratio (IR), 	<ul style="list-style-type: none"> – Economic activity and financial benefits to inhabitants – Financial income at the communal level
Environmental & Social	<ul style="list-style-type: none"> – Distance to specific area. – Policy support – Concept conflict: policy, makers... – Uncertainty of land 	<ul style="list-style-type: none"> – tons of emissions of CO₂ avoided per year (tCO₂/y) 	<ul style="list-style-type: none"> – the observer–plant minimum distance – the potential of ecological degradation – Use conflicts risks

According to the above comparative table, all used criteria could be split into four categories: Technical, Technological, Financial, Environmental and social. It also observed that all criteria have selectability or rejectability effect on the decision process. The improvement of an exhaustive and detail criterion, that could be used in the evaluation of various projects (wind, solar, geothermal or hydraulic resources) and in different locations would be very useful. These criteria could have the same impact on the process, for example the energy availability might include wind speed, solar irradiation or both in the case of hybrid resources Wind-Solar as [7].

III. THE PROPOSED NEW MULTICRITERIA APPROACH

According to previous review, the success on the building of any new renewable energy project is due to the follow of this ten steps: addressing site, obtaining zoning, obtaining environmental expertise, analyzing of the existing transmission lines, studying the securing access to land, measuring the renewable resource, establishing scenario to access to capitals, identifying reliable power purchaser or market, understanding the green energy’s policy and support. In fact the integrating of the life cycle concept allows a better understanding of the impact of the each criterion on the project. The figure1 proposes key steps needed in the design of a useful criterion, while figure 2 detailed a new criteria and sub criteria suitable for various renewable energy cases studies.

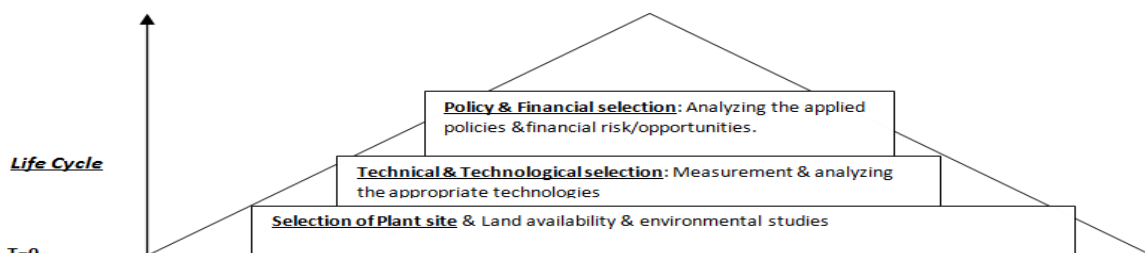


Figure 1: Proposed Renewable energy Life Cycle Project Analysis

According to the proposed new decision making process, once the studied projects are listed, the managing boards are asked to evaluate them according to the criteria & sub-criteria; these criteria are split into benefit/cost for the quantitative criterion and opportunity/risks for the qualitative criterion (see Figure 2).

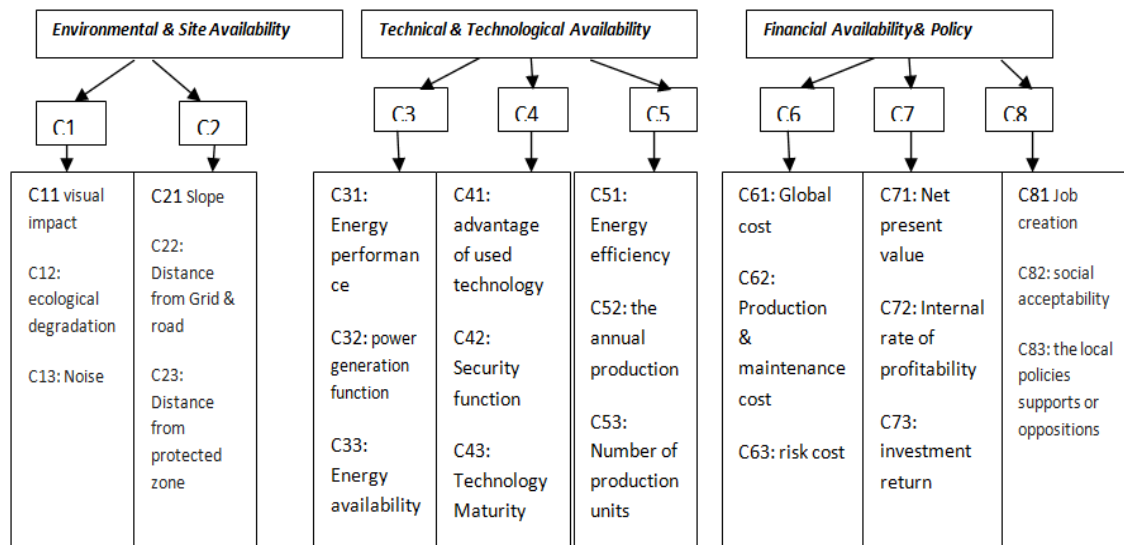


Figure 2: Proposed Global criteria and sub criteria

Finally this process proposes an aggregation of the well-known PROMETHEE II and the AHP method. This phase includes four steps (from the constitution of the decision matrix to the final ranking of alternatives).

- **Step 1:** Listing the criteria according to which the decision problem will be evaluated $C = \{c_1, \dots, c_m\}$ and splitting these Criteria into two categories: Select-ability criterions (Criteria to Maximize) and Reject-ability ones (Criteria to Minimize).
- **Step 2:** Establish a Normalized version of the initial decision matrix. The structure of the initial matrix can be expressed as follows listing of the alternatives $A = \{a_1, \dots, a_n\}$ evaluations for each criterion element.

$$Z = (z_{ij})_{n \times m} = \begin{matrix} A_1 \\ A_2 \\ \cdot \\ A_3 \end{matrix} \begin{bmatrix} z_{11} & z_{12} & \cdot & \cdot & z_{1m} \\ z_{21} & z_{22} & \cdot & \cdot & z_{2m} \\ \cdot & \cdot & \cdot & \cdot & \cdot \\ \cdot & \cdot & \cdot & \cdot & \cdot \\ z_{n1} & z_{n2} & \cdot & \cdot & z_{nm} \end{bmatrix} \quad (1)$$

The selectability criterion $\Omega_b: z_{ij} = \frac{a_{ij} - a_j^{min}}{a_j^{max} - a_j^{min}}$ (2)

The Rejectability criterion $\Omega_c: z_{ij} = \frac{a_j^{max} - a_{ij}}{a_j^{max} - a_j^{min}}$ (3)

Step 3: The “m” criteria in the same level are compared using 1-to-9 scale proposed in the AHP method, then the consistency ratio CR is calculated.

$$\sum w_j = 1 \text{ for } j = 1 \dots m \quad CR = CI/RI \text{ where } CI = (\lambda_{max} - n)/(n - 1) \quad (4)$$

- **Step 4:** The final ranking of alternative is calculated by applying the PROMETHEE II, this method use the net outranking flow to order alternatives:

$$\Phi(z) = \Phi^+(z) - \Phi^-(z) \quad (5)$$

While $\pi(a, b) = \sum_{j=1}^k P_j(a, b)w_j$ (6)

And $\Phi^+(z) = \frac{1}{n-1} \sum_{x \in A} \pi(z, x)$, $\Phi^-(z) = \frac{1}{n-1} \sum_{x \in A} \pi(x, z)$ (7)

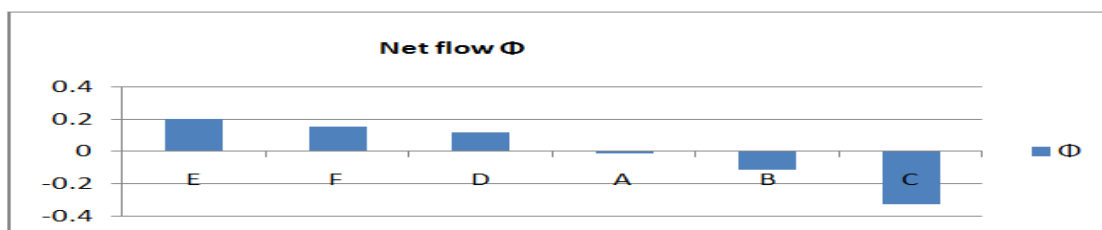
IV. THE NUMERICAL SIMULATION

Solar power plants have known considerable technological and industrial progress in recent years. These power plants use the sun’s radiation to produce electricity. Finding optimal scenario for future Concentrating Solar Power (CSP) plants is a crucial task in the early stage of project development. Therefore, this section is presenting a concentrated solar power (CSP) plant comparative study.

Table 2: The evaluated decision matrix

CRITERIA	E	F	A	B	C	D
C33: Energy availability	8	4	1	3	8	1
C32: The power generation function	4	3	4	9	1	9
C81: Job creation	1	9	8	1	1	6
C42: Security function	10	5	25	100	20	6
C83: the local policies supports or oppositions	100	120	18	30	40	50
C71 Net present value	1	9	8	4	3	6
C61: Global cost	1	3	6	8	9	1
C12 : ecological degradation	3	9	6	8	4	3
C82: social acceptability	1	3	4	9	1	9
C63: risk cost	3	9	6	8	4	3

In order to demonstrate the usefulness and efficiency of the use of the MCDM process in the real comparative studies, it was chosen to apply this study to the local construction of 6 solar complexes, A, B, C, D, E and F. The projects are evaluated according to ten sub criteria chosen from the proposed global criteria.

**Figure 3: Project's net flows ranking.**

According to the above results it can be concluded that the E project is the best one followed by F and D, while projects A, B and C are the worst ones. These results match the local CSP strategy, effectively, the first CSP projects were costly with a small power capacity, but during last years, and due to the maturity in technology and its widely use, the implanted CSP projects had became easier, cheaper and efficient. That exactly explains the better ranking of the (D, E & F) projects, which are considered by many experts as one of the most successful project around the world.

V. CONCLUSION

This paper had tried to present innovative approach to assist stakeholders in their decision making process, thought demonstration the usefulness of the MCDM theory. It had also presented a comparative study of a three decision making process, applied in different countries and applying each new MCDM method. The originality of this work is due to the proposed criteria/sub criteria and the process. One of the future works will be focused on the improvement of a new decision support system based on innovative MCDM approach, this tool will be a Web-DSS.

REFERENCES

- [1] R. Mari, L. Bottai, C. Busillo, F. Calastrini, B. Gozzini, G. Gualtieri, *A GIS-based interactive web decision support system for planning wind farms in Tuscany (Italy)*, Renewable Energy, 36 ,2011, 754-76.
- [2] A-H.I. Lee, H-H Chen, H-Y Kang, *Multi-criteria decision making on strategic selection of wind farms*, Renewable Energy, 2009, 34 120–126.
- [3] F. Cavallaro, *Multi-criteria decision aid to assess concentrated solar thermal technologies*, Renewable Energy, 2009, 34, 1678–1685.
- [4] Haurant P, Oberti P, Muselli M. *Multicriteria selection aiding related to photovoltaic plants on farming field on Corsica island: A real case study using the ELECTRE outranking framework*. Energy Policy, 39, 2011, 676–688.
- [5] P. A Beltrán, F Chaparro-González, J-P Pastor-Ferrando , A.Pla-Rubio, *An AHP (Analytic Hierarchy Process)/ANP (Analytic Network Process)-based multi-criteria decision approach for the selection of solar-thermal power plant investment projects*, 2014, 66, 222-238.
- [1] J-J Wang, Y-Y Jing, Ch-F Zhang, J-H Zhao. *Review on multi-criteria decision analysis aid in sustainable energy decision-making*, Renewable and Sustainable Energy Reviews, 13, 2009, 2263–2278.
- [2] H-H Chen , H-Y Kang, A-H.I. Lee, *Strategic selection of suitable projects for hybrid solar-wind power generation systems*, Renewable and Sustainable Energy Reviews 14, 2010, 413–421.

DEVELOPMENT OF NEW DIE FOR THE FORMING OF IMPELLER VANE AND THE INVESTIGATION OF PROCESS PARAMETERS INFLUENCING ITS PART QUALITY.

RAJESH.R¹, SARAVANAN.S²

¹(Assistant Professor, Production Engineering Department, PSG College of Technology, INDIA)

²(Associate Professor, Production Engineering Department, PSG College of Technology, INDIA)

ABSTRACT : Computer aided analysis provides optimum results to reduce the costly trial and error iterations. The component vane used in the impeller of stainless steel pump is obtained by two forming operations. The required profile is complex with the combination of five radii and is made of Stainless Steel 304. The forming of the partial shape of profile is done using the first die and then it is transferred to the second die to obtain the final shaped component. Thus, the lead time for the manufacture of vanes was observed to be high. In this work, an effort is made to design a die so that the required profile of component is obtained by a single operation. The die is modeled in PRO-E and analyzed using the DEFORM 3D software to reduce the trial and error iterations after manufacturing the die. Then the die is manufactured, checked whether it confirms to the simulation and spring back is observed which is not considered in simulation. Bio-degradable lubricants selected are sunflower, olive and castor oils. Taguchi L27 orthogonal array is employed to investigate the effect of oils along with load and dwell time as other variables. It is observed that the load, lubricant contributes most for the forming process and next is the Load and castor oil combination that influences the process.

Keywords - Impeller Vane, Stainless Steel 304, PRO-E, DEFORM 3D, Bio-degradable lubricants, Taguchi.

I. INTRODUCTION

Metal forming is a general term for a large group of sheet metal operations that includes drawing, bending and curling operations. In order to plastically deform a metal, a force is applied that must exceed the yield strength of the material. Bending refers to the operation of deforming a flat sheet around a straight axis where the neutral plane lies. Sheet forming processes generally is affected by several factors such as the shape of the die, the initial blank, the material property, friction, lubrication and so on. It is necessary to design forming processes, which can achieve specific product shapes without failures like fracture, wrinkling, surface unevenness and geometrical inaccuracies. Traditionally, the design of sheet metal products and processes is performed to a large extent by a trial-and-error approach. It is therefore unreliable, time and money consuming approach. Finite element analysis (FEA) is ideally suitable for precisely simulating the forming process taking into consideration the elasto-plastic behavior of the material, actual forming conditions such as contact and friction between the tools and the sheet.

In the field of metal forming simulation, because of the increasing people's needs, there are many mature commercial simulation software convenient for researchers using numerical simulation technique to study the industrial process. DEFORM is a finite element process simulation system to be applied for the analysis of metal forming and various forming process in related industries.

II. PROBLEM DEFINITION

In Indian pump industries, different varieties are produced and marketed. In that, phenomenal group of pumps are exported to foreign countries, mainly stainless steel pumps. In these pumps, the impeller vanes are manufactured by forming process. The profile used for these vanes is of complicate design that is combination of five radii. The metal profile used for making impellers is formed by two operations. In the first, the flat metal sheet is formed to semi circular shape (Fig 1), and then the semi circular shaped sheet is formed to required profile (Fig 2). So, efforts are made to manufacture a die that gives the required profile in single operation

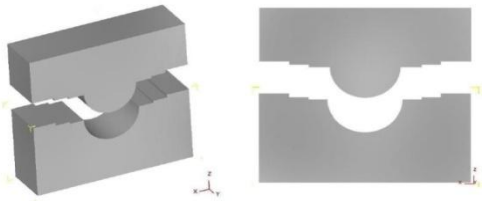


figure-1: First Forming Die.

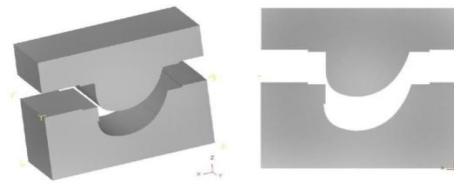


figure-2: Second Forming Die.

III. DESIGN AND MODELING OF NEW DIE

3.1. Freehand Sketching

Several designs are manually sketched and then are modeled in Pro-E. The importance of computer aided analysis is clearly understood in this stage. Here, four designs are sketched. These four designs are modeled and checked for the outcome using DEFORM 3D and fourth design seems to be satisfying. Without FEA simulation, trial and error runs should have been conducted for all the four designs which is time consuming and costly process.

3.2. Finite element model

By means of the CAD software of PRO-E, the finite element models of the forming pair and workpiece is modeled and were set according to their actual dimensions, they could be then used in DEFORM-3D simulation. In order to simplify and reduce the running time during the simulation, the upper and lower anvils were suggested as the rigid ones. Workpiece in Fig-3 is made of Stainless steel grade 304 with thickness of 1.5 ± 0.025 mm and its material properties are mentioned in Table 1.

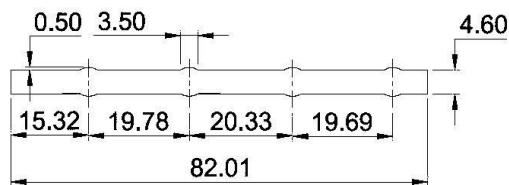


figure-3 : Workpiece

Table 1 Material Properties of SS304

Density	8 gm/cc
Ultimate Tensile strength	505Mpa
Yield Strength	215Mpa
Elastic Modulus	193-200Gpa
Poisson's Ratio	0.29

3.3. Simulation control of the forming process

In the current simulation, the coordinates system was set as that the perpendicular direction as the z-axis and the other two as the x-axis and y-axis, respectively.

- (1) During the forming process, the upper die, which is the main module, with a given speed and load moves along the negative z-axis, and the workpiece was placed on the still lower die.
- (2) Tetrahedral mesh is used to mesh the object and the punch load is given as 1.5 tons.
- (3) The friction coefficient between the dies and workpiece is given as 0.12, which is a preset for cold forming dies.
- (4) Suitable stopping criterion for the top die is assigned and step increment is assigned.
- (5) Simulation is submitted and monitored in frequent intervals.

3.4. Results of DEFORM Simulation

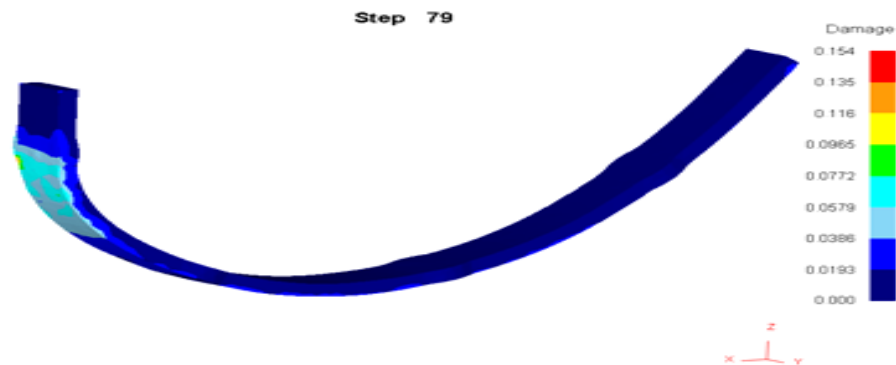


figure 4: Damage in final component

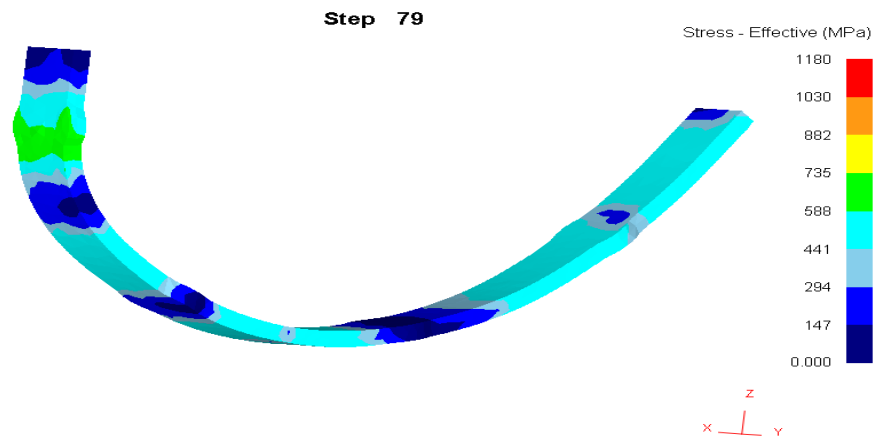


figure 5: Effective stress variations in final component

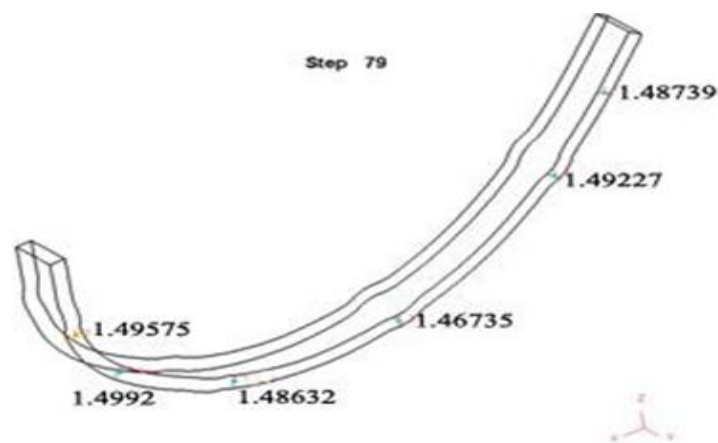


figure 6 : Variation of thickness in final component

Lesser is the damage, lesser is the chances to fracture. Damage in this case is shown in Fig 4.. It is inferred from Fig 5 that slightly higher stresses were seen in the profile indicated by green color. It cannot be eliminated because of the complex shape of the profile .The variation in thickness is indicated in Fig 6 and it is less than the permitted value of 10% change in thickness.

IV. MANUFACTURING OF DIE

The die is made up of tool steel of grade AISI D2. The die is cut form a single block using Wire EDM and the required holes are made for fasteners and threading is done. Then the die is hardened by the method of vacuum hardening. In the method of vacuum heat treatment, the die is heated gradually to 850°C in three stages of 10 minutes each. Then the die is heated to temperature of 1030°C where it hardens. Later it is to be tempered in three levels since heat treatment induces small changes in the dimensions of the die. During tempering, it is heated for 200°C two times for 240minutes and it is heated at 250°C for 240 minutes which makes the die to obtain its initial dimension and also to obtain the required HRC of 59-60.

V. DESIGN OF EXPERIMENTS

The operating variables selected in this experiment are Punch Load, Dwell Time and Lubricant used. L27 full factorial array is chosen with three operating variables at 3 levels. Punch load ranges are of 1.5, 2 and 2.5Tons. Dwell time varies from 1, 2 and 3 seconds. Due to important health, economic, and environmental issues, significant efforts are being made to develop and implement manufacturing lubricants that come from natural resources. Lubrication is selected based on the previous researches as Sunflower, Olive and Castor oils.

5.1. Experimentation

Die is placed in the hydraulic press as shown in the Fig 7. Different types of oils used are shown in Fig 8.

5.2. Experimental Analysis

Experimental results for the forming process are shown in the Table 2 and the response factor considered is the amount of spring back. The workpiece obtained by experimental process is placed on the ideal shape of the required component that is printed on the graph sheet as shown in Fig 9 and then using bevel protractor, the deviation from actual and the original is observed as shown Fig 10. For the impeller vane, outlet angle is most important than inlet angle. As the variation in inlet angle does not vary significantly, only outlet or exit angle is observed to record the amount of spring back in terms of degrees.



figure 7:Die Fixed in hydraulic press



figure 8- Lubricants

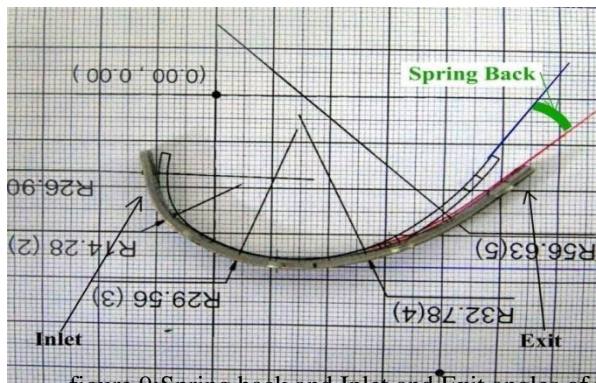


figure 9:Spring back and Inlet and Exit angles of vane



figure 10-Measurement of spring back using bevel protractor

Table 2- Experimental Table

S. No	LOAD	DWELL TIME	LUBRICANT	SPRINGBACK (Degrees)
1	1.5	1	SUNFLOWER	16.5
2	1.5	1	OLIVE	15.99666667
3	1.5	1	CASTOR	14.97
4	1.5	2	SUNFLOWER	15.85666667
5	1.5	2	OLIVE	16.02333333
6	1.5	2	CASTOR	15.16333333
7	1.5	3	SUNFLOWER	17.10666667
8	1.5	3	OLIVE	15.46666667
9	1.5	3	CASTOR	14.52333333

10	2	1	SUNFLOWER	15.85666667
11	2	1	OLIVE	16.72
12	2	1	CASTOR	15.33
13	2	2	SUNFLOWER	15.27333333
14	2	2	OLIVE	16.69333333
15	2	2	CASTOR	15.33
16	2	3	SUNFLOWER	15.69333333

5.3.Calculation of S/N ratio

The S/N ratio using the smaller the better characteristics by Taguchi Method (Minitab Software) is calculated using “equation 1” and shown in Table 3.

$$S/N = -10 * \log (\Sigma (1/Y^2)/n) \dots \dots \dots (1)$$

Table 3- S/N ratio values

S. No	SPRINGBACK	S/N Ratio
1	16.5	-24.34967888
2	15.99666667	-24.0805899
3	14.97	-23.50443601
4	15.85666667	-24.00423793
5	16.02333333	-24.09505735
6	15.16333333	-23.61589364
7	17.10666667	-24.66330786
8	15.46666667	-23.78793452
9	14.52333333	-23.2413261
10	15.85666667	-24.00423793
11	16.72	-24.46472546
12	15.33	-23.7108431
13	15.27333333	-23.6786766
14	16.69333333	-24.45086131
15	15.33	-23.7108431
16	15.69333333	-23.91430399
17	15.38666667	-23.74289091
18	13.88333333	-22.84987502
19	15.10666667	-23.58337293
20	13.13666667	-22.3697036
21	14.36	- 23.1430888
22	14.72	-23.3581562
23	15.49666667	-23.80476583
24	14.69333333	-23.34240662
25	14.22	-23.05799193
26	14.85666667	-23.43842759

VI. RESULTS AND DISCUSSION

From the experiments it is understood that the amount of spring back is less as the load acting on it increases. Load and Lubrication have more prominent effect on the amount of spring back and Dwell time has least effect on the spring back. Interaction between Load and Lubricant has also major impact on the forming process compared to other interactions. From the plots for S/N ratios, a combination of 2.5 Tons of load, 3 seconds of dwell time and Castor oil as lubricant gives the minimum amount of spring back and hence it is considered as optimum combination.

The results of ANOVA Table 4 that indicate that load is the most significant factor in affecting the spring back, followed by Lubricant used and combination of both also has major influence on spring back. Taguchi uses Signal to Noise (S/N) ratio in order to interpret the trial results data into values for the evaluation of characteristics in the optimum setting analysis. This is because the S/N ratios can reflect both the average and the variations of the quality characteristics. The main effect plot for S/N ratios is plotted between forming parameters and spring back value as shown in Fig 11.

Variable	Level			DOF	Sum of Squares	Mean Sum of Squares	F	%
	1	2	3					
Load	1.5	1	Sunflower	2	2.4968	1.2484	10.46	34.613838
Dwell Time	2	2	Olive	2	0.2979	0.149	1.25	4.1298712
Lubricant	2.5	3	Castor	2	1.3343	0.6672	5.59	18.497774
Load*Dwell Time				4	0.5779	0.1445	1.21	8.0115897
Load*Lubricant				4	0.8496	0.2124	1.78	11.778242
Dwell Time*Lubricant				4	0.7022	0.1755	1.47	9.7347954
Residual Error				8	0.9546	0.1193		13.233887
Total				26	7.2133			100

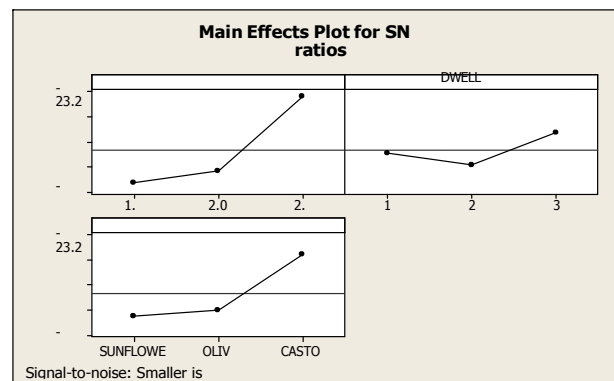


Fig.11 S/N Ratio plots for Spring back

VII. CONCLUSION

1. The simulation and experimental process is found to be in good agreement and required shape of the profile is obtained.
2. Spring back is observe, which is not considered in simulation.
3. The damage seen in simulation can be observed as scratches on the side of the specimen and excessive effective stress seen in simulation is observed as the dent on the side of the workpiece.
4. Punch load and lubricants collectively influence the spring back.

Bio-degradable lubricants can be used effectively as industrial lubricants and castor oil exhibits better lubricant as the extent of damage is very less when this is used as observed by examining the specimens.

REFERENCES

Journal Papers:

- [1] Sung-Bo Sima, Sung-Taeg Lee, Chan-Ho Jang, "A study on the development of center carrier type progressive die for U-bending part process," *Journal of material processing technology*, 2004, 1005-1010.
- [2] L.C. Sousa, C.F. Castro, C.A.C. Antonio, "Optimal design of V and U bending processes using genetic algorithms," *Journal of material processing technology*, 172, 2006, 35-41.
- [3] Sutasn Thipprakmas, Wiriyakorn Phanitwong, "Process parameter design of spring-back and spring-go in V-bending process using Taguchi technique," *Materials and design journal*, 32, 2011, 4430-4436.
- [4] M. El Sherbiny et al., "Thinning and residual stresses of sheet metal in the deep drawing process," *Materials and design journal* 55, 2015, 869-879, 2015.
- [5] A C S Reddy et al., "An experimental study on effect of process parameters in deep drawing using Taguchi technique," *International Journal of Engineering, Science and Technology*, 7(1), 21-32, 2015
- [6] Lovel M, "Increasing formability in sheet metal stamping operations using environment friendly lubricants," *Journal of Material Processing Technology*, 177, 2006, 87-90.
- [7] Salete Martins A, "Development of new cutting fluid for grinding process adjusting mechanical performance and environmental impact," *Journal of Material Processing Technology*, 179, 2006, 185-189.
- [8] Carcel AX, "Evaluation of vegetable oils as pre lube oils for stamping," *Material Design Journal*, 26, 2005, 587-593.

Books:

- [9] Deform 3D, v6.1, user guide.
- [10] Paquin J R and Vukota Boljanovic, *Die Design Fundamental*, (3rd ed., Industrial Press, New York, 2006)

Analysis of Dynamic Road Traffic Congestion Control (DRTCC) Techniques

Pardeep Mittal¹, Yashpal Singh², Yogesh Sharma³

¹Ph.D Research Scholar, JNU Jodhpur; Faculty of EEE department, Lovely Professional University, India.

²Director, SITM Rewari, India

³Professor, Jodhpur National University, Jodhpur, India

ABSTRACT : Dynamic traffic light control at intersection has become one of the most active research areas to develop the Dynamic transportation systems (ITS). Due to the consistent growth in urbanization and traffic congestion, such a system was required which can control the timings of traffic lights dynamically with accurate measurement of traffic on the road. In this paper, analysis of all the techniques that has been developed to automate the traffic lights has been done.. The efficacy of all the techniques has been evaluated, using MATLAB software. After comparison of artificial intelligent techniques , it is found that image mosaicking technique is quite effective (in terms of improving moving time and reducing waiting time) for the control of the traffic signals to control congestion on the road.

Keywords - Static and dynamic feedback control, optimal control, Neural network, fuzzy expert system, PSO,GA, Image processing and mosaicking, traffic lights.

I. INTRODUCTION

Traffic congestion is now considered to be one of the biggest problems in the urban environments. With increasing traffic on major roads controlled by traffic signals, many problems have become common. In most urbanized settings worldwide, drivers have become accustomed to undesirable congestion and excessive delay. Traffic congestion is considered to be one of the prominent issues that need attention. Traffic control and management experts and policy makers have come up with many possible solutions to solve the traffic congestion problem. Some of these solutions focused either on increasing the number of roads or lanes to cope with the demand or on limiting the traffic demand by levying tolls and raising taxes for using the system. Also, due to political concerns and feasibility constraints, both of these options did not offer a promising solution. Another solution is to use the current system in a more efficient way. This option offers high benefits and potential both on the short term and the long term. The increasing number of traffic jams, the rise in the health and environmental effects of the vehicular emissions, and the increasing fuel prices are other dimensions of the challenges of vehicular mobility in most developed countries. As a result, it has become apparent that multi-objective transportation control and management systems should be developed to address the multifaceted traffic problems. One of the well accepted and promising solutions is the use of Dynamic transportation systems. In this regard, this thesis contributes its share to improve the freeway traffic mobility by considering both environmental (emissions and dispersion of emissions) and economic concerns (travel time and energy consumption) of different stakeholders. In addition, many studies and statistics were generated in developing countries that proved that most of the road accidents are because of the very narrow roads and because of the destructive increase in the transportation means [1].

II. CONTROL DESIGN STRATEGIES

In the literature different control methodologies have been presented for controlling and managing a traffic network in which vehicles are driven by humans [2, 3]. In this section, we will discuss the control design methodologies for freeway traffic control that are currently most often used in practice such as :

2.1 FIXED CONTROL

Fixed Control is open loop control system which uses a preset cycle time to change the light. Based on the past data at that particular intersection, once the timings for RAG light has been set, controller makes On/Off the lights according to that. This type of control is easy to implement and cost is low. In an open loop control system the output is neither measured nor fed back for comparison with input. Faithfulness of an open loop control system depends on accuracy of input calibration. Fig. 2.1 shows the fixed control of traffic control.



Fig.2.1 Fixed Control System

2.2 STATIC FEEDBACK CONTROL

In static feedback control methods, the controller gets measurements from the system and determines control actions based on the current state of the system in such a way that the performance of the system is improved. The main examples of static feedback controllers are state feedback controllers (where the feedback gain can be computed using, e.g., pole placement) and PID controllers (for which several tuning rules exist,

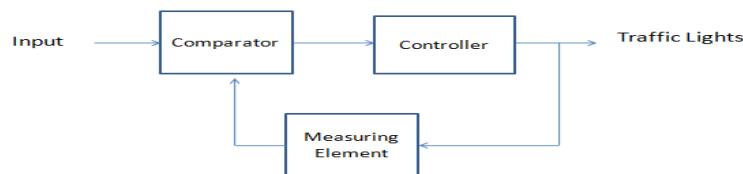


Fig. 2.2 Static feedback control

such as the Ziegler-Nichols rules) [4]. However, the static feedback strategy in general does not handle any external constraints. This is a major drawback of this control scheme. Here statics mean that the control parameters of the feedback controller are taken to be fixed.

2.3 OPTIMAL AND MODEL PREDICTIVE CONTROL

Two dynamic control methods that apply optimization algorithms to determine optimal control actions based on real-time measurements: optimal control and model predictive control. Dynamic traffic control methods continuously measure the state of the traffic network and respond accordingly. Dynamic traffic control methods can either be non-predictive or predictive [5,6]. Since traffic systems are highly non-linear and time-variant systems, model-based predictive traffic control approaches [7, 6] such as Model Predictive Control (MPC) are promising candidates. MPC is a model-based control approach that is based on the optimization of control inputs that improve a given performance criterion (objective function) over some prediction horizon. The performance criterion of MPC is formulated as a cost function of the predicted system states, outputs, or inputs. The MPC approach can be used for non-linear and time variant systems. In addition, it can incorporate constraints on the inputs, states, and outputs of the system. The MPC controller is demonstrated in two simulation-based case studies for a balanced reduction of travel time, emissions, fuel consumption, and dispersion of emissions.

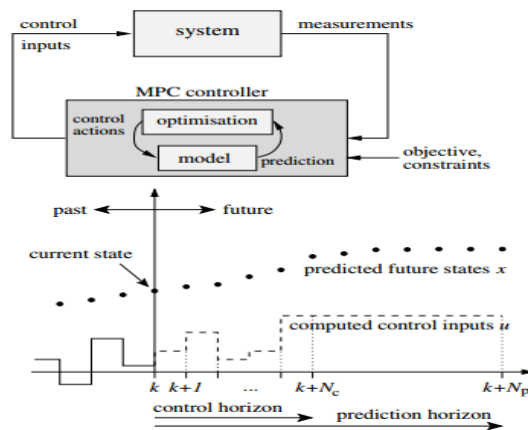


Fig. 2.3 Optimal and model predictive control

Table 2.1 Comparison between different Control strategies

Control method	Computational complexity	Constraints	Future inputs	Model based	scalability
Fixed Control	low	No	No	No	Localized
Static feedback control	Medium	No	Sometimes	Yes	Localized
MPC	High	yes	Yes	Yes	System-wide

Figure 2.3 shows the optimal and model predictive control strategy and Table 2.1 shows the comparison between different control strategies. The main advantages of MPC are that it takes the effect of the control inputs on the future system states, that it is able to take both equality and inequality non-linear constraints of the manipulated and controlled variables into account, and that it can be used for non-linear systems. Moreover, MPC can handle several process models as well as many performance criteria of significance to the system [7].MPC, and in particular, MPC for non-linear systems also has certain disadvantages. The main disadvantage of MPC for non-linear systems emanates from the non-linear and non-convex optimization problem involved. Such optimization problems do not only pose difficulty in computing optimal solutions, but also the computation time involved to get the optimal solutions may become very high. Usually, the computation time exponentially increases as the number of control inputs (optimization variables) or the prediction horizon increase.

III. TECHNIQUES FOR DRTCC

Artificial Intelligence (AI) techniques aim at enabling intelligence in machines to solve a problem using human intelligence and thinking. By human intelligence, we mean that the ability of computer programs to perceive a situation, to reason about the problem, and to act accordingly. AI techniques are mainly used in decision support systems, and one way to classify them is as follows:

3.1 ARTIFICIAL NEURAL NETWORK APPROACH

The adaptive traffic light problem was modeled using the ANN approach. The Researchers M.Patel and N. Ranganathan [8] created an ANN model which included predicting the traffic parameters for the next time frame and computing the cycle- time adjustment values. This model consisted of nine inputs (one of each past and present traffic parameters one hidden layers with 70 hidden nodes and three output nodes. The ANN model, if drawn a sketch, would like the figure shown below. The input given to the ANN models are the list of data collected by the sensors which are placed around the traffic lights. The sensors give the traffic light ANN model all the data

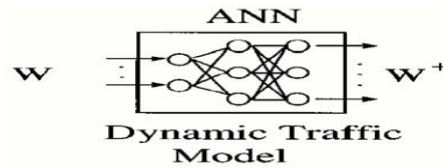


Fig. 3.1 Artificial neural network approach

The model after getting the input used the hidden layer to decide which nodes suits the current traffic situation. Each hidden nodes is given a membership function (i.e. between 0 and 1). After comparing the nodes and matching it with the current form of membership functions ranging from 0 to 1. Alternatives are selected as the output is then used by the traffic lights to set the timing for the red and green lights. The output of the ANN model will be in the form of membership functions ranging from 0 to 1.

3.2 GENETIC ALGORITHM APPROACH

Genetic algorithm [9] method proposes the use of technology to count the vehicle numbers by video image detection system. Then discusses the implementation of the genetic algorithm, and offers some suggestions intended to improve the efficiency of the system and to determine the vehicle numbers and the estimated number of people in the region by mobile cell location; where the system can makes changes in real time to avoid congestion wherever possible. The other application of the system can detect abnormal situations like car accidents, and the level of congestion. The system is based on a genetic algorithm that receives inputs from the video image detection system which will make a decision and determines the greens light time to minimize the congestions and flow of traffic jam. proposed system may compose of many technologies such as: Video Image Detection Systems, Vehicular Ad Hoc Networks and Mobile phone tracking, and Global Position System (GPS). Using these technologies with artificial intelligence could be creating an Dynamic traffic light that take a decision of green lights time by itself.

3.3 FUZZY EXPERT SYSTEM APPROACH

Fuzzy expert system [10] was used to control the traffic light in most cities. It was the most common system used in major areas. The fuzzy expert system composed of seven elements i.e. a radio frequency identification reader (RFID), an active RFID tag, a personal digital assistance (PDA), a wireless network, a database, a knowledge base and a backend server. In this system, the RFID reader detects a RF-ACTIVE code at 1024 MHz from the active tag pasted on the car. The active tag has a battery, which is inbuilt inside it, so that it can periodically and actively transmit messages stored in the tag. As soon as the data is received, the reader will save all information in the PDA. When the PDA accumulates the required amount of data, it will use its wireless card and connect to the backend server and store them in to the database in server.

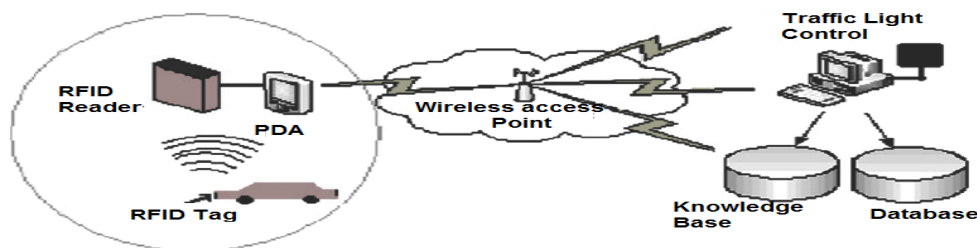


Fig. 3.2 Fuzzy Expert System

Now the server uses the data stored in the database to calculate maximum flow, interarrival time and average car speed. When all possible congestion roads and car speed are collected, then these data would be used as the input parameters of the traffic light control simulation model in the server. After getting the simulation results, the system is able to automatically give different alternatives in terms of varieties of traffic situations and then the red light or green light duration is being set via a traffic light control interface for improving the traffic congestion

problems. All the rules and reasoning are used in the IF-THEN approach, starting from a basic idea and then tries to draw conclusions format. The system is using the forward chaining approach, which is a data driven approach, starting from a basic idea and then tries to draw conclusions.

3.4 SWARM INTELLIGENCE APPRAOCH (PSO)

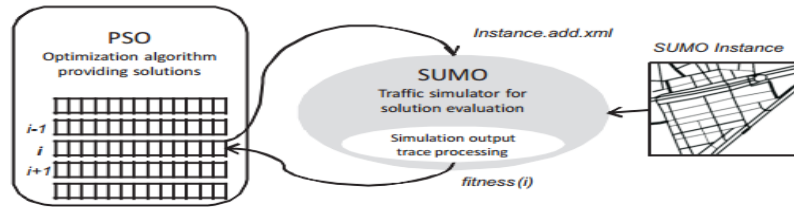


Fig. 3.3 Particle swarm optimization algorithm

When PSO [11] generates a new solution it is immediately used to update the cycle program. Then, SUMO is started, to simulate the scenario instance with streets, directions, obstacles, traffic lights, vehicles, speeds, routes, etc., under the new defined staging of the cycle programs. After the simulation, SUMO returns the global information necessary to compute the fitness function. Each solution evaluation requires only one simulation procedure since vehicle routes in SUMO are generated deterministically. In fact stochastic traffic simulators obtain similar results to deterministic ones, the latter allowing huge computing savings. In addition, we must note that each new cycle program is statically loaded for each simulation procedure. In his technique dynamically generate cycle programs during an isolated simulation as is done in agent-based algorithms has been presented which is used to obtain the optimized cycle programs for a given scenario and timetable. In fact real traffic light schedulers actually demand are constant cycle programs for specific areas and for pre-established time periods (rush hours, nocturne periods, etc.), which led them to take this approach.

3.5 HYBRID APPROACH OF FES AND ANN (IDUTC)

IDUTC [8] is a real time Dynamic decision making system that computes decisions within a dynamically changing application environment. The IDUTC model consists of seven elements. The names of the element are as follows.

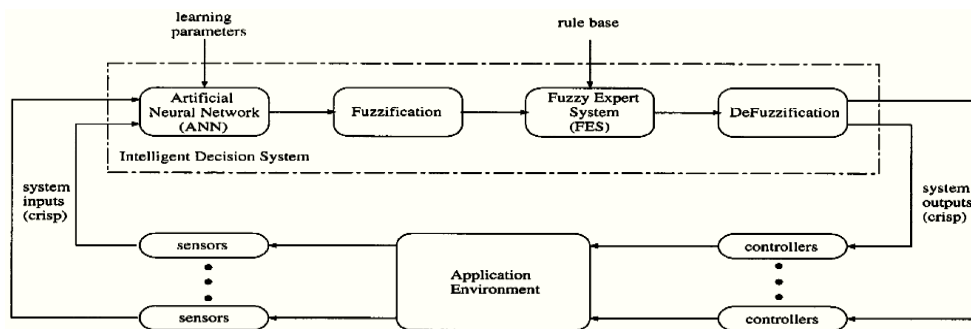


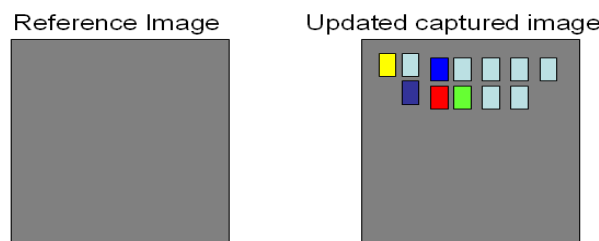
Figure 3.4 IDUTC system

- Artificial Neural Network (ANN).
- Fuzzification element
- Fuzzy expert systems (FES)
- Defuzzification Element.
- Application environment
- Controllers.
- Sensors

The architecture of the IDUTC is shown above. The system is placed at the road to sense the different parameters of the traffic conditions. The sensors are the actual input of the IDUTC model. Sensors collect the past data of the traffic conditions, which is all known as the application environments shown in the figure above. After the surrounding environmental The IDUTC is a self adjusting traffic light control system. The sensor of the ANN model collects all the data from the systems and processes it through the hidden layers and gives the desired output. Now the output of ANN model are is self-adjusting according to the situation of a domain. Then the fuzzy expert system fires the rules based on these fuzzy values. The De-fuzziification unit converts the computed decisions into crisp values that are used to control the environment through the controllers installed at the traffic lights. After running the simulation on the traffic light, past data are being collected along with the present data by the sensors.

3.6 IMAGE PROCESSING APPROACH

This approach [12] is based on the principle of matching area between reference image and updated image and this matching can be easily calculated by formula given below. The total area is the range of camera focused on the road. Reference image is black empty road image and updated image is capture when red light is on. In updated image the area covered by vehicles will reduce the area of empty road. After covering the area by vehicles rest of empty area will be compare with reference image which is already a empty road image. Thus after measuring the matching % between two images we can set the timing of RGY lights. Fig.3.5 shows the basic principle of the proposed scheme.



$$matched_area(in\ percentage) = \frac{matched_area}{total_area} \times 100$$

Fig. 3.5 Image Matching Approach

In the image matching approach, one camera is installed alongside the traffic light, which will capture image sequences. An image of the road with no traffic is captured and converted into grey level, then this image is enhanced to signify signal to appear more than the noise and to also accentuate the image features. This enhancement was implemented using Gamma- correction [13,14]. After the enhancement is done, edges are detected in the enhanced image to remove irrelevant data with preserving the important structure of the image. This can be done using Perwitt edge detection operator [13] or using canny edge detection [14]. After edge detection procedure, both reference image and other different images are captured at different time intervals are matched. The traffic light is then to be controlled based on the percentage of matching. In image matching, all edges in one image are compared to all edges in the other image. Accuracy of this approach is highly affected by the changes in illumination and weather conditions. Furthermore, it does not take stationary vehicles into consideration. The vehicles may be moving fast on one side having matching percentage between 50% and 70% and at the other side of intersection, the matching percentage is also between 50% and 70%, but they are completely stationary.

3.7 IMAGE MOSAICKING APPROACH

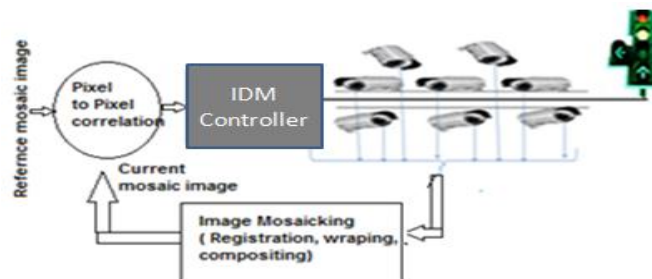


Fig.3.6 Functional block diagram of DRTCCS with MSVS

Figure 4.2 shows the components of DRTCC with multiple stable vision sensors (cameras). In this framework multiple cameras has been installed only for accurate measurement of density so that exact gap between the vehicles may be measured. One stable camera is not capable of measuring accurate density as it suffers from some installation problems (orientation adjustment). After processing the images taken from various angles, Image mosaic system gives the feedback to pixel to pixel correlation type error detector where it is compared with reference updated image. According the matching pattern of pixels, IDMC varies the timings or R-G lights.

IV. RESULT COMPARISON OF DRTCC TECHNIQUES

After closely reading the techniques for DRTCC, we could conclude that the IDUTC system provided decisions that relieve intersection congestion better than the ANN approach and was comparable to the FES approach. The ANN approach required more neural network nodes than the ANN in IDUTC, which led to slower training and higher implementation

Table 4.1 Comparative study on IDUTC, ANN and FES

System	Correct decision rate	Average wait time (m)	Number of nodes	Number of rules
IDUTC	95%	2.186	55	40
ANN	73%	2.958	83	-
FES	95%	2.975	-	40

cost. The FES system leads to correct decisions but didn't reduce time for waiting as compared to IDUTC. The IDUTC uses the current and past values or data to compute decisions, but the FES uses only current traffic flows. As shown in Table 4.1 best correct decision rate, average wait time is taken by IDUTC system. In GAs, chromosomes share information with each other. So the whole population moves like a one group towards an optimal area. In PSO, only best gives out the information to others. It is a one-way information sharing mechanism. The evolution only looks for the best solution. Compared with GA, all the particles tend to converge to the best solution quickly even in the local version in most cases. The PSO and GA provides the better decision making for optimizing the timings of lights also it takes less time to take decision but hard to implement such a method in real life applications. In image processing/matching approach better decision may be achieved in short time and can be implemented in real life but problem is that a single camera cannot measure the accurate density on road as gap between two vehicles cannot be identified with single camera. After comparing these techniques we could conclude that image processing based automatic traffic light system is best decision making system for Dynamic transportation system among all the techniques.

To compare proposed technique with conventional techniques, an experiment has been performed on one vehicle. One of the vehicles is allowed to go to in W-E direction at 40Km/hr on AimSun test bed. Total time of 450 seconds has been given to vehicle to cover the distance. Randomly traffic density is applied on road in three difference situations (heavy traffic, moderate traffic and low traffic) to check the performance. The same conditions have been applied to IDUCT, FES, ANN techniques to check their performances. After simulate the experiment, it is found that vehicle when adopts dynamic road traffic management system (DRTMS) covers 4.6Km distance in specified time period whereas distance covered by vehicle using techniques IDUCT,FES and ANN is 4.3Km, 3.9Km and 3.6Km respectively when traffic is high as shown in figure 4.1. Here A is source and B is the destination whereas AO indicates the moving time of vehicle under test, OP indicates average waiting time with DRTCCS, OQ indicates average waiting time with IDUCT, OR indicates average waiting time with FES, OS indicates average waiting time with ANN and time taken by vehicle from P to B, Q to B, R to B and S to B indicates again average moving time. And OP is the time taken by DRTCCS to make the decision as plus waiting time after measuring the density.

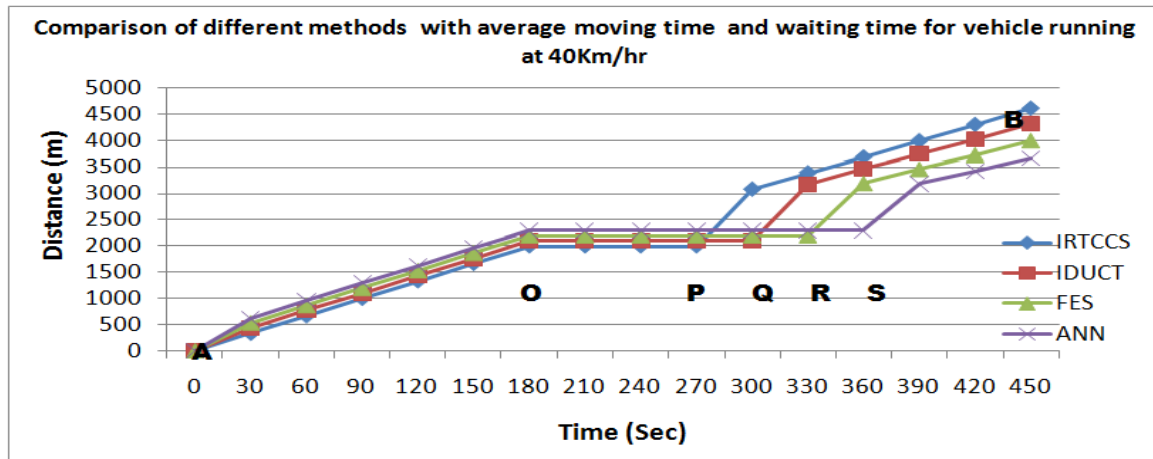


Fig.4.1 Comparison chart for DRTCC techniques

V. CONCLUSIONS AND FUTURE WORK

Problems were identified with current traffic control system. Beside, to analysis and design of new and effective system to solve the existing problems, an innovative algorithm is proposed in this research for arterial performance measurement by tracing the traffic density on road. An interesting property of the proposed model is that travel time estimation errors can be self-corrected with the signal status data, because the matching differences between a current image and updated image decides the timings of traffic lights. The efficacy of proposed method has been evaluated, using MATLAB, JAVA and LabVIEW software. The research study shows that the proposed algorithm can do better decision making to manipulate the timings of RAG lights. After comparison of proposed framework with conventional techniques, it is found that proposed method is quite effective (in terms of improving moving time and reducing waiting time) for the control of the traffic signals for controlling congestion on the road. We believe that this represents our initiative in development of low-cost, deployable strategies for alleviating congestion in developing regions. Based on the accurate dynamic traffic density measurement on road, Dynamic technique to manage the traffic lights has been developed for the purpose of maximizing traffic throughput and minimizing average waiting time at an intersection.

Some artificial Dynamic techniques like Fuzzy logic, FES, GA, PSO, ANN etc may be developed with image mosaicking for better decision making in short time on the basis of measurement of accurate density.

REFERENCES

- [1] Vasconcellos, E., "Traffic Accident Risks in Developing Countries: Su-presiding Biased Approaches," ICTCT workshop, pp. 04611-003, 2005.
- [2] C. F. Daganzo. Fundamentals of Transportation and Traffic Operations. Pergamon Press, 1997
- [3] P. Kachroo and K. Özbay. Feedback Control Theory for Dynamic Traffic Assignment., Advances in Industrial Control. Springer-Verlag, Berlin, 1999
- [4] K. J.Åström and B. Wittenmark. Computer-Controlled Systems — Theory and Applications. Prentice-Hall, Upper Saddle River, New Jersey, 3rd edition, 1997.
- [5] R. Bishop. Intelligent Vehicles Technology and Trends. Artech House, 2005.
- [6] A. Hsu, F. Eskafi, S. Sachs, and P. Varaiya. Design of platoon maneuver protocols for IVHS. Technical Report 96-21, University of California, Berkeley, California, 1991.
- [7] L. D. Baskar, B. De Schutter, and H. Hellendoorn. Dynamic speed limits and onramp metering for IVHS using model predictive control. In Proceedings of the 11th International IEEE Conference on Intelligent Transportation Systems, pages 174– 179, Beijing, China, October 2008.
- [8] M. Patel, N. Ranganathan, "An Intelligent Decision-Making System for Urban Traffic Control," IEEE Transactions-Vehicular Technology, vol.50 (3):816-829, May 2001.
- [9] Suhail M.Odeh, Management of An Intelligent Traffic Light System by Using Genetic Algorithm, Journal of Image and Graphics Vol. 1, No. 2, June 2013
- [10] W. Wen, "A dynamic and automatic traffic light control expert system for solving the road congestion problem," Expert Systems with Applications, Volume 34, Issue 4, May 2008, Pages 2370-2381
- [11] J. Garcia, E. Alba and A. Carolina Olivera, Swarm intelligence for traffic light scheduling: Application to real urban areas. Engineering Applications of Artificial Intelligence(ELSEVIER), 25, pp.274-283, 2012
- [12] P.Mittal and Y.P Singh, Design & Implementation of Image and Vision Computing based Intelligent Traffic Congestion Control Scheme (ITCCS), International Journal of IT, Engineering and Applied Sciences Research (IJIEASR), Volume 2, No. 5, May 2013
- [13] Choudekar, P., Banerjee, S. and Muju, M.K., Implementation of image processing in real time traffic light control, International Conference on Electronics Computer Technology, v.2, pp.94 -98, 2011.
- [14] Sanchi, S., Real time Traffic light control and Congestion avoidance system, International Journal of Engineering Research and Applications (IJERA) , Vol.2, pp. 925-929, 2012.

Analysis The Electrical Properties of Co, TiO₂ and Co/TiO₂ Multilayer Thin Films of Different Thickness Deposited by E-Beam Technique.

Md. Faruk Hossain¹, Md. Abdullah Al Asad², Md. Omar Faruk³, Dr. Md. Ariful Islam Nahid⁴

¹(Department of Applied Physics & Electronic Engineering, University of Rajshahi, Rajshahi, Bangladesh)

²(Department of Applied Physics, Electronics and Communication Engineering, Bangabandhu Sheikh Mujibur Rahman Science & Technology University, Bangladesh)

³(Department of Information and Communication Engineering, Pabna University of Science and Technology, Bangladesh)

⁴(Department of Applied Physics & Electronic Engineering, Rajshahi University, Bangladesh)

ABSTRACT : This paper presents the fabrication of the Co doped TiO₂ film for studying the electrical properties. In this case, at first Co/TiO₂ multilayer films were prepared by e-beam evaporation in a vacuum better than 10⁻⁵ Torr. The electrical properties of the deposited Co, TiO₂, Co/TiO₂ films had been studied. The surface morphology had been studied by Atomic Force Microscopy. In the multilayer, the thickness of Co and TiO₂ was kept same. Each layer thickness was varied from 5nm to 15 nm and repeated three times. The deposition rate of the Co and TiO₂ thin films are about 1.33 nm/sec & 1.25 nm/sec respectively. Electrical conductivity for the deposited Co, TiO₂ and Co/TiO₂ multilayer thin films had been measured as a function of temperature ranging from 300K to 470K. The deposited Co thin film, conductivity is of the order of 10⁶(Ω-m)⁻¹ that decreases with increasing temperature and the value for deposited TiO₂ and Co/TiO₂ multilayer thin films is of the order of 10²(Ω-m)⁻¹ and 10⁵(Ω-m)⁻¹ respectively. Again, the conductivity of the deposited TiO₂ thin films decreases with film thickness where in the case of as deposited Co, Co/ TiO₂ multilayer thin films increases with increasing film thickness. The sheet resistance of the as deposited Co thin films increases with increasing temperature which is to be the order of 10² Ω/sheet. It is found that the sheet resistance of the as deposited TiO₂ and Co/TiO₂ multilayer thin films to be the order of 10⁷ Ω/sheet and 10² Ω/sheet respectively which decreases with increasing temperature. Variation of temperature coefficient of resistance (T.C.R) for Co and TiO₂ thin films are metallic and insulating in nature respectively. The T.C.R. of deposited Co/TiO₂ multilayer thin films in all cases are semiconducting in nature.

Keywords - Co, e-beam, electrical properties, TiO₂ thickness.

I. INTRODUCTION

Co-doped TiO₂ has been a promising candidate for dilute magnetic semiconductor (DMS). Many researchers are investigating this system to study and further manipulate their electrical, magnetic or semiconductor properties. The cobalt doped titanium dioxide which has received widespread interest since it was discovered to be ferromagnetic at room temperature by Y. Matsumoto et al [1]. Newly discovered room-temperature ferromagnetic semiconductor cobalt-doped titanium dioxide (Co-doped TiO₂) is known as wide-bandgap diluted magnetic semiconductors (DMSs), it has a higher T_c (above room temperature), which makes it an extremely attractive material [2,3]. The magnetic material is doped in transparent oxide in a motivation that the magnetic properties can be controlled by controlling the electrical interaction. The reason for choosing cobalt and titanium dioxide in this research is because cobalt is a well-known magnetic element while the titanium dioxide has been extensively studied for several decades since it has many technologically important properties. TiO₂ is soft solid and melts at 1800°C. It absorbs ultraviolet light and has a high stability which is suitable to act as a matrix layer in semiconductor. Meanwhile, Co-doped TiO₂ naturally has high value of Curie temperature (T_c) [4], very much well above room temperature. With all these properties and a doping with cobalt magnetic ions, it would be able to control its optical, magnetic and semiconductor characters for suitable applications. Therefore, it is interesting to investigate the electrical properties of Co/TiO₂ multilayer thin film.

II. EXPERIMENTAL PROCESS

Thin film specimens for all the experimental investigations (e.g. electrical) have been prepared by e-beam technique using Edwards E-306 vacuum coating unit. The unit consists of a deposition chamber, a pumping system and electrical sources. The deposition chamber is cylindrical and has a mechanically polished interior. A stainless steel substrate holder to hold four substrates is situated just above the source. A mechanical shutter operated from outside the chamber isolates the source from the substrate for desired times. A tungsten filament (W) is used for the electron beam. The accessory is comprised of six hearth turret with rotary drive. The source turret is rotated, raised and lowered by an external control mechanism. The deposition chamber is evacuated with oil diffusion pump, which is controlled by an automatic evacuation system. The coating unit is provided with Edwards, EBS power supply unit having high tension (HT) 0-6 kV and low tension (LT) 0-500 mA. For present work HT is fixed at 4 kV and LT is varied from 40mA to 50mA. Electron bombardment heating of an evaporation source has been used. Single crystal substrates of alkali halides, mica, MgO, Si, Ge etc. are used for epitaxial growth. In the present work the ordinary microscope slides glass has been used. For patterning thin films, physical masking has been used by author. The measurement of resistivity and Hall co-efficient of the samples has been carried out by Van-der-Pauw method [5]. To fabricate a planer thin film, firstly, a suitable mask and source turret (with source-hearth contained TiO_2 or Co material) are adjusted and then shutter is placed between the substrate holder and source hearth to protect the substrate from unwanted deposition. Then the HT and LT regulators on the EBS power supply unit are ensured in the zero position. After switching ON the power supply the LT control of this supply unit is then increased slowly in order to degas the filament and evaporant, it is kept at about 60% on the LT control, and it is continued to degas the filament until the system pressure is reached a steady level and then LT control is reduced to zero. Then HT control of the EBS power supply is increased to HT voltage of 4 kV indicates on the meter and then the LT control is slowly increased until an emission current of 40mA in the case of Co material and 50mA in the case of TiO_2 material indicates on the meter. The HT voltage drops slightly. The source turret is slowly raised and hearth height is adjusted as the previous relevant steps to obtain the best film conduction. The shutter is then removed to allow deposition onto the substrate through the mask windows. When the deposition of film is completed then the shutter is replaced at the proper time. The EBS power supply is switched OFF properly. The high vacuum valve is then closed. The vacuum chamber and the fabricated devices are allowed to cool down for about an hour before air is admitted. The films are then taken out and stored them into a desiccators for various measurements. During the deposition of Co, TiO_2 and Co/ TiO_2 multilayer, two films are prepared in a single run. For the process optimization, the first set of films is deposited at various substrate heights (d_{ss}) with respect to evaporant source keeping all other deposition parameters constant at an arbitrary level. From this set of films, the optimum substrate height (d_{ss}) is selected with respect to the higher thickness as well as conductivity of films. In all sets, deposition time and thickness are monitored carefully. From these monitored data, the deposition rate has been calculated. For the present work the substrate temperature has been kept at room temperature. Optical interference method is adopted for film thickness measurement by which the thickness of the film can be measured accurately. To measure resistivity, varying temperature of Van-der-Pauw technique has been adopted. The voltage and current of the sample have been measured for different temperatures. After collected these data; the resistivity, conductivity, sheet resistance and T.C.R. of the films have been calculated for a particular temperature, respectively.

III. RESULT And DISCUSSION

Our main objective is to study the electrical properties of Co/ TiO_2 multilayer thin film. In the multilayer, the thickness of Co and TiO_2 was kept same. Each layer thickness was varied from 5nm to 15 nm and repeated three times. There are six alternative layer of Co and TiO_2 in each film and the upper layer is TiO_2 . S_1 denotes that each layer is 5nm and S_2 , S_3 denotes that each layer is 10nm and 15nm respectively. Temperature effect on conductivity has been studied for thickness variation as deposited Co, TiO_2 and Co/ TiO_2 multilayer thin films are depicted in Fig-3.1, 3.2 and 3.3 respectively.

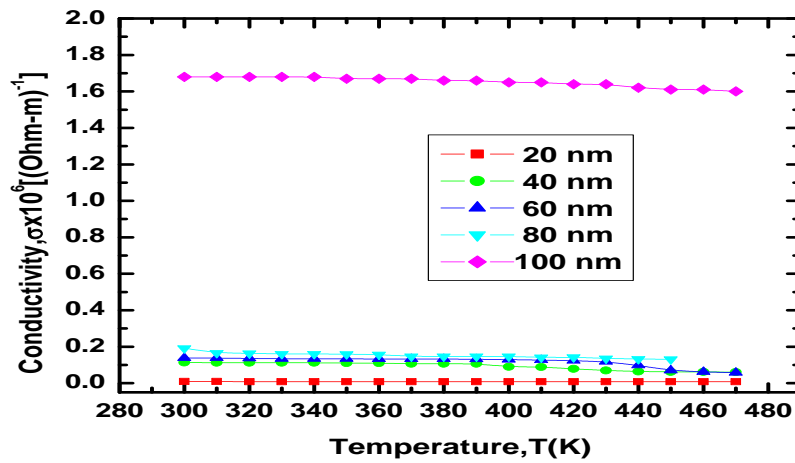


Fig-3.1: For deposited Co thin film of different thicknesses.

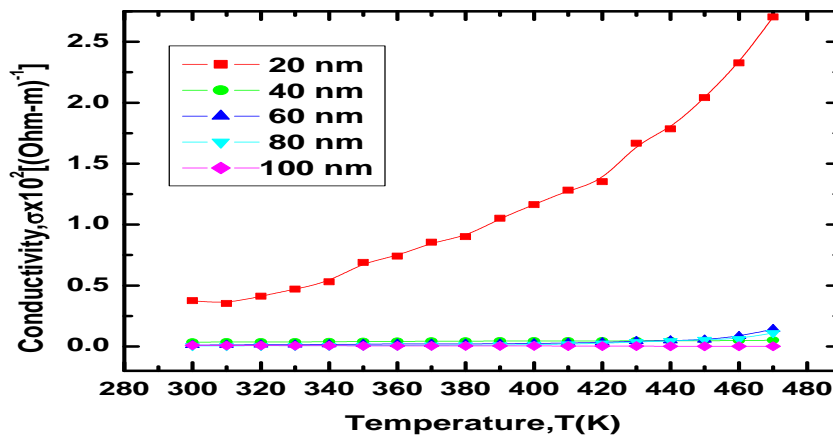


Fig-3.2: For deposited TiO_2 thin film of different thicknesses.

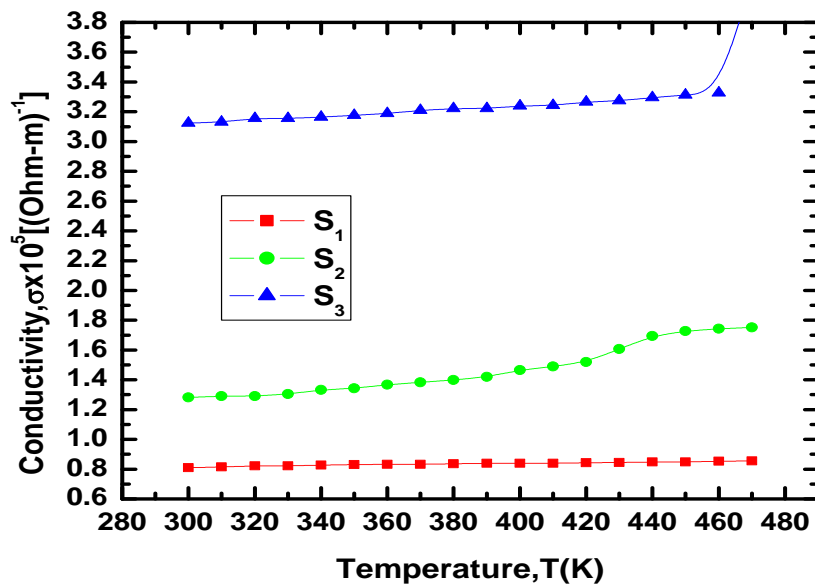


Fig-3.3: For deposited Co/ TiO_2 multilayer thin film of different thicknesses.

The temperature dependence of sheet resistance has been studied for thickness variation as deposited Co, TiO₂ and Co/TiO₂ multilayer thin films are depicted in Fig. 3.4, 3.5 and 3.6 respectively..

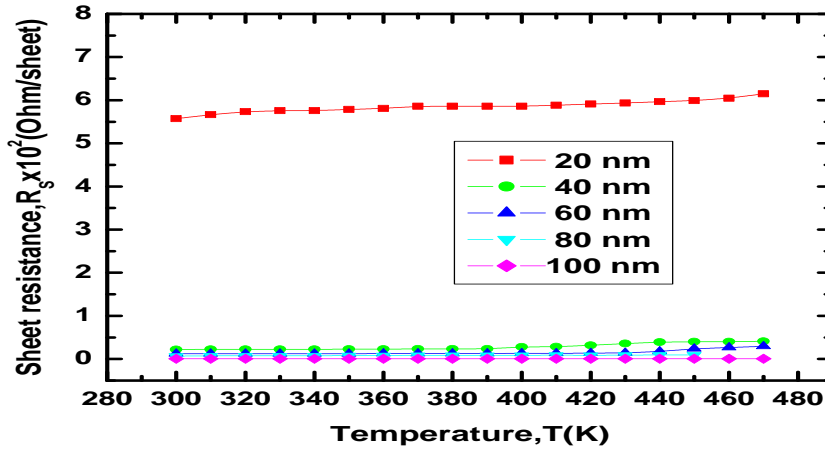


Fig-3.4: For deposited Co thin film of different thicknesses.

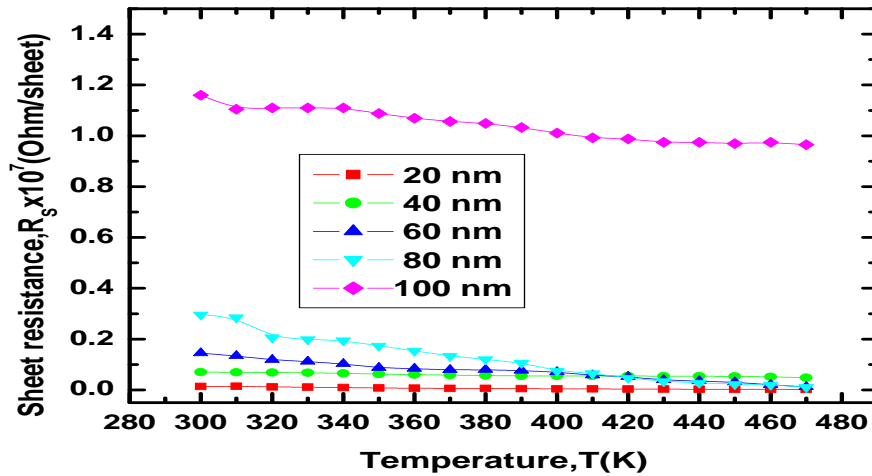


Fig-3.5: For deposited TiO₂ thin film of different thicknesses.

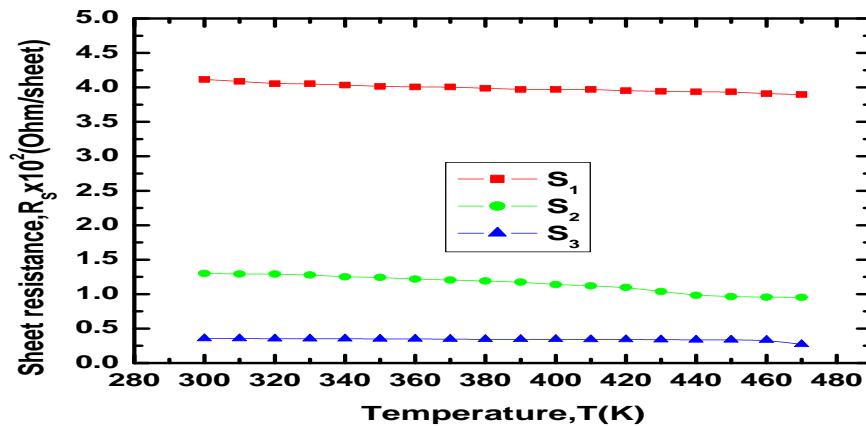


Fig-3.6: For deposited Co/TiO₂ multilayer thin film of different thicknesses.

Temperature effect on temperature coefficient of resistance (T.C.R) for thickness variation as deposited Co and TiO₂ and Co/TiO₂ multilayer thin films are depicted in fig 3.7, 3.8 and 3.9 respectively..

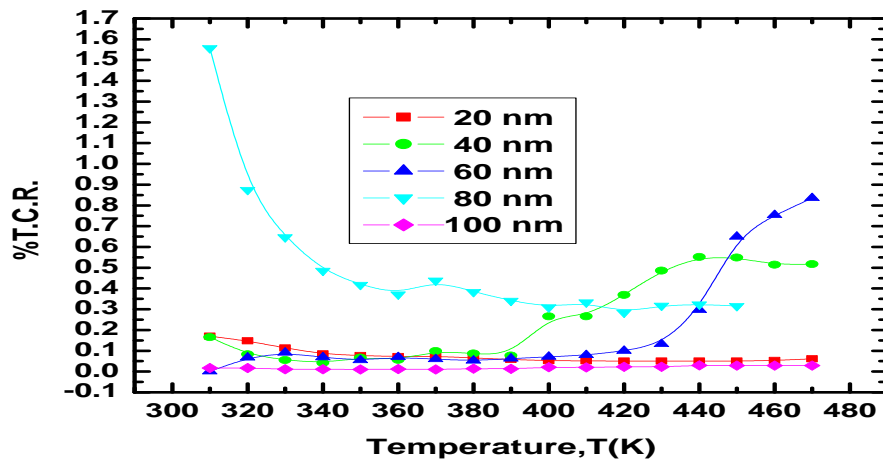


Fig-3.7: For deposited Co thin film of different thicknesses.

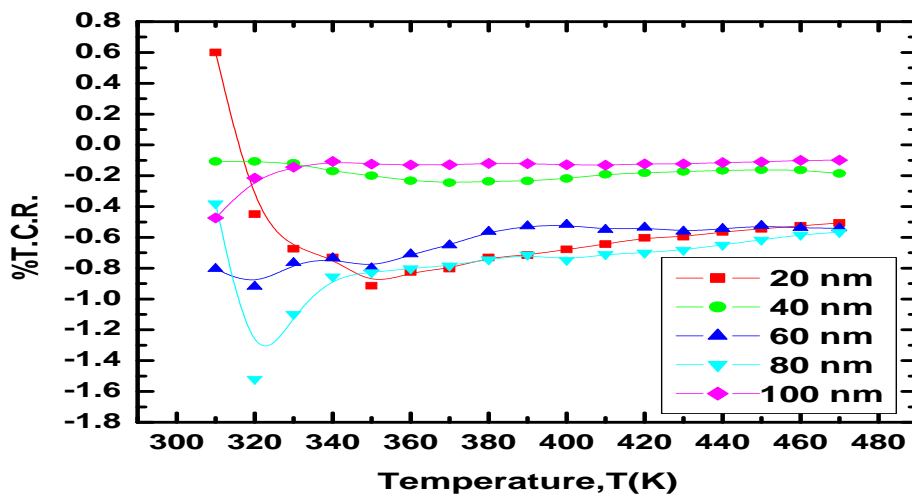


Fig-3.8: For deposited TiO₂ thin film of different thicknesses.

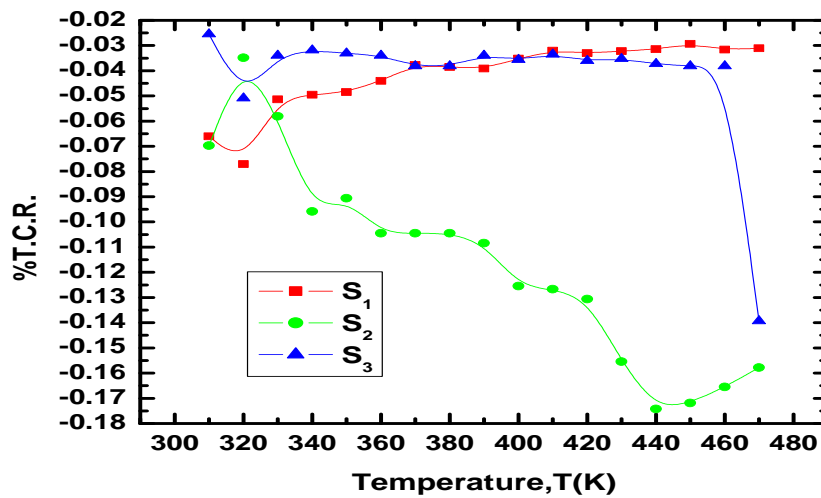


Fig-3.9: For deposited Co/TiO₂ multilayer thin film of different thicknesses.

IV. CONCLUSION

Research and development on thin films have lead to the conclusion that different classes of material are of particular interest for different applications. In the light of the experimental investigations and analysis on the electrical studies of Co, TiO₂ and Co/TiO₂ multilayer thin films of different thicknesses deposited by e-beam technique. Co, TiO₂ and Co/TiO₂ multilayer thin films with variable thickness ranges from 20 to 100 nm have been prepared onto glass substrate by e-beam evaporation technique in vacuum at a pressure of $\sim 4 \times 10^{-5}$ Pa. The deposition rate is about 1.33 nm s^{-1} for Co and 1.25 nm s^{-1} for TiO₂. The various effects on electrical properties of the films have been studied. In the case of the as deposited Co thin film, conductivity decreases with increasing temperature but conductivity increased with temperature for deposited TiO₂ thin film. Conductivity of the as deposited TiO₂ thin films decreases with film thickness where in the case of as deposited Co, Co/ TiO₂ multilayer thin films increases with increasing film thickness. In the case of TiO₂ thin films, higher thickness has higher sheet resistance however in the case of as deposited Co, Co/ TiO₂ multilayer thin films, higher thickness has lower sheet resistance. The T.C.R. of Co thin films is positive which are shown to exhibit the as deposited Co thin film are metallic in nature and T.C.R. of TiO₂ thin films is negative which indicates that the as deposited TiO₂ thin films are insulating in nature. The T.C.R. of Co/TiO₂ multilayer thin films is negative in all cases which exhibits that as deposited Co/TiO₂ multilayer thin films are semiconducting in nature.

Acknowledgements

The authors would like to thank the concerned authority of the University of Rajshahi, Rajshahi, Bangladesh for providing us laboratory facilities (Central Science Laboratory, Rajshahi University) for the purpose of completing this research work. The financial support of the ministry of information and communication technology, Bangladesh (Fellowship 2010-2011) is gratefully acknowledged.

REFERENCES

- [1] S.A. Chambers, S. Thevuthasan, R.F.C. Farrow, R.F. Marks, J.U. Thiele, L. Folks, M.G. Samant, A.J. Kellock, N. Ruzycski, D.L. Ederer and U. Diebold, Epitaxial growth and properties of ferromagnetic co-doped TiO₂ anatase, *American Institute of physics*, 79(21), 2001, 3469.
- [2] T. Fukumura, Y. Yamada, K. Tamura, K. Nakajima, Exploration of oxide semiconductor electronics of epitaxial thin films, in Y. Fujikawa (Ed), *Frontier in materials Research*, (German: Springer-berlin, 2008) 923-541.
- [3] H. Ohno, Making Nonmagnetic Semiconductors ferromagnetic, *Science Magazine*, 281(5379), 1998, 951-956.
- [4] S. A. Chambers, C. M. Wang and A. S. Lea, Transition from granular to dilute magnetic semiconducting multilayers in ion-beam-deposited ZnO/Co, *American Institute of physics*, 83(21), 2003, 4357
- [5] L.J. Vander PAUL, A method of measuring specific resistivity and hall effect of discs of arbitrary shape, *Philips Research Reports*, 13(1), 1958, 334.

Investigation of the parameters on the fast pyrolysis of wheat straw for production of bio-oil

Syed Kamal Zafar, Syed Hassan Javed Naqvi, Atif Khan

Department of Chemical Engineering, University of Engineering and Technology Lahore

ABSTRACT: Due to increase in energy demand, alternative energy resources are needed to be explored. Among these, biomass is one of the most promising, sustainable and renewable energy resources for power generation especially in agricultural countries. Several technologies are available for biomass conversion into energy but fast pyrolysis is the emerging and reliable technology among all for energy generation through biomass. Due to the continuous and abundant supply of biomass such as wheat straw, this technology is very helpful for reducing the demand and supply gap of energy. Variety of products like bio-oil, char and gases are obtained through pyrolysis of biomass. Among different type of biomasses wheat straw is selected for the study because of its abundant supply. Wheat straw is burnt in the presence of oxygen at high temperature to get pyrolysis products. The major objective of this research is to find the best and optimum temperature, particle size and heating effect at which maximum conversion of biomass into bio-oil is achieved.

Key words: Biomass, Wheat straw, fast pyrolysis, bio-oil, char

I. Introduction

Biomass is a biological material obtained from living or recently living organisms. Major purpose of obtaining this biological material is to generate electricity. Due to increase in the demand and supply gap of energy especially in the third world countries, alternative sources of energy should be considered[1]. Biomass is the best alternate and renewable source of energy, having a great potential to reduce the demand and supply gap. Biomass can be grown easily within a short interval of time that is why it is known as the renewable energy source[2]. Forest (wood), Plants (crops) and animal wastes are some common examples of biomass. The history of biomass was developed gradually over the past few decades and it continues to improve until today. Now a days, biomass heaters and dryers are being used on domestic and commercial scale to obtain biofuels[3].

Biomass is mainly composed of mixture of organic molecules such as carbon, hydrogen and oxygen. Sometimes it contains traces of nitrogen, alkali and alkaline earth metals. Wheat straw is a type of agriculture biomass. It mainly consists of cellulose (40% -60%), hemicelluloses (20% - 35%) and lignin (15 -30%). Some minerals and organic components are also present in minor proportion in the wheat straw. Cellulose exhibits a crystalline structure consisting of thousands of polymers[4]. During combustion process, cellulose usually degrades at 350°C into monomers. Hemicellulose has lower thermal stability as compared to cellulose and it usually degrades at 270°C. It consists of C₅ monomers. Unlike cellulose, lignin exists in amorphous form having large number of cross-linked chains of carbon atoms, therefore its degradation temperature is much higher than cellulose. The proximate and ultimate analysis of wheat straw is given in the Table 1.1.

Table 1.1. Proximate & Ultimate Analysis of Wheat Straw[5]

Description	Wheat Straw (%)
Volatile Matter	64
Fixed Carbon	26
Moisture	0.9
Ash	6

Carbon	44
Hydrogen	6
Nitrogen	0.48
Sulfur	0.15
Oxygen	44.37

Conversion process is one of the important parameters in order to attain maximum energy from bio-fuel. At present, several conversion technologies are being used to convert biomass into useful products. These include combustion, carbonization, gasification and pyrolysis. Other thermal conversion processes are combustion, carbonization, gasification and pyrolysis. In the combustion process, biomass is burned at high temperature in the presence of oxygen to achieve heat and energy. Carbon dioxide and water are produced as byproducts. Gasification is considered a better conversion technology than combustion that converts carbonaceous biomass into gaseous products such as CO and H₂ gas. It is carried out at high temperature. In this process, synthesis gases such as CH₄, CO, CO₂, H₂ and N₂ are produced which are of moderate heating value[6]. In gasification, sulfur is converted into H₂S. The sulfur compounds are usually in minor quantities. Pyrolysis is one of the efficient and cost effective methods to obtain energy from biomass[7]. Pyrolysis is classified into three types; slow, fast and flash pyrolysis. These three types of pyrolysis are differentiated by their operating conditions. In pyrolysis biomass is converted into useful products in the absence of oxygen at higher heating rates. 70-80 wt. % bio-oil is obtained in fast pyrolysis process[8].

Table 1.2: Bio oil properties[9]

QUANTITY	BIO OIL	HEAVY FUEL OIL
Volume Energy Density (GJ/m ³)	21	39
Bio oil density (kg/m ³)	1220	963
Viscosity at 50°C (mm ² /s)	13	351
pH	3	7
Oil water content (wt. %)	20	0.1
Ash content (wt. %)	0.02	0.03

Table 1.3: Main technology providers of fast pyrolysis in world[10]

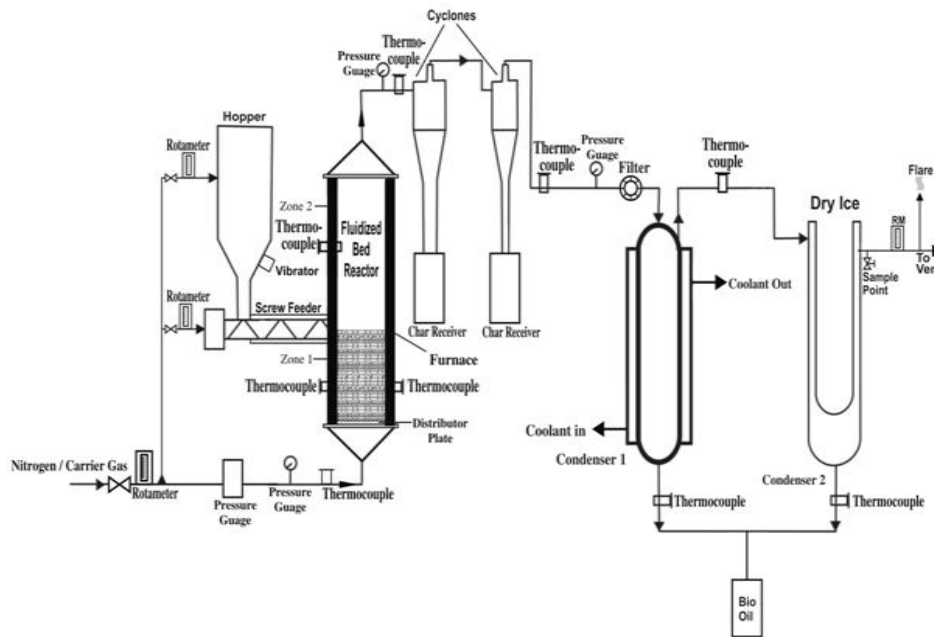
Technology provider/ trademark	Country	Scale (kg/h)	Reactor type
DynamotiveBiotherm™	Canada	400 and 4000	Fluidized bed reactor
Ensyn RTP™	Canada	1000	Circulating fluidized bed reactor
BTG	Netherlands	250	Rotating cone reactor
Pyrovac/ pyrolycycling™	Canada	50 and 3500	Vacuum reactor

II. Materials and methods

A known weight of sand is introduced into the fluidised bed reactor from the top over the distributor plate. A set point of temperature is given from the computer software system and starts the system to achieve the required temperatures. The system is initially run on air. Biomass feed is introduced from the top of hopper[11].

There is a pre-heater that heats the nitrogen gas. Nitrogen is used for purging. The nitrogen gas goes into the header from where it goes into the reactor and hopper. When the required temperature is achieved, then the feed is introduced. The screw feeder takes away the feed towards the reactor. A water cooling system is provided around the screw to prevent it from overheating[12]. As the pyrolysis reaction starts, charring of vapours take place and gases pass through the two cyclones. The char and dust is collected into the char receiver. The gases and vapours pass through the two condensers. In the first condenser water is used and in the second condenser ice is used. Bio-fuel is collected from the bottom of condensers after condensation and gases go outward from the rotameter. After the completion of the process, the bio-fuel and char are collected[13].

Fig 2.1 Schematic Diagram of Fast Pyrolysis System[14].



III. Results and Discussion

3.1 Effect of Temperature on Products

The experimental rig was operated by changing the reactor temperature between 450 and 650°C while the other parameters were kept constant. Feed (2 kg) of -30 - +60 mesh particle size and sand (2 kg) of the similar particle size were used in each run. Nitrogen gas flow rate was kept at 60 ft³/hr in the hopper. The effect of temperature on the % age yield of products is elaborated below in Table 3.1.

Table (3.1):-Effect of Temperature on the % age Yield of Products

Test Run	Reactor Temperature (°C)	N ₂ Flow Rate (m ³ /hr)	Feeder RPM	Bio oil %	Char %	Gases %
1	450	125	20	56	22	11
2	500	125	20	59	20	13
3	550	125	20	62	17	16
4	600	125	20	55	15	19
5	650	125	20	53	12	21

Fig (3.1) indicates that % age yield increases by increasing pyrolysis temperature up to 550°C and then suddenly decreases. So the maximum yield is obtained at 550°C.

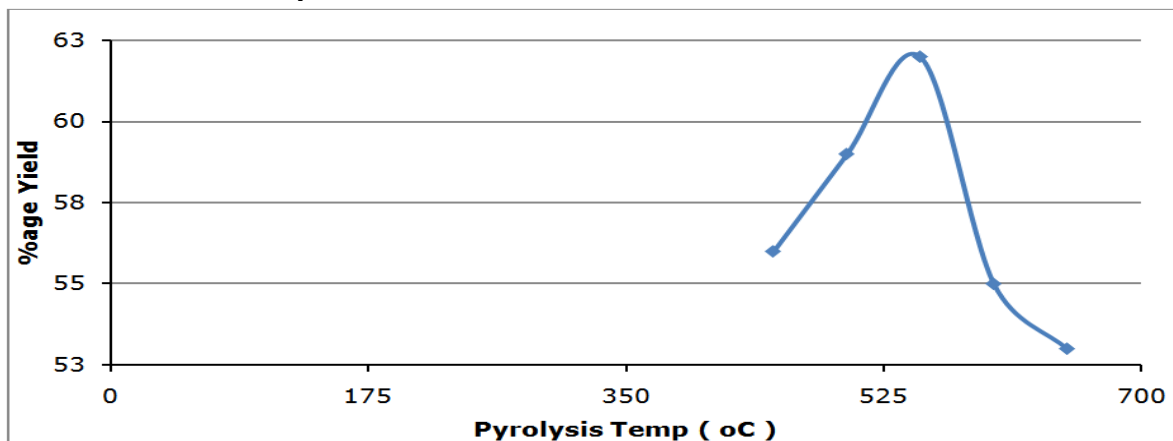


Fig (3.1):-Effect of temperature on % age Yield of Bio-oil

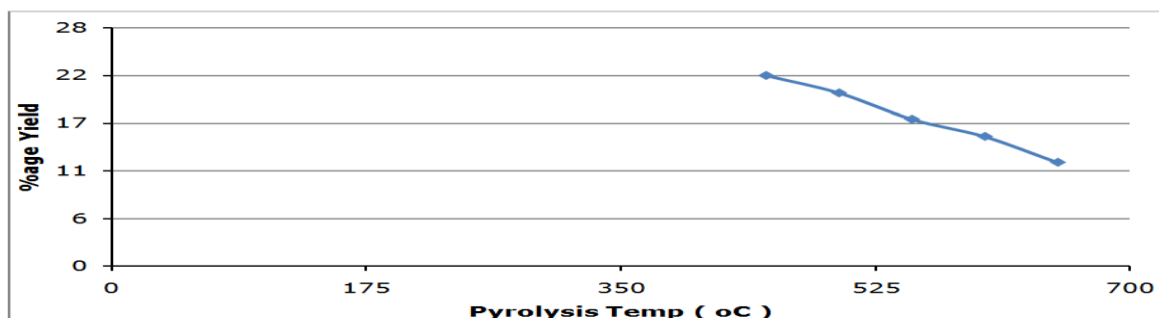


Fig (3.2):-Effect of temperature on % age Yield of Bio-char

Effect of temperature on % age yield on char is again reflected in Fig 3.2. At 450°C, the maximum yield of char is obtained at 450°C.

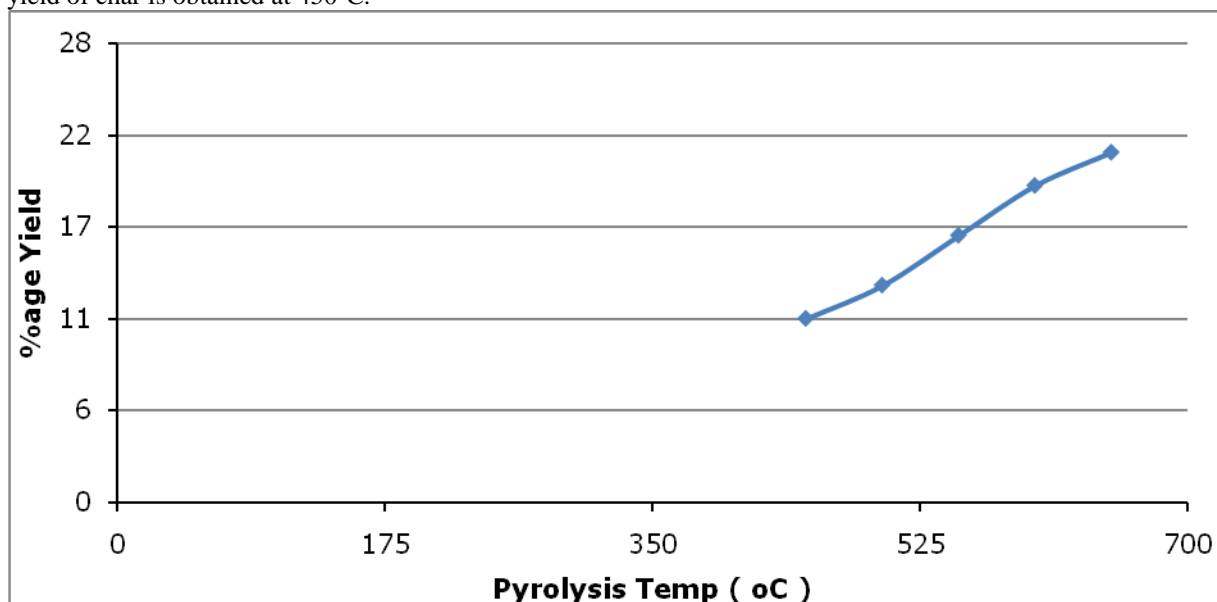


Fig (3.3):-Effect of temperature on % age Yield of gases

A linear trend is obtained in the Fig (3.3) which shows an increase in % age yield of gases with the increases in temperature in each experimental run. The maximum yield of gases is achieved at 650°C. This is because as the temperature increases, secondary reactions initiate that cause cracking and reforming. As a result formation of gases also increases.

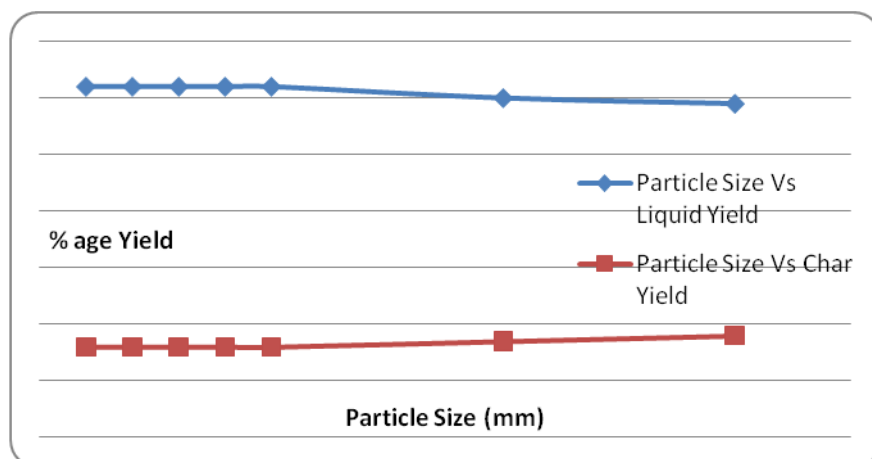
3.2 Effect of Particle Size on Products

Different runs were made to see the effect of particle size on all these products. The particle sizes were varied from 0.2-3mm, while the other parameters were kept constant.

Table 3.2.Effect of Particle size on the Products

Particle Size dp (mm)	Pyrolysis Temperature (°C)	Liquid % age yield	Char % age Yield
0.2	550	62	16
0.4	550	62	16
0.6	550	62	16
0.8	550	62	16
1	550	62	16
2	550	60	17
3	550	59	18

Fig 3.4. Effect of Particle size on the Products



This effect can be seen in Fig 3.4. The graph indicated that the liquid and char yield remains same up to 1mm dp. After 1mm, the bio-oil yield starts to decrease and bio-char yield increases. This shows that particle size also affects the product yield. The reason is that when particle size is below 1 mm, more cellulosic components are formed due to the increase in the surface area. And when the feed size is large then surface area is smaller and rate of reaction of cellulosic components decreases and thus bio-oil yield decreases.

3.3. FTIR

Fourier Transform Infrared Spectrometry (FTIR) test results of bio-oil samples were also performed during the study. The results at different wavelength showed following groups that are given below in Table 3.3

Table 3.3 FTIR results of Bio-oil

Wavelength (cm^{-1})	Groups
2927	Aromatics ,Cyclic enes
1636	Quinolones
1022	C-F group
1263	Hydroxyl group
3380	Imino-moiety of piperozinyl group
1702	Carbonyl of acids
1456	O-C-O group of acid
912	Amines

III. Conclusion

From the above analysis and behaviour it is concluded that maximum production of bio-oil is obtained at 550°C with minimum production of char and waste gases. Hence, for the production of bio-oil using fast pyro-lysis and wheat straw as a raw material, the optimum temperature evaluated is 550°C. The decrease in temperature causes an increase in the char yield and further increase in the temperature above 550°C increases the formation of gaseous products. Particle size also found as significant parameter which affects the products specially bio-oil and char. Bio-oil yield remains constant for biomass feed particle size less than 1mm. As particle size increases from 1mm bio-oil yield decreases and char yield increases. The ash content in char was found 13 % and calorific value of char is 14.307 MJ/kg which is in acceptable range.

References

- [1] J. N. Murwanashyaka, H. Pakdel, and C. Roy, "Step-wise and one-step vacuum pyrolysis of birch-derived biomass to monitor the evolution of phenols," *Journal of Analytical and Applied Pyrolysis*, vol. 60, pp. 219-231, 2001.
- [2] D. S. Scott and J. Piskorz, "The continuous flash pyrolysis of biomass," *The Canadian Journal of Chemical Engineering*, vol. 62, pp. 404-412, 1984.
- [3] G. Maschio, C. Koufopoulos, and A. Lucchesi, "Pyrolysis, a promising route for biomass utilization," *Bioresource technology*, vol. 42, pp. 219-231, 1992.
- [4] S. R. Kersten, X. Wang, W. Prins, and W. P. van Swaaij, "Biomass pyrolysis in a fluidized bed reactor. Part 1: Literature review and model simulations," *Industrial & Engineering Chemistry Research*, vol. 44, pp. 8773-8785, 2005.
- [5] M. Ayllón, M. Aznar, J. Sánchez, G. Gea, and J. Arauzo, "Influence of temperature and heating rate on the fixed bed pyrolysis of meat and bone meal," *Chemical Engineering Journal*, vol. 121, pp. 85-96, 2006.
- [6] P. T. Williams and S. Besler, "The influence of temperature and heating rate on the slow pyrolysis of biomass," *Renewable energy*, vol. 7, pp. 233-250, 1996.
- [7] A. Janse, R. Westerhout, and W. Prins, "Modelling of flash pyrolysis of a single wood particle," *Chemical Engineering and Processing: Process Intensification*, vol. 39, pp. 239-252, 2000.
- [8] W. Tsai, M. Lee, and Y. Chang, "Fast pyrolysis of rice straw, sugarcane bagasse and coconut shell in an induction-heating reactor," *Journal of Analytical and Applied Pyrolysis*, vol. 76, pp. 230-237, 2006.
- [9] D. S. Scott, J. Piskorz, M. A. Bergougnou, R. Graham, and R. P. Overend, "The role of temperature in the fast pyrolysis of cellulose and wood," *Industrial & Engineering Chemistry Research*, vol. 27, pp. 8-15, 1988.
- [10] K. Shi, S. Shao, Q. Huang, X. Liang, L. Jiang, and Y. Li, "Review of catalytic pyrolysis of biomass for bio-oil," in *Materials for Renewable Energy & Environment (ICMREE), 2011 International Conference on*, 2011, pp. 317-321.
- [11] P. A. Horne and P. T. Williams, "Influence of temperature on the products from the flash pyrolysis of biomass," *Fuel*, vol. 75, pp. 1051-1059, 1996.
- [12] S. Czernik and A. Bridgwater, "Overview of applications of biomass fast pyrolysis oil," *Energy & Fuels*, vol. 18, pp. 590-598, 2004.
- [13] P. T. Williams and N. Nugranad, "Comparison of products from the pyrolysis and catalytic pyrolysis of rice husks," *Energy*, vol. 25, pp. 493-513, 2000.
- [14] V. Seebauer, J. Petek, and G. Staudinger, "Effects of particle size, heating rate and pressure on measurement of pyrolysis kinetics by thermogravimetric analysis," *Fuel*, vol. 76, pp. 1277-1282, 1997.

A Technical Investigation of Voltage Sag

¹Vima P. Mali, ²R. L. Chakrasali, ¹K. S. Aprameya

¹Electrical and Electronics Engineering Research Centre, University B.D.T. College of Engineering, Davanagere, India.

²Department of Electrical and Electronics Engineering, SDM College of Engineering and Technology, Dharwad, India.

Abstract: Voltage sag is regarded as one of the most harmful power quality disturbances due to its costly impact on sensitive loads. The vast majority of the problems occurring across the utility, transmission and industrial sides are voltage sags. The source of sag can be difficult to locate, since it occurs either inside or outside facilities. So, this paper analyses some aspects of voltage sag such as the cost of voltage sag, their characteristics, types of voltage sag, its occurrence, percentage of sag present in power system, acceptable level of voltage sag curve, voltage sag indices, its economical impact, ways to mitigate the voltage sag and finally few devices used to mitigate voltage sag.

Keywords: Voltage sag, impact, types, occurrence etc.

I. INTRODUCTION

The name power quality has become one of the most productive concepts in the power industry since late 1980s. Power quality is the "Degree to which both the utilization and delivery of electric power affects the performance of electrical equipment" [1]. Power quality is decided by magnitude of voltage and frequency. Voltage quality problem is divided into under voltage, overvoltage, interruption, voltage sag, voltage swell and so on, and frequency quality problem could be classified into frequency variations, transient, harmonics, etc. [2].

Voltage sag or Voltage dip the two terms are equivalent. According to the IEEE defined standard (IEEE Std. 1159, 1995), voltage sag is the decrease of rms value of voltage from 0.1 to 0.9 per unit (pu), for a duration of 0.5 cycle to 1 minute. The International Electrotechnical Commission, IEC, has the following definition for a dip (IEC 61000-2-1, 1990). "A voltage dip is a sudden reduction of the voltage at a point in the electrical system, followed by a voltage recovery after a short period of time, from half a cycle to a few seconds".

Voltage sags are present in power systems, but only during the past decades customers are becoming more sensitive to the inconvenience caused [3]. Voltage sag can cause serious problems to sensitive loads, because these loads often drop off-line due to voltage sag. As a result, some industrial facilities experience production outage that results in economic losses [4, 5, 6]. In several processes such as semiconductor manufacturing or food processing plants, the voltage dip of very short duration can cost a substantial amount of money [7]. Voltage dip is the main power quality problem for the semiconductor and continuous manufacturing industries, and also to the hotels and telecom sectors [8].

International Joint Working Group (JWG) C4.1110 sponsored by CIGRE, CIREN and UIE has addressed a number of aspects of the immunity of equipment and installations against voltage dips and also identified areas where additional work is required. The work took place between 2006 and 2009 and resulted in a technical brochure distributed via CIGRE and UIE [9]. Voltage sag on a power grid can affect facilities within a 100-mile radius. According to Electric Power Research Institute the voltage sag causes 92% of distribution & transmission power quality problems.

A typical electric customer in the U.S experiences 40 to 60 sag events per year with those events resulting in the voltage dropping to between 60 to 90% and lasting several cycles to more than a second. The large majority of faults on a utility system are single line-to-ground faults (SLGF). Three phase faults can be more severe, but much less common. System wide, an urban customer on average may see 1 or 2 interruptions a year whereas the same customer may experience over 20 voltage sag occurrences a year depending on how many circuits are fed from the substation.

II. COST OF VOLTAGE SAG

Voltage sag lasting for a few cycles result in losses of several million dollars includes:

- a. Repairs cost.
- b. Increased buffer inventories.
- c. Product quality issues affect brand name, fame of the industry and even the country.
- d. Customer dissatisfaction due to huge loss in business.
- e. Penalties and disposal fees.
- f. Product-related losses, such as loss of product/materials, hampered production capacity, disposal charges, and increased inventory requirements.
- g. Labor-related losses, such as idle employees, overtime, cleanup and repair.
- h. Ancillary costs, such as damaged equipment, lost opportunity cost and penalties due to shipping delays.

III. CHARACTERISTICS OF VOLTAGE SAG

The magnitude of voltage and the frequency are the parameters that specify the voltage sag.

a. Magnitude:

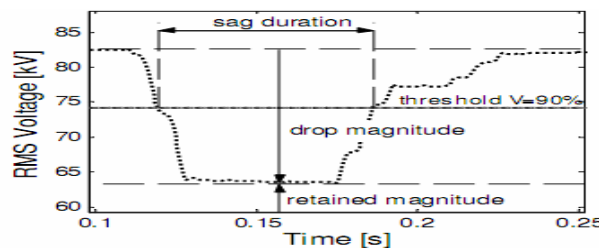


Figure 1. Voltage sag characteristics

The sag magnitude is the minimum of rms voltage and refers to the retained voltage or to the drop of the voltage (IEEE P1564). Thus, a 70% sag in a 230-V system indicates the voltage dropped to 161 V. One could be tricked into thinking that 70% sag refers to a drop of 70%, thus a remaining voltage of 30% [10]. The most common approach to obtain the sag magnitude is to use rms voltage. There are other alternatives, e.g. rms voltage of fundamental component and peak voltage [11,12]. The rms voltage is calculated over one cycle using equation 1

$$V_{rms}(k) = \sqrt{\frac{1}{N} \sum_{i=k-N+1}^k v_i^2} \quad \text{----- (1)}$$

The rms value using one half cycle is given by equation 2

$$V_{rms(1/2)}(k) = \sqrt{\frac{2}{N} \sum_{i=k-(N/2)+1}^k v_i^2} \quad \text{-----(2)}$$

Where N is the number of samples per cycles, V(i) is the instantaneous sampled voltage and k is the instant when the rms voltage is estimated.

b. Duration: Sag duration is commonly determined by the speed of the fault clearing time. The voltage sag duration is nothing but the period of time in which the voltage is lower than the stated limit; normally sag duration is less than 1 second (IEEE Std. 493, 1997). According to IEEE Std. 1159, 1995 voltage sag has been classified into three types based on their duration i) Instantaneous (0.5-30cycle) ii) Momentary (30 cycles-3sec) iii) Temporary (3sec-1min). For measurements in the three-phases systems the three rms voltages have to be considered to determine duration of the sag. The voltage sag starts when at least one of the rms voltages drops below the sag-starting threshold. The sag ends when all three voltages have recovered above the sag-ending threshold.

c. Unbalance of Sag: In the power system the faults are classified as symmetrical (balanced) and unsymmetrical (unbalanced) depending on the type of fault. If three phase fault occurs, the sag will be symmetrical but if the fault is single phase, double phase or double phase to ground faults the sag in three phases will not be symmetrical.

d. Phase-Angle Jump: A short circuit in a power system not only causes voltage sag, but also changes the phase angle of the voltage leading to phase-angle jump. The phase-angle jump is visible in a time-domain plot of the sag as a shift in voltage zero-crossing between the pre-event and the during-event voltage. If source and feeder impedance have equal X/R ratio, there will be no phase-angle jump in the voltage at the Point of Common Coupling. This is the case for faults in transmission systems, but normally not for faults in distribution systems. The distribution systems may have phase-angle jumps up to a few tens of degrees.

For unsymmetrical faults, the analysis becomes much more complicated. A consequence of unsymmetrical faults (single-phase, phase-to-phase, two-phase-to-ground) is that single-phase load experiences a phase-angle jump even for equal $X = R$ ratio of feeder and source impedance. From the measured voltage wave shape, the phase angle of the voltage during the event must be compared with the phase angle of the voltage before the event.

IV. TYPES OF VOLTAGE SAG

Based on the phases affected during the sag, the voltage sag has been classified into three types:

a. Single Phase Sags: The frequently occurring voltage sags are single phase events which are basically due to a phase to ground fault occurring somewhere on the system. On other feeders from the same substation this phase to ground fault appears as single phase voltage sag. Typical causes are lightning strikes, tree branches, animal contact etc. It is common to see single phase voltage sags to 30% of nominal voltage or less in industrial plants.

b. Phase to Phase Sags: The two phase or phase to phase sags are caused by tree branches, adverse weather, animals or vehicle collision with utility poles. These types of sags typically appear on other feeders from the same substation.

c. Three Phase Sags: These sags are caused by switching or tripping of a 3 phase circuit breaker, switch or recloser which will create three phase voltage sag on other lines fed from the same substation. Symmetrical 3 phase sags arise from starting large motors and they account for less than 20% of all sag events and are usually confined to an industrial plant or its immediate neighbors.

V. OCCURRENCE OF VOLTAGE SAG

Voltage sag occurs at almost all locations in the power system and avoiding them is only practically possible up to a certain extent. Voltage sag is caused by faults on the system, transformer energizing, or heavy load switching. Reducing the number and severity of voltage sag experienced by a customer, beyond what is normally considered as good engineering practice, can be very expensive [11].

Utility side voltage sag occurs due to operation of reclosers & circuit breakers, equipment fails(due to overloading, cable faults), bad weather (thunderstorms and lightning strikes cause a significant number of voltage sags), animals & birds(squirrels, raccoons and snakes occasionally find their way onto power lines or transformers and can cause a short circuit or either phase to phase or phase to ground), Vehicles occasionally collide with utility poles (causing lines to touch, protective devices trip and voltage sags occur), Construction activity(Digging foundations for new building construction can result in damage to underground power lines and create voltage sags).

Salt spray builds up on power line insulators over time in coastal areas, even many miles inland, can cause flash over especially in stormy weather. Dust in arid inland areas can cause similar problems. As circuit protector devices operate voltage sags appear on other feeders. If electrical equipment fails due to overloading, cable faults etc., protective equipment will operate at the sub-station and voltage sags will be seen on other feeder lines across the utility system.

Industrial side voltage sags occurs within an industrial facility (due to factory equipment, office equipment, air conditioning & elevator drive motors) or a group of facilities by the starting of large electric motors either individually or in groups. The large current inrush on starting can cause voltage sags in the local or adjacent areas even if the utility line voltage remains at a constant nominal value. Starting a large load, such as an electric motor or resistive heater, typically draw 150% to 500% of their operating current as they come up to speed. Resistive heaters typically draw 150% of their rated current until they warm up. Even 80% of all power quality problems occur in a company's distribution and grounding/bonding systems.

Electronic process controls, sensors, computer controls, PLC's and variable speed drives, conventional electrical relays are all to some degree susceptible to voltage sags. In many cases one or more of these devices may trip if there is a voltage sag to less than 90% of nominal voltage even if the duration is only for one or two cycles i.e. less than 100 milliseconds. The time to restart production after such an unplanned stoppage can typically be measured in minutes, hours or even days. Costs per event can be many tens of thousands of dollars. Voltage sag cannot be eliminated fully so, Industrial customers who have invested heavily in production equipment which is susceptible to voltage sags must take responsibility for their own solutions to voltage sags or lose some benefit from their investment.

VI. PERCENTAGE OF SAG PRESENT IN POWER SYSTEM

The most common types of voltage abnormalities are: harmonics, voltage sags, voltage swells and short interruptions. Among these, voltage sags account for the highest percentage of occurrences in equipment interruptions, as shown in Figure 1. The figure 1 indicates that voltage sags account for the highest percentage of equipment interruptions, i.e., 31%. Voltage sags are also major power quality problem that contributes to nuisance tripping and malfunction of sensitive equipment in industrial processes and Table 1 below gives causes of voltage sag on distribution system based on number of voltage sag occurrences and its percentage.

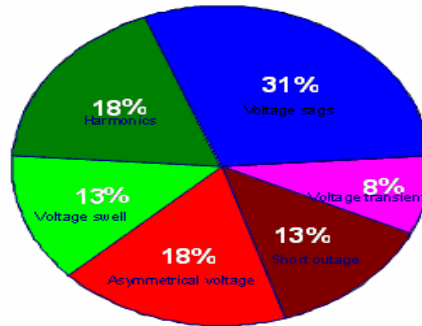


Figure 1 Power quality disturbances [28]

Table 1. Causes of voltage sag on distribution system

Sl. No	Causes	Number of Occurrences	Percentage
1.	Wind & lightning	37	46%
2.	Utility equipment failure	8	10%
3.	Construction or traffic accident	8	10%
4.	Animals	5	6%
5.	Tree limbs	1	1%
6.	Unknown	21	26%
Total		80	100%

VII. CLASSIFICATION OF VOLTAGE SAG

There are two methods for classification the three phase voltage sags i) ABC Classification (First method) ii) Symmetrical Components (Second method). Due to simplicity, first method is more used than the symmetrical components classification. However, this classification is based on a simplified model of the network and it is not recommended to use for the classification of voltage sags obtained from measured instantaneous voltages.

In the first classification, in 1997, Bollen has proposed a four type’s classification for voltage sags (A, B, C, D) based on type of fault which generates the sag [13]. This classification isn’t so good for voltage sags generated by 2PN (2 phase to neutral) faults [14, 15]. So, Bollen has proposed a new by adding another three (E, F, G) types of voltage sags. Types of voltage sag are:

Table 2. The phasor diagram and equations

Type of voltage sag	Phasor diagram	Phase to neutral equations
Type A: Voltage sag during the event is equal (symmetrical) in all the three phases and they are generated by 3P (3 phase or 3PN (3 Phase to neutral) faults.		$\bar{V}_a = V$ $\bar{V}_b = -\frac{1}{2}V - j\frac{\sqrt{3}}{2}V$ $\bar{V}_c = -\frac{1}{2}V + j\frac{\sqrt{3}}{2}V$

<p>Type B: The voltage sags generated by PN (phase to neutral) faults are classified as type B, if the consumer has star connection, these sag are rare to occur.</p>		$\bar{V}_a = V$ $\bar{V}_b = -\frac{1}{2}E_1 - j\frac{\sqrt{3}}{2}E_1$ $\bar{V}_c = -\frac{1}{2}E_1 + j\frac{\sqrt{3}}{2}E_1$
<p>Type C: Voltage sags generated by 2P (2 Phase) faults are classified as type C, if the consumer has star connection. Even voltage sag generated by PN faults, are classified as type C if the consumer has delta connection.</p>		$\bar{V}_a = E_1$ $\bar{V}_b = -\frac{1}{2}E_1 - j\frac{\sqrt{3}}{2}V$ $\bar{V}_c = -\frac{1}{2}E_1 + j\frac{\sqrt{3}}{2}V$
<p>Type D: Voltage sags generated by 2P (2 Phase) faults are classified as type D if the consumer has delta connection.</p>		$\bar{V}_a = V$ $\bar{V}_b = -\frac{1}{2}V - j\frac{\sqrt{3}}{2}E_1$ $\bar{V}_c = -\frac{1}{2}V + j\frac{\sqrt{3}}{2}E_1$
<p>Type E: It shows a symmetrical relation between PP (Phase to Phase) and PN voltage. These are also rare to occur and can be seen only when a LLG fault is located at the same voltage level or when the fault propagates through a star-star connected transformer grounded at both sides.</p>		$\bar{V}_a = E_1$ $\bar{V}_b = -\frac{1}{2}V - j\frac{\sqrt{3}}{2}V$ $\bar{V}_c = -\frac{1}{2}V + j\frac{\sqrt{3}}{2}V$
<p>Type F: It is a reduction in one phase voltage. It is caused by the propagation of a LLG fault through a delta star connected transformer. For this type of sag, when the PN voltage is zero, the minimum PP voltage is 1/3.</p>		$\bar{V}_a = V$ $\bar{V}_b = -\frac{1}{2}V - j\left(\frac{\sqrt{3}}{6}V + \frac{\sqrt{3}}{3}E_1\right)$ $\bar{V}_c = -\frac{1}{2}V + j\left(\frac{\sqrt{3}}{6}V + \frac{\sqrt{3}}{3}E_1\right)$
<p>Type G: These sags are obtained by the propagation of a sag type F through a delta – star connected transformer. For this type of sag the minimum PN voltage is 1/3 when PP voltage is zero.</p>		$\bar{V}_a = \frac{2}{3}E_1 + \frac{1}{3}V$ $\bar{V}_b = -\frac{1}{3}E_1 - \frac{1}{6}V - j\frac{\sqrt{3}}{2}V$ $\bar{V}_c = -\frac{1}{3}E_1 - \frac{1}{6}V + j\frac{\sqrt{3}}{2}V$

The pre-event voltage in phase A is denoted as E1, recalling to the equivalence between phase A voltage and positive sequence voltage in a balanced system. The voltage in the phase that has experienced the sag or between the phases that has experienced the sag is indicated as V. In table 1 sag types are shown considering phase A as the reference phase. It means that another set can be derived for phase B or C are set as the reference phase. This classification is the base for international standard IEC 61000-4-11[18], because it makes possible generation of the seven types of voltage sag.

VIII. ACCEPTABLE LEVEL OF VOLTAGE SAG CURVE

This is generally determined by power quality curves, a plot of voltage magnitude versus time. Power quality curves represent the intensity and duration of voltage disturbances. The Computer and Business Equipment Manufacturers' Association (CBEMA), and Semiconductor Equipment and Materials Institute (SEMI) have published information defining what levels of poor power quality, specifically voltage sag, equipment should be able to tolerate. Other power quality curves in common use today were developed by the American National Standards Institute (ANSI) and the Information Technology Industry Council (ITIC).

The ANSI curves plot the deviation from nominal voltage as a percentage of nominal voltage compared to the duration or the maximum length of time the voltage is permitted to reach. For example, the limit for voltage occurrences greater than 1 second duration might be $\pm 10\%$. The ITIC and CBEMA curves also plot voltage with respect to duration, but as a percentage of absolute voltage. Electronic equipment can typically withstand high voltages provided they last for less than 1 millisecond in duration, but voltages greater than $+10\%$ or -20% for between 0.5 seconds and 10 seconds duration are to likely create problems.

ITIC also shows that computer equipment should be able to ride through short-duration voltage sags, if the voltage doesn't go below 70%. For sags of longer duration, voltages below 80% could affect the equipment. Even SEMI F47 semiconductor industry standard specifies an improved voltage sag ride-through for process tools. It requires a ride-through down to 50% voltage for 200 milliseconds, which will significantly reduce the number of voltage sags that may cause process disruptions in semiconductor plants. These curves are merely guidelines, and some electronic equipment may require higher power quality conditions than those represented in these standards.

IX. VOLTAGE SAG INDICES

PQ indices are key issue to indicate the different performance experienced at the transmission, sub-transmission, substation and distribution circuit levels. There are various ways of presenting voltage sag performance [16].

- a. SARFI (System Average Rms Variation Frequency Index)
- b. SIARFI (System Instantaneous Average Rms Variation Frequency Index)
- c. SMARFI (System Momentary Average Rms Variation Frequency Index)

The most common index use is the SARFI. This index represents the average number of voltage sags experienced by an end user each year with a specified characteristic. For SARFI_X, the index would include all of the voltage dips where the minimum voltage was less than X (where X is a number between 0 and 100) gives the number of events with a duration between 10 milliseconds and 60 seconds and a retained voltage less than X%. SARFI₇₀ gives the number of events with retained voltage less than 70% [17, 18]. Standard voltage thresholds are 140, 120, 110, 90, 80, 70, 50, and 10 % of nominal.

X. ECONOMICAL IMPACT OF VOLTAGE SAG

The cost associated with the voltage sag is more compared to other power quality issues:

- a. The cost to North American industry of production stoppages caused by voltage sags now exceeds US\$250 billion per annum [9].
- b. In South Africa, a recent study showed that major industries suffer annual losses of more than 200 US\$ million due to voltage sag problems [11].
- c. A study in United States (U.S.), the total damage by voltage sag may amount to 400 Billion Dollars [12].
- d. Manufacturing facilities have cost ranging up to millions of dollars attributed to a single disruption of the process whereas the cost to commercial customer (e.g., banks, data center, customer service centers, etc.) can be just as high if not higher [14].
- e. In automotive industry, four-cycle voltage sag can lost over 700,000 US\$ in the following 72 minutes due to shut down of process and required rework from malfunction of programmable controllers and drive systems working in a real-time process environment [19].
- f. One automaker estimated that the total losses from momentary voltage sag at all its plants runs to about \$10M a year [1].
- g. Manufacturing facilities have costs ranging from Rs.4, 00,000 to millions of rupees associated with a single interruption to the process. Momentary interruptions or voltages sags lasting less than 100 ms can have the same impact as in outage lasting many minutes [20].
- h. If an interruption costs Rs.16, 00,000, the total costs associated with voltage sags and interruptions would be Rs.2, 70, 40,000/-year. (The total cost is approx. 17 times the cost of an interruption) [21].

The table 3 shows some industries and their loss per event due to voltage sag and table 4 shows Cost of Momentary interruption due to voltage sag.

Table 3. Industries and their loss per event

Sl.No	Industry	Loss per event (US\$)
1.	<i>Semiconductor industry</i>	2,500,000
2.	<i>Credit card processing</i>	250,000
3.	<i>Equipment manufacturing</i>	100,000
4.	<i>Automobile industry</i>	75,000
5.	<i>Chemical industry</i>	50,000
6.	<i>Paper Manufacturing</i>	30,000

Table 4. Shows industries & their Cost of Momentary interruption [22]

Sl.No	Industry	Cost of Momentary interruption	
		Minimum	Maximum
1.	<i>Semiconductor Manufacturing</i>	\$20.0	\$60.0
2.	<i>Pharmaceutical</i>	\$5.0	\$50.0
3.	<i>Electronics</i>	\$8.0	\$12.0
4.	<i>Communications, Information Processing</i>	\$1.0	\$10.0
5.	<i>Automobile manufacturing</i>	\$5.0	\$7.5
6.	<i>Food processing</i>	\$ 3.0	\$ 5.0
7.	<i>Glass</i>	\$4.0	\$6.0
8.	<i>Petrochemical</i>	\$3.0	\$5.0
9.	<i>Textile</i>	\$2.0	\$4.0
10.	<i>Rubber & plastics</i>	\$3.0	\$4.5
11.	<i>Metal fabrication</i>	\$2.0	\$4.0
12.	<i>Mining</i>	\$2.0	\$4.0
13.	<i>Hospitals, Banks, Civil services</i>	\$2.0	\$3.0
14.	<i>Paper</i>	\$1.5	\$2.5
15.	<i>Printing (News Paper)</i>	\$1.0	\$2.0
16.	<i>Restaurants, bars, hotels</i>	\$0.5	\$1.0
17.	<i>Commercial shops</i>	\$0.1	\$0.5

XI. MITIGATION OF VOLTAGE SAG

There are several ways to mitigate the voltage sag:

a. From Fault to Trip: The equipment trip is the main cause of voltage sag, if there are no equipment trips due to short-circuit fault, there is no voltage sag problem. Due to short circuit at the fault position, the voltage drops to zero, or to a very low value. This zero voltage is changed into an event of a certain magnitude and duration at the interface between the equipment and the power system. If the fault takes place in a radial part of the system, the protection intervention clearing the fault will also lead to an interruption. If there is sufficient redundancy present, the short circuit will only lead to voltage sag. If the resulting event exceeds a certain severity, it will cause an equipment trip. The equipment trip due to short circuit fault can be minimized by:

- Reducing the fault-clearing time.
- Changing the system such that short-circuits faults result in less severe events at the equipment terminals or at the customer interface.
- Connecting mitigation equipment between the sensitive equipment and the supply.
- Improving the immunity of the equipment.

b. Reducing the Number of Faults:

Short circuits cannot be entirely eliminated. The majority of failures are due to faults on one or two distribution lines. Below mentioned fault mitigation measures may be expensive, especially for transmission systems but their costs have to be weighed against the consequences of the equipment trips. The actions taken are:

- Replacing overhead lines with cables.
- The use of insulated conductors on overhead lines.
- Regular tree cutting in the area of the transmission line and fencing against animal.
- Shielding overhead conductors with additional shield wires and by increasing insulation level.
- Increased frequency of overhaul and periodic maintenance, cleaning insulators etc.

c. Reducing the Fault-Clearing Time: To minimize the fault clearing time several types of fault current limiters (able to clear a fault within one half-cycle) are in use for low and medium voltage systems i.e. few tens to kilovolts, but actually they do not clear the fault, they only reduce the current magnitude within one or two cycles. Reducing the fault clearing time of any event does not reduce the number of events occurring, but can reduce the severity of fault impact. Recently introduced static circuit breaker has the same characteristics as fault current limiters. Fault-clearing time is not only the time needed to open the breaker, but also the time needed for the protection to make a decision.

d. Changing the Power System: The cost associated with changing the supply system may be high, especially for transmission and sub transmission voltage levels. But in case of industrial systems, the design stage will outweigh the cost. Some other ways to mitigate the voltage sags are:

- By installing a generator near the sensitive load. The generators will keep up the voltage during remote sag.
- Split buses or substations in the supply path to limit the number of feeders in the exposed area.
- Determine the frequency, depth & duration of the voltage sag. Collection of data is essential if the optimal solution is to be determined.
- In order to provide a cost effective solution to voltage sag problems, it is necessary to determine which equipment is more subjected to voltage sag.

XII. INSTALLING VOLTAGE SAG MITIGATING EQUIPMENT

There are number of mitigating devices used to mitigate the voltage sag:

a. Device Voltage Restorer (DVR): DVR uses modern power electronic components to insert a series voltage source between the supply and the load. The voltage source compensates for the voltage drop due to the sag. The DVR is a series connected FACTS device to protect sensitive loads from supply side disturbances; it can also act as a series active filter, isolating the source from harmonics generated by loads. This is often the best solution when voltage sags are the dominant concern. DVR is also used for protecting individual loads or group of loads.

b. Uniform Power Quality Conditioner (UPQC): is the integration of series and shunt active filters, connected back to back on the dc side and share a common DC capacitor. The series connected UPQC is responsible for mitigation supply side disturbances such as voltage sags, flickers, voltage unbalance and harmonics. The shunt component is responsible for mitigating the current quality problems caused by consumer: poor power factor, load harmonic currents, load unbalance etc. It can perform the function of both DSTATCOM and DVR [23].

c. Uninterruptible Power Supply (UPS): Utilize batteries to store energy that is converted to a usable form during outage or voltage sag. This is the most commonly used device to protect low-power equipment (computers, etc.) against voltage sags and interruptions. During the sag or interruption, the power supply is taken over by an internal battery. The battery can supply the load for, typically, between 15 and 30 minutes.

d. Motor-Generator Sets (M-G Sets): It usually utilizes flywheels for energy storage. They completely decouple the load from the electric power system. Rotational energy in the flywheel provides voltage regulation and voltage support during under voltage conditions. M-G sets have relatively high efficiency and low initial capital cost. They are only suitable for industrial environment due to noise and the maintenance required compare to office environment.

e. Ferro resonant, Constant Voltage Transformers (CVTs): can be used to improve voltage sag ride through capability. CVTs are especially attractive for constant, low power loads, variable loads, especially with high inrush currents, present more of a problem for CVTs because of the tuned circuit on the output. CVTs are basically 1:1 transformers which are excited high on their saturation curves, thereby providing output voltage which is not significantly affected by input voltage variations.

f. Static transfer switch: A static transfer switch switches the load from the supply with the sag to another supply within a few milliseconds. This limits the duration of sag to less than one half cycle, assuming that a suitable alternate supply is available.

XIII. CONCLUSION

Voltage sag is an avoidable natural phenomenon in a power system; faults in the system are the main reason for the voltage sag. The issues related to voltage sag are gaining importance because a small power outage has a great economical impact especially on the industrial consumers. A longer interruption harms practically all operations of modern society sensitive equipment. So it is necessary to have awareness regarding damages caused by voltage sag by analyzing their characteristics, types, its places of occurrence, percentage of damages caused by the presence of sag, acceptable level of sag curve and its indices. Lastly by taking following some strict measures and by installing mitigating equipment the voltage sag can be avoided upto certain extent.

REFERENCES

- [1] Alexander Eigel Emanuel, John A. McNeill "Electric Power Quality". Annu. Rev. Energy Environ 1997.22:263-303.
- [2] Bong-Seok Kang et al; "A Study of the Impact of Voltage Sags and Temporary Interruptions on 3-Phase Induction Motors", Dept. of Electrical Engineering, Soongsil University, Sangdo-dong, Dongjak-Gu, Seoul, 156-743, Korea.
- [3] Pirjo Heine and Matti Lehtonen, "Voltage sag distributions caused by power systems faults," IEEE Transactions on Power Systems, vol.18, No.4, pp.1367-1373, November 2003.
- [4] Ward, D.J. (2001). Power quality and the security of electricity supply. Proceedings of the IEEE, Vol. 89, Issue: 12, Dec. 2001, pp: 1830 –1836.
- [5] M. Firouzi et al; "Proposed New Structure for Fault Current Limiting and Power Quality Improving Functions", International Conference on Renewable Energies and Power Quality (ICRE PQ'10) Granada (Spain), 23rd to 25th March, 2010.
- [6] Ward, D.J. (2001). Power quality and the security of electricity supply. Proceedings of the IEEE, Vol. 89, Issue: 12, Dec. 2001, pp: 1830 –1836.
- [7] P.Zanchetta et al, "New power quality assessment criteria for supply systems under unbalanced and nonsinusoidal conditions", IEEE trans. on Power Delivery, vol.19, no.3, July.2004 pp1284-1290.
- [8] Sharmistha Bhattacharyya et al; "Consequences of Poor Power Quality – An Overview", Technical University of Eindhoven The Netherlands.
- [9] CIGRE/CIREP/UIE JWG C4.110, Voltage dip immunity of equipment and installations, CIGRE Technical Brochure 412, published in 2010.
- [10] Halpin, S.M. "Power Quality" *The Electric Power Engineering Handbook* Ed. L.L. Grigsby Boca Raton: CRC Press LLC, 2001.
- [11] Suresh Kamble et al; "Characteristics Analysis of Voltage Sag in Distribution System using RMS Voltage Method", ACEEE Int. J. on Electrical and Power Engineering, Vol. 03, No. 01, Feb 2012.
- [12] Suresh Kamble et al; "Characterization of Voltage Sag Due To Balanced and Unbalanced Faults in Distribution Systems" International Journal Of Electrical Engineering. Volume 3, Issue 1, January- June (2012), pp. 197-209.
- [13] M.H.J. Bollen, "Characterization of Voltage Sag Experienced by Three-Phase Adjustable-Speed Drives", *IEEE Transactions on Power Delivery*, Vol.12, No.4, pp.1666-1671, Oct. 1997.
- [14] Math H. J. Bollen, "Understanding Power Quality problems: Voltage Sags and Interruptions", IEEE Press, 2000.
- [15] Florin MOLNAR-MATEI et al; "New Method for Voltage Sags Characteristics Detection in Electrical Networks", 978-1-4244-5794-6/10/\$26.00 ©2010 IEEE.
- [16] J. Wang, S. Chen, and T. T. Lie, "System voltage sag performance estimation," *IEEE Transactions on Power Delivery*, vol. 20, pp. 1738-1747, April 2005.
- [17] David B. Vannoy et al; "Roadmap for Power-Quality Standards Development" , Ieee Transactions On Industry Applications, Vol. 43, No. 2, March/April 2007.
- [18] L.P. Singh et al; "A New Approach for Analysing Voltage Sag Severity Based on Power Quality Indices", International Journal on Emerging Technologies 4(1): 1-5(2013).
- [19] Nita R. Patne et al; "Factor Affecting Characteristic of Voltage Sag Due to Fault in the Power System", Serbian Journal Of Electrical Engineering Vol. 5, No. 1, May 2008, 171-182.
- [20] S. GUPTA, "Power Quality: Problems, Effects And Economic Impacts" International Journal of Electrical and Electronics Engineering (IJEEE) Vol.1, Issue 1 Aug 2012 83-91 © IASET.
- [21] M.Mc Granaghan et al, "Economic evaluation of power quality", IEEE Power engineering review, Vol.22, no.2, Feb.2002, pp8-12.
- [22] Recommended Practice for Monitoring Electric Power Quality, 1995. IEEE Std. 1159, IEEE.
- [23] L. Dinesh et al; "Simulation of Unified Power Quality Conditioner for Power Quality Improvement Using Fuzzy Logic and Neural Networks" Innovative Systems Design and Engineering ,Vol 3, No 3, 2012.

Electrical Energy Potential from Municipal Solid Waste in Rajshahi City Corporation, Bangladesh

A.Z.A. Saifullah

¹Department of Mechanical Engineering, IUBAT- International University of Business Agriculture and Technology, Dhaka 1230, Bangladesh

Abstract: -This paper presents the assessment of the electrical power generation potential from municipal solid waste (MSW) in Rajshahi City Corporation (RCC), Bangladesh. RCC generates huge amount of solid waste (SW) which is left very poorly managed due to crisis in governance. About 80% of organic food wastes are the major constituents of SW generated in RCC in the year 2012. Electrical energy can be produced from SW generated in RCC as a sustainable commercial solution. The average calculated value of heat content of MSW of the year 2012 based on the data of MSW of 2005 (MSW: 2005) and MSW of 2012 (MSW: 2012) is 7234.5 kJ/kg, which is sufficient to produce electricity. Integrated sustainable waste management (ISWM) has to be put into operation to harness energy from MSW. A 645.543 ton/day energy recovery Mass Burn Incinerator (MBI) system of 19.71% overall efficiency is to be used. It is found that potential of electrical energy generation from MSW in RCC during the years 2012 and 2025 is 5.336 MW and 10.568 MW respectively.

Keywords: -Rajshahi City Corporation; Municipal Solid Waste; Renewable Energy; Integrated Sustainable Waste Management; Mass Burn Incinerator

I. INTRODUCTION

Fast rising population level, explosion of economic growth, rapid urbanization and the ascend in community living standards are the detrimental factors responsible for the accelerated rate of municipal solid waste (MSW) generation in developing countries [1, 2]. Solid waste management (SWM) appears to be a worldwide growing challenge in urban areas, especially in the rapidly rising towns and cities of the developing countries [3-6]. SWM reflects a foremost environmental and economic issue almost in all countries [7, 8]. But municipal solid waste management (MSWM) is an extremely ignored spot mostly in urban cities of developing countries [9-15]. Due to progressive urbanization, the management of SW is appearing as a major threat to environment and public health in urban zones. But SWM is a vital environmental health service. It is a primary indispensable urban service. From the primitive era efforts have been made for safe disposal of SW. In those days habitations were scanty and land was abundant. With the rapidly growing urbanization a large number of people have started to flock in short spaces to hunt their livelihoods. As a result of the increase in density of population in the places of congregation, the waste generation per unit area has been also increased. Available land for waste disposal has been proportionately reduced. Disposal has been recognized as the most awkward functional element of SWM in developing countries. The factors causing the problems of SWM in developing countries are mainly technical and financial deficiencies [16, 17]. Other factors which hamper the effective SWM are institutional, economic and social ones [18].

In developing countries, the common problems associated with SWM are manifestation of irregular collection services and low collection coverage, poorly managed and illegal open dumping, burning without air, pollution of ground and surface water sources, breeding of vermin and flies and handling of informal waste picking or scavenging activities [84, 88]. Industrialization with rapid urbanization altered the distinctiveness of SW produced. It signifies the need of updating the solid waste management system (SWMS) to suit the waste quality, quantity and composition [15, 18, 19]. It may be noted that waste composition and characteristics varies from source to source [21].

Saving the space of disposal sites and reducing illegal open crude dumping and thereby cutting down on potential from SW can be achieved through minimizing waste generation by modifying the management practices at the source [17].

Urbanization is now a worldwide trend, but its growth is rapid predominantly in developing countries. The world urban population is anticipated to double to more than 5 billion people in the next 35 years, having 90% of this growth in the developing world [20, 22]. Statistics reveals that the world population touched 6 billion in 2001 with 46% of it dwelling in urban areas [23]. The SW generated globally was 0.49 billion tons, the estimated annual growth rate being 3.2-4.5% in developed nations and 2-3% in developing nations [24].

Every place from small house to large industry produces waste. The population and use of resources is higher in urban areas. Consequently, the waste generation rate in those areas is also high. Urban areas produce two to three times more SW than rural ones. According to the estimation of a report by World Bank, the SW generation in urban areas of East Asia alone will shift from 760,000 ton/day to 1.8 million ton/day within 25 years. Consequently, waste management costs will be approximately double from US \$ 25 billion per year to US \$ 47 billion by 2025 [25, 26].

The awareness of the adverse impact of improper handling of MSW has led the developing nations to address this issue with increasing necessity [10, 27]. Usually, about 50% of the residents in urban areas of low and middle income countries do not get MSW collection services. This is, because, municipal authorities are either unwilling or unable to provide services to all residents. The openings for the development of a sustainable MSW system are inadequate for the limitation of government budgets. Proper disposal of SW is considered as something costly [28, 29]. Municipalities are mainly responsible for MSWM in the cities. It is too difficult for them to make available an effective and efficient SWMS to the residents. The issues they face in SWMS are legal, socio-cultural, environmental, political, economic, institutional, technical and available resources. These factors are interrelated which causes the MSWM multidimensional and complex [30-33]. All these issues require to be addressed properly to accomplish a sustainable solution for MSWM. Instead of environmental legislation itself, generally, what it counts is need of implementation and/or doable substitutes [34]. Integrated Sustainable Waste Management (ISWM) Model is the model which implements an integral method to study complex and multidimensional systems. WASTE advisers on urban environment and development [35] and partners or organizations working in developing countries in the mid-1980s developed this model. Collaborative Working Group (CWG) developed it further in mid-1990s [36]. The model recognizes the significance of three dimensions in analyzing, developing or changing waste management system (WMS). The dimensions are the stakeholders who have an interest in SWM, the elements or stages of the movement or flow of materials from the generation points towards treatment and final disposal and the facets through which the system is analyzed [37-44].

It is obvious that decreasing the amount of waste generated is the technique to evade the brunt on the environment. If it does not work, recycling or re-using the waste is the best option. When these alternatives are unbecoming, burning (incinerating) the waste to generate electricity with recent advantages of combustion technology, materials and recycling technology is attractive. Utilization of landfills is the last choice [45-47].

Studies have been reported on electrical energy recovery potential from MSW generated in different countries. A study in Jordan estimated the energy content of MSW generated on its physical composition. It shows that the MSW generated is 2150 ton/day by 4.3 million population of Jordan in 1996. It would yield electrical energy of 1.77 MW/day [48].

The ratio of total MSW incinerated electricity generation (2.616×10^9 KWh) to total electricity production (1.738×10^{11} kWh) in Taiwan during the year of 2003 was about 1.51%. It signifies effective conversion of MSW-to-energy [49].

An assessment of the electricity generation potential from MSW in Kuala Lumpur, Malaysia was conducted by Kathirvale et al. They estimated the energy potential from an incineration plant operating on SW of 1500 ton/day to be 640 kW/day [50].

In Bangladesh, Alam and Bole analyzed the possibility for the SW to electrical energy generation and its economic viability in Dhaka City. It is mentioned that the annual 1.28 million of MSW generation could produce 71 MW of electricity [51].

A system dynamics model has been developed for investigating MSW produced in Dhaka city, Bangladesh and to estimate its potential to generate electricity. Electrical energy generation potential was 456,900 MWh in 1995, which increases to 1,894,400 MW in 2025 [52]. Potential electrical energy generation was calculated in a similar way as performed by Alam and Bole [51] and Islam and Saifullah [53].

A comprehensive analysis of power production from MSW incineration plants in Taiwan since 2000 has been given by Tsai and Kuo. Waste-to-energy (WTE) power generated (i.e., 2967 GWh) in 2008 has been taken as the basis. Preliminary calculation showed that the environmental benefit of mitigating CO₂ emissions was around 1.9×10^6 tons and the economic benefit of selling electricity was US\$ 1.5×10^8 [54].

MSW generation, collection and disposal data of Kampala City, Uganda was analyzed using Microsoft Excel and LandGEM model to find out the electrical energy generation potential at landfill. MSW collection of Kampala City has elevated from 7.76% in 1997 to 38.8% in 2007 of the calculated MSW generated. 70% of the MSW in the landfill is organic, enabling the landfill a high potential of methane generation [55].

A novel WTE technology was implemented in Changchun MSW power plant, China. This technology applies co-firing of MSW with coal in a grate-circulating bed (CFB). Two 260 ton/day incinerators incinerated 137,325 tons in 2006, which is nearly 1/6 of the MSW generated in Changchun. It saved landfill space of more than of 0.2 million m³. In total, 46.2 KWh of electricity was generated, and emission of air pollutants was low [56].

Renewable power generation opportunity from MSW has been studied for Lagos Metropolis (Nigeria). The electrical energy generation potential from MSW through the route of thermo-chemical conversion has been remarkably discussed as an alternative step to landfilling and open dumping of waste commonly practiced in the metropolis. Around 442 MWe can be achieved for a population of over 16 million recorded in 2006 [57].

A mathematical model based on the composition of the waste in India has been investigated on the power generation from MSW. Linear equations have been written to represent various flow paths of waste. Then the mass balance equations have been solved for minimum cost as the main objective [58].

The energy recovery potential from MSW in Chile has been evaluated by a proposed methodological approach on the basis of a techno-economic assessment. Electrical energy options considered are landfill gas-to-energy (LGTE), direct WTE and landfill gas recovery and upgrading to feed into the grid (LGU) [59].

Bangladesh is one of the densely populated (1,125 per sq km) Least Developed Asian Countries (LDACs). MSW is generated at a very high increasing rate in the urban areas of Bangladesh mainly due to rapid urbanization and population growth. 40 – 60% of MSW are not properly stored, collected or ultimately disposed in the designated sites. This unmanaged MSW appears as an environmental, social and professional threat to city dwellers, urban planners and other concerned stakeholders [60, 61]. This scenario is distinctly visible in all the city corporations of Bangladesh, namely, Barishal City Corporation, Chittagong City Corporation, Dhaka (North) City Corporation, Dhaka (South) City Corporation, Khulna City Corporation, Komilla City Corporation, Narayanganj City Corporation, Rajshahi City Corporation, Rangpur City Corporation, Sylhet City Corporation and Gazipur City Corporation.

It is necessary to think and analyze whether waste is really waste, and if it is possible to manage MSW in such a way so that trash can be translated into cash. To find a sustainable commercial solution for MSW produced in RCC by generating electrical energy is the purpose of this paper. More specifically the objectives of the study are:

- (i) To implement ISWM.
- (ii) To estimate population till 2025.
- (iii) To estimate the amount of MSW produced per day till 2025 and estimate how suitable it is for energy production.
- (iv) To estimate the amount of energy produced by the MBI.
- (v) To ascertain the possibility whether it can be established as a power generation system as well as SWMS in RCC.

The volume, the density and proportions of components of the MSW generated vary from city to city depending upon level of socio-economic development, weather and geographic location [103, 104]. Populated cities of developed countries generate more quantity of wastes and their quality, i.e., heating value is higher [62].

WTE policy not only ensures effective and efficient MSWM but also solve the problem of scarcity of electricity. This study encompasses (a) the heating values of all the components of MSW with different moisture contents, (b) the amount of energy produced for conversion into electricity and the total possible electrical energy generation and (c) the justification of the electricity generation from the MSW in RCC is feasible or not.

II. METHODOLOGY

2.1 MSW

Garbage, refuse, trash and rubbish are the synonyms to SW. The term MSW implies to SW generated from houses, streets, public places, shops, offices, hospitals and industrial processes, which are mainly the responsibility of the municipal or other government authorities [63]. Domestic waste, commercial waste, institutional waste, industrial waste and street sweeping waste belong to MSW.

Fossil fuel and other conventional energy sources supply 90% of the global energy needs, whereas other 10% comes from biomass. Excessive combustion of fossil fuel for energy generation results in serious environmental hazards such as global warming. Power generation from renewable energy sources is increasingly becoming popular for rational benefits. MSW is composed of both organic and inorganic components. Organic fraction of MSW (OFMSW) is its most useful part. OFMSW is biodegradable. MSW is generated on daily basis. MSW is considered as a new source of energy called renewable energy source as it is available in abundance and contains biomass in huge amount [64, 65].

2.2 Description of study area

July 2006 estimation shows that Bangladesh is the seventh highest populated nation, having population of 147.36 million [66]. Rapid urbanization is taking place in the densely populated country and a large quantity of people is moving from rural to urban regions each year [33, 67].

The annual increase of the total population of the country is about 1.4%, whereas the annual growth of its urban population is about 3.27%. The above comparison simply indicates rapid urbanization. The current urban population of Bangladesh is 40 million, which is about 28% of the total population of the country. It is expected that the urban population will be 116 million by 2040 which is but 50% of the total population [69]. It may be mentioned that estimated total urban population of Bangladesh was 32,765,516 in 2005 and total waste generation was 13,332.89 ton/day. In 2025, total urban population is estimated to be 78,440,000, which is 40 percent of total population. The corresponding total urban waste generation will be 47,000 ton/day [70 - 72].

2.2.1 Rajshahi City Corporation (RCC)

The head quarter of Rajshahi Division of Bangladesh is Rajshahi City. It stands on the north of the river Padma. Rajshahi Municipality earlier known as Rampur Boalia was formed a municipality in 1876. It was renamed as Rajshahi Pourashava and finally endowed the status of a City Corporation in 1991. The minimum and the maximum temperature range between 10 to 27^oC and 24 to 36^oC respectively from year to year. Rajshahi experiences the highest temperature during April and May. The annual rainfall is around 1400 mm. The current population of RCC is 795,451. The male population and the literacy rate (more than 7 years old) are 53.63% and 69.3% respectively as per 2001 census. RCC covers an area of 96.69 sq. km. The entire area is served by 384 km metalled and 96 km unmetalled road networks. There are about 118 km brick-built and 162 km unbrick-built drains in the City Corporation. RCC is distributed in 30 wards. RCC generates MSW of about 292.323 ton/day. About 50% of MSW are collected and dumped in the open dumping ground. The rest of the MSW remain uncollected and gets littered around the city.

The drains of Rajshahi City are typically uncovered and as such they collect a lot of MSW. Some of the smaller drains are lined but the main arteries are plain. These surface run-offs drains act as sewers and receive a large majority of the grey water in the city including domestic wastes and also wastes from commercial units, markets and small industries. A proportion of MSW ends up in the storm water drains which in turn flow to the field. There are facilities for door to door collection only in 13 wards. RCC possesses only one landfill (3.5 feet deep in 15.98 acre area) site located at Tikhor Vagar. Besides, there are 35 collection points and 1200 dustbins [73-76].

Migration from rural to urban area is leading to unplanned urbanization and slum development.

A huge amount of unmanageable SW is produced in these areas in all major cities of Bangladesh including Rajshahi city [68, 77]. This has given rise to a great increase in need for waste management facilities. The issue of poor MSWM is detrimental to environment, public health and safety. To ensure betterment of MSWM necessitates storage, collection and proper disposal of SW [78, 79]. The capacity of the city instruments has become inadequate to provide efficient and effective conservancy services to the rapid increase in urban population growth. About 50% of the refuse produced daily is left unattended in the six city corporations of Bangladesh. The crisis of the urban governance can be overcome by public-private partnerships for efficient MSWM [78, 80]. The MSW of RCC is only used as a material for landfilling and is a serious issue. Still rooms are there for further improvement to achieve an effective MSWM.

The demand of electricity in Rajshahi is 65 MW, whereas Power Development Board supplies only 25 MW. No electricity generation unit has been set up yet. As a consequence, the city has to face acute load-shedding and unpredictable power supply quite so often. Mills and factories are experiencing slow down due to frequent load shedding. Instant power supply appliances have got their sale sharply elevated at the outskirts. In this situation, alternative source of electric power generation is an absolute necessity [81, 82].

2.3 Integrated Sustainable Waste Management (ISWM)

MSWM is a crucial financial, environmental and social concern in the city lives of RCC. RCC cannot administer the increasing amount of waste generated. The reasons for the incapability of RCC to handle MSW are insufficient facilities, lacked environmental controls, inadequate institutional structure, poor understanding of complex systems and deficient sanitation, etc. [83-85].

A sustainable solution for SW produced in RCC is possible through ISWM. ISWM, defined by Tchobanoglous et al. as integrated solid waste management, is the choice and implementation of suitable technologies and management procedures for incorporating more environmental and economic friendly concepts to rationalize all the stages of SWM, i.e., the separation of source, gathering and haulage, transfer stations and material recovery, treatment and resource recovery and final disposal by legalizing the informal schemes, public participation and partial privatization. In industrialized nations, the general waste hierarchy is in the order: reduce, reuse, recycle, recover waste through physical, biological or chemical processes (e.g. composting, incineration) transformations and landfilling [21, 85, 86]. Thus far, Bangladesh has adapted a national strategy for ISWM solely based on the approach of 3R (reduce, reuse and recycle).

2.4 Disposal of MSW

Disposal of MSW must be properly carried out to lessen degradation of land resources and environmental health impact. MSW is generally disposed of by transporting and releasing it in open dumps in LDCAs. This is environmentally insecure. Systematic disposal methods are as described below:

2.4.1 Composting

Composting is the controlled biological decomposition of organic waste such as plants or food by bacteria, fungi, worms and other organisms under aerobic conditions. It is applicable to organic waste only. It is a very slow process. It is one of the oldest methods of SWM [87].

2.4.2 Land Filling

Land filling is one of the easiest and cheapest methods of SWM burn out mines. Dumping of SW is done in low level areas to level the ground for useful purpose. But land filling releases poisonous gases like methane causing environmental deterioration [87]. A few resource recovery plants are available in Bangladesh. Land filling is the only means in most cases of MSW disposal here [78].

2.4.3 Waste to energy (WTE) plants

The concept of biomass application for energy generation is of growing demand throughout the world. Exploitation of renewable energy resources specifically MSW is possible and it will aid to supply primary energy needs at households and for some commercial applications. Electric power can be harnessed from OFMSW. Power plants using MSW are also known as WTE plants. The technologies adopted are based on thermo-chemical and bio-chemical conversion. The three common WTE technologies are gasification, anaerobic digestion and combustion [28, 57]. Thermal treatment can reduce the volume of MSW by up to 90% and thus at a time deal with two problems: disposal of MSW and electricity generation [57, 89]. Besides, effective use of natural resources is a great step towards sustainable development [90].

2.4.3.1 Gasification of MSW

Gasification of MSW to generate energy needs thermo-chemical conversion reactions. The process brings on production of various gases like carbon dioxide, methane, steam and other byproducts such as tar and ash at elevated temperature and low concentration of pure oxygen or air. Methane is the main product in this process. Undergoing through some cleaning processes it can be directly used to run an internal combustion (IC) engine to generate electricity [57]. Gasification may reduce the mass of MSW by 70-80% and volume by 80-90% while it preserves the land area for waste land filling [91, 92]. The process involves waste collection, transportation, sorting, and conversion process, then electricity generation via a generator.

2.4.3.2 Anaerobic digestion

Anaerobic digestion is entirely a process of bio-chemical conversion for production of energy-fuel in a well-controlled enclosed space called digester. It is used to treat both dry and wet biomass resources. It implies microbial actions on bio-waste in absence of oxygen to produce biogas. The complete process is multifarious and involves a series of heterogeneous chemical reactions such as hydrolysis, acetogenesis and methanogenesis. These integrated processes degrade organic waste resulting in biogas and other energy-rich organic compounds [93, 94]. It is suitable for small scale electricity production in remote corners of developing countries.

2.4.3.3 Incineration

Incineration is another process of thermo-chemical conversion to generate energy from MSW either in the form of heat or electricity. WTE plants are fabricated for MSW disposal and electricity generation as a byproduct of the incineration. The most common WTE technology is mass burn of MSW as fuel. The MSW can be in unprocessed or minimally processed form [114, 116].

In a mass burn incinerator (MBI), incoming trucks carry the MSW into pits. The MSW is mixed by crane there and bulky or large un-combustible items are taken away. To prevent odors from being released to the environment, the MSW storage area is kept at pressure lower than atmospheric. The cranes carry the MSW to the combustor charging hopper to feed the boiler.

Heat of combustion is used to convert water into steam turning a turbine generator assembly. The steam is then condensed by traditional methods and taken back to the boiler. Residues are bottom ash, fly ash and residue from the flue gas cleaning system.

Incineration converts heterogeneous wastes into more homogeneous residues. The most significant advantage of MSW incineration is the weight decrement by up to 75% and reduction of volume by up to 90%. This can be cost-effective if landfill space is scarce [95-97].

Waste incineration technology is composed of three basic components: incinerator, energy recovery unit and air pollution control system [68, 98]. Due to combustion MSW is converted into ash, flue gas (oxides of sulphur, carbon and nitrogen) and heat. Mostly the inorganic fraction of MSW forms the ash. The flue gases have to be cleaned of gaseous and particulate pollutants by incorporating a pollution control system in a complete set-up of MBI to avoid atmospheric pollution. The operating temperature range of a MBI is 800-1000⁰C [57, 87]. Air is continuously supplied during incineration to ascertain complete combustion of the components to stable and natural molecular forms. The solid residues can either be transferred to landfills or can be used off-site for specific construction purposes after cleaning up [116].

For a sustainable commercial solution of MSW generated in RCC, an energy recovery MBI system will be used which is the same as shown by Islam and Saifullah [53]. Figure 1 shows the energy recovery MBI system for MSW of RCC.

2.5 Estimation

The SW generated in RCC is mainly non-hazardous type. These are food wastes (vegetable trimming, part of food not taken, slough of onion, green pepper, garlic, etc.), papers, packages, plastic bags, polythene, animal and fish bones, weeds, ashes, broken glass, tin, worn cloth, casing, cover of pharmaceuticals and many other things. Industrial wastes are also there. Most of the times, the wastes are piling up on roads, junction of roads, buildings, shops, schools, colleges, etc. The wastes are generated from different sources and have various components. Figure 2 (a) shows typical components of SW in RCC in % by weight during the period 1991-2001. Figure 2 (b) shows different sources of SW generation in RCC in % by weight during the period 1991-2001 [53, 99].

Urbanization of RCC has been taking place through area expansion, population growth and rural to urban migration. Right from the independence of Bangladesh in 1971, the population growth of RCC has been rising at a high rate due to migration of a large number of people from different regions of Bangladesh to RCC for education, job and business opportunities. This has given rise the total population to be increased by about 10% due to floating population from 2005 and onward [70, 100]. It may be mentioned that low income countries are, especially, facing rapid urbanization. In 1985, the world population living in urban areas was 41%, and is expected to increase to 60% by 2015 [101, 102].

The estimated total population of RCC in 1991 and 2001 was 294,056 and 388, 811 respectively.

Due to lack of information, the amount of MSW generated in RCC in 1991 and 2001 was estimated to be 53 ton/day and 113.33 ton/day [53, 99]. This estimation is based on empirical relation, i.e., the information of other cities and countries having similar socio-economic condition to that of RCC. Some simple practical procedures like counting trucks and containers were also employed to calculate MSW generation. These predictions for waste generation were, thus, not realistic [83, 21].

Without any processing MSW of RCC contains about 60% moisture, and its average calorific value is 4.63 MJ/kg. When dried in the air the moisture content of MSW reaches 5-8%, and its average calorific value then becomes 8.37 MJ/kg. And, drying MSW by flue gases makes its average calorific value stand 11.04 MJ/kg. Possible emission of SO_x, NO_x and CO during combustion of MSW is very low [53, 114].

Considering mass-fired incinerator-boiler efficiency of 0.63 and steam turbine-generator system efficiency of 0.29 the overall efficiency of the MBI energy recovery system becomes 0.183. With station service allowance of 6% and unaccounted heat losses of 5% the net electric power export (NEPE) of the years 1991 and 2001 are evaluated to be 1.103 MW and 2.358 MW respectively.

Later detailed survey was done for waste generation in both dry and wet seasons using primary and secondary data as well to estimate for 2005, 2010, 2015, 2020 and 2025 with respect to the estimated population projected for those years. Waste generation in wet season has an increase of 46% by weight is considered [70, 100]. Including 10% floating population, total population of RCC in the years 2005, 2010, 2012, 2015, 2020 and 2025 are 468,378, 606,122, 661,219, 743,865, 881,609 and 1,019,352 respectively. The corresponding waste generation in these years in ton/day is 172.83, 282.14, 325.864, 391.45, 500.77 and 610.08. Figure 3(a) shows physical composition of SW of RCC in 2005 [100]. Figure 3 (b) shows SW generated daily in RCC from different sources in % by weight in 2005 [61]. Waste generation rate (WGR) in 2005 is 0.369 kg/capita/day.

The energy content of MSW has been determined for the OFMSW only by the Modified Dulong Formula as given below [105].

$$\text{Heat (kJ/kg)} = 337C + 1428 (H - O/8) + 9S$$

where

C = carbon (%)

H = hydrogen (%)

O = oxygen (%)

S = sulfur (%)

The value of the percentage of moisture content of individual component of MSW and data on ultimate analysis of the combustible components of MSW have been used to get finally the overall chemical composition of MSW of RCC [20, 81, 105-108].

The heat content of MSW of RCC in 2005 is found to be 8.299 MJ/kg.

In the MBI energy recovery (steam turbine – generator) plant using unprocessed MSW, 70% of heat energy is converted to steam energy. It may be mentioned that heat released from combustion of MSW is partly stored in the products of combustion (gases and ash) and partly transferred by conduction, convection and radiation to the incinerator walls and to the incoming waste. For the station or process power needs and unaccounted process heat losses allowance of 6% and 5% are considered respectively [105].

Energy available in MSW is found to be 16.601 MW and the NEPE is 3.269 MW for the year 2005. For the years 2010, 2012, 2015, 2020 and 2025 energy available in MSW are determined to be 27.100 MW, 31.300 MW, 37.601 MW, 48.101 MW and 58.600 MW respectively. And, the NEPE in those years is 5.336 MW, 6.163 MW, 7.403 MW, 9.471 MW and 11.538 MW respectively. Overall efficiency of the plant is found to be 19.69%.

Fig. 4 (a) shows physical composition of SW of RCC in % by weight in 2010 [81]. Figure 4 (b) shows SW generated daily in RCC from different sources in % by weight in 2010 [81]. Both primary and secondary data have been used collecting sample from different sources and in three main seasons: summer, monsoon and winter. In addition to domestic waste there are street sweeping, commercial including market waste, industrial waste, clinical waste and other source which includes packing materials, rags and other torn fabrics, garment materials and other trash [81, 109]. Including 10% increase for floating population, total population of RCC in 2010 was 825000 [110, 111]. WGR was 0.401 kg/capita/day. Total waste generated in RCC in 2010 was 330.825 ton/day. The heat content of MSW of RCC in 2010 is determined to be 7.673 MJ/kg. Energy available in MSW is estimated to be 29.38 MW and NEPE is 5.778 MW for the year 2010. Overall efficiency of the plant is found to be 19.666%.

Fig. 5(a) shows physical composition of MSW of RCC at landfill site in % by weight in 2012 [69]. Figure 5 (b) shows MSW generated daily in RCC from different sources in % by weight in 2012 [69]. Table 1 shows population, growth rate and area of RCC [112, 113].

Table 1: Population, Growth Rate and Area of RCC

Year	Population	Average Annual Growth Rate (%)	Area (sq km)
1981	165,821		29.83
1991	294,056	7.733	96.68
2001	388,811	3.222	96.68
Average Annual Growth Rate (1981-2001)		6.723	

For the decade (1991-2001) the annual population growth rate in RCC is 3.222%, which is considered as the low growth rate. The medium growth rate is the average annual growth rate 6.723% over the period (1981-2001). The high growth rate is the annual growth rate 7.733% over the decade (1981-1991).

Considering 2001 census population of 388,811 as the base population the projected total population including 10% increase for floating people under medium growth rate for the years 2005, 2010, 2012, 2015, 2020 and 2025 are found to be 554,851, 768,216, 874,996, 1,063,629, 1,472,640 and 2,038,936 respectively. Overall WGR in RCC in 2012 is 0.334 kg/capita/day. Total MSW generation in RCC is 292.323 ton/day in 2012. This study is mainly based on primary data. Survey was conducted during dry season only. Average weight of MSW generation has been determined considering increase of weight by 46% during wet season.

The heat content of MSW of RCC in 2012 is determined to be 6.17 MJ/kg. Energy available in MSW is estimated to be 20.875 MW and the NEPE is 4.119 MW for the year 2012. The corresponding waste generation in the years 2005, 2010, 2015, 2020 and 2025 in ton/day is 185.320, 256.584, 355.252, 491.862 and 681.005 respectively. For the years 2005, 2010, 2015, 2020 and 2025 energy available in MSW are determined to be 13.234 MW, 18.323 MW, 25.369 MW, 35.125 MW and 48.632 MW respectively. And, the NEPE in those years is 2.611 MW, 3.616 MW, 5.006 MW, 6.931 MW and 9.597 MW respectively. Overall efficiency of the plant is found to be 19.73%.

Figure 6 shows population in RCC in 1991, 2001 and estimated population in 2005 to 2025 based on information with MSW: 2005, MSW: 2010 and MSW: 2012. Figure 7 shows MSW generation in RCC in 1991, 2001 and estimated MSW generation in 2005 to 2025 based on information with MSW: 2005, MSW: 2010 and

MSW: 2012. Figure 8 shows the NEPE from MSW in RCC in 1991, 2001 and NEPE from MSW in RCC in 2005 to 2025 based on information with MSW: 2005, MSW: 2010 and MSW: 2012.

III. RESULTS AND DISCUSSION

A study on the MSW generated in RCC shows that during the period 1991-2001 domestic waste is only 30% by weight, which stands the highest value of 77.2%, 61.5% and 68.246% by weight among all the sources of MSW: 2005, MSW: 2010 and MSW: 2012 respectively. Food and vegetable waste is the dominating one among all the waste components and attains a value of 78.70%, 62.43%, 66.68% and 79.4% by weight in MSW: (1991-2001), MSW: 2005, MSW: 2010 and MSW: 2012 respectively. Grass/Leaves have a value of 10% by weight in MSW: (1991-2001) which gradually decreases to attain a value of 0.225% by weight in MSW: 2012. MSW: (1991-2001) shows paper and packages content of 6% by weight, whereas paper itself only is 6.32% by weight in MSW: 2005 and gradually decreases in MSW: 2010 and MSW: 2012. MSW: (1991-2001) contains paper and polyethylene of 4.50% by weight whereas plastics itself is 7.99% by weight in MSW: 2005 and 0.425% and 3.23% by weight in MSW: 2010 and MSW: 2012 respectively. Polyethylene is 4.50% by weight in MSW: 2010, and it has no trace in MSW: 2005 and MSW: 2012. Wood is 0%, 5.5%, 0.02% and 0.225% by weight in MSW: (1991-2001), MSW: 2005, MSW: 2010 and MSW: 2012 respectively. MSW: (1991-2001) contains clothes 1% by weight and jute/textile of 3.41, 1.11% and 2.2% by weight in MSW: 2005, MSW: 2010 and MSW: 2012 respectively. Bones has been mentioned as 0.48% and 0.37% by weight in MSW: 2005 and MSW:2012 respectively. MSW: 2010 contains bones and various other wastes of 2.05% by weight.

The heat content of MSW: (1991-2001), MSW:2 005, MSW: 2010 and MSW: 2012 are 11.04 MJ/kg, 8.299 MJ/kg, 7.673 MJ/kg and 6.17 MJ/kg respectively. It may be mentioned that percentage of waste component of MSW: 2012 is less as this MSW is landfill site and thus results in a comparatively lower value of heat content.

Waste generation is 0.369, 0.401 and 0.334 kg/capita/day for MSW: 2005 in 2005 MSW: 2010 in 2010 and MSW: 2012 in 2012 respectively. It is noted that total population in 2010 from the information of MSW: 2005, MSW: 2010 and MSW: 2012 are 606, 122, 825,000 and 768,216.

The first two values resemble LGR and HGR respectively. The NEPE in 2005 for MSW: 2005, 2010 for MSW: 2010 and 2012 for MSW: 2012 are 3.269, 5.778 and 4.119 MW respectively. The NEPE in 2010 for MSW: 2005 is 5.336 MW. This value is identical to that of 2010 for MSW: 2010. The results based MSW: 2005 and MSW: 010 are more authentic as both primary and secondary data have been used directly for different seasons. The results of MSW: 2012 is based on primary data and data for wet season has been estimated from data of dry season. Moreover, the nature and quantity MSW has been changed depending on urbanization, development, industrialization and standard of living of the people with time.

It is wise to take an average value of the results obtained for MSW: 2005 and MSW: 2012 for the required MBI energy recovery system. Figure 9 shows population in RCC in 1991, 2001 and average estimated population in 2005 to 2025 for MSW: 2005 and MSW: 2012. Figure 10 shows MSW generation in RCC in 1991, 2001 and average estimated MSW generation in 2005 to 2025 for MSW: 2005 and MSW: 2012. Figure 11 shows the NEPE from MSW in RCC in 1991, 2001 and the average NEPE from MSW in RCC in 2005 to 2025 for MSW: 2005 and MSW: 2012.

A 645.543 ton/day energy recovery system with an overall efficiency of 19.71% would generate 5.336, 6.205, 8.201 and 10.568 MW NEPE in the years 2012, 2015, 2020 and 2025 respectively from MSW of RCC. The minimum heating value of MSW required for sustainable combustion is between 5.024 – 5.861 MJ/kg [115]. The heat content of MSW of RCC is 7234.5kJ/kg. A 12 MW MBI energy recovery powerplant may be installed depending on the quality and current generation of SW based on the quality and current generation of SW.

It may be mentioned that WTE plants minimize the transport of MSW to distant landfills, reduce emissions and shorten fuel consumption [117]. Extra fuel is needed to run the process of MBI, but electric power generation his higher. Associated with this method is the drying of MSW during monsoon season. This problem can be overcome by providing a shed in a large area and using additional fuel for heating. Other methods need MSW of low moisture content and dry land which is unavailable in this area.

The main contributor to greenhouse gas (GHG) emissions during MSW incineration (MSWI) is CO₂ emissions from the combustion of inherent fossil carbon in MSW. GHG emissions can be lessened by increasing the efficiency of electricity and heat recovery. This appears to be significantly effective to optimize the energy conversion strategies of MSWI plants in China [118]. In Asia, most of the WTE plants are incineration-based. Incineration is an established and simpler technology compared to others [119, 120]. The WTE technology is considered as one of the cleanest source of technology by the U.S. environmental Protection Agency (EPA) because of the gradually diminishing levels of dioxin, furan, mercury and other volatile metal emissions over the last 20 years [121].

IV. CONCLUSIONS

- Population of RCC in the years 2012, 2015, 2020 and 2025 are 768,108, 903,747, 1,177,125 and 1,529,144 and respective WGR are 309.094 ton/day, 373.351 ton/day, 496.316 ton/day and 645.543 ton/day.
- Heating value of MSW of RCC is 7234.5 kJ/kg
- Net power generation during the years is 5.336 MW, 6.205 MW, 8.201 MW and 10.568 MW respectively.
- Capacity of the MBI to be used is 646 ton/day.
- Overall efficiency of the energy –recovery plant is 19.71%
- A 12 MW experimental power plant may be installed in RCC.
- Substantial reduction of waste quantity and safe disposal of SW in a controlled manner.
- Public health is ensured, environmental pollution is controlled and electric power is generated.
- MSW can be used as a renewable source of energy.
- Power generation by incineration of waste can reduce the costly fossil fuel utilization.

REFERENCES

- [1] Z. Minghua, F. Xiumin, A. Rovetta, H. Qichang, F. Vicentini, L. Binkai, A. Gusti, L. Yi, Municipal solid waste management in Pudong new area, China, *Waste Management* 29 (2009) 1227-1233.
- [2] L.A. Guerrero, G. Mass, W.Hogland, Solid waste management challenges for cities in developing countries, *Waste Management* 33 (2013) 220-232.
- [3] S. Seo, T. Aramaki, Y. Hwang, K. Hanaki, Environmental impact of solid waste treatment methods in Korea, *Journal of Environmental Engineering Div., ASCE* 130 (1) (2004) 81-89.
- [4] I.A. Al-Khatib, M. Monou, A.S.F.A. Zahra, H.Q. Shaheen, D.Kassinou, Solid waste characterization, quantification and management practices in developing countries. A case study: Nablus district – Palestine, *Journal of Environmental Management* 91 (2010) 1131-1138.
- [5] T.S. Foo, Recycling of domestic waste: early experiences in Singapore, *Habitat International* 21 (1997) 277-289.
- [6] L. A. Manaf, M. A. A. Samah, N. I. M. Jukki, Municipal solid waste management in Malaysia: Practices and challenges, *Waste Management* 29 (2009) 2902-2906.
- [7] A. Demirbas, Waste management, waste resource facilities and waste conversion processes, *Energy Conversion and Management* 52 (2010) 1280-1287.
- [8] Q. H. Bari, K. M.Hasan, R. Haque, Scenario of solid waste reuse in Khulna City of Bangladesh, *Waste Management* xxx (2012) xxx – xxx.
- [9] L. Zhen-shan, Y. Lei, Q. Xiao-Yan, S. Yu-mei, Municipal solid waste management in Beijing City, *Waste Management* 29 (10) (2009) 2618-2624.
- [10] S.A. Batool, M.N. Chuadhry, Municipal solid waste management in Lahore city district, Pakistan, *Waste Management* 29 (2009) 1971-1981.
- [11] E. Metin, A. Erztürk, C. Neyim, Solid waste management practices and review of recovery and recycling operations in Turkey, *Waste Management* 23 (5) (2003) 425-432.
- [12] M. Berkum, E. Aras, S. Nemlioglu, Disposal of solid waste in Istanbul and along the black sea coast of Turkey, *Waste Management* 25 (2005) 847-855.
- [13] S.S. Chung, C.W.H. Lo, Local waste management constraints and waste administrators in China, *Waste Management* 28 (2) (2008) 272-281.
- [14] A. Imam, B. Mohammed, D.C. Wilson, C.R. Cheeseman, Solid waste management in Abuja, Nigeria, *Waste Management* 28 (2) (2008) 468-472.
- [15] S.A. Ahmed, M. Ali, Partnerships for solid waste management in developing countries: linking theories to realities, *Habitat International* 28 (2004) 467-479.
- [16] M.E.Kasseva, S.E.Mbuligwe, Ramifications of solid waste disposal site relocations in urban areas of developing countries: a case study in Tanzania, *Resources, Conservation and Recycling* 1999; 28 (2000) 147-161.
- [17] S.E. Mbuligwe, Institutional solid waste management practices in developing countries: a case study of three academic institutions in Tanzania, *Resource, Conservation and Recycling* 35 (2002) 131-146.
- [18] H. Ogawa, Sustainable solid waste management in developing countries. In: 7th ISWA International Congress and Exhibition. World Health Organization. Kuala Lumpur, Malaysia. Online: <http://www.eoc.titech.ac.jp/uem/waste/swm-fogawal.htm> (29 July 2000).
- [19] D.C. Wilson, C. Velis, C.Cheeseman, Role of informal sector recycling in waste management in developing countries, *Habitat International* 30 (2006) 197-808.
- [20] N.J. Themelis, Y.H. Kim, Material and energy balances in large-scale aerobic bioconversion cell, *Waste Management and Research* 20 (2002) 234 – 242.
- [21] G. Tchobanoglous, H. Theisen, S.A. Vigil, *Integrated solid waste management: Engineering principles and management issues*. McGraw-Hill, Inc., New York, USA, 1993.
- [22] World Resources institute, *World resources report 1996-1997*, Oxford University Press, New York, USA, 1997.
- [23] HMGN, MoPE, 2003, *Nepal population report 2060*. Published by His Majesty's Government of Nepal (HMGN), Ministry of Poulation and Environment (MoPE) (in Nepali).
- [24] D. Suochong, K.W. Tong, Y. Yuping, Municipal solid waste management in China: using commercial management to solve a growing problem, *Utilities Policy* 10 (2001) 7-11.
- [25] What cities do with their waste, *Urban Age* 6 (1999) 32-33.
- [26] World Bank, 1999, *What a waste: solid waste management in Asia*, urban development sector unit. East Asia and Pacific Region. The International Bank for Reconstruction and Development, Washington DC, USA.
- [27] M. Sharholi, K. Ahmad, G. Mahmood, R.C. Trivedi, Municipal solid waste management in Indian cities – a review, *Waste Management* 28 (2) (2008) 459-467.
- [28] K. Parizeau, V. Maclaren and L. Chanthy, Waste characterization as an element of waste management planning: Lessons learned from a study in Siem Reap, Cambodia, *Resources, Conservation and Recycling* 49 (2) (2006) 110-128.

- [29] E.A. McBean, E. Rosso, F.A. Rovers, Improvement in financing for sustainability in solid waste management, *Resources, Conservation and Recycling* 43 (2005) 391-401.
- [30] H.A.A. Qdais, Techno-economic assessment of municipal solid waste management in Jordan, *Waste Management* 27 (11) (2007) 1666-1672.
- [31] V. Kum, A. Sharp, N. Harnpornchai, Improve the solid waste management in Phnom Penh City: a strategic approach, *Waste Management* 25 (1) (2005) 101-109.
- [32] S.J. Burntley, A review of municipal solid waste composition in the United Kingdom, *Waste Management* 27 (10) (2007) 1274-1285.
- [33] M. Sujauddin, S.M.S. Huda, A.T.M. Rafiqul Hoque, Household solid waste characteristics and management in Chittagong, Bangladesh, *Waste Management* 28 (2008) 1688-1695.
- [34] A. Forie, Municipal solid waste management as a luxury item, *Waste management* 26 (2006) 801-802.
- [35] WASTE 2004, Integrated sustainable waste management click on ISWM under "Approaches". <http://waste.nl>.
- [36] J. Anschutz, J. Ijgosse, A. Scheinberg, Putting ISWM to Practice, WASTE, Gouda, The Netherlands, 2004.
- [37] L.F. Zuilen, Planning of an integrated solid waste management system in Suriname: a case study in Greater Paramaribo with focus on households, PhD Thesis, Ghent University, Belgium,
- [38] C. Zurbrügg, S. Drescher, I. Rytz, M. Sinha, I. Enayetullah, Decentralized composting in Bangladesh, a win-win situation for all stakeholders, *Resources, Conservation and Recycling* 43 (2005) 281-292.
- [39] D.C. Wilson, A. Araba, K. Chinwah, C.R. Cheeseman, Building recycling rates through the informal sectors, *Waste Management* 29 (2009) 629-635.
- [40] M.S. Müller, A. Sheinberg, Genderlinked livelihoods from modernizing the waste management recycling sector: a framework for analysis and decision making. Gender and waste economy. Vietnamese and international experiences. CIDA funded project, 2002.
- [41] M.S. Müller, A. Iyer, M. Keita, B. Sacko, D. Traore, Differing interpretations of community participation in waste management in Bamako and Bangalore: some methodological considerations, *Environment and Urbanization* 14 (2002) 241-258.
- [42] A. Sheinburg, D.C. Wilson, L. Rodic, Solid waste management in the World's Cities, UN-Habitat's Third Global Report on the State of Water and Sanitation in the World's Cities, Earth Scan, Newcastle-upon-Tyne, UK, 2010.
- [43] A. Sheinburg, S. Spies, M.H. Simpson, A.P.J. Mol, Assessing urban recycling in low-and-middle income countries: Building on modernized mixtures, *Habitat International* 35 (2011) 188-198.
- [44] ISSOWAMA Consortium, Integrated sustainable solid waste management in Asia. In: Seventh Framework Programme, European Commission, 2009.
- [45] A. Messino, D. Panno, Municipal waste management in Sicily: practices and challenges, *Waste Management* 28 (2008) 1201-1208.
- [46] Mohammad Osman Saeed, MohdNasir Hassan, M. Abdul Mujeebu, Assessment of municipal solid waste generation and recyclable materials potential in Kuala Lumpur, Malaysia, *Waste Management* 29 (2009) 2209-2213.
- [47] B.A/K Abu-Hijleh, M. Mousa, R. Al-Dwairi, M. Al-Kumoos and S. Al-Tarazi, Feasibility Study of Municipality Solid Waste Incineration Plant in Jordan, *Energy Conversion and Management* 39(11) (1998) 1155-1159.
- [48] M. Abu-Qudais, H.A. Abu-Qudais, Energy content of municipal solid waste in Jordan and its potential utilization, *Energy Conversion and Management* 41 (2000) 983 – 991.
- [49] W.T. Tsai, Y.H. Chou, An overview of renewable energy utilization from municipal solid waste (MSW) incineration in Taiwan, *Renewable and Sustainable Energy Reviews* 10 (2006) 491-502.
- [50] S. Kathirvale, M.N.M. Yunus, K. Sopian, A.H. Samsuddin, Energy potential from municipal solid waste in Malaysia, *Renewable Energy* 29 (2003) 559-567.
- [51] M.J. Alam, B. Bole, Energy recovery from municipal solid waste in Dhaka city. In: Proceedings of the International Conference on Mechanical Engineering, Dhaka, 26-28 December 2001, pp. 125-130.
- [52] M.A. Sufian, B.K. Bala, Modeling of electrical energy recovery from urban solid waste system: The case of Dhaka city, *Renewable Energy* 31 (2006) 1573-1580.
- [53] M.D. Islam and A.Z.A. Saifullah, Solid waste and sugarcane bagasse – A renewable source of energy in Rajshahi City, Bangladesh. In: Proceedings of the 4th International Conference on Mechanical Engineering, Dhaka, Bangladesh, December 26-28, 2001, pp. 133-36.
- [54] Wen-Tien Tsai, Kuan-Chi Kuo, An analysis of power generation from municipal solid waste (MSW) incineration plants in Taiwan, *Energy* 35 (2010) 4824-4830.
- [55] A. Mwesigye, S.B. Kucel, A. Sebbit, Opportunities for Generating Electricity from Municipal Solid Waste: Case of Kampala City Council Landfill. [www.mak.ac.ug/documents/Makfiles/act 2011/Mwesigye.pdf](http://www.mak.ac.ug/documents/Makfiles/act%202011/Mwesigye.pdf)
- [56] H. Cheng, Y. Zhang, A. Meng, and Q. Li, Municipal Solid Waste Fueled Power Generation in China: A Case Study of Waste-to-Energy in Changchun City. www.aseanenvironment.info/Abstract/41016304.pdf
- [57] M.Y. Suberu, A.S. Mokhtar, N. Bashir, Renewable Power Generation Opportunity from Municipal Solid Waste: A Case Study of Lagos Metropolis (Nigeria), *Journal of Energy Technologies and Policy* 2(2) (2012)1-14. www.iiste.org
- [58] S.B. Karajgi, Udaykumar.R.Y, G.D. Kamalapur, Modelling of Power Generation using Municipal Solid Waste in India, *International Journal of Electrical and Computer Engineering (IJECE)* 2 (2) (2012) 197-202.
- [59] C. Bidart, M. Fröhling, F.Schultmann, Municipal solid waste and production of substitute natural gas and electricity as the energy alternatives, *Applied Thermal Engineering* 51 (2013) 1107-1115.
- [60] A. Ahsan, M. Alamgir, R. Islam, K.H. Chowdhury, Initiatives of Non-Governmental Organizations in Solid Waste Management at Khulna City. Proc. 3rd Annual Paper Meet and Intl. Conf. on Civil Engineering, IEB, Dhaka, Bangladesh, March 9 – 11, 2005, pp. 185-196.
- [61] M. Alamgir, A. Ahsan, Municipal solid waste and recovery potential: Bangladesh perspective, *Iran. J. Environ. Health Sci. Eng.* 4(2)(2007) 67-76.
- [62] C.S.Rao, Environmental pollution control engineering, Willy Eastern Limited, New Delhi, India, 1992, pp. 396-414.
- [63] Chris Zurbrugg, SANDEC / EAWAG, Solid Waste Management in Developing Countries. bscw.ihe.nl/pub/bscw.cgi/d1354352/basics_of_SWM.pdf
- [64] Y. Hamzeh, A. Ashori, B.Mirzaei, A. Abdulkhani, M.Molaei, Current and potential capabilities of biomass for green energy in Iran, *Renewable and Sustainable Energy Reviews* 15 (9) (2011) 4934-4938.
- [65] F.A.M. Lino, W.A. Bizzo, E.P. Da Silva, K.A.R. Ismail, Energy impact of waste recyclable in a Brazilian metropolitan, *Resources, Conservation and recycling* 54(1) (2010) 916-922.
- [66] M.R. Alam, Environmental management in Bangladesh – A study on municipal solid management system in Chittagong, The Cost and Management May-June, (2008) 23-30.

- [67] M. Salequzzaman, Perceptions of vehicle air pollution in Khulna, Bangladesh. In: Proceedings of the Habitus 2000, Conference in Perth, Western Australia, September 05-09, 2000.
- [68] Incineration of municipal solid waste. A state-of-the art, Pub. Works 121 (1990) 1-5.
- [69] Joint Venture (JV) of AQUA Consultant & Associates Ltd. (BD), Hifab International AB, Sweden, Resource Planning and Management Consultants Ltd. (BD) & Engineering & Planning Consultants Ltd. (BD), Study on Municipal Solid Waste Management, Final Report, Bangladesh Municipal Development Fund (BMDF) June 21, 2012.
- [70] I.Enayetullah, Q.S.I. Hashmi, Community based solid waste management through public-private-community partnerships: experience of Waste Concern in Bangladesh, 3R Asia Conference, Tokyo, Japan, October 30 to November 1, 2006. Web: www.wasteconcern.org
- [71] A.I. Chowdhury, Instruments of local financial reform and their impact on service delivery, institutional and development concerns: Bangladesh Case Study, Dhaka: Center for Urban Studies, 2008
- [72] S. Suryanarayanan, Sustainable Waste Management in Bangladesh, December, 2010. http://www.strategicforesight.com/waste_management.htm
- [73] A. Clemett, M.M. Amin, S. Ara, M.M.R. Akan, Background information for Rajshahi City, Bangladesh, WASPA Asia Project Report 2, 2006.
- [74] en.wikipedia.org/wiki/Rajshahi
- [75] A. Ali, Faulty Solid waste Management in Rajshahi City: Dumping in Open Spaces Poses Health Hazard to Dwellers, 2011. <http://www.bangladesh2day.com/newsfinance/2010/February/11/Faulty-solid-waste-management-in-Rajshahi-city.php>
- [76] N. Akter, M. Rahman & L. Sharmin, Medical waste management at Rajshahi City Corporation public-private partnership model development: A collaborative effort on medical waste management in Bangladesh (baseline and status report), Antocom Online Journal of Anthropology 6(2) (2010) 173-186.
- [77] M. Salequzzaman, M. Awal, M. Alam, Willingness to pay community based solid waste management and its sustainability in Bangladesh. In: Proceedings of the International Conference 'The Future is Here', RMIT, Melbourne, Victoria, January 15-19, 2001.
- [78] S.H. Bhuiyan, A crisis in governance: Urban solid waste management in Bangladesh, Habitat International 34 (1) (2010) 125-133.
- [79] S.M. Kassim, M. Ali, Solid waste collection by the private sector: households' perspectives – findings from a study in Dar-es-Salaam city, Tanzania, Habitat International, 30 (4) (2006) 769-780.
- [80] S.H. Bhuiyan, Benefits of social capital: urban solid waste management in Bangladesh. Münster: LIT.
- [81] M.A. Rouf, Prospect of Electric Energy from Solid Wastes of Rajshahi City Corporation: A Metropolitan City in Bangladesh, 2011 2nd International Conference on Environmental Engineering and Applications, IPCBEE vol. 17 (2011) © (2011) IACSIT Press, Singapore. www.ipcbee.com/vol_17/9-L022.pdf
- [82] NFB (news From Bangladesh. Business & Economy: Rajshahi People Facing Acute Load-Shedding. 2004 <http://www.bangladesh-web.com/view.php?hidRecord=4484>
- [83] T.A. Chowdhury, S.R. Afza, Waste management in Dhaka City – A theoretical marketing model, BRAC University Journal III(2) (2006) 101-111.
- [84] C. Furedy, Social aspects of solid waste recovery in Asian cities, Environmental Sanitation Reviews, No. 30, December, 1990.
- [85] U. Glawe, C. Visvanathan, M. Alamgir, Solid waste management in least developed Asian countries -A comparative analysis. In: Proceedings of international conference on integrated solid waste management in Southeast Asian cities, 5-7 July, 2005, Siem Reap, Cambodia.
- [86] M.A. Memon, Integrated solid waste management based on the 3R approach. <http://www.springerlink.com/content/cmnu81374n412898/4/29/2010>
- [87] A. Ojha, Abhishek C. Reuben, D. Sharma, Solid Waste Management in Developing Countries through Plasma Arc Gasification – An Alternative Approach, APCBEE Procedia 1 (2012) 193-198.
- [88] M.M. Rahman, K.R. Sultana, M.A. Haque, Suitable sites for urban solid waste disposal using GIS approach in Khulna City, Bangladesh, In: Proc. Pakistan Acad. Sci. 45 (1) (2008) 11-22.
- [89] C. Smith, K. Whitty, M. Quintero & B.S. Ozeda, Opportunities for Energy Production from Solid waste in The Mexicali Region, Annual Meeting of the American Institute of Chemical Engineers, November 2-5, 2007.
- [90] P.S. Phillips, R.M. Pratt & K. Pike, An analysis of UK waste minimization clubs: key requirements for future cost effective developments, Waste Management 21 (2001) 389-404.
- [91] U. Arena, Process and technological aspects of municipal solid waste gasification. A review, Waste Management 32 (2012) 625–639.
- [92] S. Consonni, M. Giugliano, M. Grosso, Alternative strategies for energy recovery from municipal solid waste Part A: Mass and energy balances, Waste Management 25(2) (2005) 123-135.
- [93] K. Lata, K.V. Rajeshwari, D.C. Pant, V.V.N. Kishore, Volatile fatty acid production during anaerobic mesophilic digestion of tea and vegetable market wastes, World Journal of Microbiology and Biotechnology 18(6)(2002) 589-592.
- [94] G. Lastella, C. Testa, G. Cornacchia, M. Notornicola, F. Voltasio, V. K. Sharma, Anaerobic digestion of semi-solid organic waste: biogas production and its purification, Energy Conversion and Management 43 (1) (2002) 63–75.
- [95] Electricity from municipal solid waste. http://www.powerscorecard.org/tech_detail.cfm?resource_id=10 4/20/2010
- [96] Municipal solid waste power plants – waste to energy (WTE) & biomass in California. <http://www.energy.ca.gov/biomass/msw.html> 4/24/2010
- [97] Municipal solid waste management. http://www.unep.or.jp/ietc/estdir/pub/msw/sp/sp5/sp5_1.asp 4/25/2010
- [98] K. C. Lee, K. C. M. Kwok, W. H. Cheung, G. McKay, Operation of a municipal solid waste co-combustion pilot plant, Asia-Pacific Journal of Chemical Engineering 2(6) (2007) 631-639.
- [99] M.K. Huda, A.Z.A. Saifullah, Solid waste management in Rajshahi City Corporation of Bangladesh – A case study. In: Proceedings of the thirteenth international conference on solid waste technology and management, Vol 1, Philadelphia, PA U.S.A., November 16-19, 1997.
- [100] I. Enayetullah, A.H.M.M. Sinha, S.S.A. Khan, Urban Solid waste Management Scenario of Bangladesh: Problems and Prospects, West Concern Technical Documentation, June 06, 2005. www.wasteconcern.org/Publication/Waste%20Survey-05.pdf
- [101] R. Schertenleib, W. Meyer, Municipal Solid waste management in DC's: problems and issues; need for future research, IRCWD News, Duebendorf, Switzerland, No. 26, 1992.
- [102] C. Zurbrugg, Urban solid waste management in low-income countries of Asia. How to cope with the garbage crisis. Presented for: Scientific committee on problems of the environment (SCOPE), Urban solid waste review session, Durban, South Africa, November 2002.

[103] T.B. Yousuf, M. Rahman, Monitoring quantity and characteristics of municipal solid waste in Dhaka City, Environ Monit Assess, 135(1-3) (2007) 3-11.

[104] EEA (European Environment Agency), Case studies on waste minimization practices in Europe. Copenhagen:EEA. (2002).

[105] H. S. Peavy, D. R. Rowe, G.Tchobanoglous, Environmental Engineering, McGraw Hill Book Company, International Edition, 1985.

[106] www. weiku.com

[107] P. Phiraphynio, S.Taepakpurenat, P. Lakkanatinaporn, W. Suntornsuk and I.Suntornsuk, Physical and Chemical properties of fish and chicken bones as calcium source for mineral substances, Sonklanakarim J. Sci. Technol. 28 (2) (2006) 327-335.

[108] D. Okanović, M. Ristić, M. Popović, T. Tasić, P. Ikonić, J. Gubić, Biotechnology in Animal Husbandry 25 (5-6) (2009) 785-790. Publisher: Institute for Animal Husbandry, Belgrade – Zemun. www.istocar.bg.ac.rs/radovi8/2/23.engl.Dj.OkanicSR.pdf

[109] M.R. Alam & M.H. Sohel, Environmental management in Bangladesh – A study on municipal solid waste management in Chittagong. Chittagong: University of Chittagong, 2008.

[110] BBS (Bangladesh Bureau of Statistics). Census reports. Dhaka: BBS, 2001.

[111] RCC (Rajshahi City Corporation). Rajshahi City Corporation Report – 2010. Rajshahi: RCC, 2010.

[112] Bangladesh Bureau of Statistics (BBS). 1997. “Bangladesh Population Census 1991, Urban Area Report.” Dhaka: Statistics Division, Ministry of Planning, Government of Bangladesh.

[113] Bangladesh Bureau of Statistics (BBS). 2002. “Statistical Pocket Book of Bangladesh.” Dhaka: Statistical Division, Ministry of Planning, Government of Bangladesh.

[114] The PREGA National Technical Experts from Bangladesh Centre for Advanced Studies, Dhaka City solid waste to electrical energy project (A pre-feasibility study report), April 2005.

[115] P. J. Reddy, Municipal Solid Waste Management: Processing - Energy Recovery - Global Examples, BS Publications, pp. 120 books.google.com.bd/books?isbn=0415690366

[116] H. Cheng and Y. Hu, Municipal solid waste (MSW) as a renewable source of energy: Current and future practices in China, Biosource Technology 101 (2010) 3816-3824.

[117] P.O. Kaplan, J. DeCarolis and S. Thorneloe, Is it better to burn or bury waste for clean electricity generation? Environmental Science & Technology 43(6) (2009) 1711-1717.

[118] N. Yang, H. Zhang, M. Chen, L. Shao, P. He. Green House gas emissions from MSW incineration in China: Impacts of waste characteristics and energy recovery, Waste Management 32 (2012) 2552-2560.

[119] X. Xu and J. Liu, Status and development prospect on municipal solid waste incineration technology in our country, ZhongguoHuanbaoChanye 11 (2007) 24-29.

[120] K. Yuan, H. Xiao and X. Li, Development and application of municipal solid waste incineration in China, NengyuanGongcheng 5 (2008) 43-46.

[121] C. Psomopoulos, A. Bourka, N. Themelis, Waste-to-energy: a review of the status and benefits in USA, Waste Management 29 (2009) 1718-1724.

FIGURES

FLOW DIAGRAM OF ENERGY RECOVERY SYSTEM FROM MSW OF RCC

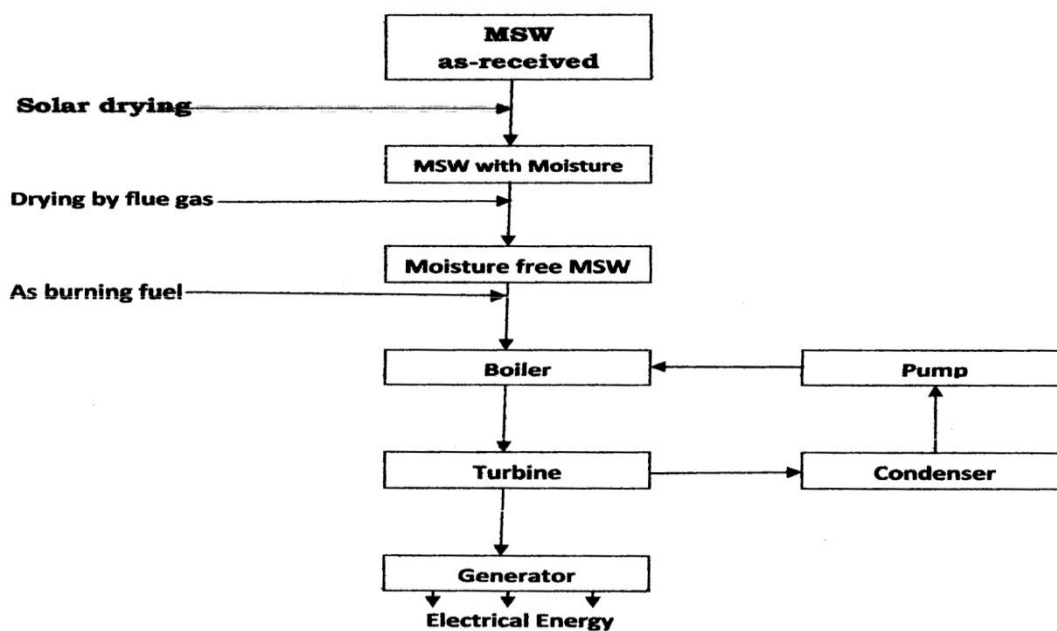


Figure 1: Energy Recovery MBI System for MSW of RCC

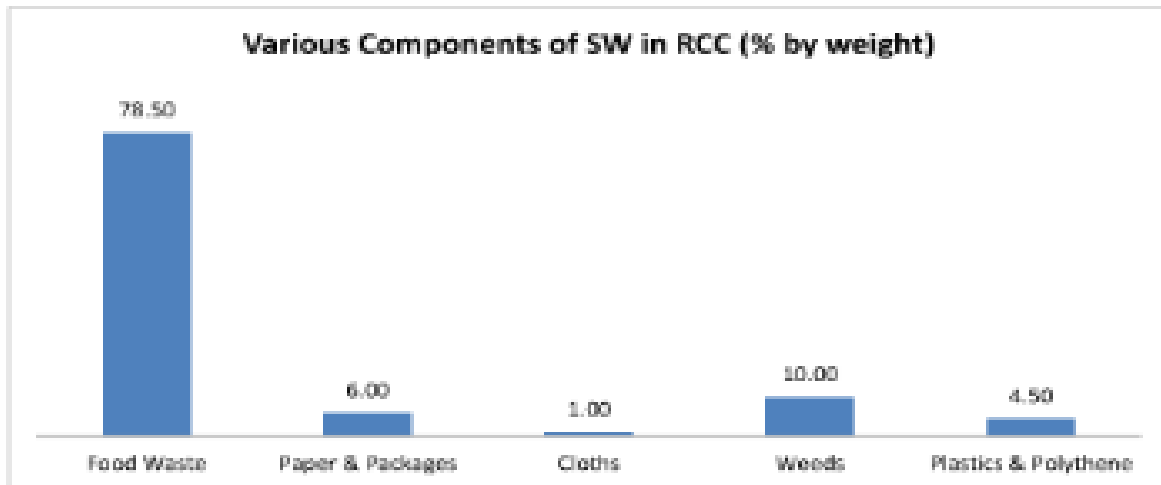


Figure 2 (a): Typical components of SW in RCC in % by weight during the period 1991- 2001

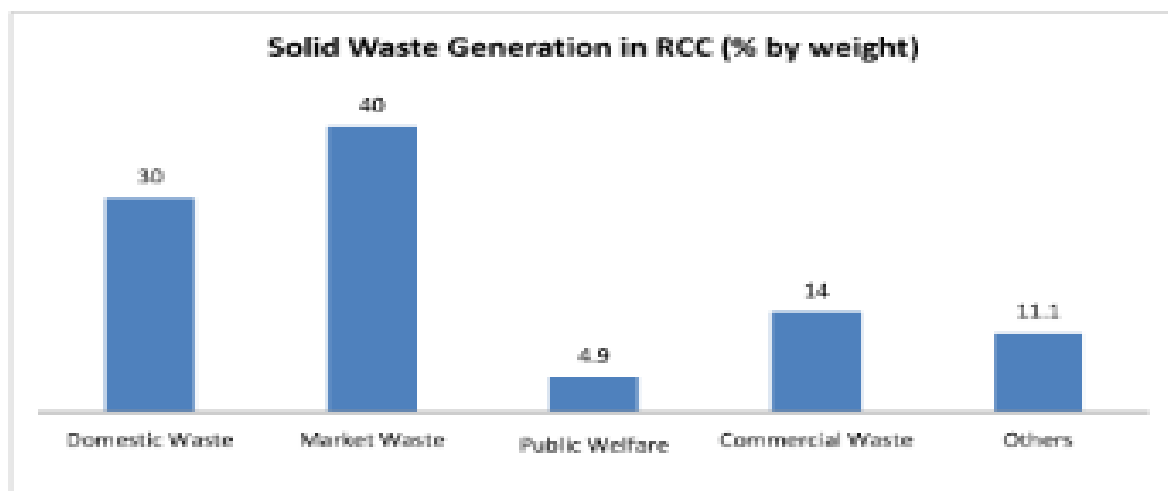


Figure 2 (b): Various sources of SW generated in RCC in % by weight during the period 1991- 2001

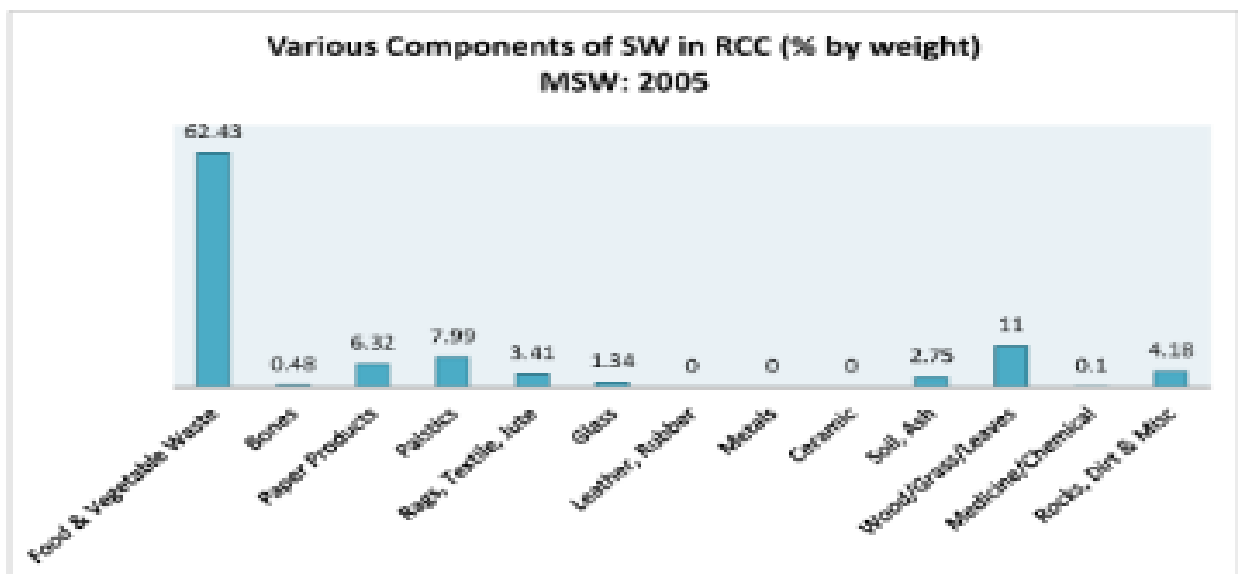


Figure 3 (a): Physical composition of SW of RCC in % by weight in 2005

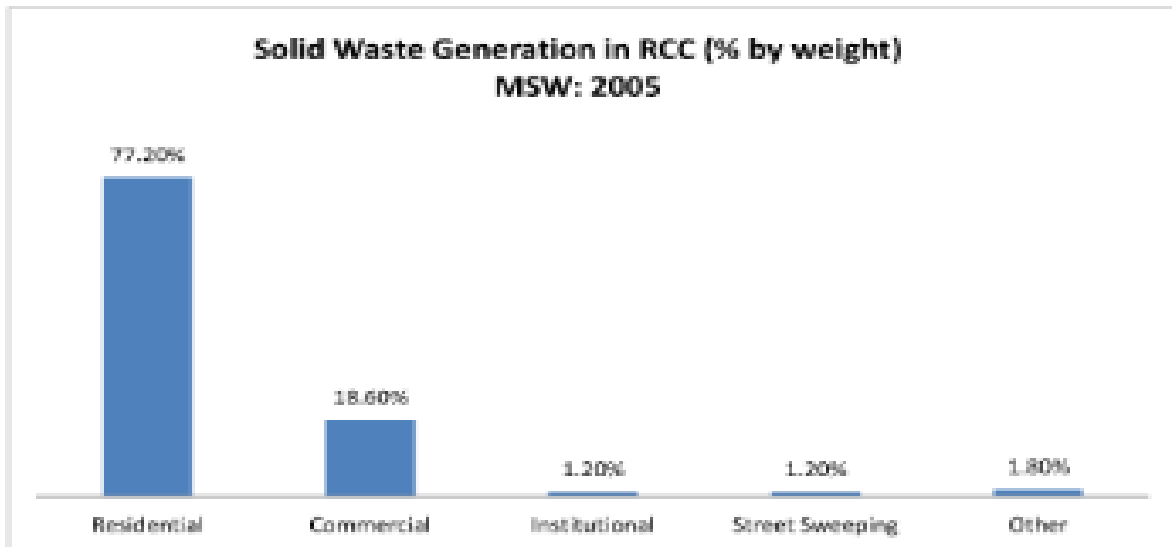


Figure 3 (b): Various sources of SW generated daily in RCC in % by weight in 2005

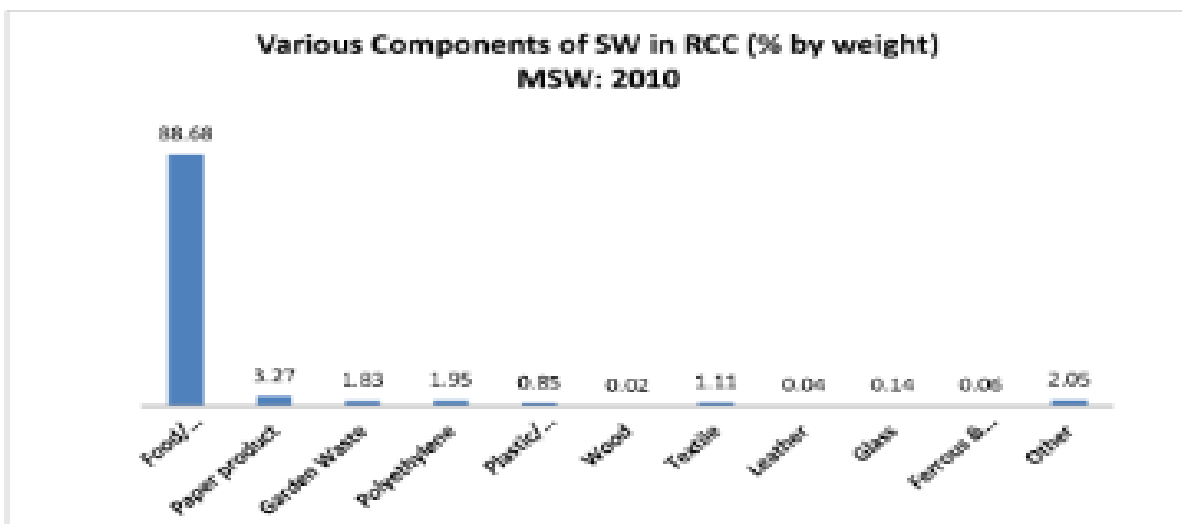


Figure 4 (a): Physical composition of SW of RCC in % by weight in 2010

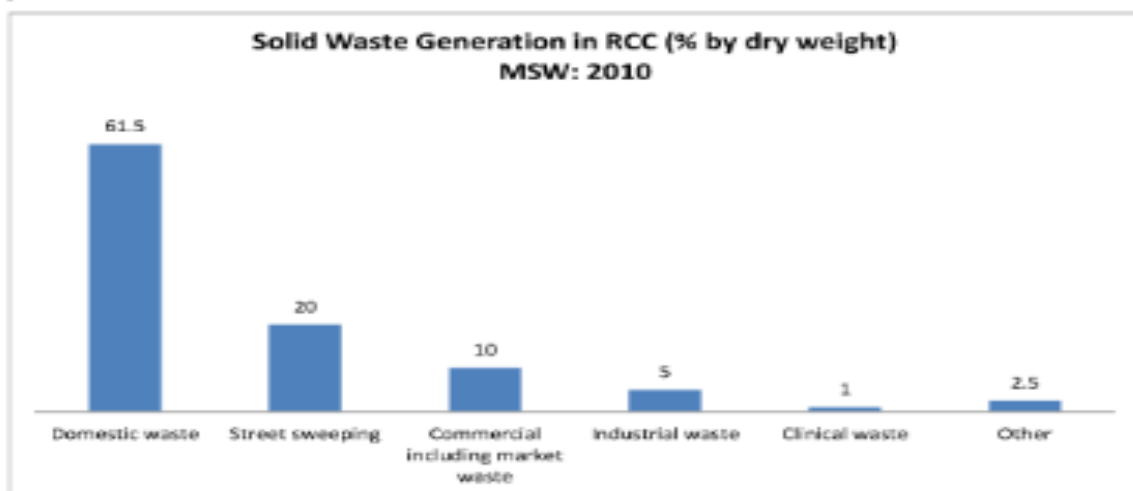


Figure 4 (b): Various sources of SW generated daily in RCC in % by dry weight in 2010

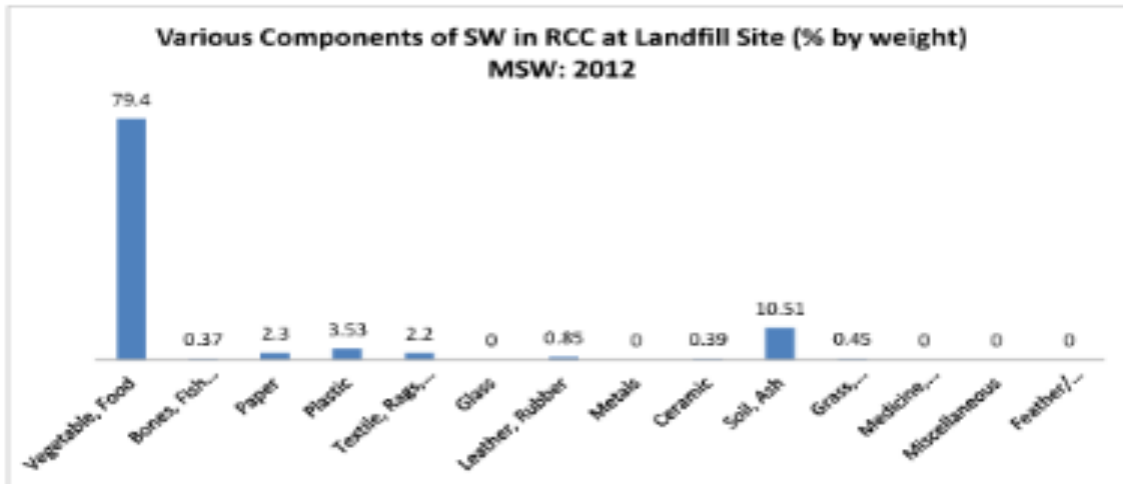


Figure 5 (a): Physical composition of SW of RCC at landfill site in % by weight in 2012

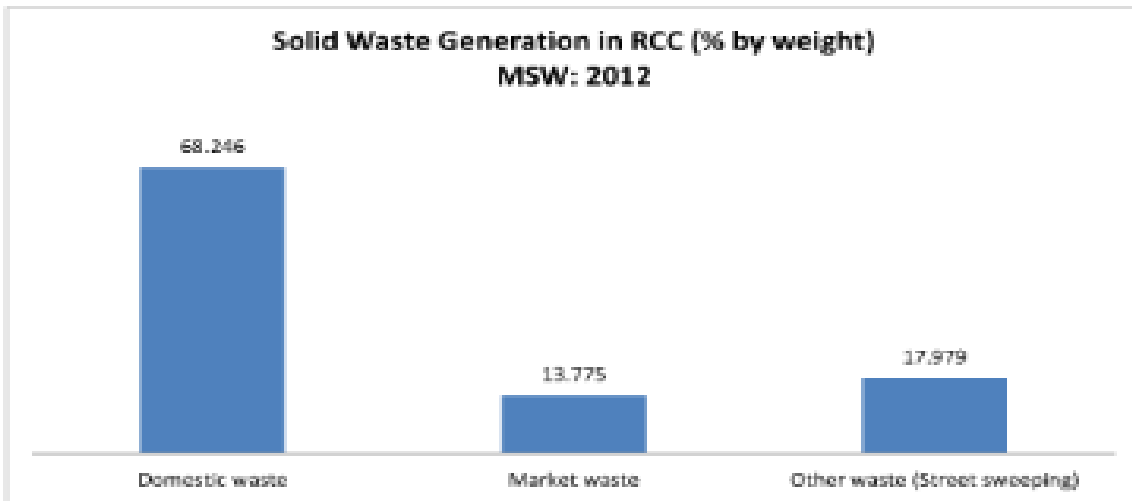


Figure 5 (b): Various sources of SW generated daily in RCC in % by weight in 2012

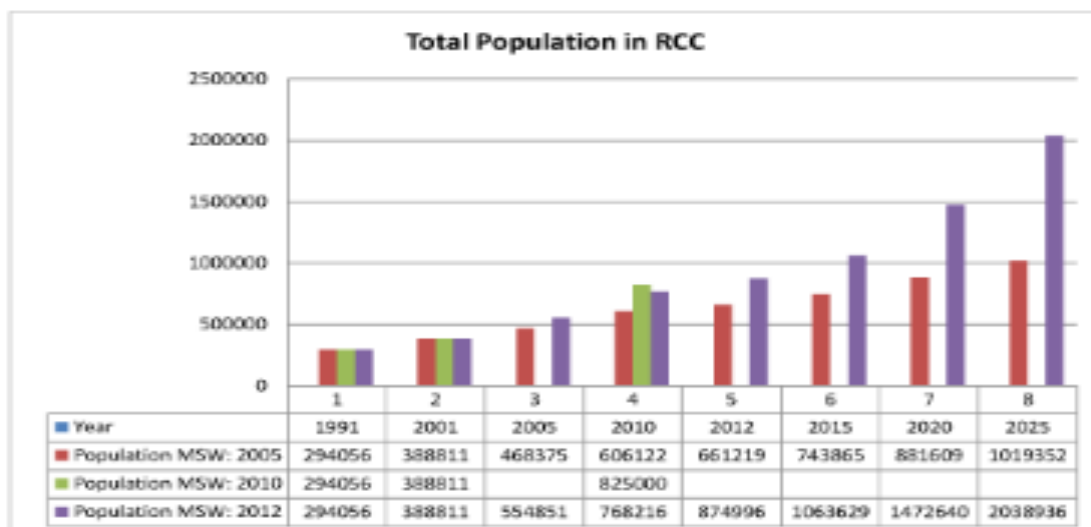


Figure 6: Population in RCC in 1991, 2001 and estimated population in 2005 to 2025 based on information with MSW: 2005, MSW: 2010 and MSW: 2012



Figure 7: MSW generation in RCC in 1991, 2001 and estimated MSW generation in 2005 to 2025 based on information with MSW: 2005, MSW: 2010 and MSW: 2012

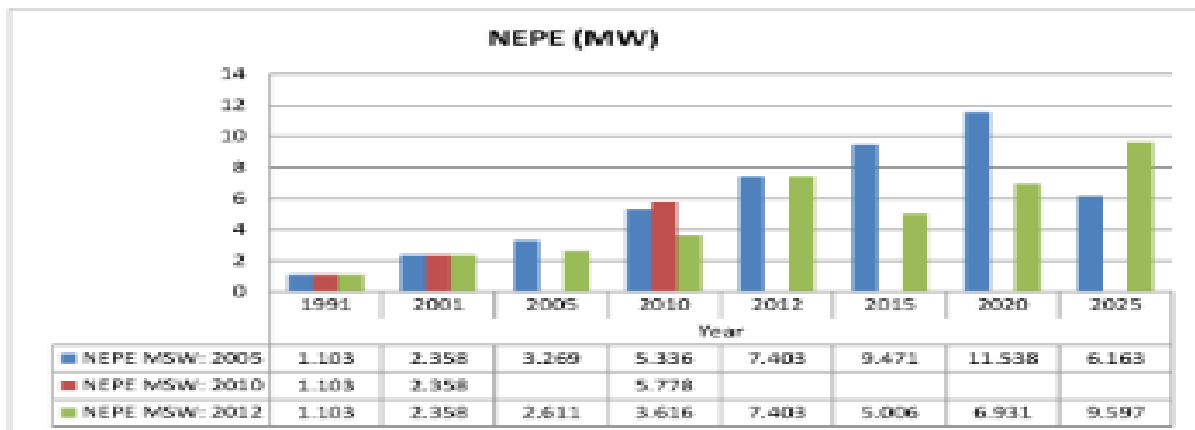


Figure 8: The NEPE from MSW in RCC in 1991, 2001 and NEPE from MSW in RCC in 2005 to 2025 based on information with MSW: 2005, MSW: 2010 and MSW: 2012

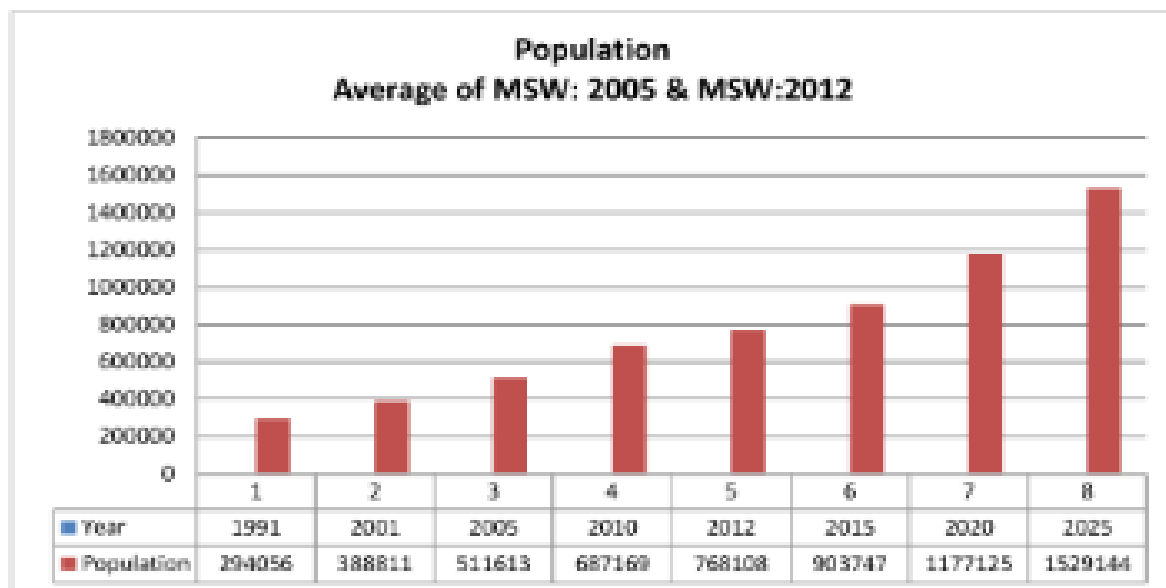


Figure 9: Population in RCC in 1991, 2001 and average estimated population in 2005 to 2025 for MSW: 2005 and MSW: 2012



Figure 10: MSW generation in RCC in 1991, 2001 and average estimated MSW generation in 2005 to 2025 for MSW: 2005 and MSW: 2012

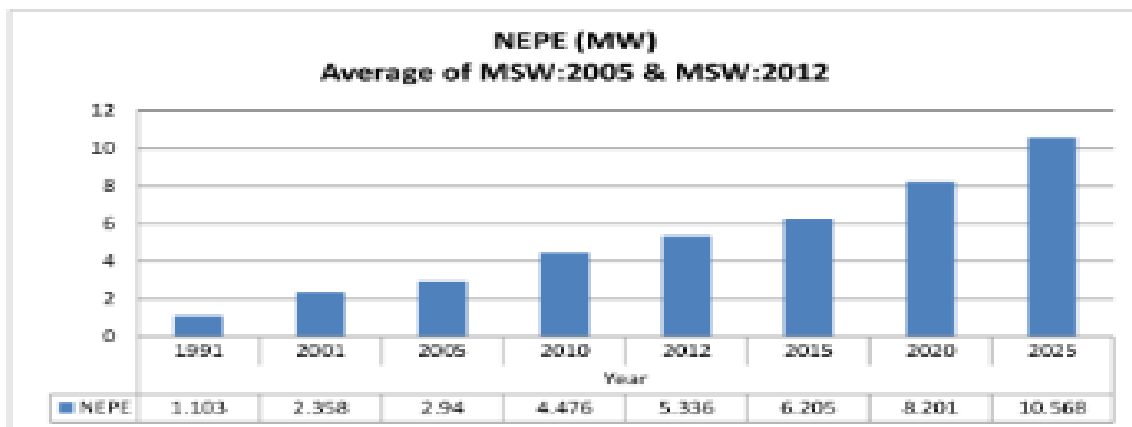


Figure 11: The NEPE from MSW in RCC in 1991, 2001 and the average NEPE from MSW in RCC in 2005 to 2025 for MSW: 2005 and MSW: 2012

CMOS BASED CURRENT FEEDBACK OP-AMP WITH IMPROVED BANDWIDTH

Akshay Dubey

Research Scholar, Electronics Engineering department,
Institute of Engineering and Technology, Lucknow, India.

ABSTRACT : A current mode feedback operational amplifier designed using a complimentary MOS circuit technology has been discussed in this paper. A class AB amplifier has been used in the design and the design results in improvement of values of number of parameter when compared to the previously reported architecture. The circuit is designed using 0.35 μ m technology. Bandwidth of the presented architecture was obtained, that was always greater than 50MHz. On the other hand, bandwidth in case of previously reported circuit was coming out to be always more than 2MHz. Thus in our proposed circuit, there is a considerable improvement in the bandwidth of the circuit. Also the Slew rate, which was improved from 5.2V/ μ sec to 8.1V/ μ sec. Settling time of the proposed circuit has been reduced to 134 nsec which was of order of 212 nsec in case of the previous design.

Keywords - Amplifiers, CMOS, current-feedback operational amplifiers (CFOAs), Slew Rate.

I. INTRODUCTION

An operational amplifier (op amp) is a device whose output is the multiplication of its internal gain and the differential voltage applied to its input terminals. It was initially used for analog computation and instrumentation. It wasn't until the mid 1960's and the invention of the integrated circuit (IC) that the op amp's full versatility was realized.

Earlier, an ideal op amp has been classified as a differential input, single ended output amplifier with infinite gain, infinite input resistance, and zero output resistance. But after the invention of the first IC, manufacturers of op amps have almost got very closer to approximate these characteristics of an ideal op amp. There are continuous researches going all over the globe to find the ways to increase the input impedance, lower the output impedance, offset currents and voltages and noise. Simultaneously, researchers have been trying to push the bandwidths of the devices higher, and lower the settling-time characteristics. These characteristics are very important, specially in applications such as high speed digital to analog conversion (DAC) buffers, sample and hold (S-H) circuits, switching applications and video and IF drivers.

In spite of all electronic systems prominently being dominated by digital circuits and systems, the analog circuits have neither become obsolete nor avoidable. In fact, analog circuits and techniques continue to be indispensable and unavoidable in many areas since all real life signals are analog in nature [8]. Also many basic functions such as amplification, rectification, continuous time filtering, analog to digital conversion and digital to analog conversion etc. need analog circuits and techniques. Therefore analog circuits act as a bridge between the real world and digital systems. Current feedback operational amplifiers (CFOAs) are the modified version of conventional voltage op-amps and are used in number of applications [1]–[4] for their inherent advantages over conventional op-amps, which are generally expressed in terms of high-speed properties [5], [6]. Also, the (inverting) closed-loop bandwidth of operational amplifier have becomes independent of the closed loop gain, provided, the feedback resistance is kept constant. Besides, the input (output) stage of current feedback op-amp are the voltage buffer that can be easily implemented through class-AB topologies. This enable us achieving a reasonably high slew rate values.

In this paper, we will discuss the implementation of two CFOA architectures. The former was originally proposed by one of the authors in [7], is based on a low-voltage alternative and is modified version of the architecture that was presented in [8] which was based on a well-known class AB differential amplifier stage

with high drive capability. The class AB differential amplifiers are here utilized in unity feedback, and thus allowing us to achieve high slew rate and relatively low input and output resistances. This property also enables a large variation of the closed-loop gain, while maintaining constant the bandwidth. Both the circuit topologies are described in Sections 2 and 3, respectively. Simulations and experimental measurements are given in Section 4. Conclusions are summarized in Section 5.

II. EXISTING ARCHITECTURE

In the architecture presented in [8], the problem of high voltage requirement have been solved by adopting a class-AB unity-gain buffer ,and thus the new architecture require low-voltage supply. The resulting simplified schematic of the low-voltage CFOA is depicted in Fig. 1. M1-M13 form the first unity-gain closed-loop voltage buffer. The input current at the inverting terminal is conveyed to the high impedance node at the drain of M22-M23. Transistors M1b-M13b implement the output buffer. The minimum supply voltage is now reduced to $V_{GS} + 3V_{DS, SAT}$ (path formed by M9b-M1b-M23-M24) and the maximum input swing is $V_{GS} + 3V_{DS, SAT}$ from $V_{DD} - V_{SS} - V_{GS} - 2V_{DS, SAT}$ that was derived in [8].

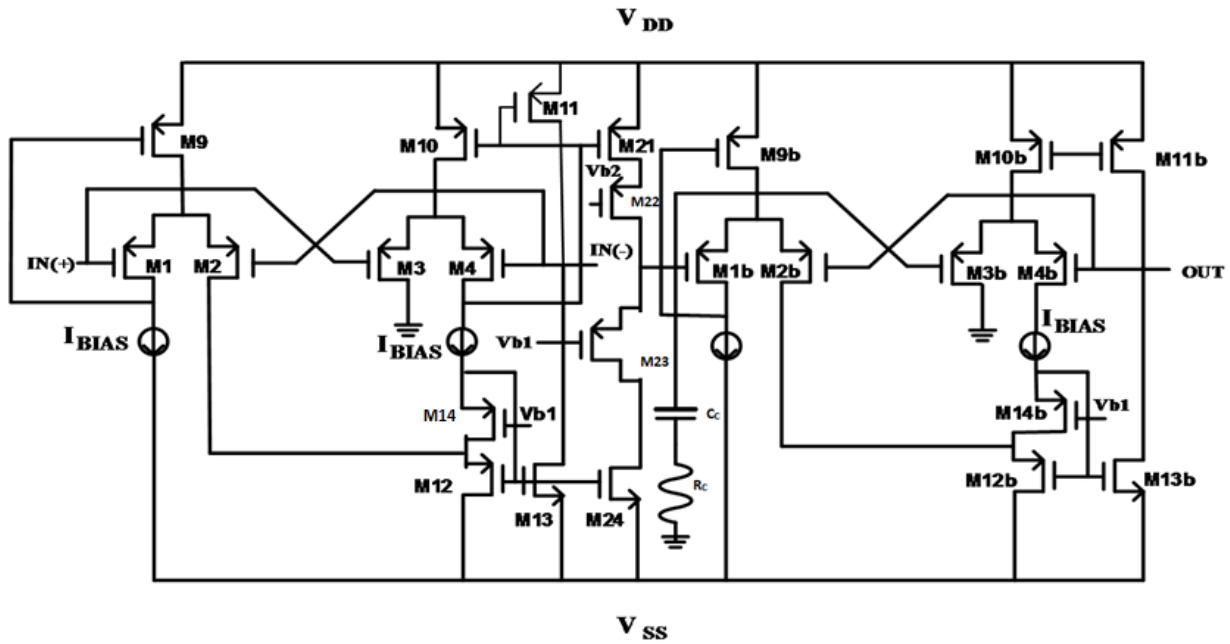


Figure 1. Existing Architecture.

III. PROPOSED ARCHITECTURE WITH IMPROVED BANDWIDTH.

In the circuit presented in fig 3, M1-M13 form the first unity-gain closed-loop voltage buffer. The input current at the inverting terminal is conveyed to the high impedance node at the drain of M22-M23. Transistors M1b-M13b implement the output buffer. In the circuit shown in fig 1, the transistor such as M14, M14b, M11, M22 and M23 is intended to provide stability to the circuit and they are not performing any such special function. Since all the MOS are operating in saturation region and if we are in a position to sacrifice the stability of the circuit to some extent, in order to achieve some fruitful results such as improvement in various parameter, then we can propose a circuit that is shown in fig 3.

In the proposed circuit shown in fig 3, MOSFET M11, M14, M14b, M22 and M23 has been removed and the resultant circuit results were studied on a Tanner EDA tool. By doing so, we have achieved improvement in the verious parameter.

Dominant-pole frequency compensation is obtained through capacitor C_C whereas resistor R_C introduces, as usual, a negativezero. The input resistance, (at the inverting input terminal) and the output resistance are expressed by:

$$r_{in}^- = \frac{1}{g_{m4}} \parallel \frac{1}{g_{m8}} \tag{1}$$

$$r_{out} = \frac{1}{g_{m4b}} \parallel \frac{1}{g_{m8b}} \tag{2}$$

The gain bandwidth product is given by:

$$\omega_{GBW} = \frac{1}{(r_{in}^- + r_{out})C_c} \tag{3}$$

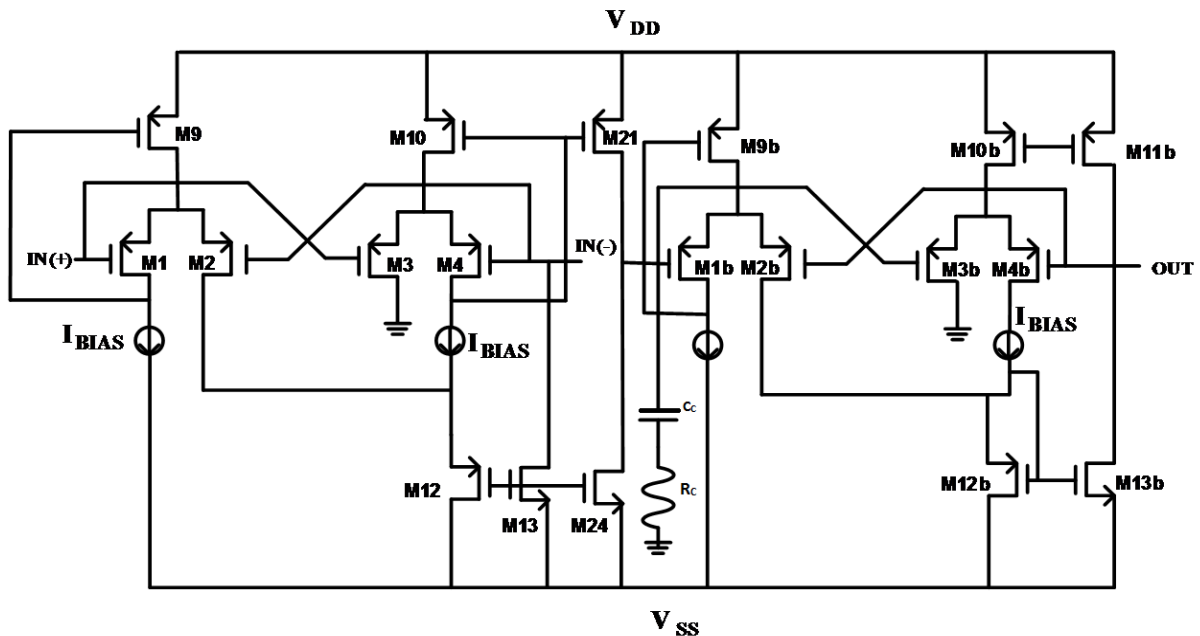


Figure 2. Proposed Architecture.

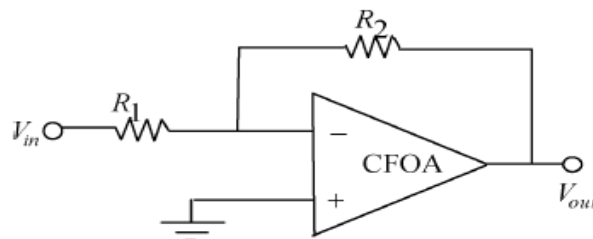


Figure 3. CFOA in inverting configuration.

III. PERFORMANCE COMPARATIVE ANALYSIS OF FIGURES AND TABLES

The proposed architecture shown in figure 2 has number of distinguished features. The number of MOS transistors has been reduced and thus the architecture become much simplified. The aspect ratio of the various transistors used in the proposed architecture has been summarized below in Table I.

TABLE I :TRANSISTOR ASPECT RATIO OF FIGURE 1

TRANSISTOR	W/L
M1-M4, M1b-M4b	180/0.6
M9-M10,M21,M9b-M10b	40/1
M11b	80/1
M12-M13,M24,M12b	130/1
M13b	260/1

III A. SIMULATION

The two proposed solutions have been designed using the 0.35 μ m technology and the results are verified using tanner EDA tool version 14.11. Bandwidth of the modified architecture shown in fig 3. was obtained around 63MHz and 70 MHz for value of the feedback resistor of 3K Ω and 9K Ω respectively. On the other hand, bandwidth in case of base circuit shown in fig 3.2 was coming out to be always more than 2MHz. Thus in our proposed circuit, it can be said that there is a considerable improvement in the bandwidth of the circuit and the bandwidth is always found to be greater than 50MHz. Also, improvement in slew rates and setting time have been reduced. Slew rates was coming out to be 8.1V/ μ sec, which is more than the slew rate obtained for circuit shown in Fig 1. Transistor dimensions of both circuits are summarized in Tables I and II, respectively. The two circuits are here dimensioned for off-chip applications and to account for a larger capacitive load of 20 pF. Also the power supply in both cases are kept equal to 2V. Total harmonic distortion of the modified architecture was found to be almost same as that of the base architecture, but, the number of the MOS used has also been reduced thus the complexity of the circuit had been improved.

TABLE II :COMPARISON OF PERFORMANCE OF THE EXISTING AND PROPOSED CIRCUITS.

PARAMETER	FIG 1.	FIG 3.
Bandwidth	>2MHz	>50MHz
Slew rate	5.2 V/us	8.1 V/us
Offset voltage	4.1 mV	6.7 mV
Settling time	212 ns	134 ns
Technology	350nm	350nm
Supply voltage	2 V	2 V
Load capacitance	20pF	20pF
THD	-76.8 dB	-75.5 dB
Impedence	577 Ω	1.4 K Ω

III B. EXPERIMENTAL RESULTS

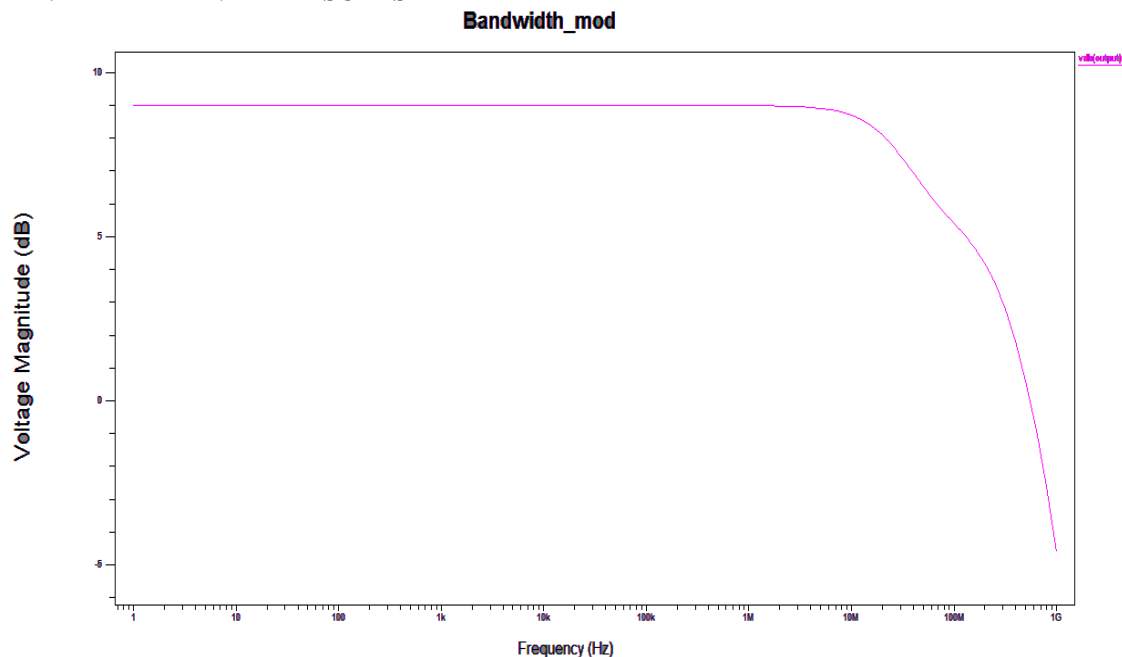


Figure 3. Gain vs Frequency characteristics of proposed circuit.

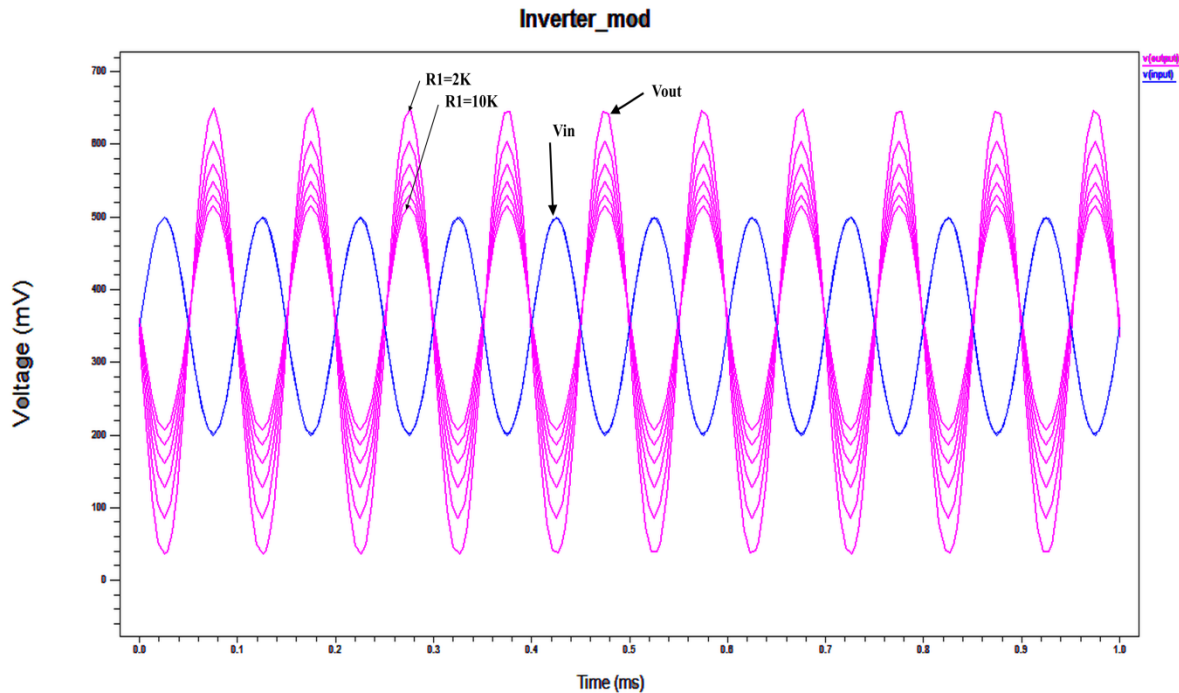


Figure 4. Response of CFOA with improved bandwidth, operating in inverting mode for different value of feedback resistor.

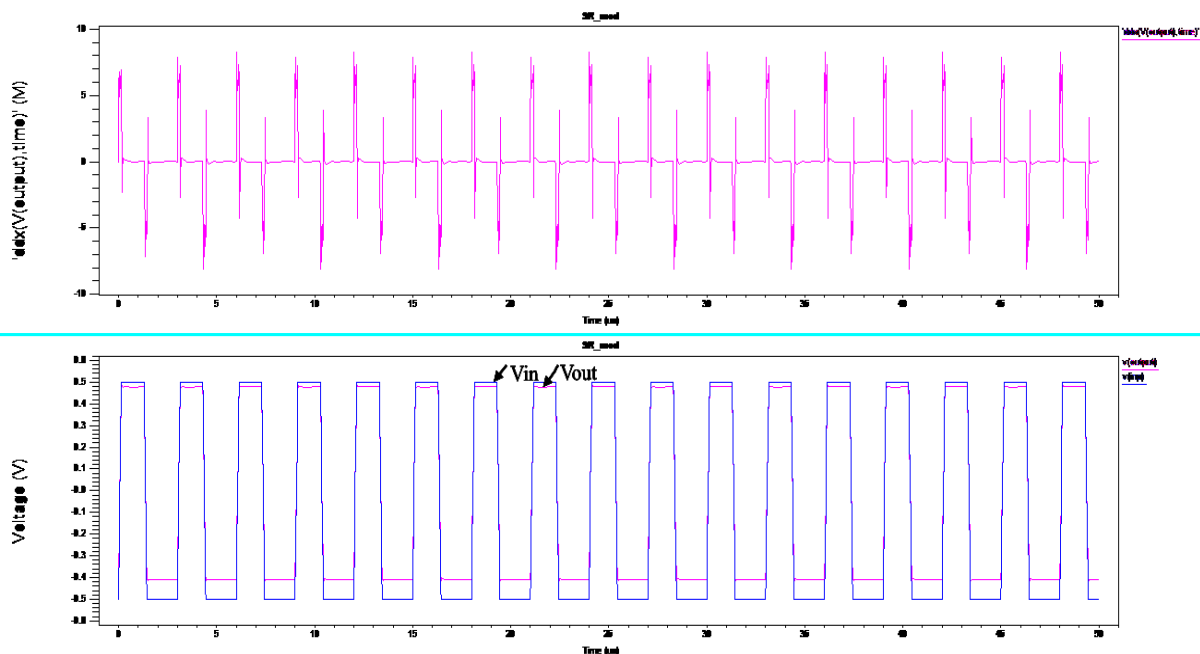


Figure 3. output voltage and slew rate characteristics of proposed circuit.

IV. CONCLUSION

CMOS based current-feedback operational amplifiers with improved bandwidth proposed here. It was obtained from two class AB voltage buffer configurations exploiting local feedback and providing low output resistance and both high current drive and slew-rate capability. Number of improvements in various parameter have been observed and the circuit has also been simplified. Comparison of the proposed circuit with the previous one has been summarized in tabular form. Design examples using a 0.35- μm process were presented and simulations along with experimental results, confirming the effectiveness of the solutions are also provided. The proposed architecture gives high value of offset voltage. Also, circuit is not as stable as its previous counterpart.

REFERENCES

- [1] A. Soliman, "Applications of the current feedback operational amplifiers," *Analog Integrated Circuits Signal Process.*, no. 11, pp. 265–302, 1996.
- [2] S. A. Mahmoud and A. M. Soliman, "New MOS-C biquad filter using the current feedback operational amplifier," *IEEE Trans. Circuits Syst. I, Reg. Papers*, vol. 46, no. 12, pp. 1510–1512, Dec. 1999.
- [3] A. K. Singh and R. Senani, "Active-R design using CFOA-poles: New resonators, filters, and oscillators," *IEEE Trans. Circuits Syst. II, Exp. Briefs*, vol. 48, no. 5, pp. 504–511, May 2001.
- [4] J. Bayard and M. Ayachi, "OTA- or CFOA-based LC sinusoidal oscillators-Analysis of the magnitude stabilization phenomenon," *IEEE Trans. Circuits Syst. I, Reg. Papers*, vol. 49, no. 8, pp. 1231–1236, Aug. 2002.
- [5] D. Smith, M. Koen, and A. Witulski, "Evolution of high-speed operational amplifier architectures," *IEEE J. Solid-State Circuits*, vol. 29, pp. 1166–1179, Oct. 1994.
- [6] C. Toumazou and J. Lidge, "Current feedback OpAmps: A blessing in disguise?," *IEEE Circuits Devices Mag.*, pp. 34–37, Jan. 1994.
- [7] Giuseppe Di Cataldo, Alfio Dario Grasso, and Salvatore Pennisi, "two CMOS current feedback operational amplifier"
- [8] S. Pennisi, "High-performance CMOS current-feedback operational amplifier," in *Proc. IEEE ISCAS '05*, Kobe, May 2005, pp. 1573–1576.
- [9] Harvey B., "Current feedback op-amp limitations: a state-of-the-art review" *IEEE International Symposium on Circuits and Systems*, pp. 1062–1069, 1993.
- [10] Smith S.O., "The good, the bad and the ugly: Current feedback technical contributions and limitations" *IEEE International Symposium on Circuits and Systems*, pp. 1058–1061, 1993.
- [11] R. Senani, "Realization of a class of analog signal processing/signal generation circuits: Novel configurations using current feedback op-amps" *Frequenz*, vol. 52, no. 9/10, pp. 196–206, 1998.
- [13] K. Smith, A. Sedra, "The current-conveyor-a new circuit building block," *IEEE Proc.*, vol. 56, pp. 1368–69, 1968.
- [14] A. Sedra, K. Smith, "A second-generation current-conveyor and its applications," *IEEE Trans.*, vol. CT-17, pp. 132–134, 1970.
- [15] R. Senani, D. R. Bhaskar, A. K. Singh, V. K. Singh, "Current Feedback Operational Amplifiers and their Applications" *Springer* New York Heidelberg Dordrecht London, 2013, chapter (3–4).
- [16] Tammam AA, Hayatleh K, Lidgey FJ : "High CMRR current feedback operational amplifier". *Int J Electron* 90:87-97, 2000.
- [17] Tammam AA, Hayatleh K, Han BL, Lidgey FJ: "A Novel current feedback operational amplifier exploiting bootstrapping technique". *Int J Electron* 94: 1157-1170, 2007.
- [18] G. Palumbo, "Bipolar current feedback amplifier: Compensation guidelines," *Analog Integrated Circuits Signal Processing*, vol. 19, no. 2, pp. 107–114, May 1999.
- [19] P. W. Li, M. J. Chin, P. R. Gray, and R. Castello, "A ratio-independent algorithmic analog-to-digital conversion technique," *IEEE J. Solid-State Circuits*, vol. SC-19, pp. 828–836, Dec. 1984.
- [20] B. J. Maundy, A. R. Sarkar, and S. J. Gift, "A new design for low voltage CMOS current feedback amplifiers," *IEEE Trans. Circuits Syst. II, Exp. Briefs*, vol. 53, no. 1, pp. 34–38, Jan. 2006.
- [21] R. Mancini, "Understanding Basic Analog -Active Devices" Application Report SLOA026A - April 2000.

Appendix

The proposed circuit design has been investing the parameters such as bandwidth, slew rate and settling time with the CAD EDA tool. The netlist created and simulate the following extracted parameters such as bandwidth >50MHz, slew rate 8.1V/ μ sec and settling time 134 nsec. The theoretical description of these parameters are described below.

(I) BANDWIDTH

Bandwidth can be defined as a measure of the width of a range of frequencies. It is measured in hertz. It is also defined as the difference between the upper and lower frequencies in a continuous set of frequencies.

If f_H and f_L are the high cutoff and low cutoff frequency respectively, then bandwidth can be given by expression:

$$\text{Bandwidth(B.W)} = f_H - f_L \quad (5)$$

(II) SLEW RATE

Slew rate is defined as the maximum rate of change of output voltage per unit of time and is expressed as volts per second. Limitations in slew rate capability can give rise to non linear effects in electronic amplifiers. Expression for slew rate is given by:

$$SR = \left[\frac{\partial v_o}{\partial t} \right]_{\max} \quad (6)$$

(III) SETTLING TIME

The settling time of an amplifier is defined as the time it takes the output to respond to a step change of input and come into, and remain within a defined error band, as measured relative to the 50% point of the input pulse. Expression for settling time is given by:

$$T_s = 4/\zeta\omega_n \quad (7)$$

Development of Distribution Feeder Reliability Profile: A Case Study of Egbu Feeders in Imo State Nigeria

Raymond OkechukwuOpara, NkwachukwuChukwuchekwa, Onojo James Ondoma¹ and Joy Ulumma Chukwuchekwa²

¹Electrical/Electronic Engineering Department, Federal University of Technology Owerri, Nigeria)

²Mathematics Department, Federal University of Technology Owerri, Nigeria))

ABSTRACT: The evaluation of a system reliability model has proven importance just as the load flow model in system planning, expansion and security level determination. Power system reliability parameters and indices evaluation is important in determining system behavior. The techniques employed for system reliability evaluation are predictive, deterministic or probabilistic. This paper evaluates the Egbu 33kV feeder using the probabilistic approach and state transition from the Markovian model. From the feeder's analysis, it was observed that the feeders experience low reliability quotient due to the high failure rates. The feeder reliabilities are 12.75%, 45.4%, 11.53%, 37.94%, 52.74% and 18.82% for Umuahia, Owerri main, Owerri Airport, Oguta, Orlu, and Okigwe respectively.

Keywords -reliability profile feeder, reliability parameter, Markovian model, transition matrix

I. INTRODUCTION

The provision of reliable, uninterrupted and secured power supply for all customers has been the major problem of power system designers and operators. This has led most of the power driven nations to device means of measuring the system reliability through the use of some customer based metrics [1]. Distribution system delivers power from bulk power system to the system load (customers). For this, it is a normal practice for utility companies to measure the coefficient of power availability to the customer at a particular security and quality. The economic and social effects of loss of electric service have significant impacts on both the utility supplying electric energy and the customers. The power system is vulnerable to system abnormalities such as control failures, protection or communication system failures, and disturbances, such as lightning, and human operational errors. Therefore, maintenance is a very important issue for power systems design and operation. The function of an electric power system is to satisfy the system load requirement with a reasonable assurance of continuity and quality. The ability of the system to provide an adequate supply of electrical energy is usually designated by the term of reliability, but if all generation and transmission supply condition is met, the system reliability will simply be distribution system bound [1]. The concept of power system reliability is extremely broad and covers all aspects of the ability of the system to satisfy the customer requirements. There is a reasonable subdivision of the concern designated as "system reliability", which is shown in figure 1.

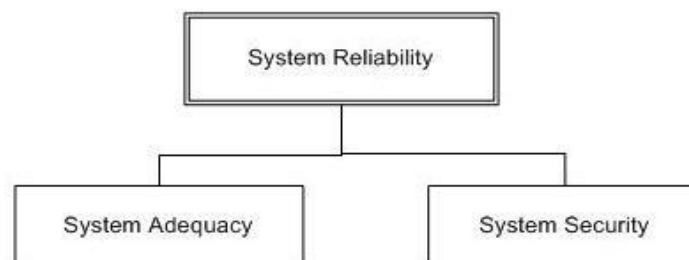


Fig.1:Sub-division of system reliability

According to reliability of power system describes the security of that system and avoidance of outage to the customers [2], while defines reliability as the ability of a system/component to perform its desired function [3]. Similarly, [4] defines reliability as simply the ability of the power network to deliver uninterrupted power to its customer at a prescribed level of quality and security. From the above definitions, it can be inferred that power system reliability is a measure of power availability to the customer at an acceptable security limit and avoidance of outage. The distribution system reliability can therefore, be defined as the probability of supply to the customer if all supply conditions is met by the generation and transmission system.

Distribution system reliability assessment is complex because of its direct connection to the system load, sparsity of components, large number of components, and radial design of network. As a result for a customer with 90 minutes of interruption per year, 70-80 minutes of interruption is as a result problems from the distribution end of the network [5].

Prior to the 1960's, the reliability of proposed power systems was often estimated by extrapolating the experience obtained from existing systems and using rule-of-thumb methods to forecast the reliability of new systems [6]. This approach is referred to as deterministic technique. During this period, considerable work was done in the field of power system reliability and some excellent papers were published. The most significant publications were two company papers by a group of Westinghouse Electric Corporation, and Public Service and Gas Company authors [7], [8]. These papers introduced the concept of a fluctuation environment to describe the failure rate of transmission system components. The techniques presented were approximations which provided results within a few percent of those obtained using more theoretical techniques, such as Markov processes [5]. Indeed, randomly occurring or probabilistic events in the system are easy to recognize: forced outages of distribution system components, failure of overhead lines, and uncertainty in customer demand. Probabilistic methods can provide more meaningful information to be used in design and resource in planning and allocation. There are two main approaches for probabilistic evaluation of power systems reliability; Analytical methods and Monte Carlo simulation [2]-[5].

Analytical techniques represent the system by mathematical models and use direct analytical solutions to evaluate a priori reliability indices from the model [9]. Monte Carlo simulation estimates posterior reliability indices by simulating the actual random behavior of the system [2]. Whichever approach is used, the predicted indices are as good as the derived models, the relevance of each technique and the quality of the data.

The Nigeria Electricity Regulatory Commission (NERC) is an independent regulatory body which is saddled with the regulation of electric power industry in Nigeria. NERC which is analogous to North American Electricity Reliability Council was formed in 2005 for:

- Electricity Tariffs
- Transparent power Policies regarding subsidies
- Promotion of power policies that are efficient and environmentally friendly
- Enforcing of standards in the creation and use of electricity in Nigeria.

The primary duties of NERC as regards Power Holding Company of Nigeria (PHCN) unbundling and privatizations are:

- Protect interest of customer, which was divided into
 - Regulation of Tariffs
 - Creation of safe and friendly work environment
 - Improvement of reliability of the electricity supply
- Licensing of operators.

Since NERC has to guide the duty of the utility in providing power to the customer, the reliability computation of the distribution system supply will help in penalizing defaulters based on the degree of default below a threshold point.

II. EXPONENTIAL DISTRIBUTION

Probability distribution functions are mathematical equations allowing a large amount of information, characteristics and behavior of a system to be described by a small number of parameters. Probability distribution density is the likelihood that a random variable, t , will be a particular value. Probability density function $f(t)$ value lies between 0 and 1, the limits inclusive. The integral over all possible outcomes must be unity.

$$f(t) \in [0,1] \quad 1$$

$$\int_{-\infty}^{\infty} f(t) dt = 1 \quad 2$$

Cumulative distribution function $F(t)$ is the integral of the probability density function, and reflects the probability that $f(t)$ will be equal to or less than t .

$$F(t) = \int_{-\infty}^{\infty} f(t)dt \quad 3$$

Probability distribution density function is the probability that the component has already failed.

Hazard rate, $\lambda(t)$, is the probability of a component failing if it has not already failed. It is also called hazard function if it is constant.

$$\lambda(t) = \frac{f(t)}{1 - F(t)} \quad 4$$

Expected value (μ) is the average of the entire data collected for analysis.

$$\text{expected value } (\mu) = \int_{-\infty}^{\infty} tf(t)dt \quad 5$$

Variance is the measure of how the function varies from the mean.

$$\text{variance} = \int_{-\infty}^{\infty} [f(t) - \mu]^2 dt \quad 6$$

Standard deviation (σ) is the normalization of the variance to a smaller value for critical analysis.

$$\sigma = \sqrt{\text{variance}} \quad 7$$

$$\% \sigma = 100 * \frac{\sigma}{\mu} \quad 8$$

Reference [2] defines reliability as the probability of a device or system performing its function adequately, for the period of time under an intended operating conditions. This definition not only gives the probability of failure, but also its magnitude, duration and frequency.

The probability of a component/system failure can be described by a function of time as

$$P(T \leq t) = F(t); \quad t \geq 0 \quad 10$$

where T is a random variable representing

the failure time

$F(t)$ is the probability that component will

fail by time t

The probability that the component/system will not fail in performing its intended function at a time t is defined as the reliability of the component/system.

$$R(t) = 1 - F(t) \quad 11$$

$F(t)$ is failure distribution function

also called unreliability function

$R(t)$ is reliability distribution function

If the time to failure random variable has a density function $f(t)$

$$R(t) = 1 - \int_0^t f(t) dt \quad 13$$

$$R(t) = \int_t^{\infty} f(t) dt \quad 14$$

The exponential distribution is used to express components failure rate because of the assumption of a constant failure rate at the components useful life period.

But for an exponential distribution function

$$f(t) = \lambda e^{-\lambda t} \quad 15$$

$$R(t) = e^{-\lambda t} \quad 16$$

If $Q(t)$ is defined as unreliability distribution function

$$Q(t) + R(t) = 1 \quad 17$$

$$\therefore Q(t) = \int_0^t f(t) dt \quad 18$$

Expected life or mean $E(t)$

$$E(t) = \int_0^{\infty} e^{-\lambda t} dt = \frac{1}{\lambda} \quad 19$$

If after failure, the component is not repaired but wholly replaced, $E(t)$ is referred to as mean time to failure (MTTF).

$$MTTF = \bar{m} = \frac{1}{\lambda} \quad 20$$

If after failure, the component is repaired and put back in service, $E(t)$ is referred to as mean time between failures (MTBF)

$$MTBF = \bar{T} = \bar{m} + \bar{r} \quad 21$$

where \bar{r} is mean time to repair

Mean time to repair (MTTR) is the reciprocal of the average repair rate.

$$MTTR = \bar{r} = \frac{1}{\mu} \quad 22$$

where μ is the average repair rate

III. SYSTEM MODELLING

The system is modelled using Markov probabilistic technique based on system states and transition between these states. It makes two basic assumptions regarding system behavior [8]:

- i. System is memory – less – (i.e. probability of event is solely a function of the existing state of the system and not what has occurred prior to the system entering the present state).
- ii. The system is stationary – (i.e. transition probabilities between states are transient and do not vary with time).

Markov models can either be discrete or continuous. Discrete models have state transitions that occur at specific time steps while continuous models have constant state transition. Discrete Markov chain characterizes a system as a set of states and transition between these states that occur at a discrete time interval. Whereas the Markov process is described by a set of states and transition between these states. It processes state transition rates for this purpose. Markov processes are easily applied to distribution system reliability model which describes the failure rates - λ_i , repair rates - μ_i and switching rates of the system components as shown in Fig. 2 below.

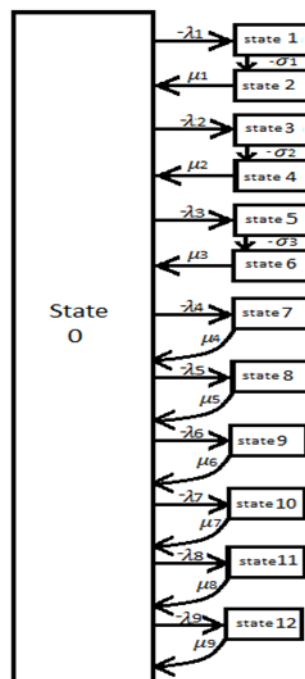


Fig. 2: System transition state

$$P'_0 = -\lambda_1 P_0 + \mu_1 P_2 - \lambda_2 P_0 + \mu_2 P_4 - \lambda_3 P_0 + \mu_3 P_6 - \lambda_4 P_0 + \mu_4 P_8 - \lambda_5 P_0 + \mu_5 P_{10} - \lambda_6 P_0 + \mu_6 P_{12} + \mu_7 P_{10} - \lambda_8 P_0 + \mu_8 P_{11} - \lambda_9 P_0 + \mu_9 P_{12} \quad 23$$

$$P'_1 = \lambda_1 P_0 - \sigma_1 P_1 \quad 24$$

$$P'_2 = \sigma_1 P_1 - \mu_1 P_2 \quad 25$$

$$P'_3 = \lambda_2 P_0 - \sigma_2 P_3 \quad 26$$

$$P'_4 = \sigma_2 P_3 - \mu_2 P_4 \quad 27$$

$$P'_5 = \lambda_3 P_0 - \sigma_3 P_5 \quad 28$$

$$P'_6 = \sigma_3 P_5 - \mu_3 P_6 \quad 29$$

$$P'_7 = \lambda_4 P_0 - \mu_4 P_7 \quad 30$$

$$P'_8 = \lambda_5 P_0 - \mu_5 P_8 \quad 31$$

$$P'_9 = \lambda_6 P_0 - \mu_6 P_9 \quad 32$$

$$P'_{10} = \lambda_7 P_0 - \mu_7 P_{10} \quad 33$$

$$P'_{11} = \lambda_8 P_0 - \mu_8 P_{11} \quad 34$$

$$P'_{12} = \lambda_9 P_0 - \mu_9 P_{12} \quad 35$$

where P_0 = probability of

V COMPONENT RELIABILITY PARAMETER

Simple reliability models are based on component failure rate and repair rates of the system components.

- Permanent Short Circuit Failure Rate(λ_p): Describes the number of times per year a component expected to experience a permanent short circuit.
- Temporary Short Circuit Failure Rate(λ_T): Describes the number of times per year a component is expected to experience a temporary short circuit.
- Open Circuit Failure Rate(λ_{oc}): Describes the number of times a component will interrupt the flow of current without causing fault current to flow.
- Schedule Maintenance Frequency(λ_m): The frequency of schedule maintenance for a component
- Mean Time to Repair(MTTR): Expected time it will take to repair a fault. A single MTTR is typically used for each component, but may be different for different failure modes.
- Mean Time to Switch(MTTS): The mean time it will take a sectionalizing switch to operate after a fault occurs on the system.
- Probability of Operation Failure(POF): Conditional statement that a component will not operate when called to operate.
- Mean Time to Maintain(MTTM): The average time taken to perform schedule maintenance on a component.

VI INTERRUPTION CAUSES

Customer's interruptions are caused by a wide range of phenomena which include equipment failure, tree, animals, severe weather and human error [10]. The interruption causes are at the distribution system primarily and understanding these phenomena will allow for practical perspective to reliability studies analysis [11]. Of all these phenomena, the most frequent and severe is equipment failure.

A EQUIPMENT FAILURES

All distribution system equipment has a probability of failure associated to it [12]. When first installed, a piece of equipment can fail due to poor manufacturing, damage during shipping or installation [13]. Healthy equipment may fail as a result of high current or voltage, animals, severe weather etc., equipment will also fail for reasons such as chronological age, thermal aging, state of chemical decomposition, state of contamination and state of mechanical wear [14].

B SEVERE WEATHER

Hash weather conditions are extreme situations which can be grouped under contingency [5][10]. They include: Tornadoes, Hurricanes, Earthquakes, and Heat Storm etc. The weather condition contingency that will be considered for the purpose of this paper is lightning Storm.

C HUMAN FACTOR

These are reliability concern based on human. It is divided into three groups which would not be considered by this paper.

- Schedule Interruption
- Human Switching errors and
- Vehicular accidents

VII TRANSITION MATRIX GENERATION AND EVALUATION OF FEEDER RELIABILITY INDEX:

The procedure for the evaluation of feeder reliability quotient; indices and availability are evaluated as shown below:

- Evaluate average feeder failure rate.
- Evaluate feeder mean down time
- Evaluate components failure; repair rate and switching rate.
- Evaluate feeder availability and distribution system reliability index.

System Average Interruption Frequency Index (SAIFI): measure of how many sustained interruptions an average customer will experience over the course of a specified time.

$$SAIFI = \frac{\sum \text{customer sustained interruption}}{\text{Total number of customers served}}^{37}$$

System Average Interruption Duration Index (SAIDI): measure of how many interruptions an average customer will experience over the course of a specified time.

$$SAIDI = \frac{\sum \text{customer outage duration}}{\text{Total number of customers served}} \quad 38$$

CAIDI: measure of how long an average interruption lasts. It is a measure of utility response time.

$$CAIDI = \frac{\sum \text{customer interruption duration}}{\text{Total number of customers served}} \quad 39$$

Average System Availability Index (ASAI): measure of customer weighted availability.

$$ASAI = \frac{\text{Total customer served hour}}{\text{Total customer served time required}} \quad 40$$

VIII RESULTS AND DISCUSSION

Figures 3 and 4 below show the monthly and daily feeder consumptions respectively.

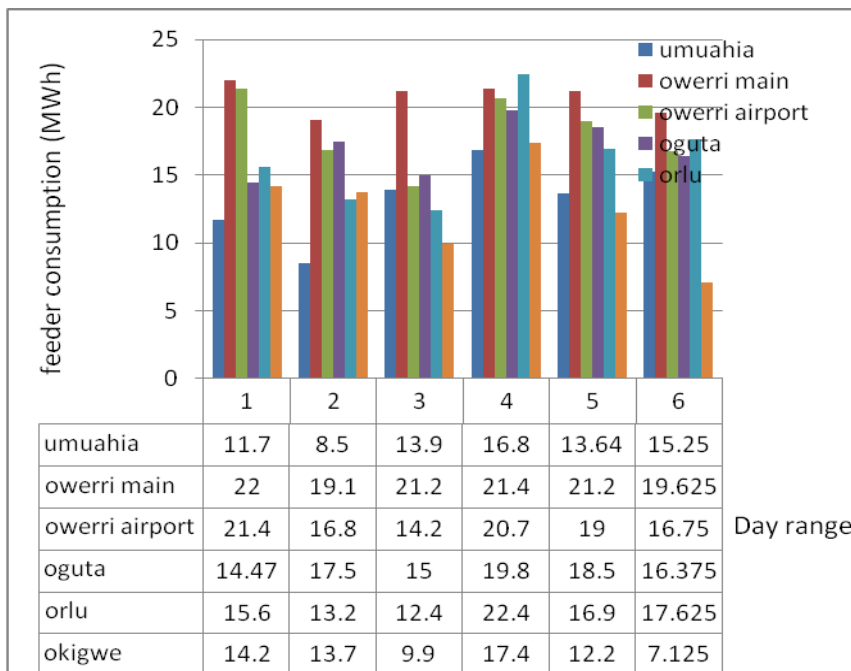


Fig.3. Monthly feeder consumption

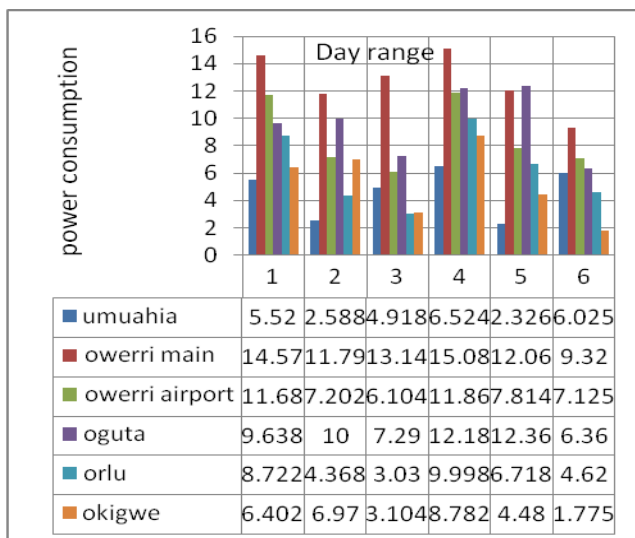


Fig.4. Daily feeder consumption

From the monthly and daily bar chart, it can be observed that Owerri main is the most industrialized feeder and the daily consumptions of the feeder are relatively high.

Table 1 below shows the actual, modified failure rates and reliability of the feeders. The actual failure rates of the system gives an approximately zero reliability but with the failure rate modification, some reasonable reliability quotient was obtained.

Table1: Feeder failure rates and reliability.

Feeder	Original failure rate	Modified failure rate	Reliability (%)
Umuahia	41.203	0.41203	12.74
Owerri main	15.972	0.15972	45.4
Owerri airport	43.117	0.43117	11.53
Oguta	19.381	0.19381	37.94
Orlu	12.795	0.12795	52.74
Okigwe	33.406	0.33406	18.82

Table 2 shows the feeder reliability indices against the other. The worst performing feeder can be observed to be Owerri airport and the factor necessitating the ill performance can be corrected.

Table2: Feeder down time and reliability index

Feeders	Total down time	ASAI	SAIDI	SAIFI	CAIDI
Umuahia	1406.69	0.3781	0.0354	0.005275	0.1760
Owerri main	152.40	0.041	0.0038	0.001975	0.0190
Owerri airport	359.49	0.0966	0.0090	0.054	0.0450
Oguta	454.78	0.1222	0.0114	0.002425	0.0570
Orlu	314.44	0.0845	0.0079	0.00135	0.0398
Okigwe	969.30	0.2606	0.0242	0.04175	0.1212

Table 3 shows the energy not served and cost of energy not served incurred by the utility.

Table 3: Total Energy Not Served(ENS) and Cost

Feeder	Total ENS (MWh)	Average ENS (MWh)	Cost of ENS (N million)
Umuahia	393.9	78.78	1.010
Owerri main	167.25	33.45	0.429
Owerri airport	161.89	32.38	0.415
Oguta	122.37	24.46	0.313
Orlu	350.41	70.08	0.898
Okigwe	583.62	116.72	1.496

$P_0 = 0.8684; P_1 = 0.0419;$

$P_2 = 0.03673; P_3 = 0.00125;$

$P_4 = 0.00334;$

$P_5 = 0.000119; P_6 = 0.000297;$

$P_7 = 0.000397; P_8 = 0.0465;$

$P_9 = 0.000397; P_{10} = 0.000238;$

$P_{11} = 0.000238; P_{12} = 0.000238$

IX CONCLUSION

From the analysis performed on the systems parameter, it can be observed that the feeders exhibit high average failure rates, high repair rates and low switching rates. The nature of the system parameter undoubtedly makes the system have the following:

- i. Low Reliability quotient

- ii. Average availability quotient
- iii. High SAIFI
- iv. High SAIDI
- v. High CAIDI and
- vi. Low ASAI

With these observable problems of the feeders, a customer would rather resort to the back-up supply rather than the utility supply. From the analysis performed, the factors causing the system low reliability and reliability quotients are:

- a. Feeders component high failure rates due to
 - i. Maintenance problem
 - ii. System components overloading
 - iii. Operators operation
- b. Feeders high repair rates due to
 - i. Low utility response to fault clearance
 - ii. Manual operation of system
- c. High energy not served during fault because of the feeder is not segmented.

X RECOMMENDATION

The feeder as analyzed above shows the reliability quotient and feeder indices. For optimal performance of the system the following recommendation should be considered.

- Increase the ratings of components employed in the feeder. Most of the feeder failure is due to component overloading.
- Adopt preventive maintenance schedule. The schedule for maintenance can be allocated using the consumption bar chart presented in figure 1.
- Dividing system into segment so as to reduce energy not served. Utility incur high cost of energy not served (CENS) when faults occur. If the feeder circuit is increased and divided by fuses, the amount of energy not served will reduce and hence cost of energy not served
- Creation of Performance Based Rating (PBR) Regulatory. The regulation has to place a stipulation on the reliability quotient and reliability indices of utility to help improve service to customer.

Adopting Customer Cost of Reliability technique. Making the customers has their reliability contracts.

XI ACKNOWLEDGEMENT

The authors are grateful to Mr. Isiofialkechukwu Moses for his help in this study. The contribution of Federal University of Technology, Owerri, Nigeria through provision of facilities used in this study is hereby appreciated.

REFERENCES

- [1] C.C. Liu, G.T. Heydt, A. G. Phadke et al, "The Strategic Power Infrastructure Defense (SPID) System", IEEE Control System Magazine, Vol. 20, Issue 4, August 2000, pp. 40 - 52.
- [2] T. Gonën "Electric Power Distribution System Engineering 2nd edition" CRC Press Taylor and Francis Group Boca Raton London New York 2007.
- [3] L. L. Grigsby "Electric Power Engineering Handbook: Power System" CRC Press Taylor & Francis Group Boca Raton London New York 2007.
- [4] A.J. Momoh "Electric Power Distribution, Automation, Protection and Control" CRC Press Taylor & Francis Group Boca Raton London New York 2008.
- [5] Richard E. Brown "Electric Power Distribution Reliability 2nd Edition", CRC Press, Taylor & Francis Group Boca Raton London, NY 2009
- [6] D.P. Gaver, F.E. Montmeat, A.D. Patton, "Power System Reliability I: Measures of Reliability and Methods of Calculation", IEEE Transaction Power Apparatus System, vol. 83, pp. 727-737, July, 1964.
- [7] C.E. Montmeat, A.D. Patton, J. Zemkowski, D.J. Cumming, "Power System Reliability II: Applications and a Computer Program", IEEE Transaction on Power Apparatus System, vol. PAS-87, pp. 636-643, July 1965.
- [8] R. Billinton, Kenneth E. Bollinger, "Transmission System Reliability Evaluation using Markov Processes", IEEE transaction on Power Apparatus System, vol. PAS-87 no. 2 pp. 538-547, Feb. 1968.
- [9] Richard E. Brown and B. Howe, "Optimal Deployment of Reliability Investment", E-source Report PQ-6, April 2000
- [10] "Risk-Based Resource Allocation for Distribution System" PSERC Publication 05-06, December 2005.
- [11] "IEEE Standard 1366, Guide for Electric Power Distribution Reliability Indices", 2003.
- [12] J.M Clummenson, "A System Approach to Power Quality", IEEE Spectrum, June 1993.
- [13] S.V Nikolajeric, "The Behavior of water in XLPE and EPR Cables and its Influence on the Electrical Characteristics of Insulation", IEEE transaction on Power Delivery, Vol. 14, No. 1, Jan. 1999, pp. 39-45.
- [14] B.S Bernstein, W. A Thue, M.D Walton, and J.T Smith III, "Accelerated Aging of Extruded Dielectric Power Cables, Part II: Life Testing of 15kV XLPE-Insulated Cables", IEEE Transaction on Power Delivery Vol. 7, No.2, April 1992, pp. 603-608.

TCP-IP Model in Data Communication and Networking

Pranab Bandhu Nath¹, Md.Mofiz Uddin²

¹(MS in ITM, Sunderland University, UK)

²(MS in CSE, Royal University of Dhaka, Bangladesh)

ABSTRACT : The Internet protocol suite is the computer networking model and set of communications protocols used on the Internet and similar computer networks. It is commonly known as TCP/IP, because it's most important protocols, the Transmission Control Protocol (TCP) and the Internet Protocol (IP), were the first networking protocols defined in this standard. Often also called the Internet model, it was originally also known as the DoD model, because the development of the networking model was funded by DARPA, an agency of the United States Department of Defense. TCP/IP provides end-to-end connectivity specifying how data should be packetized, addressed, transmitted, routed and received at the destination. This functionality is organized into four abstraction layers which are used to sort all related protocols according to the scope of networking involved. From lowest to highest, the layers are the link layer, containing communication technologies for a single network segment (link); the internet layer, connecting hosts across independent networks, thus establishing internetworking; the transport layer handling host-to-host communication; and the application layer, which provides process-to-process application data exchange. Our aim is describe operation & models of TCP-IP suite in data communication networking.

Keywords – TCP-IP, OSI, Protocol, layers, Stack.

I. INTRODUCTION

TCP/IP is a two-layer program. The higher layer, Transmission Control Protocol, manages the assembling of a message or file into smaller packets that are transmitted over the Internet and received by a TCP layer that reassembles the packets into the original message. The lower layer, Internet Protocol, handles the address part of each packet so that it gets to the right destination. Each gateway computer on the network checks this address to see where to forward the message. Even though some packets from the same message are routed differently than others, they'll be reassembled at the destination [1]. TCP/IP uses the client/server model of communication in which a computer user requests and is provided a service by another computer in the network. TCP/IP communication is primarily point-to-point, meaning each communication is from one point in the network to another point or host computer. TCP/IP and the higher-level applications that use it are collectively said to be "stateless" because each client request is considered a new request unrelated to any previous one. Being stateless frees network paths so that everyone can use them continuously Any Internet users are familiar with the even higher layer application protocols that use TCP/IP to get to the Internet. These include the World Wide Web's Hypertext Transfer Protocol (HTTP), the File Transfer Protocol (FTP), Telnet (Telnet) which lets you logon to remote computers, and the Simple Mail Transfer Protocol (SMTP). These and other protocols are often packaged together with TCP/IP as a "suite." Personal computer users with an analog phone modem connection to the Internet usually get to the Internet through the Serial Line Internet Protocol (SLIP) or the Point-to-Point Protocol (PPP). These protocols encapsulate the IP packets so that they can be sent over the dial-up phone connection to an access provider's modem [2]. Protocols related to TCP/IP include the User Datagram Protocol (UDP), which is used instead of TCP for special purposes. Other protocols are used by network host computers for exchanging router information. These include the Internet Control Message Protocol (ICMP), the Interior Gateway Protocol (IGP), the Exterior Gateway Protocol (EGP), and the Border Gateway Protocol (BGP).

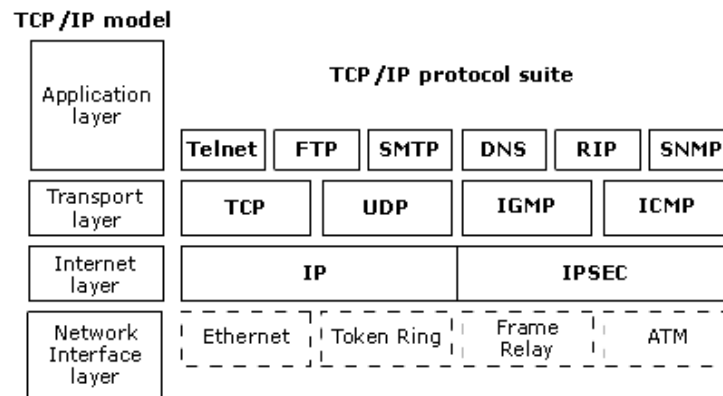


Figure 1: TCP-IP Protocol Suite.

II. EARLY RESEARCH ON TCP-IP

The Internet protocol suite resulted from research and development conducted by the Defense Advanced Research Projects Agency (DARPA) in the late 1960s. After initiating the pioneering ARPANET in 1969, DARPA started work on a number of other data transmission technologies. In 1972, Robert E. Kahn joined the DARPA Information Processing Technology Office, where he worked on both satellite packet networks and ground-based radio packet networks, and recognized the value of being able to communicate across both. In the spring of 1973, Vinton Cerf, the developer of the existing ARPANET Network Control Program (NCP) protocol, joined Kahn to work on open-architecture interconnection models with the goal of designing the next protocol generation for the ARPANET [3]. By the summer of 1973, Kahn and Cerf had worked out a fundamental reformulation, in which the differences between network protocols were hidden by using a common internetwork protocol, and, instead of the network being responsible for reliability, as in the ARPANET, the hosts became responsible. Cerf credits Hubert Zimmermann and Louis Paulin, designer of the CYCLADES network, with important influences on this design. The design of the network included the recognition that it should provide only the functions of efficiently transmitting and routing traffic between end nodes and that all other intelligence should be located at the edge of the network, in the end nodes. Using a simple design, it became possible to connect almost any network to the ARPANET, irrespective of the local characteristics, thereby solving Kahn's initial problem.

A computer called a router is provided with an interface to each network. It forwards packets back and forth between them. Originally a router was called gateway, but the term was changed to avoid confusion with other types of gateways.

III. ARCHITECTURAL PRINCIPLE

End-to-end principle: This principle has evolved over time. Its original expression put the maintenance of state and overall intelligence at the edges, and assumed the Internet that connected the edges retained no state and concentrated on speed and simplicity. Real-world needs for firewalls, network address translators, web content caches and the like have forced changes in this principle.

Robustness Principle: "In general, an implementation must be conservative in its sending behavior, and liberal in its receiving behavior. That is, it must be careful to send well-formed datagrams, but must accept any datagram that it can interpret. The second part of the principle is almost as important: software on other hosts may contain deficiencies that make it unwise to exploit legal but obscure protocol features.

IV. MODEL LAYERS OF TCP-IP

The Internet protocol suite uses encapsulation to provide abstraction of protocols and services. Encapsulation is usually aligned with the division of the protocol suite into layers of general functionality. In general, an application uses a set of protocols to send its data down the layers, being further encapsulated at each level. The layers of the protocol suite near the top are logically closer to the user application, while those near the bottom are logically closer to the physical transmission of the data [5]. Viewing layers as providing or consuming a service is a method of abstraction to isolate upper layer protocols from the details of transmitting bits over, for example, Ethernet and collision detection, while the lower layers avoid having to know the details of each and every application and its protocol. Even when the layers are examined, the assorted architectural documents—there is no single architectural model such as ISO 7498, the Open Systems Interconnection (OSI) model have fewer and less rigidly defined layers than the OSI model, and thus provide an easier fit for real-world protocols.

One frequently referenced document, RFC 1958, does not contain a stack of layers. The lack of emphasis on layering is a major difference between the IETF and OSI approaches. It only refers to the existence of the internetworking layer and generally to upper layers; this document was intended as a 1996 snapshot of the architecture: "The Internet and its architecture have grown in evolutionary fashion from modest beginnings, rather than from a Grand Plan. While this process of evolution is one of the main reasons for the technology's success, it nevertheless seems useful to record a snapshot of the current principles of the Internet architecture."

RFC 1122, entitled Host Requirements, is structured in paragraphs referring to layers, but the document refers to many other architectural principles not emphasizing layering. It loosely defines a four-layer model, with the layers having names, not numbers, as follows:

- The Application layer is the scope within which applications create user data and communicate this data to other applications on another or the same host. The applications, or processes, make use of the services provided by the underlying, lower layers, especially the Transport Layer which provides reliable or unreliable pipes to other processes. The communications partners are characterized by the application architecture, such as the client-server model and peer-to-peer networking. This is the layer in which all higher level protocols, such as SMTP, FTP, SSH, HTTP, operate. Processes are addressed via ports which essentially represent services.
- The Transport Layer performs host-to-host communications on either the same or different hosts and on either the local network or remote networks separated by routers. It provides a channel for the communication needs of applications. UDP is the basic transport layer protocol, providing an unreliable datagram service. The Transmission Control Protocol provides flow-control, connection establishment, and reliable transmission of data.
- The Internet layer has the task of exchanging datagrams across network boundaries. It provides a uniform networking interface that hides the actual topology (layout) of the underlying network connections. It is therefore also referred to as the layer that establishes internetworking, indeed, it defines and establishes the Internet. This layer defines the addressing and routing structures used for the TCP/IP protocol suite. The primary protocol in this scope is the Internet Protocol, which defines IP addresses. Its function in routing is to transport datagrams to the next IP router that has the connectivity to a network closer to the final data destination.
- The Link layer defines the networking methods within the scope of the local network link on which hosts communicate without intervening routers. This layer includes the protocols used to describe the local network topology and the interfaces needed to effect transmission of Internet layer datagrams to next-neighbor hosts [6].

The Internet protocol suite and the layered protocol stack design were in use before the OSI model was established. Since then, the TCP/IP model has been compared with the OSI model in books and classrooms, which often results in confusion because the two models use different assumptions and goals, including the relative importance of strict layering.

V. Data Encapsulation and the TCP/IP Protocol Stack

The packet is the basic unit of information that is transferred across a network. The basic packet consists of a header with the sending and receiving systems' addresses, and a body, or payload, with the data to be transferred. As the packet travels through the TCP/IP protocol stack, the protocols at each layer either add or remove fields from the basic header. When a protocol on the sending system adds data to the packet header, the process is called data encapsulation [7]. Moreover, each layer has a different term for the altered packet, as shown in the following figure.

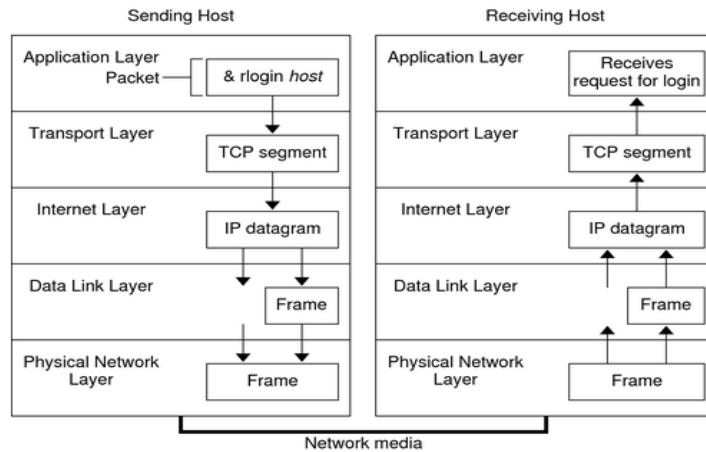


Figure 2: How a Packet Travels Through the TCP/IP Stack

IP attaches an IP header to the segment or packet's header, in addition to the information that is added by TCP or UDP. Information in the IP header includes the IP addresses of the sending and receiving hosts, the datagram length, and the datagram sequence order. This information is provided if the datagram exceeds the allowable byte size for network packets and must be fragmented. TCP/IP provides internal trace support by logging TCP communication when an RST packet terminates a connection. When an RST packet is transmitted or received, information on as many as 10 packets, which were just transmitted, is logged with the connection information.

VI. TCP PROTOCOLS WITH INTERNETS

TCP/IP is most commonly associated with the UNIX operating system. While developed separately, they have been historically tied, as mentioned above, since 4.2BSD UNIX started bundling TCP/IP protocols with the operating system. Nevertheless, TCP/IP protocols are available for all widely-used operating systems today and native TCP/IP support is provided in OS/2, OS/400, all Windows versions since Windows 9x, and all Linux and UNIX variants [8]. When the user accesses a Web site on the Internet, the NAT server will translate the "private" IP address of the host (192.168.50.50) into a "public" IP address (220.16.16.5) from the pool of assigned addresses. NAT works because of the assumption that, in this example, no more than 27 of the 64 hosts will ever be accessing the Internet at a single time.

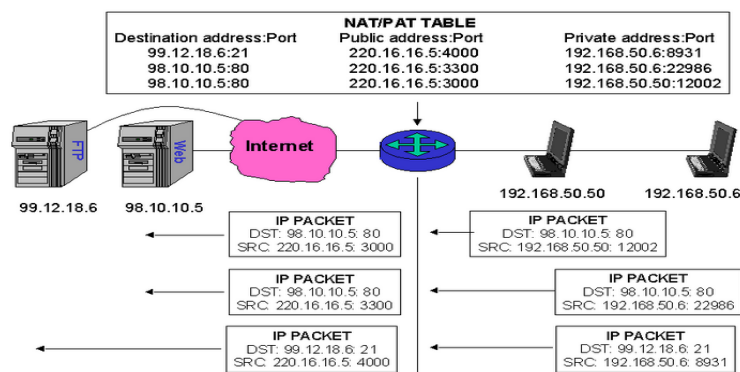


Figure 3: TCP-IP

A pool of IP addresses can be shared by multiple hosts using a mechanism called Network Address Translation (NAT). NAT, described in RFC 1631, is typically implemented in hosts, proxy servers, or routers. The scheme works because every host on the user's network can be assigned an IP address from the pool of RFC 1918 private addresses; since these addresses are never seen on the Internet, this is not a problem. Consider the scenario shown in Figure 3.

Port numbers are used by higher layer protocols (e.g., TCP and UDP) to identify a higher layer application. A TCP connection, for example, is uniquely identified on the Internet by the four values (aka 4-tuple) <source IP address, source port, destination IP address, destination port>. The server's port number is defined by the standards while client port numbers can be any number greater than 1023. The scenario in Figure 7 shows the following three connections:

- The client with the "private" IP address 192.168.50.50 (using port number 12002) connects to a Web server at address 98.10.10.5 (port 80).
- The client with the "private" IP address 192.168.50.6 (using port number 22986) connects to the same Web server at address 98.10.10.5 (port 80).
- The client with the "private" IP address 192.168.50.6 (using port number 8931) connects to an FTP server at address 99.12.18.6 (port 21).

PAT works in this scenario as follows. The router (running PAT software) can assign both local hosts with the same "public" IP address (220.16.16.5) and differentiate between the three packet flows by the source port. A final note about NAT and PAT. Both of these solutions work and work fine, but they require that every packet be buffered, disassembled, provided with a new IP address, a new checksum calculated, and the packet reassembled. In addition, PAT requires that a new port number be placed in the higher layer protocol data unit and new checksum calculated at the protocol layer above IP, too. The point is that NAT, and particularly PAT, results in a tremendous performance hit.

One advantage of NAT is that it makes IP address renumbering a thing of the past. If a customer has an IP NET_ID assigned from its ISP's CIDR block and then they change ISPs, they will get a new NET_ID. With NAT, only the servers need to be renumbered [9].

VII. COMPARISON BETWEEN TCP-IP & OSI

The three top layers in the OSI model, i.e. the application layer, the presentation layer and the session layer, are not distinguished separately in the TCP/IP model which only has an application layer above the transport layer. While some pure OSI protocol applications, such as X.400, also combined them, there is no requirement that a TCP/IP protocol stack must impose monolithic architecture above the transport layer. For example, the NFS application protocol runs over the external Data Representation (XDR) presentation protocol, which, in turn, runs over a protocol called Remote Procedure Call (RPC). RPC provides reliable record transmission, so it can safely use the best-effort UDP transport. Different authors have interpreted the TCP/IP model differently, and disagree whether the link layer, or the entire TCP/IP model, covers OSI layer 1 (physical layer) issues, or whether a hardware layer is assumed below the link layer. Several authors have attempted to incorporate the OSI model's layers 1 and 2 into the TCP/IP model, since these are commonly referred to in modern standards. This often results in a model with five layers, where the link layer or network access layer is split into the OSI model's layers 1 and 2. The IETF protocol development effort is not concerned with strict layering. Some of its protocols may not fit cleanly into the OSI model, although RFCs sometimes refer to it and often use the old OSI layer numbers. The IETF has repeatedly stated that Internet protocol and architecture development is not intended to be OSI-compliant. RFC 3439, addressing Internet architecture, contains a section entitled: "Layering Considered Harmful".

For example, the session and presentation layers of the OSI suite are considered to be included to the application layer of the TCP/IP suite. The functionality of the session layer can be found in protocols like HTTP and SMTP and is more evident in protocols like Telnet and the Session Initiation Protocol (SIP). Session layer functionality is also realized with the port numbering of the TCP and UDP protocols, which cover the transport layer in the TCP/IP suite. Functions of the presentation layer are realized in the TCP/IP applications with the MIME standard in data exchange.

Conflicts are apparent also in the original OSI model, ISO 7498, when not considering the annexes to this model, e.g., the ISO 7498/4 Management Framework, or the ISO 8648 Internal Organization of the Network layer (IONL). When the IONL and Management Framework documents are considered, the ICMP and IGMP are defined as layer management protocols for the network layer. In like manner, the IONL provides a structure for "sub network dependent convergence facilities" such as ARP and RARP.

VIII. CONCLUSION

The Internet protocol suite does not presume any specific hardware or software environment. It only requires that hardware and a software layer exists that is capable of sending and receiving packets on a computer network. As a result, the suite has been implemented on essentially every computing platform. A minimal implementation of TCP/IP includes the following: Internet Protocol (IP), Address Resolution Protocol (ARP), Internet Control Message Protocol, Transmission Control Protocol (TCP), and User Datagram Protocol. In addition to IP, Internet Protocol version 6 requires Neighbor Discovery Protocol and IGMPv6 and is often accompanied by an integrated IPsec security layer. Application programmers are typically concerned only with interfaces in the application layer and often also in the transport layer, while the layers below are services provided by the TCP/IP stack in the operating system. Most IP implementations are accessible to programmers

through sockets. Unique implementations include Lightweight TCP/IP, an open source stack designed for embedded systems a stack and associated protocols for amateur packet radio systems and personal computers connected via serial lines. Microcontroller firmware in the network adapter typically handles link issues, supported by driver software in the operating system. Non-programmable analog and digital electronics are normally in charge of the physical components below the link layer, typically using an application-specific integrated circuit chipset for each network interface or other physical standard. High-performance routers are to a large extent based on fast non-programmable digital electronics, carrying out link level switching.

IX. Acknowledgements

We are earnestly grateful to one our group member, Pranab Bandhu Nath, MS in ITM, Sunderland University, UK. For providing us with his special advice and guidance for this project. Finally, we express our heartiest gratefulness to the Almighty and our parents who have courageous throughout our work of the project.

REFERENCES

- [1] S. Zaman S., F. Karray. Fuzzy ESVDf approach for Intrusion Detection System. *The IEEE 23rd International Conference on Advanced Information Networking and Applications (AINA-09)*, May 26-29, 2009.
- [2] I. Onut and A. Ghorbani. A Feature Classification Scheme for Network Intrusion Detection. *International Journal of Network Security*, Page(s): 1-15, July 2007.
- [3] A. Tamilarasan, S. Mukkamala, A. Sung, and K. Yendrapalli. Feature Ranking and Selection for Intrusion Detection Using Artificial Neural Networks and Statistical Methods. *2006 International Joint Conference on Neural Networks (IJCNN'06)*, Page(s):4754-4761, July 16-21, 2006.
- [4] A. Sung, S. Mukkamala. Identifying Important Features for Intrusion Detection Using Support Vector Machines and Neural Networks. *Symposium on Application and Internet (SAINT'03)*, Page(s): 209-216, 27-31 Jan. 2003.
- [5] V. Golovko, L. Vaitsekhovich, P. Kochurko and U. Rubanau. Dimensionality Reduction and Attack Recognition using Neural Network Approaches. *International Joint Conference on Neural Networks, 2007*, Page(s): 2734-2739, 12-17 Aug. 2007.
- [6] S. Srinoy. Intrusion Detection Model Based On Particle Swarm Optimization and Support Vector Machine. *The 2007 IEEE Symposium on Computational Intelligence in Security and Defense Applications (CISDA 2007)*, Page(s): 186-192, 1-5 April 2007.
- [7] H. Gao, H. Yang, X. Wang. Ant Colony Optimization Based Network Intrusion Feature Selection and Detection. *The Fourth International Conference on Machine Learning and Cybernetics, Guangzhou*, Page(s): 18-21, August 2005.
- [8] Kh. Shazzad, J. Sou Park. Optimization of Intrusion Detection through Fast Hybrid Feature Selection. *The Sixth International Conference on Parallel and Distributed Computing, Applications and Technologies, 2005, (PDCAT'05)*, Page(s): 264 - 267, 05-08 Dec, 2005.
- [9] M. Yasin, and A. Awan. A Study of Host-Based IDS using System Calls. *INCC 204, International Conference on Networking and Communication 2004*, on page(s): 36-41, June 2004.

Drying of Chilli Pepper Using a Solar Dryer with a Back-Up Incinerator under Makurdi Humid Climate

Ibrahim, J. S¹, Barki, E², Edeoja, A. O.¹

¹Department of Mechanical Engineering, University of Agriculture, Makurdi, Nigeria

²Department of Mechanical Engineering, Benue State Polytechnic, Ugbokolo, Nigeria.

Abstract: The drying of chilli pepper using a solar dryer with a back-up incinerator to determine the drying rate and efficiency was undertaken. The dryer was used to dehydrate the pepper during sunny (clear) and cloudy (dull) weather with the view to improve the quality of the pepper for storage. Drying was assumed to have taken place in the falling rate period so that only one drying rate constant was used. Different batches of the pepper were dried under various drying conditions. The solar dryer was used for drying during sunny weather while the incinerator assisted dryer was used during cloudy weather. Open air sun drying was carried out as control. The respective weight losses of the dried samples were measured and used to determine the reduction in moisture contents. The efficiencies of the equipment and the drying rate efficiencies were computed. The drying rate efficiencies for solar dryer and solar-incinerator dryer were obtained as 99.6 %, and 92.9 % respectively. The corresponding computed efficiencies for the equipment were 56 % and 13 % respectively. The results obtained showed that drying rate was highest during the solar drying and least during the incinerator-assisted and control drying respectively indicating good prospects for solar drying of chilli pepper in Makurdi.

Keywords: Solar dryer, incinerator, chilli pepper, drying rate, efficiency, humid climate

I. Introduction

Drying is a thermal process in which heat and moisture transfer occur simultaneously. Heat is transferred by convection from heated air to the product to raise the temperatures of both the solid and moisture that is present [1]. Moisture transfer occurs as the moisture travels to the evaporative surface of the product and then into the circulating air as water vapour [2]. The heat and moisture transfer rates are therefore related to the velocity and temperature of the circulating drying air [3]. Agricultural crops need to be dehydrated by drying to moisture content suitable for storage [4 – 11].

Active drying systems for the small scale rural development are not common because of the motorised fans which calls for grid connected electricity or photovoltaic (PV) generators. While PV systems are expensive, grid connected electricity is either unavailable or unreliable or both [12 – 16]. Hence, the traditional open sun drying is still common and widespread in Nigeria. The products under the open drying are of poor quality due to the unavoidable presence of rain, wind, moisture and dust [17 – 20]. Also, they are attacked by rodents, insects and fungi among others. The process is also time-consuming and it requires a large area for spreading out the produce to dry.

Solar drying is an alternative which offers several advantages over the traditional (open sun) method of drying [21 – 23]. It is economically viable and environmentally friendly. It saves energy, time, occupies less area, improves product quality, and makes processing industries to produce hygienic, good quality food products. At the same time, it can be used to promote renewable energy sources as an in-come generating option [20]. Several attempts have been made to improve the quality of the dried agro-products by harnessing solar energy [24, 25]. Makurdi is the capital of Benue State in the middle belt region of Nigeria. The town is located on coordinates 7^o 43' 50"N, 8^o32'10"E. Several efforts have been carried out in this location to take advantage of the abundant solar radiation available [17, 22, 26].

Most crops and grains are harvested during the peak periods of raining season and preservation by sun drying proves difficult. These result in agricultural produce to be dumped in villages and major cities as waste [23, 26]. Rehydration of the crops during cloudy weather and at nights results to poor dehydrated products for storage [27].

The solar dryer with a backup incinerator therefore focuses on dehydrating agricultural produce during clear weather, cloudy weather and at nights to improve the quality of agricultural products for storage. It will enhance the dehydration of agricultural products especially during the harvest period in order to improve storage life [21, 28 – 33].

Generally, the drying of a mass of moist solid can be described under three parts namely the initial adjustment, constant rate and the falling rate periods. According to [34], natural convection drying in the falling rate period can be represented with equation 1.

$$\ln(M_0 - M) = Kt \quad (1)$$

where, M_0 = initial moisture content and M = moisture content at time t and K = drying constant.

II. Materials and Methods

The dryer comprises of three major units namely the flat plate collector; an incinerator and the drying chamber. The incinerator is incorporated in the design for drying during cloudy weather and night periods. The schematic diagram of the complete assembly of the Solar dryer with incinerator is shown in figure 1.

No-load tests were carried out on the system. The tests involved measuring the temperature of the air stream and the ambient temperature using thermometer. The average velocity of air delivered into the drying chamber was also measured using a cup anemometer. The biomass (charcoal) used in the incinerator was burnt and the heat conveying fluid (water) was allowed to flow by gravity. The initial and final temperatures of the fluid were measured and the temperature of the dryer was also measured using a thermometer.

On-load tests were ran for different drying conditions for solar, solar-incinerator and control experiment of chilli pepper (*Capsicum annuum*) respectively. To compare the performance of the dryer with that of the sun drying, equal weights of control samples of chilli pepper (1000 g) to that introduced into the dryer were respectively placed on a tray beside the dryer in the open sun. Before starting the experimental runs, the whole apparatus was operated for a period of one hour to stabilize the air temperature and air velocity in the dryer each day from 09.00 hours. Drying was started after completion of loading, usually at about 10.00 hours and discontinued when it reached the final acceptable moisture content for chilli pepper of 5%. The sample was weighed every one hour to determine the moisture lost. The drying process was continued until acceptable moisture content was achieved. The same experiment was repeated for dull weather and the equipment, solar collector, incinerator and dryer connected and ran to determine the equipment efficiency and dry rate.

Weight losses of the samples during the drying process were measured using a digital weighing balance. A Vaisala humidity and temperature indicator HMI 31 was used for measuring relative humidity, ambient temperature and the temperatures of the collector and the dryer respectively. A micro processor AM 4822 Anemometer was used for measuring air speed. Temperatures of the glass cover, absorber plate of the collector were measured using thermometers at 1 hour intervals during the no-load test and 2 hours interval during the on-load test. The moisture content of the chilli pepper was determined using analytical balance moisture analyzer. The dried chilli pepper samples were collected cooled in the shade to the ambient temperature and sealed in plastic bags for storage.

III. Results and Discussions

Tables 1 to 3 show the mean mass (moisture) profile of chilli pepper for the control, solar dryer, and solar-incinerator dryer experiments respectively. The results indicate that the percentage moisture lost by the open sun drying and the solar –incinerator drying were quite close at the end of the second day (41.34 % and 48.80 % respectively). A wide gap of the moisture loss was observed at the end of the second day for the sample in the solar dryer (61.54 %). At the end of the third day (after 26 hrs), it could be said that the solar dried sample had lost all its expellable moisture content (85.96 %) whereas the open sun dried sample had lost only 51.99 % moisture content and the solar –incinerator lost only 67.91 % of its expellable moisture content. At the end of 32 hrs it could be said that the solar–incinerator dryer also lost virtually all the expellable moisture content (86.14 %) whereas the control sample lost only 80.67 %. It took (38 hrs) for the control sample to lose all its expellable moisture content (86.21 %).

Figure 2 shows that efficiency of the collector (η_c), increases with increase in ambient temperature. Figure 3 shows the drying pattern distribution rate for pepper drying. The Figure 3 shows that the drying rate is faster in solar drying, followed by solar incinerator drying, then the open sun drying. The efficiencies of the equipment were also determined using the drying distribution rates and constants of the four equipment. The drying rate efficiency for solar dryer and solar-incinerator dryer was obtained as 99.6 %, and 92.9 % respectively.

IV. Conclusion

The solar dryer can be used efficiently during cloudy, rainy and sunny weather conditions and at nights. The drying rate efficiency for solar dryer and solar-incinerator dryer was obtained as 99.6 %, and 92.9 % respectively. The computed efficiencies for the equipment were 56 % and 13 % for solar dryer and solar-incinerator dryer respectively. The solar dryer had a better drying rate. The system can be adopted in both rural and urban areas with high humid conditions such as Makurdi for drying of agricultural produce.

References

- [1] Sarsavadia, P.N. (2007). Development of a solar-assisted dryer and evaluation of energy requirement for the drying of Onion, *Renewable Energy*, 32: 2529-2549
- [2] Sreekumar, A. Manikantan, P.E., Vijayakumar, K.P. (2008). Performance of indirect solar cabinet dryer, *Energy Conversion and Management*, 49: 1388-1395.
- [3] Madhlopa, A., Ngwalo, G. (2007). Solar dryer with thermal storage and biomass-backup heater, *Solar Energy* 81: 449-462.
- [4] Thirugnanasambandam, M., Iniyan, S., Goic, R. (2010). A review of solar thermal technologies. *Renewable and Sustainable Energy Reviews*, 14: 312-322
- [5] Fudholi, A. Sopian, K., Ruslan, M.H., Alghoul, M.A., Sulaiman, M.Y. (2010). Review of solar dryers for agricultural and marine products. *Renewable and Sustainable Energy Reviews*, 14: 1-30
- [6] Çakmak, G., Yıldız, C. (2009). Design of a new solar dryer system with swirling flow for drying seeded grape. *International Communications in Heat and Mass Transfer*, 36: 984-990
- [7] Afriyie, J.K., Rajakaruna, H., Nazha, M.A.A., Forson, F.K. (2011). Simulation and optimisation of the ventilation in a chimney-dependent solar crop dryer. *Solar Energy*, 85: 1560-1573
- [8] Bennamoun, L. (2011). Reviewing the experience of solar drying in Algeria with presentation of the different design aspects of solar dryers. *Renewable and Sustainable Energy Reviews*, 15: 3371- 3379
- [9] Amer, B.M.A., Hossain, M.A., Gottschalk, K. (2010). Design and performance evaluation of a new hybrid solar dryer for banana. *Energy Conversion and Management*, 51: 813-820
- [10] Afriyie, J.K., Nazha, M.A.A., Rajakaruna, H., Forson, F.K. (2009). Experimental investigations of a chimney-dependent solar crop dryer, *Renewable Energy*, 34: 217-222
- [11] Murthy M.V.R. (2009). A review of new technologies, models and experimental investigations of solar driers, *Renewable and Sustainable Energy Reviews*, 13: 835-844
- [12] Montero, I., Blanco, J., Miranda, T., Rojas, S., Celma, A.R. (2010). Design, construction and performance testing of a solar dryer for agro-industrial by-products, *Energy Conversion and Management*, 51: 1510-1521
- [13] Li, Z. Zhong, H., Tang, R. (2006). Experimental investigation on solar drying of salted greengages, *Renewable Energy*, 31: 837-847.
- [14] Jairaj, K.S., Singh, S.P., Srikant, K. (2009). A review of solar dryers developed for grape drying, *Solar Energy*, 83: 1698-1712
- [15] Janjai, S., Lamler, N., Intawee, P., Mahayothee, B., Bala, B.K., Nagle, M., Müller, J. (2009). Experimental and simulated performance of a PV-ventilated solar greenhouse dryer for drying of peeled longan and banana, *Solar Energy*, 83: 1550-1565
- [16] Singh, S., Kumar, S. (2012). Testing method for thermal performance based rating of various solar dryer designs, *Solar Energy*, 86: 87-98
- [17] Edeoja, A.O., Kucha, E.I., Itodo, I. N. (2009). Development of an active solar crop dryer with a manually-tracking concentrating collector. *Int. Journal of Electrical & Elect.* 1(1).
- [18] Barki, E., Ibrahim, J. S., Eloka-Eboka, A. C. (2012). Performance Evaluation of an Efficient Solar Dryer with a Backup Incinerator for Grated Cassava under Makurdi Humid Climate. *International Journal of Environment and Bioenergy*. 1(2): 118-125
- [19] Bal, L. M., Satya, S., Naik, S.N. (2010). Solar dryer with thermal energy storage systems for drying agricultural food products: A review. *Renewable and Sustainable Energy Reviews*, 14: 2298-2314
- [20] Sharma, A., Chen, C.R., Vu Lan, N. (2009). Solar-energy drying systems: A review. *Renewable and Sustainable Energy Reviews*, 13: 1185-1210
- [21] Ibrahim, J. S., Eloka-Eboka, A. C., Barki, E. (2014). Comparative Analysis and Performance of Solar Dryers with Backup Incinerators for Nsukka Sub-tropical and Makurdi Humid Locations Using Selected Farm Produce. *British Journal of applied science and technology*, 4(3): 525-539.
- [22] Ibrahim, J. S., Edeoja, A. O., Barki, E. (2013). Comparative Performance Analysis of Solar Dryers with Backup Incinerators under Subtropical and Humid Climate Using Cassava Grates. *Jurnal Mekanikal*, 36: 24-33
- [23] Bala, B. K., Mondol, M. R. A., Biswas, B. K., Chowdury B. L. K., Janjai S. (2003). Solar Drying of Pineapples using solar Tunnel Drier, *Renewable Energy*, 28: 183-190.
- [24] Mumba, J. (1995). Economic analysis of a photovoltaic, forced convection solar grain drier, *Energy*, 20(9): pp. 923-928.
- [25] Okonkwo, W. I., Okoye, E. C. (2004). Integrated pebbled Bed passive solar energy crop dryer, proceedings of 5th international conference and AGM of the Nigerian Institution of Agricultural Engineers, 26: 417 - 423.
- [26] Itodo, I.N., Obetta, S.E., Satimehin, A.A. (2002). Evaluation of a solar crop dryer for rural application in Nigeria, *Botswana J. Tech.*, 11(2): 58 - 62.
- [27] Ayensu, A. (1997). Dehydration of food crops using a solar dryer with convective heat flow, *Solar Energy* 59 (4/6): 121-126.
- [28] Unachukwu, G.O., Anyanwu, C.N. (2010). Small-scale Incinerator for Domestic Hot Water Generation from Municipal Solid Wastes. Vol. 39; pp 430-439.
- [29] Kaewkiew, J., Nabnean, S., Janjai, S. (2012). Experimental investigation of the performance of a large-scale greenhouse type solar dryer for drying chilli in Thailand. *Procedia Engineering*, 32: 433 - 439
- [30] Aktaş, M., Ceylan, İ., Yilmaz, S. (2009). Determination of drying characteristics of apples in a heat pump and solar dryer, *Desalination*, 239: 266-275
- [31] Boughali, S., Benmoussa, H., Bouchekima, B., Mennouche, D., Bouguettaia, H., Bechki, D. (2009). Crop drying by indirect active hybrid solar-Electrical dryer in the eastern Algerian Septentrional Sahara, *Solar Energy*, 83: 2223-2232
- [32] Maiti, S., Patel, P., Vyas, K., Eswaran, K., Ghosh, P. K. (2011). Performance evaluation of a small scale indirect solar dryer with static reflectors during non-summer months in the Saurashtra region of western India, *Solar Energy*, 85: 2686-2696
- [33] Banout, J., Ehl, P., Havlik, J., Lojka, B., Polesny, Z., Verner, V. (2011). Design and performance evaluation of a Double-pass solar drier for drying of red chilli (*Capsicum annum L.*), *Solar Energy*, 85: 506-515
- [34] Coulson J. M., Richardson J. F. (1977). Chemical Engineering Vol. 1, 3rd Ed. A wheaton and CO, Exeter, G.B.

Table 1: Mean Mass (Moisture) Profile of Pepper Sample (Control)

Time (Hrs)	Mass before drying, W (g)	Mass after drying, W _s (g)	M (%)	M ₀ -M (%)	$\ln (M_o - M)$	Time (days)
1000 – 1200	1000	824	21.30	65.30	4.17	1
1200 – 1400	824	805	24.08	62.52	4.13	
1400 – 1600	805	809	23.50	63.10	4.14	
1600 – 1800	809	786	27.09	59.51	4.08	
0800 – 1000	786	773	29.31	7.29	4.05	2
1000 – 1200	773	765	30.60	56.00	4.02	
1200 – 1400	765	761	31.33	55.27	4.01	
1400 – 1600	761	722	38.49	48.11	3.87	
1600 – 1800	722	707	41.34	45.26	3.81	3
0800 – 1000	707	677	47.60	39.00	3.66	
1000 – 1200	677	671	48.98	37.62	3.62	
1200 – 1400	671	683	46.30	40.30	3.69	
1400 – 1600	683	657	51.99	34.61	3.54	4
1600 – 1800	657	611	63.43	23.17	3.14	
0800 – 1000	611	595	67.89	18.71	2.93	
1000 – 1200	595	553	80.67	5.93	1.78	
1200 – 1400	553	556	79.23	7.37	1.99	4
1400 – 1600	556	552	81.13	5.47	1.69	

Table 2: Mean Mass (Moisture) Profile of Pepper Sample (Solar Dryer)

Time (Hrs)	Mass before drying (W) (g)	Mass after drying W _s (g)	M (%)	M ₀ -M (%)	$\ln (M_o - M)$	Time (days)
1000 – 1200	1000	816	22.42	64.18	4.16	1
1200 – 1400	816	812	23.04	63.56	4.15	
1400 – 1600	812	800	24.94	61.66	4.12	
1600 – 1800	800	767	30.30	56.30	4.03	
0800 – 1000	767	756	32.17	54.43	3.99	2
1000 – 1200	756	730	36.93	49.67	3.91	
1200 – 1400	730	717	39.29	47.31	3.86	
1400 – 1600	717	643	55.40	31.20	3.44	
1600 – 1800	643	619	61.54	25.06	3.22	3
0800 – 1000	619	600	66.59	20.01	2.99	
1000 – 1200	600	582	71.76	14.84	2.69	
1200 – 1400	582	564	77.28	9.32	2.23	
1400 – 1600	564	537	85.96	0.64	- 0.44	

Table 3: Mean Mass (Moisture) Profile of Pepper Sample (Solar-Incinerator Dryer)

Time (Hrs)	Mass before drying W (g)	Mass after drying W _s (g)	M (%)	M ₀ -M (%)	$\ln (M_o - M)$	Time (days)
1000 – 1200	1000	821	21.8	64.74	4.17	1
1200 – 1400	821	794	25.81	60.79	4.11	
1400 – 1600	794	802	24.61	61.99	4.13	
1600 – 1800	802	789	26.61	59.99	4.09	
0800 – 1000	789	775	29.03	57.57	4.05	2
1000 – 1200	775	755	32.45	54.15	3.99	
1200 – 1400	755	719	39.01	47.59	3.86	
1400 – 1600	719	702	42.36	44.24	3.79	
1600 – 1800	702	672	48.80	37.80	3.66	3
0800 – 1000	672	668	49.50	37.10	3.61	
1000 – 1200	668	606	64.89	21.71	3.07	
1200 – 1400	606	650	53.66	32.94	3.49	
1400 – 1600	650	595	67.91	18.69	2.93	4
1600 – 1800	595	555	80.11	6.49	1.87	
0800 – 1000	555	544	83.66	2.94	1.08	
1000 – 1200	544	537	86.14	0.46	- 0.77	

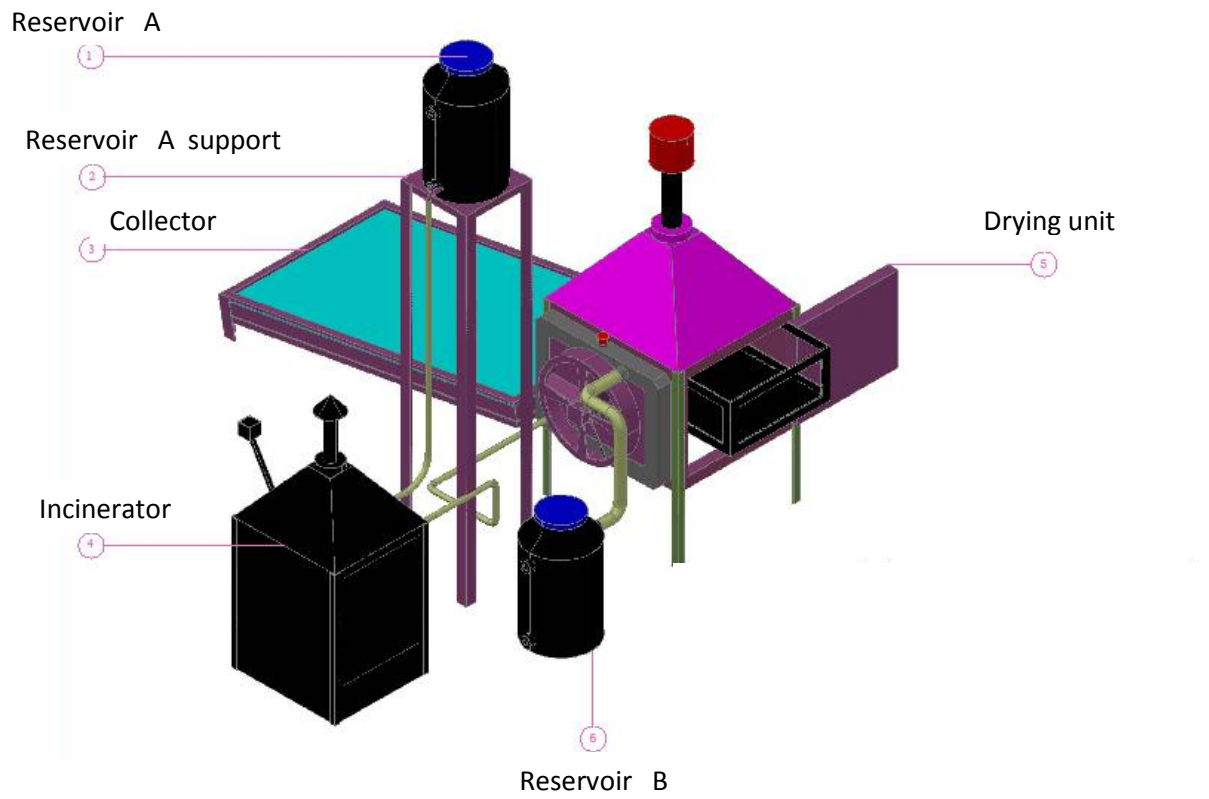


Fig. 1: Solar dryer with a back-up incinerator

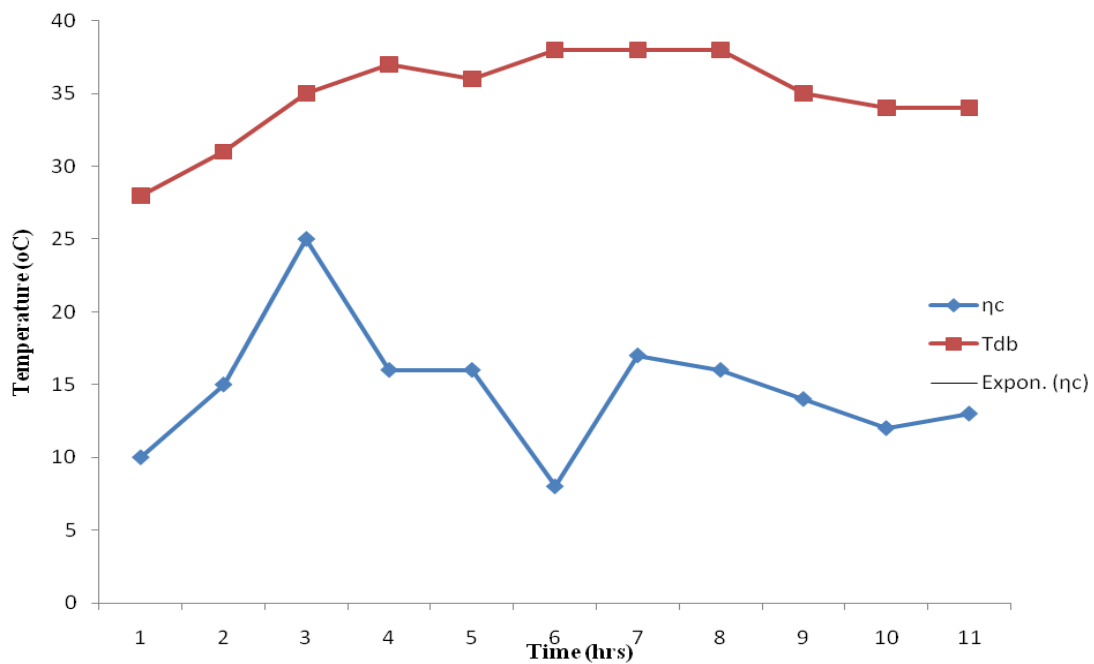


Fig. 2: Effect of Ambient Temperature on the Efficiency of Collector during No-load test

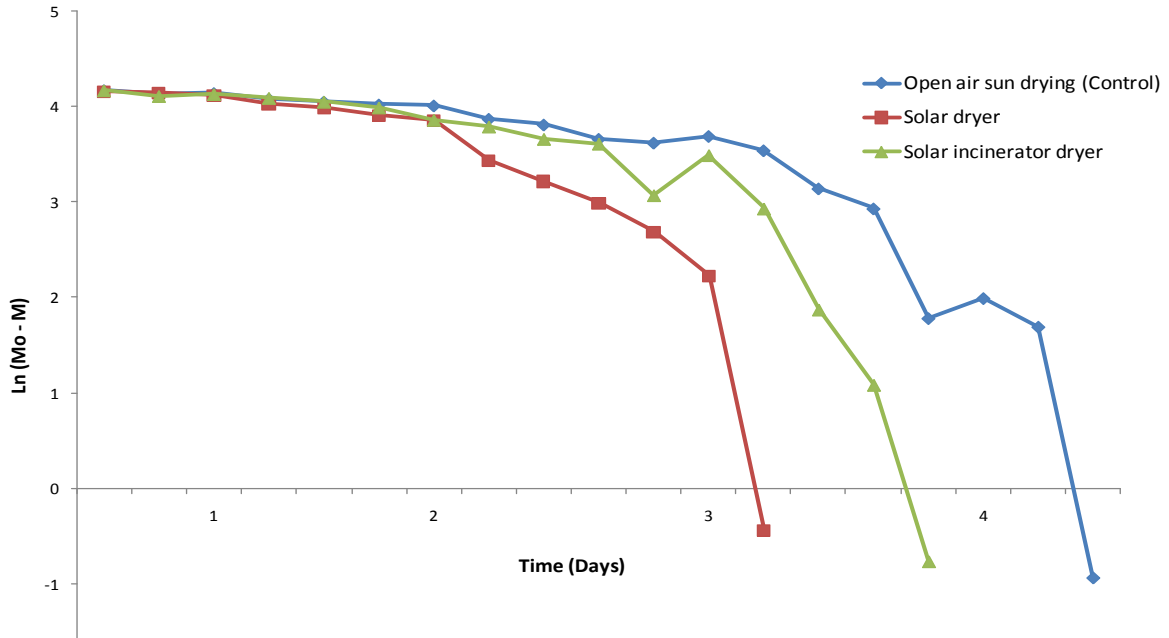


Fig. 3: Drying rates of Pepper for various drying conditions

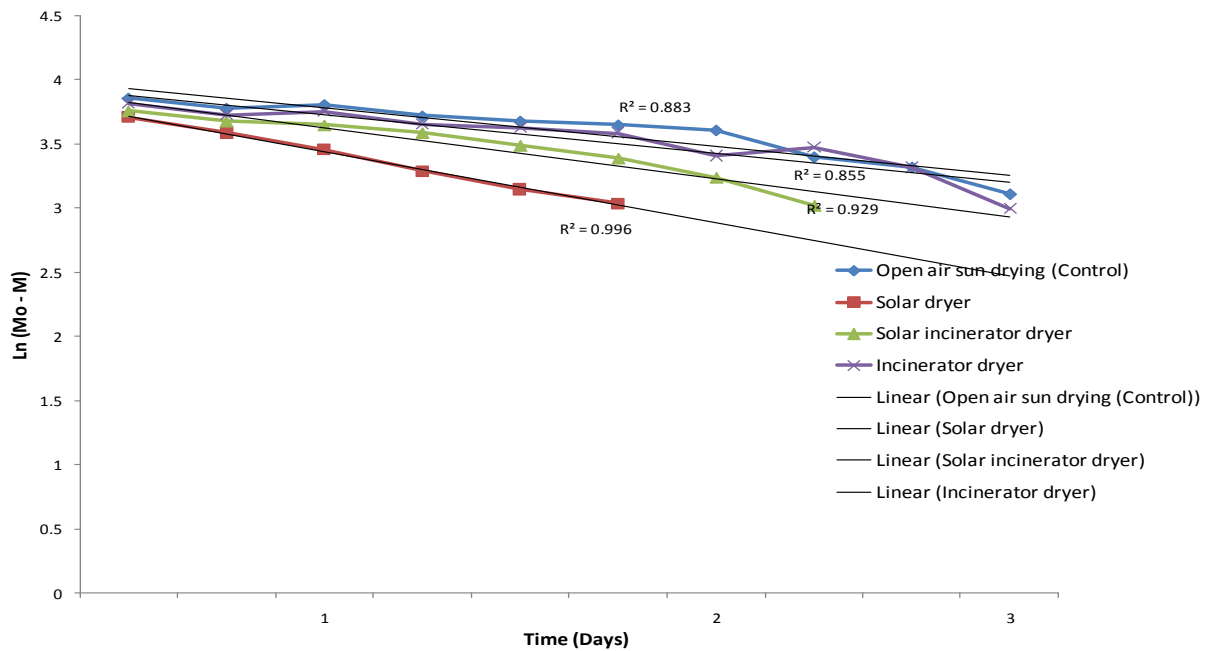


Fig. 4: Drying distribution rates and constants of the four Equipment

Experimental Study of Crushed Palmyra Palm Shells As Partial Replacement For Coarse Aggregate In Concrete

*Osakwe C .E, Nasiru A and Vahyala P

(Department of Civil Engineering, Modibbo Adama University of Technology Yola, Adamawa state, Nigeria)

ABSTRACT : In the study, effects of replacing crushed granite aggregate commonly used in concrete with crushed palmyra palm shells (CPPS) on the workability, strength and density of concrete were examined. Preliminary tests were carried out to determine some physical and mechanical properties of CPPS, so as to comparatively evaluate it with crushed granite. It was found that, CPPS had a relatively higher Water Absorption value compared to crushed granite. Conversely, crushed granite had a relatively higher aggregate impact value and specific gravity. Furthermore of the compressive strength, workability and density of concrete containing 10, 20, 30, 40 and 50% of CPPS as replacement to crushed granite in concrete mix of ratio 1:2:4 was studied. Concrete cubes of size 150 X 150 X 150 mm³ were casted, cured in water for 7, 14, and 28 days after which compressive strengths of casted cubes were determined. The result of the tests showed that the compressive strength of concrete as well as the density of the concrete decreases as the percentage of the CPPS increases in the concrete mix.

Keywords- Crushed palmyra palm shells, concrete, compressive strength, workability, density

I. INTRODUCTION

Increase in the construction activities worldwide over time has made the demand for concrete to be on the increase. Concrete can be defined as a composite consisting of the dispersed phase of aggregates (ranging from its maximum size coarse aggregates down to the fine sand particles) embedded in the matrix of cement paste [1]. Aggregates essentially constitute over seventy percent of the volume of concrete [2] and [3]. With this large proportion of the concrete occupied by aggregates, it is expected that aggregates will have profound influence on the concrete properties and its general performance. Aggregates tend to give concrete its volumetric stability. It also has a remarkable influence on the reduction of moisture-related deformation like shrinkage of concrete. In developed countries, many construction industries have identified the use of waste natural materials as the potential alternatives to conventional aggregates. This has brought immense change in the development of high rise structures using Light Weight Concrete (LWC). At present, the most commonly used coarse aggregates for concrete production is the crushed granite rock due mainly to the presence of granite rocks deposits. With the high cost of constituent materials for the production of concrete especially coarse aggregates, coupled with the need for environmental sustainability, the need for the search for materials especially residual agricultural waste materials becomes imperative hence, the reason why many researchers are in search of replacing coarse aggregate to make concrete less expensive as well as enhancing sustainable development [3].

CPPS which is a residual agricultural waste material is obtainable in relatively large quantities especially in the northern parts of Nigeria where palmyra palms are mostly observed to thrive. CPPS is observed to be of little value in itself, being a residual agricultural waste, hence the need to integrate it as one of the components in concrete production thus opening a new horizon in agro-concrete research and at the same time offering alternatives to preserve natural coarse aggregate for the use of future generation. This paper investigates the performance of concrete mix in terms of workability and compressive strength upon addition of CPPS as partial replacement material for coarse aggregate. In previous research works, various types of waste materials have been investigated based on their potential to be used as partial coarse aggregate replacement material in concrete production such as palm kernel shell [4], crushed burnt bricks [2], crushed coconut shell [5], cockle shell [6], ceramic scrap [7] periwinkle shell [8], break tile [9], Date palm seed [10], Expanded polystyrene beads [11]. However, the use of CPPS is rare in literature, hence the need for the documentation of the potentials of its use as a partial replacement for coarse aggregate in concrete.

II. METHODS AND MATERIALS

2.1 MATERIALS

Basically, materials used for this research work include: River sand, crushed granite, CPPS samples and ordinary Portland cement.

2.2 METHODS

Tests carried out were done in accordance to the methods as prescribed in the BS code.

- Specific gravity test was carried out in accordance with the procedure as outlined in [12].
- Particle size distribution analysis test was carried out in accordance with the procedure as outlined in [13].
- Aggregate water Absorption (AWA) test was conducted in accordance with the procedure as outlined in [14].
- Aggregated impact value (AIV) test conducted in accordance with the procedure as outlined in [15].
- Slump test was carried out on the fresh concrete in accordance with the procedure as outlined in [16].

The cube moulds used were cleaned and oiled before each casting. 150 cubes of 150mm x 150mm x 150mm were produced with mix ratio of 1:2:4. Water/Cement ratio of 0.55, was used. De-moulding of the cubes was done between 18hours to 24hours after casting. The hardened cubes, were transferred into a curing tank at room temperature. The cubes were removed at the end of 7th, 14th and 28th days from the curing tank and air dried for between 3 to 5 hours before testing. Partial replacement of crushed granite with CPPS was in of percentages 10%, 20%, 30%, 40%, and 50%.

III. RESULTS AND DISCUSSIONS

The specific gravity test result shows that the values for crushed granite and CPPS are 2.66 and 1.26 respectively as given in Table 1 below. This shows that crushed granite is denser than CPPS. Also, the Aggregate Impact Value (AIV) test for crushed granite and CPPS were found to be 18.85% and 14.25% respectively as shown. The average impact values calculated falls within the acceptable limits as stated in [17] which prescribes maximum value of 45% for aggregate to be used in concrete for non-wearing surfaces. Furthermore, it can be observed that the aggregate impact value (AIV) of CPPS aggregates are much lower compared to that of crushed granite aggregates, which indicates that these aggregates have good absorbance to shock. The Aggregate Water Absorption test result for crushed granite and CPPS were found to be 0.90% and 26.18% respectively hence, CPPS has higher water absorption and this is because of the porosity in its shell.

Table 1: Physical and Mechanical Properties of CPPS and Crushed Granite

S/No.	Physical and Mechanical Property	CPPS	Crushed Granite
1	Specific gravity	1.26	2.66
2	Aggregate Water Absorption (%)	26.18	0.90
3	Aggregate Impact Value (%)	14.25	18.85

Table 2: Varying Percentages of CPPS in concrete in relation to Slump Height.

CPPS in concrete (%)	Crushed granite in concrete (%)	Water/Cement Ratio	Slump (mm)
0	100	0.5	27
10	90	0.5	48
20	80	0.5	41
30	70	0.5	39
40	60	0.5	35
50	50	0.5	32

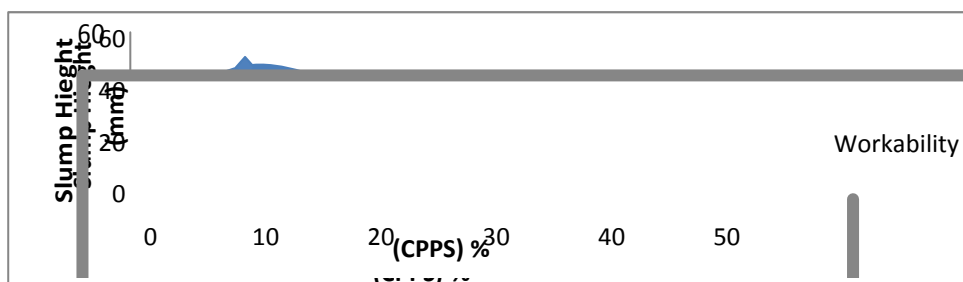


Figure 1: Plot of slump height against percentage of CPPS in concrete

The workability of concrete batches for different percentages of CPPS using slump test is shown in Table 2 and represented Fig.1. It can be observed that workability of concrete increased as the percentage of CPPS increased up to a maximum value of 48mm at 10% replacement of crushed granite with CPPS beyond which a decreasing trend in the workability of the concrete was observed as the percentage of CPPS increased. A w/c ratio of 0.55 was used for all the mixes. The hydrated cement paste produced enabled the penetration of cement into the CPPS aggregate. Results obtained by [19] using Oil Palm Shells (OPS) as the replacement of control aggregate shows similar trend the same as that of CPPS aggregate. This can be explained by the fact that, as the percentage CPPS increases, the workability of the concrete reduces, hence reducing the height of slump.

Table 3: Compressive Strength of concrete at varying percentages of CPPS in concrete (MPa).

Design Strength (MPa)	PPS content (%)	7 days (MPa)	14 day (MPa)	28 days (MPa)
	0	20	24	27.7
	10	14.36	16.52	18.45
25	20	12.15	14.81	17.04
	30	10.30	11.78	14.30
	40	8.89	10.30	12.00
	50	7.18	9.41	10.15

The compressive strengths of weight-batched concrete cubes at varying percentages of CPPS are shown in Table.3. The effect of replacement of crushed granite with CPPS on compressive strengths of the concrete cubes is as represented in Fig.2. It can be observed that the compressive strength decreased as the percentage of CPPS increased. The compressive strength is maximum at 0% replacement of crushed granite with CPPS and minimum at 50% replacement. The 28-day strength represented by 10and 20% replacement of crushed granite with CPPS satisfies the criteria for lightweight concrete [18].

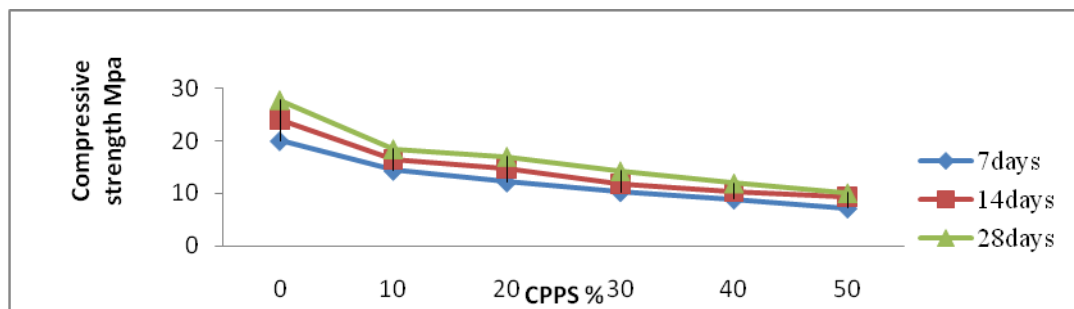


Figure 2: Plot of compressive strength against percentage of CPPS in concrete

DENSITY:

Densities of the concrete cubes at varying percentage replacement of crushed granite with CPPS are as given in table 4 and represented in fig.3.

Table 4: Density of the Concrete of all Percentage of CPPS

CPPS content (%)	7 days (Kg/m ³)	14 days (Kg/m ³)	28 days (Kg/m ³)
0	2586	2622	2623
10	2202	2338	2426
20	2115	2240	2328
30	2053	2181	2319
40	1940	2128	2187
50	1884	2058	2133

It can be observed from figure 3 that density of concrete reduces as percentage of CPPS increases and vice versa. The range of densities for CPPS (at 10-50% replacement of crushed granite with CPPS) in concrete for 28days was between 2426 – 2133 Kg/m³ while at, 0% CPPS in concrete (100% crushed granite used as coarse aggregates) the density was 2623 kg/m³. The least density was at 50% replacement of CPPS with a value of 2133 kg/m³.

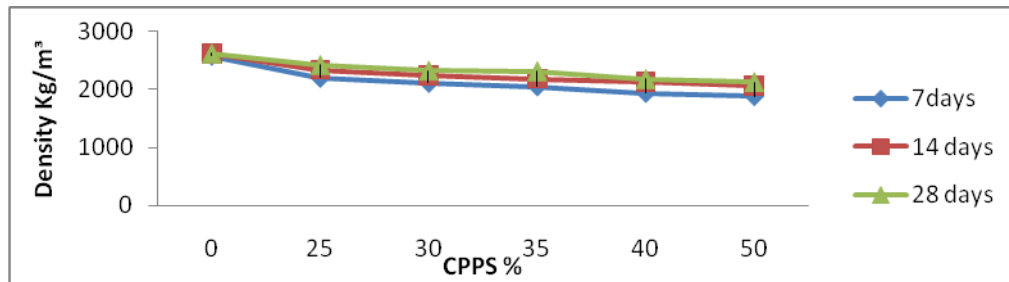


Figure 3: Plot of Density of concrete at varying percentage of CPPS in Concrete

The densities of all the concrete cubes casted within the range of 0-50% replacement of crushed granite with CPPS in concrete was found to be above 2000 kg/m³ making it suitable for use as lightweight concrete[18].

IV. CONCLUSIONS

From the study, it can be observed that, the 28-day compressive strength of the concrete made using CPPS as coarse aggregate (at 10 and 20% replacement of granite with CPPS) produced concrete with a compressive strength above the minimum value required for structural lightweight concrete [18]. This is similar to findings of [20]. Hence, CPPS can be recommended for use as partial replacement of aggregate for light weight concrete for non structural members. Furthermore, the CPPS indicates that CPPS has good absorbance to shock. However, it is recommended that durability studies on concrete made using CPPS as aggregates should be carried out to assess its behavior in aggressive environments.

REFERENCES

- [1] Neville, A. M. (1995). *Properties of Concrete (Fourth and Final Edition)*. Delhi: Pearson Educational Limited.
- [2] Apebo, N. S., Iorwua, M. B., & Agunwamba, J. C. (2013). Comparative analysis of the compressive strength of concrete with gravel and crushed over burnt bricks as coarse aggregates. *Nigerian journal of technology (NIJOTECH)*, 32(1), 7-12.
- [3] Daniel, Y. (2013). Experimental assessment on coconut shells as aggregate in concrete. *International Journal of Engineering Science Invention*, 2(5), 7-11.
- [4] Olanipekun, E. A., Olusola, K. O., & Ata, O. (2006). A comparative study of concrete properties using coconut shell and palm kernel shell as coarse aggregates. *Building and Environment*, 41, 297- 301.
- [5] Akshay, S., Kalyani, R., Pooja, P., & Shraddha, P. (2014). Coconut Shell as Partial Replacement for Coarse Aggregate. *International Journal of Civil Engineering Research*, 5, 211-214.
- [6] Muthusamy, K., & Sabri, N. A. (2012). Cockle shell, A potential parcial coarse. *International Journal of Science, Enviroment and Technology*, 1(4), 260-267.
- [7] Veera Reddy, M. (2010). Investigations on stone dust and ceramic scrap as aggregate replacement in concrete. *International Journal of Civil and Structural Engineering*, 1(3), 213-223.
- [8] Adewuyand, A., & T., A. (2008). Exploratory study of Periwinkle shells as coarse Aggregate in concrete works. *ARPN Journal of Engineering and Applied Sciences*, 3(6), 121-211.
- [9] Kamala, K., & Krishna, B. (2012). Reuse of Solid Waste from Building Demolition for the Replacement of Natural Aggregates. *International Journal of Engineering and Advanced Technology (IJEAT)*, 2(1), 432-456.
- [10] Aka, A., Muhammad, H., Ephraim, T., & Idris, A. (2013). Exploratory Study of Date Seed as Coarse Aggregate in Concrete Production Environmental Research. *www.iiste.org*, 3(1).
- [11] Thomas, T., Rajendra, P., Katta, V., & Subhash, C. (2014). Partial Replacement of coarse Aggregates by Expanded Polystyrene Beads in Concrete. *IJRET: International Journal of Research in Engineering and Technology*.
- [12] BS-EN 1377-2. (1990). Soils for Civil engineering purposes. London: British Standard Institution.
- [13] BS-812-103.1. (1985). Sieve tests. *Methods for determination of particle size distribution*. London: British Standard Institution.
- [14] BS-812-109. (1990). Testing Concrete. *Methods for determination of moisture content*. London: British Standard Institution.
- [15] BS-812-112. (1990). Testing aggregates. *Methods for determination of aggregate impact value (AIV)*. London: British Standard Institution.
- [16] BS-1881-102. (1983). Testing Concrete. *Method for determination of slump*. London: British Standard Institution.
- [17] BS-882. (1992). Specifications of Aggregates for Natural Sources for Concrete. London: British Standard Institution.
- [18] BS-8110-1. (1997). The structural use of Concrete. London: British Standard Institution.
- [19] Saman, D., & Omidreza, S. (2011). influence of oil palm shell on workability and compressive strength of high strength concrete. *International journal of Engineering Tome IX Fascicule 2*.
- [20] Mannan M. & Ganapathy, C. (2001). Mix design for oil palm shell concrete. *International Journal of Cement and Concrete Research*, 1323- 1325.

Designing and Analysis of Microstrip Patch Antenna for Wi-Fi Communication System Using Different Dielectric Materials

Raja Rashidul Hasan¹, Md. Moidul Islam², Kazi Saiful Islam³, Md. Mostafizur Rahman⁴, Md. Tanvir Hasan⁵

¹²³⁴⁵(Electrical and Electronic Engineering, American International University-Bangladesh, Bangladesh)

ABSTRACT : Wireless communications has become very popular now-a-days. Wireless communication and networking system has become an important area for research in academic and industrial institutes. Wires provide less free space and non-mobility, thus indoor wireless communication system takes interest. Microstrip patch antennas has low weight and low profile, conformability, easy and cheap fabrication costing, that's why it has been widely used in a various useful applications now a days. Microstrip patch antenna is designed for Wi-Fi communication which operates using 2.4 GHz frequency band. This research paper represents the effort of designing and performance analysis of microstrip patch antenna for Wi-Fi communication system. The main objective of this paper is to design and observe the performance of the designed microstrip patch antenna using different dielectric materials. Better performance is observed for FR4. For FR4 the return loss, S_{11} is obtained -11.4 dB at 2.4 GHz, this indicates the return loss is much lower comparing to the other dielectric materials used in this research. Also VSWR is found 1.74 which is desirable. In this paper we also observed and analyzed the radiation pattern of far field region, gain, radiation efficiency and total efficiency for different dielectric materials.

Keywords –Wi-Fi communication system, Microstrip patch antenna, Return loss, Far field, Different dielectric materials.

I. INTRODUCTION

Technology is making rapid progress and is making many things easier. As the innovative thinking of persons is increasing day-by-day, new methods for wireless communication have been evolved of which our present topic Wi-Fi is the most accepted technology. Wi-Fi allows to connect to the internet from virtually anywhere at speeds of up to 54Mbps. The computers and handsets enabled with this technology use radio technologies based on the IEEE 802.11 standard to send and receive data anywhere within the range of a base station.

Antenna is the most important equipment for wireless communication systems which is used for both transmitting and receiving electromagnetic waves. Microstrip antennas are relatively inexpensive to manufacture and design because of the simple two dimensional physical geometry. They are usually employed at UHF and higher frequencies because the size of the antenna is directly tied to the wavelength at the resonant frequency. With the development of MIC and high frequency semiconductor devices, microstrip has drawn the maximum attention of the antenna community in recent era. In spite of its various attractive features like, light weight, low cost, easy fabrication, conformability on curved surface and so on, the microstrip element suffers from an inherent limitation of narrow impedance bandwidth.

We focused on improving the performance of Wi-Fi communication by designing of a microstrip patch antenna [3]. To increase the performance of a microstrip patch antenna there are several methods like increasing the thickness of substrate, using low dielectric substrate, using of various impedance matching and feeding techniques [4].

Microstrip patch antenna consists of a conducting patch of any planar or non-planar geometry on one side of a dielectric substrate with a ground plane on other side. It is a popular printed resonant antenna for narrow-band microwave wireless links that require semi-hemispherical coverage. Due to its planar configuration and ease of integration with microstrip technology, the microstrip patch antenna has been heavily studied and is often used as elements for an array [5].

This research paper is organized as follows: Section II explains the structure and design specifications of a microstrip patch antenna. Section III describes the simulations of designed device. Analysis of the simulations for the designed microstrip patch antennas are described in this section. This paper ends with a conclusion in Section IV. CST Microwave Suite simulation results show better performance in terms of return loss, radiation efficiency and total efficiency.

II. STRUCTURE AND DESIGN SPECIFICATIONS

A Microstrip patch antenna consists of a radiating patch on one side of a dielectric substrate which has a ground plane on the other side as shown in Fig 1. The patch is generally made of conducting material such as copper or gold and can take any possible shape. The radiating patch and the feed lines are usually photo etched on the dielectric substrate [2].

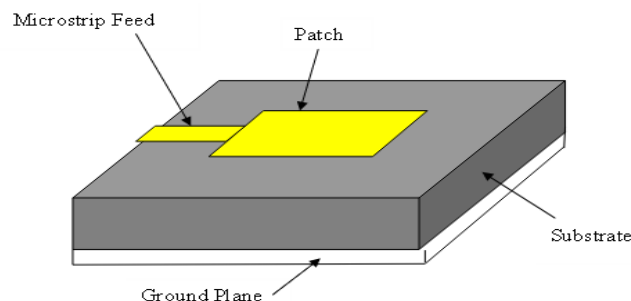


Figure 1: Structure of Patch antenna [8].

Different materials are used in different layer in the antenna. In substrate layer different dielectric substrate materials are used. Copper is used in ground plane, patch and microstrip line. In this research different dielectric materials were used for specific cut-off frequency to analyze the performance of the antenna for Wi-Fi application. Table I shows the name of the layers and materials used in the microstrip patch antenna. In simulation software materials with loss effect were selected to get practical simulated results.

Table I: Name of the layers and materials used in the layers of a microstrip patch antenna.

Layer Name	Material Name
Microstrip Line	Copper
Patch	Copper
Substrate	Dielectric substrate materials
Ground plane	Copper

Table II shows the list of the dielectric materials used in this research purpose to analyze the performance of the antenna for 2.4 GHz.

Table II: List of different dielectric materials used in this research and their dielectric constants.

Name of the dielectric materials	Dielectric constants (ϵ_r)
FR4	4.3
RTDuroid 5880	2.2
Arlon Di 522	2.5
Taconic RF 35P	3.5
Bakelite	4.8
Dupont-951	7.8

The essential parameters require designing Microstrip Patch Antenna are:

Frequency of operation (f_0): The resonant or cut-off frequency of the antenna must be selected appropriately. Wi-Fi communication system uses 2.4 GHz frequency. Thus the designed antenna must be able to operate at this frequency [6].

Dielectric constant of the substrate (ϵ_r): Six different dielectric materials were used in this research. Name of the dielectric materials and their dielectric constants are mentioned in table. A substrate with a high dielectric constant has been selected since it reduces the dimensions of the antenna [6].

Height of dielectric substrate (h): For the microstrip patch antenna used in Wi-Fi communication system should not be bulky. Hence, the height of the dielectric substrate used to design the antenna is 1.5 mm [6].

Calculation of effective dielectric constant, ϵ_{reff} : Effective dielectric constant, ϵ_{reff} can be calculated from the below equation.

$$\epsilon_{\text{reff}} = \frac{\epsilon_r + 1}{2} + \frac{\epsilon_r - 1}{2} \left[1 + 12 \frac{h}{W} \right]^{1/2} \quad (1)$$

Calculation of the width of the patch, W : The width of the patch can be calculated from the below equation.

$$W = \frac{c}{2f \sqrt{\frac{\epsilon_r + 1}{2}}} \quad (2)$$

Calculation of the length of the patch, L : The effective length of the patch can be calculated from the below equation.

$$L_{\text{eff}} = \frac{c}{2f \sqrt{\epsilon_{\text{reff}}}} \quad (3)$$

The length extension can be calculated from the below equation.

$$\Delta L = 0.412h \frac{(\epsilon_{\text{reff}} + 0.3) \left(\frac{W}{h} + 0.264 \right)}{(\epsilon_{\text{reff}} - 0.258) \left(\frac{W}{h} + 0.8 \right)} \quad (4)$$

The actual length of the patch can be calculated from the below equation.

$$L = L_{\text{eff}} - 2\Delta L \quad (5)$$

Calculation of the length of the ground plane, L_g : The length of the ground plane can be calculated from the below equation.

$$L_g = 6h + L \quad (6)$$

Calculation of the width of the ground plane, W_g : The width of the ground plane can be calculated from the below equation.

$$W_g = 6h + W \quad (7)$$

Calculation of the length of the feed line, L_f : The length of the feed line can be calculated from the below equation.

$$L_f = \frac{\lambda_0}{4\sqrt{\epsilon_r}} \quad (8)$$

$$\text{Where, } \lambda_0 = \frac{c}{f_0} \quad (9)$$

Calculation of the width of the feed line, W_f : If $Z_c = 50 \Omega$, the width of the feed line can be calculated from the below equation.

$$Z_c = \frac{120\pi}{\sqrt{\epsilon_{\text{reff}}} \left[\frac{W_f}{h} + 1.393 + 0.667 \ln \left(\frac{W_f}{h} + 1.444 \right) \right]} \quad (10)$$

Calculation of the gap of the feed line, G_{pf} : The gap of the feed line can be calculated from the below equation.

$$G_{pf} = \frac{4.65 \times 10^{-9} x c}{f_0 \sqrt{2\epsilon_{\text{reff}}}} \quad (11)$$

In fig. 2 parameters required to design microstrip patch antenna are identified.

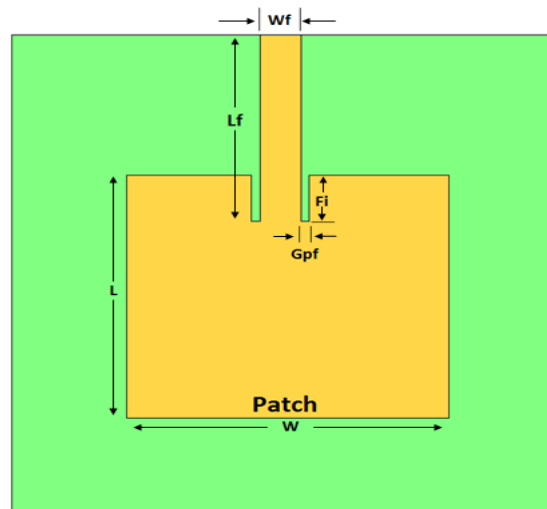


Figure 2: Parameters of microstrip patch antenna.

III. SIMULATIONS AND ANALYSIS

Microstrip patch antenna was designed in CST Microwave Suite for 2.4 GHz resonant frequency for different dielectric materials. Then the performance for different substrate materials were compared to observe for which materials the designed antenna performs better. All the simulations were done by CST Microwave Suite. Parameters were calculated individually using the equations and different dielectric constants. Table III shows the values of the parameters for different dielectric materials used in this research.

Table III: Values of different parameters of microstrip patch antenna for different dielectric materials for 2.4 GHz.

Expression	Substrate Materials					
	FR4	RTDuroid 5880	Arlon Di 522	Taconic RF 35P	Bakelite	Dupont-951
L (mm)	29.7786	41.3484	38.8568	32.9573	28.2022	22.1492
W (mm)	38.3934	49.4106	47.2456	41.6667	36.7013	29.7957
L _f (mm)	15.07	21.069	19.7642	16.7038	14.2636	11.1893
W _f (mm)	3.0389	4.9284	4.2525	3.5613	2.7796	1.7867
Fi (mm)	11.0213	14.5014	13.7273	11.9577	10.5556	8.7202
G _{pf} (mm)	0.20558	0.283	0.2663	0.22679	0.19507	0.1547
h (mm)	1.6	1.6	1.6	1.6	1.6	1.6
M _t (mm)	0.1	0.1	0.1	0.1	0.1	0.1

Fig. 3 shows the designed microstrip patch antenna for 2.4 GHz using 6 different dielectric materials.

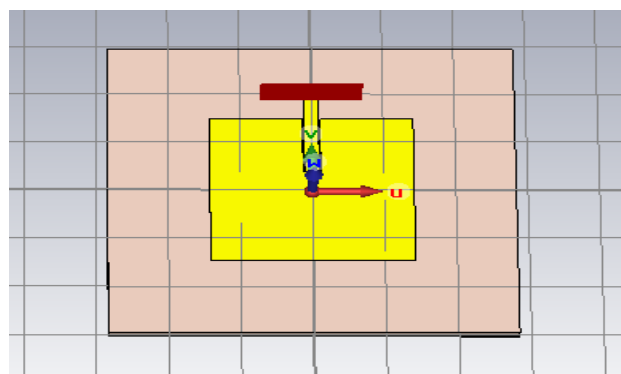


Figure 3: Designed microstrip patch antenna in CST Microwave Suite.

A. Performance of the antenna for FR4:

Fig. 4 shows of the designed microstrip patch antenna using FR4 substrate material. Fig. 5 shows the s-parameter graph for FR4. S-parameter represents how much power is reflected from antenna and is known as reflection coefficient or return loss. In the figure the value of S11 parameter is -11.401291 dB at 2.4 GHz, which is better for antenna performance. The less the value of S11 is, the better the performance. For better performance of microstrip patch antenna the value of return loss or S₁₁ parameter should be less than -10 dB.

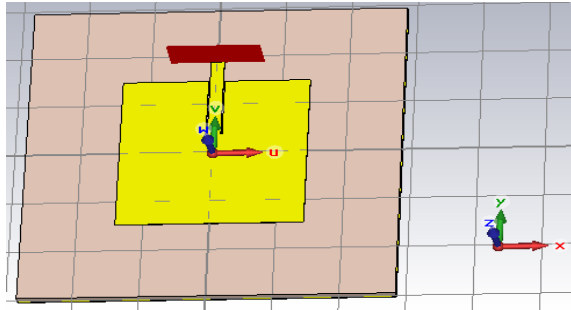


Figure 4: Designed microstrip patch antenna for FR4.

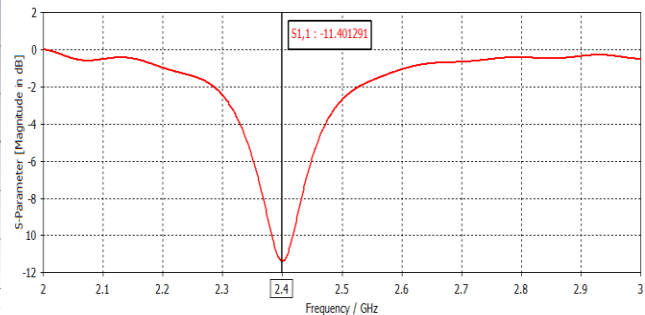


Figure 5: Return loss for FR4.

Fig.6 shows the far field region. In the figure the total efficiency and radiation efficiency are mentioned. From the figure it can be seen that the directivity is in Z-axis on the XY plane. At 2.4 GHz the radiation efficiency is -2.763 dB and total efficiency is -3.305 dB, which is better for the performance of antenna. Directivity is 6.316 dBi. The top red color shows the radiation. Radiation increased from green to red in Z direction. Fig.7 shows the far field polar view. According to the figure at 2.4 GHz angular width of half power beam is 94.4° and side lobe level is -13.1dB.

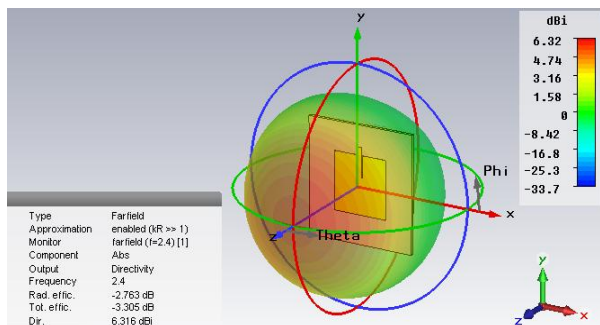


Figure 6: Far field region for FR4.

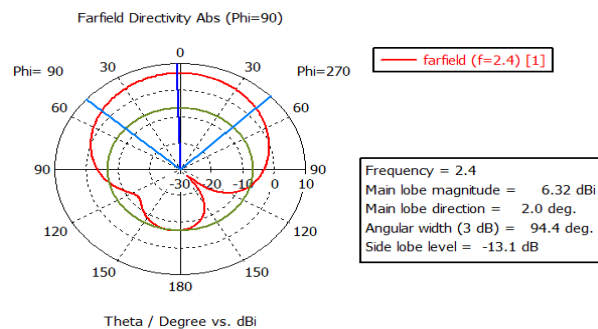


Figure 7: Far field in polar view for FR4.

B. Performance of the antenna for RTDuroid 5880:

Fig. 8 shows the designed antenna for RTDuroid 5880. Fig.9 shows the s-parameter graph for RTDuroid5880. According to the figure the value of S11 parameter is -8.3849 dB at 2.4 GHz. The value of return loss is less for better performance.

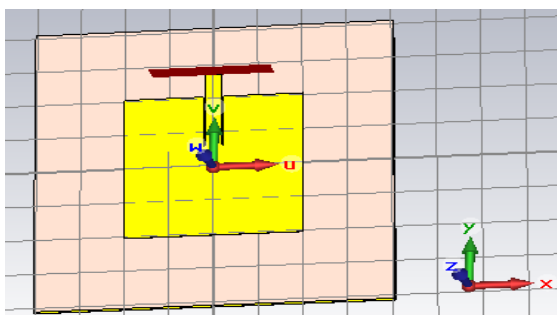


Figure 8: Designed microstrip patch antenna for RTDuroid 5880.

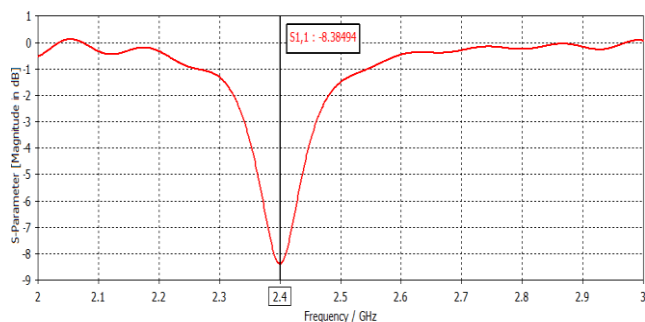


Figure 9: Return loss for RTDuroid 5880.

Fig.10 shows the far field region. According to the figure the directivity is in Z-axis on the XY plane. At 2.4

GHz the radiation efficiency is -0.8413 dB and total efficiency is -1.731 dB, which is better for the performance of antenna. Directivity is 7.559 dBi. Radiation increased from green to red in Z direction. Fig. 11 shows the far field polar view. According to the figure at 2.4 GHz angular width is 81.1° and side lobe level is -19.6 dB.

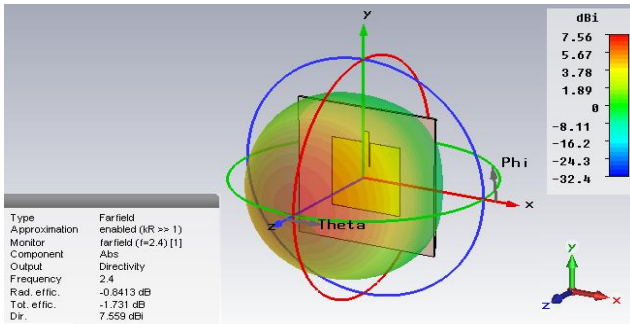


Figure 10: Far field region for RTDuroid 5880.

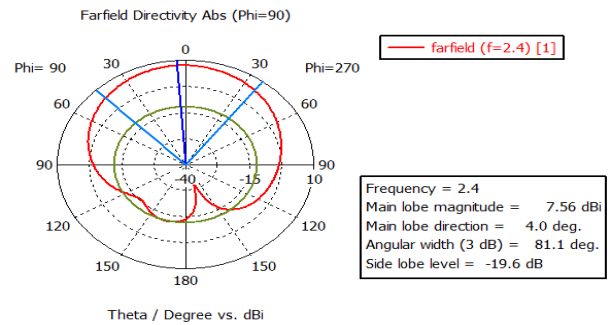


Figure 11: Far field in polar view for RTDuroid 5880.

C. Performance of the antenna for Arlon Di 522:

Fig. 12 shows the designed antenna for Arlon Di 522 dielectric material. Fig. 13 shows the return loss graph for Arlon Di 522. In the below figure the value of S11 parameter is -9.5806 dB at 2.4 GHz.

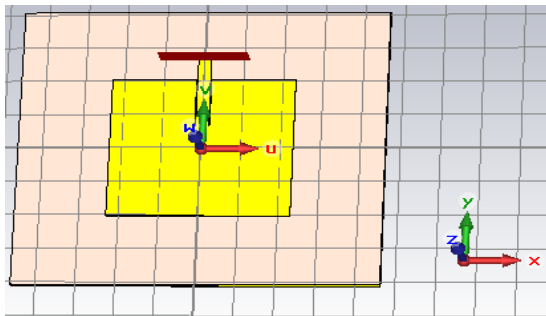


Figure 12: Designed microstrip patch antenna for Arlon Di 522.

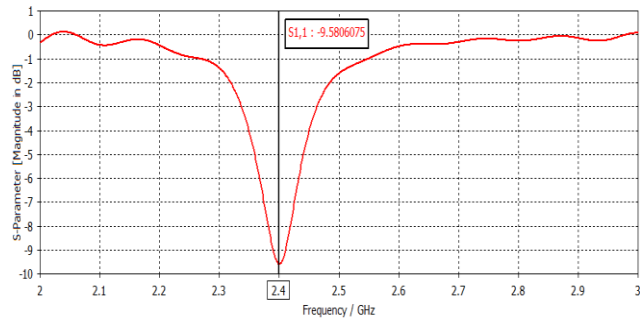


Figure 13: Return loss for Arlon Di 522.

Fig. 14 shows the far field region. From the figure it can be seen the total efficiency and radiation efficiency. According to the figure directivity is in Z-axis on the XY plane. At 2.4 GHz the radiation efficiency is -0.7555 dB and total efficiency is -1.580 dB, which is better for the performance of antenna. Directivity at 2.4 GHz is 7.899 dBi. Fig. 15 shows the far field polar view. From the figure we can measure angular width and side lobe level. At 2.4 GHz angular width is 80.3° and side lobe level is -18.8 dB.

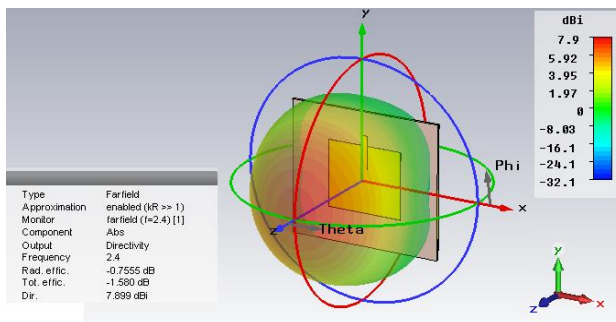


Figure 14: Far field region for Arlon Di 522.

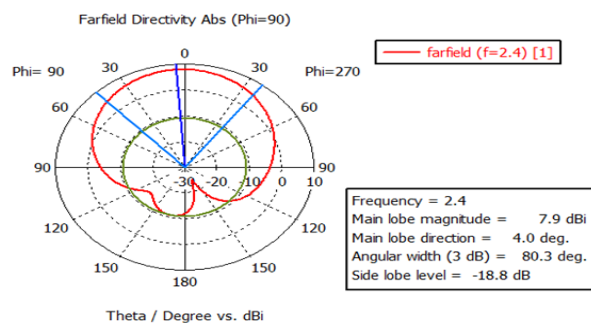


Figure 15: Far field in polar view for Arlon DI 522.

D. Performance of the antenna for Taconic RF 35P:

Fig. 16 shows the designed antenna for Taconic RF 35P in substrate layer. Fig. 17 shows the return loss graph for Taconic RF 35P. The value of S11 parameter is -6.4270911 dB at 2.4 GHz.

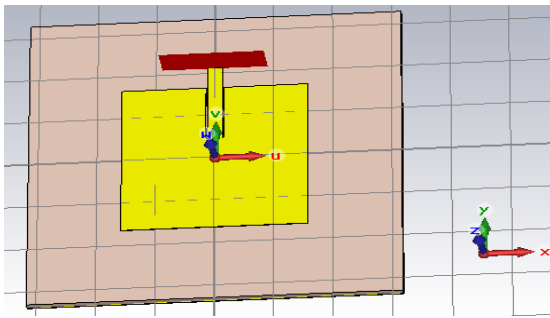


Figure 16: Designed microstrip patch antenna for Taconic.

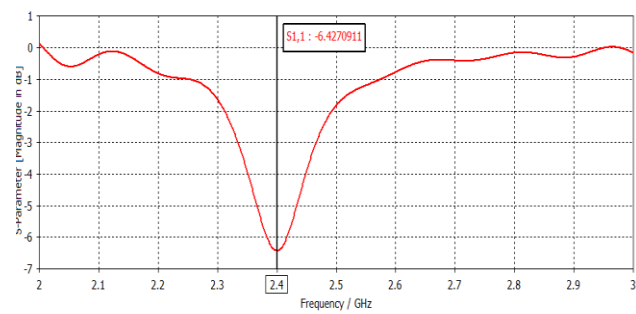


Figure 17: Return loss for Taconic RF 35P.

Fig. 18 shows the far field region. According to that figure the directivity is in Z-axis on the XY plane. At 2.4 GHz the radiation efficiency is -1.346 dB and total efficiency is -2.735 dB, which is better for the performance of antenna. Directivity is 6.671 dBi. Fig. 19 shows the far field polar view. At 2.4 GHz angular width is 90.8° and side lobe level is -15.6 dB.

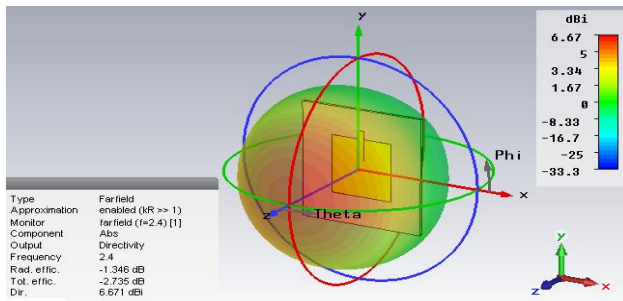


Figure 18: Far field region for Taconic RF 35P.

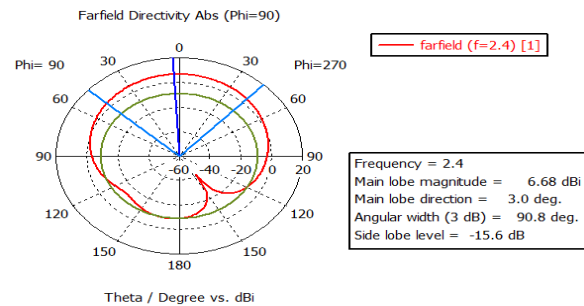


Figure 19: Far field polar view for Taconic RF 35P.

E. Performance of the antenna for Bakelite:

Fig. 20 shows the designed antenna for Bakelite substrate material. Fig. 21 shows the return loss graph for Bakelite. According to the below figure the value of S11 parameter is -7.7358 dB at 2.4 GHz. The performance for bakelite is very poor.

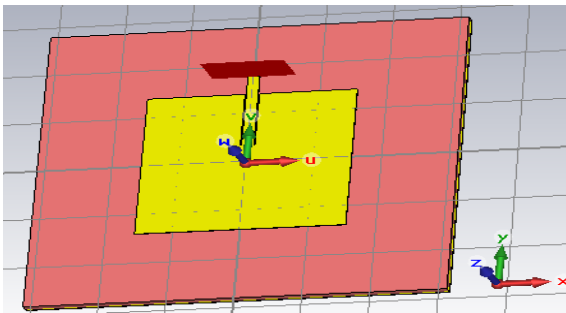


Figure 20: Designed microstrip patch antenna for Bakelite.

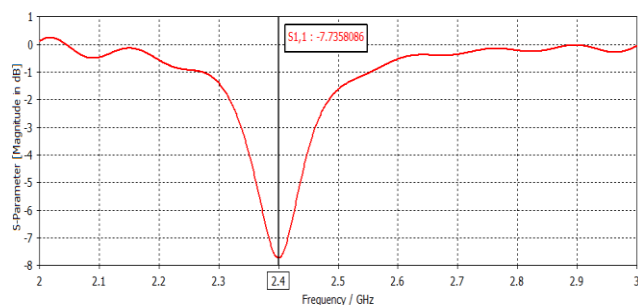


Figure 21: Return loss for Bakelite.

Fig. 22 shows the far field region. In fig. 16 the directivity is in Z-axis on the XY plane. At 2.4 GHz the radiation efficiency is -0.7625 dB and total efficiency is -1.871 dB, which is better for the performance of antenna. Directivity is 6.481 dBi. Radiation increased from green to red in Z direction. Fig. 23 shows the far field polar view. According to the figure at 2.4 GHz angular width is 95.7° and side lobe level is -11.9 dB.

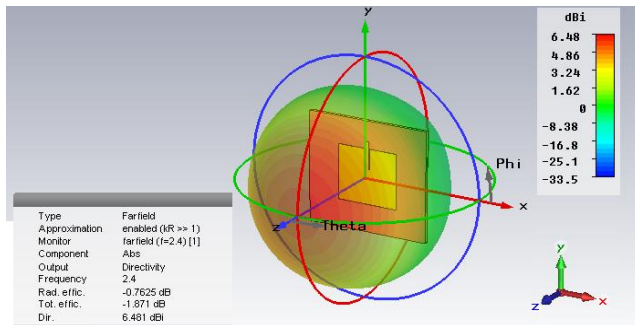


Figure 22: Far field region for Bakelite.

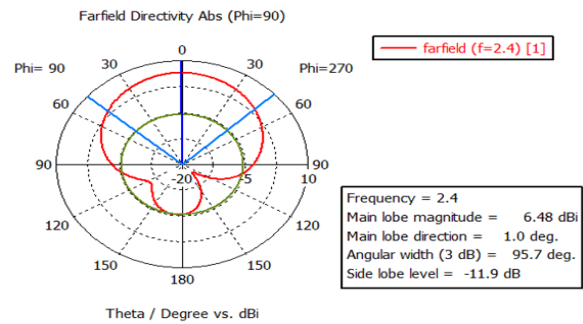


Figure 23: Far field polar view for Bakelite.

F. Performance of the antenna for Dupont-951

Fig. 24 shows the designed antenna for Dupont-951 in substrate layer. Fig. 25 shows the return loss graph for Dupont-951. According to the below figure the value of S11 parameter is -10.768469 dB at 2.4 GHz.

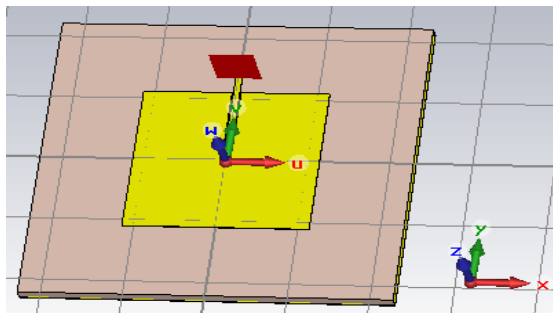


Figure 24: Designed microstrip patch antenna for Dupont-951.

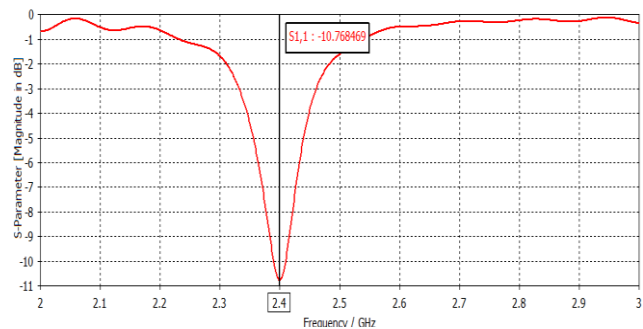


Figure 25: Return loss for Dupont-951.

Fig. 26 shows the far field region. From the figure it can be seen that that the directivity is in Z-axis on the XY plane. At 2.4 GHz the radiation efficiency is -1.068 dB and total efficiency is -1.940 dB, which is also better for the performance of antenna. Directivity at 2.4 GHz is 5.565 dBi. Figure 27 shows the far field polar view. At 2.4 GHz angular width is 100° and side lobe level is -7.7 dB.

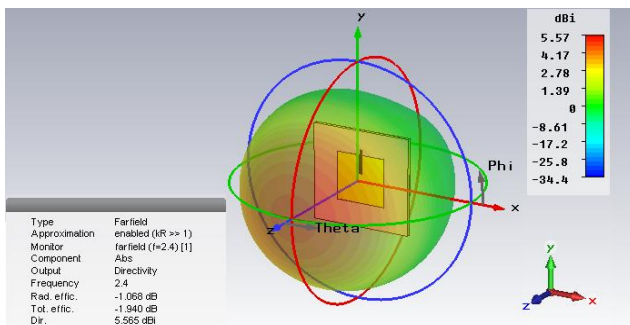


Figure 26: Far field region for Dupont-951.

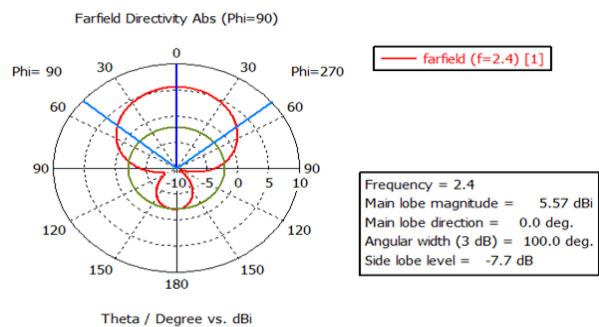


Figure 27: Far field polar view for Dupont-951.

Table IV shows the performance analysis of the designed 2.4 GHz microstrip patch antenna for all the 6 dielectric materials used in this research. From the above table we can see that the highest value of return loss or reflection coefficient is 11.4 dB for FR4, which it better for performance. Also highest total efficiency is achieved for FR4 which is -3.30 dB and radiation efficiency is -2.76 dB. So the best performance of microstrip patch antenna at 2.4 GHz is achieved for FR4 dielectric material. If FR4 is used as substrate material in the microstrip patch antenna it will give the best performance comparing to the other 6 dielectric materials.

Table IV: Performance analysis of the designed microstrip patch antenna for different dielectric materials at 2.4 GHz

Parameters	Substrate Materials					
	FR4	RTDuroid 5880	Arlon Di 522	Taconic RF 35P	Bakelite	Dupont- 951
Dielectric Constant	4.3	2.2	2.5	3.5	4.8	7.8
Resonant Frequency (GHz)	2.4	2.4	2.4	2.4	2.4	2.4
Return Loss (dB)	-11.4	-8.38	-9.58	-6.43	-7.74	-10.8
Side Lobe (dB)	-13.1	-19.6	-18.8	-15.6	-11.9	-7.7
Gain (dB)	3.55	6.72	7.14	5.33	5.72	4.50
VSWR	1.74	2.23	1.99	2.83	2.39	1.81
Directivity (dBi)	6.32	7.56	7.90	6.67	6.48	5.57
Radiation Efficiency (dB)	-2.76	-0.84	-0.76	-1.35	-0.77	-1.1
Total Efficiency (dB)	-3.31	-1.73	-1.58	-2.74	-1.87	-1.9

IV. CONCLUSION

Microstrip patch antenna is widely used in mobile communication, Wi-Fi and WiMAX communication sectors. To develop the communication, several things need to be consider and they are minimize the cost, weight, power consumption and profile of antennas which are capable of maintaining high performance over a wide spectrum of frequencies which was the goal in our work. For designing and analysis of microstrip patch antenna for Wi-Fi communication here different dielectric materials like FR4,RTDuroid 5880,Arlon Di 522,Taconic RF 35P,Bakelite and Dupont-951 were used in substrate layers. By analyzing the performance of the designed microstrip patch antenna for all the six different dielectric materials, better performance was observed for FR4 at 2.4 GHz resonant frequency. The value of return loss was better for FR4 substrate material at 2.4 GHz. Total efficiency and radiation efficiency is also higher for FR4.If FR4 is used in the substrate layer better return loss, radiation efficiency and total efficiency will be observed. Thus FR4 is very suitable for designing this type of antenna for Wi-Fi application.

REFERENCES

- [1] *Microstrip Patch Antenna for 2.4GHz Wireless Applications*, International Journal of Engineering Trends and Technology (IJETT) Volume 48-August 2013.
- [2] *Antenna Theory: Analysis and Design*, Constantine A. Balanis, 3rd Edition 2005.
- [3] Yahya S. H. Khraisat (2012) Design of 4 Elements Rectangular Microstrip Patch Antenna with High Gain for 2.4 GHz Applications. *Modern Applied Science* .6(1), 68-74.
- [4] G. Sharma, D. Sharma and A. Katariya (2012) An Approach to Design and Optimization of WLAN Patch Antennas for Wi-Fi Applications. *IJECCT*,2(2),18-23.
- [5] Indrasen Singh, Dr. V.S. Tripathi, *Microstrip Patch Antenna and its Applications: A Survey*, Indrasen Singh et al, Int. J. Comp. Tech. Appl., Vol 2 (5), 1595-1599.
- [6] Joshua Madhukar Singh, Mayank Mishra, Prafull Sharma, *Design & Optimization of Microstrip Patch Antenna*.
- [7] Escortradarforum.com, 'Kustom Falcon HR & Raptor RP-1 - Escort Radar Forum', 2015. [Online] Available: <http://escortradarforum.com/forums/showthread.php?t=9611>. [Accessed: 08- July- 2015].
- [8] Dakir, R. et al. 'Rectangular Planar Antenna Using U-Slot For Bandwidth Improvement'. *Electrical and Electronic Engineering* 3.4 (2013): 118-121. Web. 4 Oct. 2015.

Solution of the Linear and Non-linear Partial Differential Equations Using Homotopy Perturbation Method

Abaker. A. Hassaballa.

¹Department of Mathematics, Faculty of Science, Northern Border University,
Arar, K. S. A. P.O. Box 1321,

²Department of Mathematics, College of Applied & Industrial Sciences, Bahri University, Khartoum, Sudan

Abstract:- In recent years, many more of the numerical methods were used to solve a wide range of mathematical, physical, and engineering problems linear and nonlinear. This paper applies the homotopy perturbation method (HPM) to find exact solution of partial differential equation with the Dirichlet and Neumann boundary conditions.

Keywords:- homotopy perturbation method, wave equation, Burgers equation, homogeneous KdV equation.

I. INTRODUCTION

The notion of homotopy is an important part of topology and thus of differential geometry. The homotopy continuation method or shortly speaking homotopy was known as early as in the 1930s. Thus, in 1892, Lyapunov [1] introduced the so called “artificial small parameters method” considering a linear differential

equation with variable coefficient in the form
$$\frac{du}{dt} = M(t)u$$

with $M(t)$ a time periodic matrix. He replaced this equation with the equation
$$\frac{du}{dt} = \varepsilon M(t)u$$

To get the solution of the last equation, Lyapunov developed the power series over ε for the variable u and then setting $\varepsilon = 1$.

Later, this method was used by kinematicians in the 1960s in the US for solving mechanism synthesis problems [29]. The latest development was done by Morgan at General Motors [3]. There are also two important literature studies by Garcia and Zangwill [5] and Allgower and Georg [8]. The HPM was introduced by Ji-Huan He of Shanghai University in 1998, [9-13]. The HPM is a special case of the homotopy analysis method (HAM) developed by Liao Shijun in 1992 [25]. HPM has been applied by many authors, to solve many types of the linear and nonlinear equations in science and engineering, boundary value problems [2,11], Cauchy reaction–diffusion problem [4], heat transfer[6],nonlinear wave equations [9], non-linear oscillators with discontinuities [12], Sumudu transform[21], and to other fields [13-28].

The method employs a homotopy transform to generate a convergent series solution of linear and nonlinear partial differential equations. The homotopy perturbation method is combination of perturbation and homotopy method

II. HOMOTOPY PERTURBATION METHOD

To illustrate the basic idea of this method, we consider the following non-linear differential equation:

$$A(u) - f(r) = 0, \quad r \in \Omega \quad (1)$$

With the following boundary conditions:

$$B\left(u, \frac{\partial u}{\partial n}\right) = 0, \quad r \in \Gamma \quad (2)$$

Where A is a general differential operator, B is a boundary operator, $f(r)$ is a known analytical function and Γ is the boundary of the domain Ω . The operator A can be decomposed into a linear and a non-linear, designated as L and N respectively. The equation (1) can be written as the following form.

$$L(u) + N(u) - f(r) = 0 \quad (3)$$

Using homotopy perturbation technique, we construct a homotopy $v(r, p) : \Omega \times [0, 1] \rightarrow \mathbf{R}$ which satisfies

$$H(v, p) = (1 - p)[L(v) - L(u_0)] + p[A(v) - f(r)] = 0 \quad (4)$$

Where $p \in (0, 1)$ is an embedding parameter, u_0 is an initial approximation solution of (1), which satisfies the boundary, from equation (4) we obtain

$$H(v, 0) = L(v) - L(u_0) = 0 \quad (5)$$

$$H(v, 1) = A(v) - f(r) = 0 \quad (6)$$

Changing the process of p from zero to unity, a change $v(r, p)$ from $u_0(r)$ to $u(r)$.

In topology, this is called homotopy. According to the HPM, we can first use the embedding parameter p as a small parameter, and assume that the Solutions of equation (4) can be written as a power series in p as the following

$$v = v_0 + p v_1 + p^2 v_2 + p^3 v_3 + \dots \quad (7)$$

Setting $p = 1$ results in the approximate of equation (7), can be obtained

$$u = \lim_{p \rightarrow 1} v = v_0 + v_1 + v_2 + v_3 + \dots \quad (8)$$

III. Applications

In this section, we apply Homotopy perturbation method for solving linear and nonlinear problems.

Example 1.

Use the Homotopy perturbation method to solve the Laplace equations:

$$\begin{cases} u_{xx} + u_{yy} = 0, & 0 < x, y < \pi \\ u(0, y) = 0, & u(\pi, y) = \sinh \pi \sin y \\ u(x, 0) = 0, & u(x, \pi) = 0 \end{cases} \quad (9)$$

Using HPM, we construct a homotopy in the following form

$$H(v, p) = (1 - p) \left[\frac{\partial^2 v}{\partial y^2} - \frac{\partial^2 u_0}{\partial y^2} \right] + p \left[\frac{\partial^2 v}{\partial x^2} + \frac{\partial^2 v}{\partial y^2} \right] = 0 \quad (10)$$

We select $u_0(x, y) = y \sinh x$ as in initial approximation that satisfies the two conditions. Substituting equation (7) into equation (10) and equating the terms with identical powers of p , we drive

$$p^0 : \begin{cases} \frac{\partial^2 v_0}{\partial y^2} - \frac{\partial^2 u_0}{\partial y^2} = 0, \\ v_0(x, 0) = 0, & v_0(0, y) = 0 \end{cases} \quad (11)$$

$$p^1 : \begin{cases} \frac{\partial^2 v_1}{\partial y^2} + \frac{\partial^2 u_0}{\partial y^2} + \frac{\partial^2 v_0}{\partial x^2} = 0, \\ v_1(x, 0) = 0, & v_1(0, y) = 0 \end{cases} \quad (12)$$

$$p^2 : \begin{cases} \frac{\partial^2 v_2}{\partial y^2} + \frac{\partial^2 v_1}{\partial x^2} = 0, \\ v_2(x, 0) = 0, \quad v_2(0, y) = 0 \end{cases} \quad (13)$$

$$p^3 : \begin{cases} \frac{\partial^2 v_3}{\partial y^2} + \frac{\partial^2 v_2}{\partial x^2} = 0, \\ v_3(x, 0) = 0, \quad v_3(0, y) = 0 \end{cases} \quad (14)$$

⋮

Consider $v_0 = u_0(x, y) = y \sinh x$. From equations (12),(13) and (14), we have

$$v_1 = -\frac{y^3}{3!} \sinh x$$

$$v_2 = \frac{y^5}{5!} \sinh x$$

$$v_3 = -\frac{y^7}{7!} \sinh x$$

⋮

Therefore, the solution of equation(9) when $p \rightarrow 1$ we will be as follows:

$$u(x, y) = \left(y - \frac{y^3}{3!} + \frac{y^5}{5!} - \frac{y^7}{7!} + \dots \right) \sinh x = \sinh x \sin y$$

Because the boundary conditions are Neumann boundary conditions, an arbitrary constant must be added. Therefore, the exact solution in will be as follows:

$$u(x, y) = \sinh x \sin y + C.$$

Example .2

Use the Homotopy perturbation method to solve the inhomogeneous wave equation

$$\begin{cases} u_{tt} - u_{xx} + 2 = 0, \quad 0 < x < \pi, \quad t > 0 \\ u(0, t) = 0, \quad u(\pi, t) = \pi^2 \\ u(x, 0) = x^2, \quad u_t(x, 0) = \sin x \end{cases} \quad (15)$$

Using HPM, we construct a homotopy in the following form

$$H(v, p) = (1 - p) \left[\frac{\partial^2 v}{\partial t^2} - \frac{\partial^2 u_0}{\partial t^2} \right] + p \left[-\frac{\partial^2 v}{\partial x^2} + \frac{\partial^2 v}{\partial t^2} - 2 \right] = 0 \quad (16)$$

We select $u_0(x, t) = x^2 + t \sin x$ as in initial approximation that satisfies the three conditions. Substituting equation (7) into equation (16) and equating the terms with identical powers of p , we drive

$$p^0 : \begin{cases} \frac{\partial^2 v_0}{\partial t^2} - \frac{\partial^2 u_0}{\partial t^2} = 0, \quad v_0(0, t) = 0 \\ v_0(x, 0) = x^2, \quad v_0(\pi, t) = \pi^2 \end{cases} \quad (17)$$

$$p^1 : \begin{cases} \frac{\partial^2 v_1}{\partial t^2} + \frac{\partial^2 u_0}{\partial t^2} - \frac{\partial^2 v_0}{\partial x^2} + 2 = 0, & v_1(0,t) = 0 \\ v_1(x,0) = 0, & v_1(\pi,t) = 0 \end{cases} \quad (18)$$

$$p^2 : \begin{cases} \frac{\partial^2 v_2}{\partial t^2} - \frac{\partial^2 v_1}{\partial x^2} + 2 = 0, & v_2(0,t) = 0 \\ v_2(x,0) = 0, & v_2(\pi,t) = 0 \end{cases} \quad (19)$$

$$p^3 : \begin{cases} \frac{\partial^2 v_3}{\partial t^2} - \frac{\partial^2 v_2}{\partial x^2} + 2 = 0, & v_3(0,t) = 0 \\ v_3(x,0) = 0, & v_3(\pi,t) = 0 \end{cases} \quad (20)$$

⋮

Consider $v_0 = u_0(x, t) = x^2 + t \sin x$. Form equations (18),(19) and (20), we have

$$v_1 = -\frac{t^3}{3!} \sin x$$

$$v_2 = \frac{t^5}{5!} \sin x$$

$$v_3 = -\frac{t^7}{7!} \sin x$$

⋮

Therefore, the solution of equation(15) when $p \rightarrow 1$ we will be as follows:

$$u(x, t) = x^2 + \left(t - \frac{t^3}{3!} + \frac{t^5}{5!} - \frac{t^7}{7!} + \dots \right) \sin x = x^2 + \text{sint} \sin x$$

Because the boundary conditions are Neumann boundary conditions, an arbitrary constant must be added. Therefore, the exact solution in will be as follows:

$$u(x, t) = x^2 + \text{sint} \sin x + C .$$

Example.3

Use the Homotopy perturbation method to solve the Burgers equation

$$u_t + uu_x - u_{xx} = 0, \quad u(x, 0) = x \quad (21)$$

Using HPM, we construct a homotopy in the following form

$$H(v, p) = (1 - p) \left[\frac{\partial v}{\partial t} - \frac{\partial u_0}{\partial t} \right] + p \left[\frac{\partial v}{\partial t} + v \frac{\partial v}{\partial x} + \frac{\partial^2 v}{\partial x^2} \right] = 0 \quad (22)$$

Substituting equation (7) into equation (22) end equating the terms with identical powers of p , we drive

$$p^0 : \begin{cases} \frac{\partial v_0}{\partial t} - \frac{\partial u_0}{\partial t} = 0, & v_0(x,0) = x \end{cases} \quad (23)$$

$$p^1 : \begin{cases} \frac{\partial v_1}{\partial t} + \frac{\partial u_0}{\partial t} + v_0 \frac{\partial v_0}{\partial x} - \frac{\partial^2 v_0}{\partial x^2} = 0, & v_1(x,0) = 0 \end{cases} \quad (24)$$

$$p^2 : \begin{cases} \frac{\partial v_2}{\partial t} + v_0 \frac{\partial v_1}{\partial x} + v_1 \frac{\partial v_0}{\partial x} - \frac{\partial^2 v_1}{\partial x^2} = 0, & v_2(x,0) = 0 \end{cases} \quad (25)$$

$$p^3 : \begin{cases} \frac{\partial v_3}{\partial t} + v_0 \frac{\partial v_2}{\partial x} + v_1 \frac{\partial v_1}{\partial x} + v_2 \frac{\partial v_0}{\partial x} - \frac{\partial^2 v_2}{\partial x^2} = 0, & v_3(x,0) = 0 \end{cases} \quad (26)$$

⋮

Consider $v_0 = u_0(x, t) = x$, as a first approximation for solution that satisfies the initial conditions. Form equations (24),(25) and (26), we have

$$\begin{aligned} v_1 &= -xt \\ v_2 &= xt^2 \\ v_3 &= -xt^3 \\ &\vdots \end{aligned}$$

Therefore, the solution of equation(21) when $p \rightarrow 1$ we will be as follows:

$$u(x, t) = x(1 - t + t^2 - t^3 + \dots) = \frac{x}{1-t}, \quad |t| < 1$$

Because the boundary conditions are Neumann boundary conditions, an arbitrary constant must be added. Therefore, the exact solution in will be as follows:

$$u(x, t) = \frac{x}{1-t} + C, \quad |t| < 1.$$

Example.4

Use the Homotopy perturbation method to solve the homogeneous KdV equation

$$u_t - 6uu_x + u_{xxx} = 0, \quad u(x, 0) = 6x \quad (27)$$

Using HPM, we construct a homotopy in the following form

$$H(v, p) = (1-p) \left[\frac{\partial v}{\partial t} - \frac{\partial u_0}{\partial t} \right] + p \left[\frac{\partial v}{\partial t} - 6v \frac{\partial v}{\partial x} + \frac{\partial^3 v}{\partial x^3} \right] = 0 \quad (28)$$

Substituting equation (7) into equation (28) and equating the terms with identical powers of p , we drive

$$p^0 : \begin{cases} \frac{\partial v_0}{\partial t} - \frac{\partial u_0}{\partial t} = 0, & v_0(x,0) = 6x \end{cases} \quad (29)$$

$$p^1 : \begin{cases} \frac{\partial v_1}{\partial t} + \frac{\partial u_0}{\partial t} - 6v_0 \frac{\partial v_0}{\partial x} + \frac{\partial^3 v_0}{\partial x^3} = 0, & v_1(x,0) = 0 \end{cases} \quad (30)$$

$$p^2 : \begin{cases} \frac{\partial v_2}{\partial t} - 6v_0 \frac{\partial v_1}{\partial x} - 6v_1 \frac{\partial v_0}{\partial x} + \frac{\partial^3 v_1}{\partial x^3} = 0, & v_2(x,0) = 0 \end{cases} \quad (31)$$

$$p^3 : \begin{cases} \frac{\partial v_3}{\partial t} - 6v_0 \frac{\partial v_2}{\partial x} - 6v_1 \frac{\partial v_1}{\partial x} - 6v_2 \frac{\partial v_0}{\partial x} + \frac{\partial^3 v_2}{\partial x^3} = 0, & v_3(x,0) = 0 \end{cases} \quad (32)$$

⋮

Consider $v_0 = u_0(x, t) = 6x$, as a first approximation for solution that satisfies the initial conditions. Form equations (30), (31) and (32), we have

$$\begin{aligned}v_1 &= 6^3 x t \\v_2 &= 6^5 x t^2 \\v_3 &= 6^7 x t^3 \\&\vdots\end{aligned}$$

Therefore, the solution of equation (1) when $p \rightarrow 1$ we will be as follows:

$$u(x, t) = 6x + 6^3 x t + 6^5 x t^2 + 6^7 x t^3 + \dots = 6x \left(1 + 36t + (36t)^2 + (36t)^3 + \dots \right) = \frac{6x}{1 - 36t}, \quad |36t| < 1$$

Because the boundary conditions are Neumann boundary conditions, an arbitrary constant must be added. Therefore, the exact solution in will be as follows:

$$u(x, t) = \frac{6x}{1 - 36t} + C, \quad |36t| < 1.$$

IV. Conclusion

In this paper, linear and nonlinear partial differential equations are solved by using Homotopy Perturbation Method. Analytical solution obtained by this method is satisfactory same as the exact results to these models. The homotopy perturbation method is powerful and efficient technique to find the solution of linear and nonlinear equations.

References:

- [1] A.M. Lyapunov, General Problem on Stability of Motion (Taylor and Francis, London, 1992)
- [2] A. Golbabai, M. Javidi, Application of homotopy perturbation method for solving eighth-order boundary value problems, Applied Mathematics and Computation 191 (1) (2007) 334–346.
- [3] A.P. Morgan, Solving Polynomial Systems using Continuation for Engineering and Scientific Problems (Prentice Hall, Englewood, New York, 1987).
- [4] A. Yildirim, Application of He's homotopy perturbation method for solving the Cauchy reaction–diffusion problem, Computers and Mathematics with Applications 57 (4) (2009) 612–618.
- [5] C.B. Garcia, W.S. Zangwill, Pathways to Solutions. Fixed Points and Equilibrium (Prentice-Hall, Book Company, Englewood Cliffs, NY, 1981)
- [6] D.D. Ganji, The application of He's homotopy perturbation method to nonlinear equations arising in heat transfer, Physics Letters A 355 (2006) 337–341.
- [7] D. Lesnic, "A nonlinear reaction-diffusion process using the Adomian decomposition method," International Communications in Heat and Mass Transfer, vol. 34, no. 2, pp. 129–135, 2007.
- [8] E.L. Allgower, K. Georg, Numerical Continuation Methods, an Introduction (Springer, New York, NY, 1990)
- [9] He, J.H, Application of homotopy perturbation method to nonlinear wave equations, Chaos Solitons Fract. 26 (3) (2005) ,pp. 695–700.
- [10] He, J.H, Asymptotology by homotopy perturbation method, Appl. Math. Compute. 156 (3) (2004), pp. 591–596.
- [11] He, J.H. Homotopy perturbation method for solving boundary problems, Phys. Lett. A 350 (1–2) (2006), pp. 87–88.
- [12] He, J.H, The homotopy perturbation method for non-linear oscillators with discontinuities, Appl. Math. Comput. 151(1)(2004), pp. 287–292.
- [13] J. Biazar, M. Eslami, H. Ghazvini, Homotopy perturbation method for systems of partial differential equations, International Journal of Nonlinear Sciences and Numerical Simulation 8 (3) (2007) 411–416.
- [14] J. Biazar, K. Hosseini, P. Gholamin. Homotopy Perturbation Method for Solving KdV and Sawada-Kotera Equations. Journal of Applied Mathematics, 6(21)(2009):23-29.
- [15] J. Biazar, H. Ghazvini. Exact solution for non-linear Schrodinger equations by Hes Homotopy perturbation method. Physics Letters A 366(2007):79-84.
- [16] J.H. He, Homotopy perturbation technique, Computer Methods in Applied Mechanics and Engineering 178 (1999) 257262.
- [17] J.H. He. A coupling method of homotopy technique and perturbation technique for nonlinear problems. Int. J. Nonlinear Mech. 35(2000):37-43.
- [18] J.H. He. Comparison of homotopy perturbation method and homotopy analysis method. Appl. Math. Comput. 156(2004):527-539.
- [19] J.H. He. Homotopy perturbation method, a new nonlinear analytical technique. Appl. Math. Comput. 135(2003):73-79.
- [20] M.A. Jafari, A. Aminataei, Application of homotopy perturbation method in the solution of Fokker–Planck equation, Physica Scripta 80 (5) (2009) Article ID055001.
- [21] M.A. Rana, A.M. Siddiqui, Q.K. Ghor, Application of He's homotopy perturbation method to Sumudu transform, International Journal of Nonlinear Sciences and Numerical Simulation 8 (2) (2007) 185–190.
- [22] Muhammad Aslam Noor, Syed Tauseef Mohyud-Din, Homotopy perturbation method for solving sixth-order boundary value problems, Computers and Mathematics with Applications 55 (2008) 2953–2972.

- [23] N. H. Sweilam, M. M. Khader. Exact solutions of some coupled nonlinear partial differential equations using the homotopy perturbation method. *Computers and Mathematics with Applications*. 58 (2009):2134-2141.
- [24] Saadatmandi, A; Dehghan, M; Eftekhari, Application of He's homotopy perturbation method for non-linear system of second-order boundary value problems, *Nonlinear Analysis: Real World Applications*, V(10) A, (2010), pp.1912-1922.
- [25] S. J. Liao. *Beyond Perturbation, Introduction to Homotopy Analysis Method*. Chapman and Hall/Crc Press, Boca Raton. 2003.
- [26] T.M. Wu, A new formula of solving nonlinear equations by Adomian decomposition method and homotopy methods. *Appl. Math. Comput.* 172, 903907 (2006)
- [27] T. Ozis, A. Yildirim, Traveling wave solution of Korteweg–de Vries equation using e's homotopy perturbation method, *International Journal of Nonlinear Sciences and Numerical Simulation* 8 (2) (2007) 239–242.
- [28] Zaid Odibat, Shaher Momani. A reliable treatment of homotopy perturbation method for Klein-Gordon equations. *Physics Letters A* 356(2007):351-357.
- [29] V. Marinca, N. Herisanu, *Nonlinear Dynamical Systems in Engineering—Some Approximate Approaches* Springer, Heidelberg, 2011)

On Resiliency in Cyber-Road Traffic Control System using Modified Danger Theory based Optimized Artificial Immune Network

Lokesh M R, Research Scholar¹, Dr.Y.S Kumaraswamy, Professor & Dean²

¹(Department of Computer Science and Engineering, Sathyabama University, Chennai, India)

²(Department of Computer Science and Engineering, Nagarjuna College of Engineering and Technology, Devanahalli, Bangalore, India)

ABSTRACT : Cyber-Road Traffic control is a sub domain of Intelligent Transport System to make daily road traffic system as smart. Towards this various types of heterogeneous, federated, distributed infrastructure are in use, with diverse has be robust, reliable and secure for nominal operation of successful utilization of smart infrastructure, needs resiliency operation. The resiliency is a nonfunctional software requirement define as maintaining state awareness among them and if abnormality identified healing process occur to rollback normal operation. The proposal of road traffic infrastructure differentiates into In-vehicle, vehicle-vehicle, vehicle-infrastructure and, infrastructure-infrastructure and identify its infrastructural compounds, working operations, and possible nominal and abnormal behaviour of infrastructure. This infrastructure maintain nominal operation, by population based various multi Agent paradigm using Modified Danger Theory based Optimized Artificial Immune Network. This Artificial Immune network interaction is demonstrates in different infrastructure of road traffic system and validate through numerical and simulation environment.

Keywords – Cyber-Road Traffic control system, resiliency, Artificial Immune Network, Multi Agent System

I. INTRODUCTION

Cyber-Physical system (CPS) is viewed as a new technology with next generation architecture to incorporate the computation and communication with the physical world. The application like cyber-road Traffic Control system where the environment is diverse in nature needs resiliency, which plays a major role in developing reliability and robustness [1]. The Traffic management is widely accepted as an important problem in modern society as it is responsible for keeping a steady flow of people, goods and services within cities. The quality of this flow directly affects the city's economy and general well-being of the population. Recently Various CPS based approaches have been introduced such as GPS equipped smart phones and sensor based frameworks which have been proposed to provide various services i.e. environment estimation, road safety improvement but they encounter certain limitations like high energy consumption and high computation cost.

To achieve efficient and safe road transportation is one of the motivations to carry out the research on CPS and is one of the most challenging areas, as it possesses the information, physical and social features [2] Cyber-Road Traffic control System can play a major role in reducing risks, high accidents rate, traffic congestion, carbon emissions, air pollution and on the other hand increasing safety and reliability, travel speeds, traffic flow and satisfied travelers for all modes. To meet safety and high reliability requirements, the Cyber-Road Traffic control System is modeled in the lines of Cyber-Road Traffic control system with Multi Agent Paradigm [3] and biological inspired Danger Theory based-modified Artificial immune Network is applied in MAS to develop resiliency. The proposal develops algorithm, defines resiliency as state awareness and healing process, with dendritic cells as Threshold-based agent population concentration and Artificial Recognition Ball as memory agent correspondingly [4]. This algorithm is validated with simulation results as well as numerical analysis.

TABLE I
COMPARISON OF MULTI AGENT SYSTEM ARTIFICIAL IMMUNE SYSTEM AND PROPOSED DANGER THEORY BASED-MULTI AGENT CYBER-PHYSICAL SYSTEM ARCHITECTURE[4]

Multi Agent System	Artificial Immune System	Proposed Architecture
Distributed System	Cooperative work by Immune cell	Heterogeneous Multi Agent
Self Maintained System	Seeing and Being seen	State awareness
Adaptive System	Somatic Level evolution by selection	Self healing Module

The contribution of the paper is to model the Cyber-Road Traffic control System with Multi Agent System Paradigm and apply biological inspired Human Immune System of Danger theory based optimized Artificial Immune Network Algorithm methodology as shown in Table 1. An outcome of these is to achieve resiliency operation in real time, diverse environment. Hence overall goal of this paper is to integrate all the Cyber-Road Traffic control System characteristics as multi agent population of Artificial immune network, where focus is on information flow and information processing such as recognition, learning, memory, and adaptation to achieve state awareness and healing process towards resiliency in cyber-physical system as shown in Figure 1.

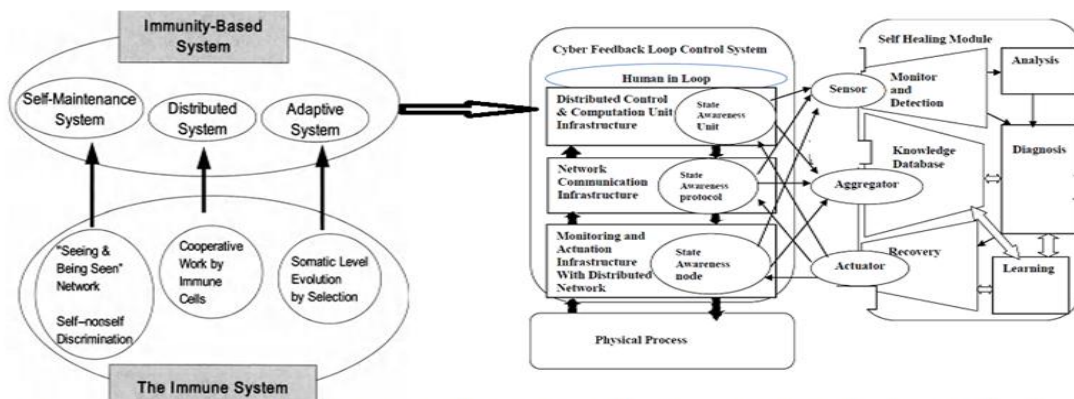


Fig. 1.Features of immunity-based system [5] and Autonomic Self Healing Architecture for Resiliency in Cyber Physical System [6]

The flow of the paper as follows: In Section 2 resiliency development methods and resiliency in Cyber-Road Traffic control System. Section 3 explains propose model of cyber-physical system through Multi Agent Paradigm on resiliency development. Section 4 Danger Theory Based Artificial Immune Network Algorithm is modified as a resiliency algorithm with state awareness and healing process. Section 5 Simulation parameter setting towards validating proposed algorithm and results is discussed.

II. RELATED WORK

Cyber physical system has been recognized as a key technique for providing next generation application which improves electricity delivery and usage, health care, transportation management system [7]. For the road traffic control, CPS studies elaborate, coordinated, efficient information space operations, realizing the traffic system control and travel behavior control [8] to make road traffic more safely and efficiently. The domain of traffic and transportation systems is well suited to an agent-based approach because of its geographically distributed nature and its alternating busy-idle operating characteristics [9], [10]. To meet the high reliability and safety requirements for these systems, various GPS based applications, frameworks have been proposed. [7] Describe how the mobile internet is changing the face of transportation CPS. They built a traffic monitoring system known as mobile millennium by using GPS equipped mobile devices, in this system collect traffic data from GPS-equipped mobile phones and estimate traffic condition in real time. The major drawback of this approach is high battery consumption, each mobile phone should be GPS equipped.CPS is not about the application methods of advanced information technology, but about the theory constructing new systems by integration of information processes and physical processes. Therefore, the research of traffic control physical systems start from the re-analysis of the model and construction [11]. Proposed a web of-thing based CPS architecture to improve road safety and to achieve high demand response in smart grids. [12] Proposed a framework on SIP/ ZigBee architecture. In this by using SIP and its extension, a seamless convergence of traffic measurement and short-range wireless sensor and equator networks can be achieved. [13] Proposed traffic monitoring system based on vehicle based sensor networks. These vehicle based sensors are embedded in vehicle

for monitoring the traffic. These sensors are used due to its low communication cost and avoid the network congestion. The major drawback of this system is that it does not define the relationship between accuracy and number of speed elements (SE). So, these proposed systems suffer with some drawbacks and does not provide the services efficiently. To provide these services like Environment estimation, Road Condition estimation, Velocity and Travel Time estimation and Traffic Congestion information [14] TIS based on QCPS that provides services according to user’s query. But the implementation of this needs a lot of server maintenance and highly qualified professionals which elevates the actual cost.

III. CYBER-ROAD TRAFFIC CONTROL SYSTEM WITH ARTIFICIAL IMMUNE MULTI AGENT SYSTEM PARADIGM

This section gives a broad overview of layered cyber-physical system [6], with the agent based paradigm. In each layer, different agents are defined with their roles for developing resiliency in cyber-physical system [15][16]. We understood the generic system of cyber process that is applicable to road traffic control system (intelligent transportation system). Cyber-Road Traffic control System has diverse environment with large scale, federated, distributed, heterogeneous components. For monitoring and actuation of these processes with communication and computation capabilities, it needs a real time abnormality monitoring, quick and accurate healing process [17][18]. Due to the nature of Cyber-Road Traffic control System discussed, developing nonfunctional requirement like resiliency are proposed with a multi-agent paradigm and Biological inspired computational methodology of Artificial Immune System which is adopted for Multi-level defense in both parallel and sequential fashion[5].

We understand the comparison between Cyber Physical Multi Agent Paradigm System and Road Traffic Control System. Also, the various interaction between vehicles and infrastructure or we can say the different entities along the road, how they interact by using different standards and their various applications and features. It is composed of three levels [11],

- the application of the CPS theory of integrating information process into transportation process
- traffic detection and control of information on the implementation of technical solutions
- support of modern computing, communication and control technology

Road Traffic Process with Multi Agent Paradigm

The road transportation system is a large-scale human-made engineering system which cannot operate safely and efficiently. The mechanics changing process of key transportation infrastructure like bridge, culvert, tunnel, subgrade, and slope, roadside and so on are Traffic physical processes. While, the ubiquitous sensing detection in a wide range of reliable interconnected, depth perception, forecast, warning and monitoring are Information processes. The Functions of this system are to achieve real-time monitoring of road facilities and transportation, meteorological environment detection. As in the figure 2,

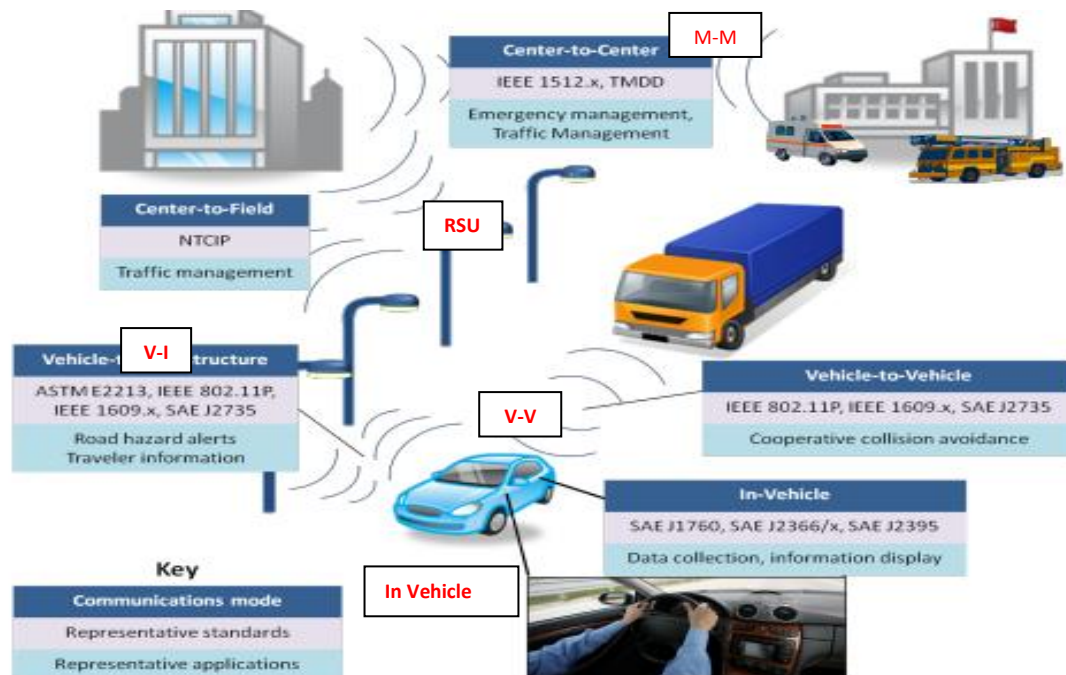


Fig. 2. Intelligent Road Traffic control system and its infrastructure [19]

In-Vehicle:

The evolution in mobile and wireless communication technology has led to use of Built-in equipment in cars or trucks can easily access traveling-related dynamic information, such as the current situation on the roads, weather forecasts, or information on local points of interests using internet. However, personal information of the vehicle’s passengers – which could be also very useful for their travel. This information is not easily accessible by the driver or the built-in equipment.

To help manage the information, we need a mechanism to orchestrate the operations of the in-vehicle devices so that such frustration due to an influx of individual messages from a lot of new devices can be eased. In this study, we propose an in-vehicle communication scheme for multi-system integration, where an effective system service discovery protocol is used. This proposed design also contains mutual communication methods and the data exchange methodologies for system integration. In- vehicles the information useful for traveling is usually not located at one device – it is distributed over various mobile and handheld devices: The mobile phones contain their phone books, PDAs (Personal Digital Assistants) manage the passengers’ time schedules. The navigation unit has the current information of the road situation and is able to specify the route with the estimated time to reach the specified destination, vehicle’s radio receives periodically the current weather conditions, Laptop contains e-mails or documents that should be sent.

The various standards used are: SAE J1760, SAE J2366/x, SAE J2395.

CPS Infrastructure	simple sensors with limited capabilities
CPS Nominacy Behavior	Set of sensors are used to gather continuous information about the physical system.
Effect due to internal and External source	Electromechanical transducer which measures certain attributes of the physical system such as speed, temperature, and pressure and converts it to an electrical signal
Issue to be handle	Control System centric-multiple control loops
Agents Type	Reactive
Local Decision	<ul style="list-style-type: none"> • Sensor Agent • Resource Agent • Tactical Survival Agent
Global Performance	<ul style="list-style-type: none"> • Tactical Survival Agent • Resource Agent • Connection Admission control Agent

- The monitor network shown in figure 2 has set of sensors, and is of Reactive Agents as a proposal, Sensor Agent, Resource Agent ,Tactical Survival Agent, Connection Admission control Agent are define as shown
- The actuator network shown in figure 2 has set of actuator device as Actuator Agent, Tactical Survival Agent, Resource Agent and Connection Admission control Agent are proposal and it is reactive Agent in Nature.

Vehicle-Vehicle:

Vehicle-to-Vehicle Communications is used for cooperative collision avoidance. By exchanging anonymous, vehicle-based data regarding position, speed, and location (at a minimum), V2V communications enables a vehicle to: sense threats and hazards with a 360 degree awareness of the position of other vehicles and the threat or hazard they present; calculate risk; issue driver advisories or warnings; or take pre-emptive actions to avoid and mitigate crashes. At the heart of V2V communications is a basic application known as the Here I Am data message. This message can be derived using non-vehicle-based technologies such as GPS to identify location and speed of a vehicle, or vehicle-based sensor data wherein the location and speed data is derived from the vehicle’s computer and is combined with other data such as latitude, longitude, or angle to produce a richer, more detailed situational awareness of the position of other vehicles. Because the Here I Am data message can be derived from non-vehicle-based technologies.

The Features are Emergency Brake Light Warning, Forward Collision Warning, Intersection Movement Assist, Blind Spot and Lane Change Warning, Do not pass Warning, Control Loss Warning.

- The monitor network shown in figure 2 has set of sensors, Reactive Agents as a proposal, Sensor Agent, Resource Agent ,Tactical Survival Agent, Connection Admission control Agent are define as shown

- The actuator network shown in figure 2 has set of actuator device as Actuator Agent, Tactical Survival Agent, Resource Agent and Connection Admission control Agent are proposal and it is reactive Agent in Nature.

Example of Application: Traffic control technology, e.g. Intelligent Transportation System,

– **Realise traffic control**

The road traffic system process and the traffic control process is the Traffic physical process. Traffic control system model description, traffic system control and traffic behaviour control instruction optimization calculation is Information process

The Function is to achieve a more secure and efficient dynamic road traffic control

CPS Infrastructure	Simple Sensors with limited capabilities
CPS Nominalcy Behavior	Set of sensors are used to gather continuous information about the physical system.
Affect due to internal and External source	Electromechanical transducer which measures certain attributes of the physical system such as speed, temperature, and pressure and converts it to an electrical signal
Issue to be handle	Control system centric- <i>multiple control loops</i>
Agents Type	Reactive
Local Decision	<ul style="list-style-type: none"> • Sensor Agent • Resource Agent • Tactical Survival Agent
Global Performance	<ul style="list-style-type: none"> • Tactical Survival Agent • Resource Agent • Connection Admission control Agent

Vehicle-to-Infrastructure:

Vehicle-to-Infrastructure (V2I) Communications for Safety is the wireless exchange of critical safety and operational data between vehicles and roadway infrastructure, intended primarily to avoid motor vehicle crashes. V2I provides road hazards alert and traveler information. V2I communications for safety is a key research program of the Intelligent Transportation Systems. Data and communication standards have been developed through this research effort which includes the SAE J2735 Basic Safety Message; and a standard communications architecture/ platform communicating in the 5.9 GHz band of radio spectrum. V2I applications can be designed to help improve critical safety situations. The various standards used are: ASTM E2213, IEEE 802.11P, IEEE 1609.x, SAE J2735.

The Features are intersection safety, roadway departure prevention, speed management, transit safety and operations, commercial vehicle enforcement and operations, at-grade rail crossing operations, priority assignment for emergency vehicles

- The monitor network shown in figure 2 has set of sensors, and it as Reactive Agents as a proposal, Sensor Agent, Resource Agent ,Tactical Survival Agent, Connection Admission control Agent are define as shown
- The actuator network shown in figure 2 has set of actuator device as Actuator Agent, Tactical Survival Agent, Resource Agent and Connection Admission control Agent are proposal and it is reactive Agent in Nature.

Example of Application: Connected vehicles and autonomous driving have been rapidly gaining momentum in recent years

– **cyber transportation systems (CTS)**

The relation between the synergic relationship process of car-to-car and car-to-road which are running in the road and communication process is the Traffic physical process. The Wireless, high-speed, high reliability, security communications, automatic driving safer and self-adaption is Information process. The Functions are High speed information exchange, in order to guarantee the safety of vehicles in efficient access.

CPS Infrastructure	wired and wireless communication and networking devices
CPS Nominalcy Behavior	Real-time data between sensors, computing subsystems, and actuators
Affect due to internal and External source	Communication between different CPS elements is vulnerable to various computer network threats such as eaves-dropping, DDoS, data modification, man-in-the-middle, and many other attacks
Issue to be handle	Buffer Maintenance, ability to share, and ultimately negotiate resource- <i>a wireless network segment</i>
Agents Type	Hybrid
Local Decision	<ul style="list-style-type: none"> • Tactical Survival Agent • Resource Agent • Connection Admission control Agent
Global Performance	<ul style="list-style-type: none"> • Tactical Survival Agent • Resource Agent • Connection Admission control Agent

Cyber Process with Multi Agent Paradigm

The Communication layer and computation and control layer shown in Figure 2, enhances embedded control system in physical process as

Center-to-Field:

This is used for traffic management. The National Transportation Communication for Intelligent system transportation protocol is a family of standards designed to achieve Interoperability and interchangeability between computers and electronic traffic control equipment from different manufacturers. NTCIP has enabled the center to field communication and command/control of equipment from different manufacturers to be specified, procured, deployed, and tested.

The Features are Improved collaboration and cooperation between jurisdictions, Improved traveler information quality and timeliness, Decreased emergency response times which reduces the impact to traffic and reduces the number of secondary crashes, Cost savings to emergency responders as the appropriate response equipment is identified much earlier, and inappropriate response equipment is not dispatched to the incident scene, Improved response across jurisdictional boundaries. This includes reduced delay as traffic signals are optimized across jurisdictional boundaries, reduced delay and improved mobility for the traveler

- The communication network layer has hybrid Multi Agent of Tactical Survival Agent, Resource Agent, Connection Admission control Agent in this layer as shown figure 2.
- The population based Artificial Immune methodology for optimal resources utilization in communication layer.

Center-to-Center:

Center to center (C2C) communication involves peer-to-peer communications between computers involved in information exchange in real-time transportation management in a many-to-many network. This is used for traffic management, emergency management. This type of communication is similar to the Internet, in that any center can request information from, or provide information to, any number of other centers. An example of center to center communications is two traffic management centers that exchange real-time information about the inventory and status of traffic control devices. This allows each center system to know what timing plan, for example, the other center system is running to allow traffic signal coordination across center geographic boundaries. The various standards used are: IEEE 1512.x, TMDD.

Connection Admission control Agent in communication layer as shown in figure 2.

- The Computation and Control Unit layered shown in figure 2 and it as hybrid Multi Agent of Computation Agent, Control Agent and Tactical Survival Agent as shown in Figure 2.
- The Computation Agent which helps in generation control command with the Control Agent. Control Agents take higher level policy either by expert system or human in loop, is managed by utilizing available resources through a resource agent. The Resource Agent is used to maintain control command to be generated by the service provider. There will be each Resource Agent for Souce-Destination pair of request as shown in figure 2. The Connection Admission control Agent is responsible for providing available resources to computation Agent and control Agent for operation for local and global stability is maintained on resiliency development.

TABLE V COMPUTATION AND CONTROL UNIT AS CENTRE – CENTRE	
CPS Infrastructure	Embedded computing systems
CPS Nominalcy Behavior	A number of embedded controllers process sensing data and compute feedback decisions
Affect due to internal and External source	Computational Platform incorporating a mixture of software-based and hardware-based processing devices, storage elements, I/O peripherals, and communication devices interacting together
Issue to be handle	Consensus Fuzzy Logic -predictable network traffic and legacy components
Agents Type	Hybrid
Local Decision	<ul style="list-style-type: none"> • Computation Agent • Control Agent • Tactical Survival Agent • Resource Agent
Global Performance	<ul style="list-style-type: none"> • Computation Agent • Control Agent • Tactical Survival Agent

IV. APPLICABLE OF IMMUNE CONCEPT IN DEFINED AGENTS

This section defines immune agents used in the developing resiliency in cyber-physical system as Multi Agent Paradigm. The previous section defines generic agent in each layer of cyber-physical system, defined agents are applied immune charactertics as shown in Table 2. In the context of Immune system antigen,

Dendritic Cell, T-cell and Responding, properties are defined as Antigen Agent, Dendritic Cell Agent, T-Cell Agent, and Responding Agent [15] and for healing process and Preliminary information for healing process is adopted in [16]. Signals are represented as real-valued numbers, proportional to values derived from the context information of the dataset in use. The antigen is only used for the labeling and tracking of data. This is applied to propose application.

- **Antigen Agent:** The Antigen is represented as binary strings extracted by neighbor Agent in the population. An Agent that contains an abnormal profile of data item in the data set.
- **Dendritic Cell Agent:** The Dendritic Cell has special characteristics for sensitivity of input signal to collect and capable of data Per-processing that is classify collected signal and transform to either one of the state, this state is formed through the population of agent having same decision have mature context antigen value (MCAV) for triggering T-cell Agent activation for response. -
- **T-Cell Agent:** The Agent receives mature context antigen value depends on the MCAV value take appropriate decides for different type of cause.
- **Responding Agent:** The agent acts like a helper to all agent operations mentioned.
- **Training Agent:** the Training Agent is the Antigen of same class represent by cells like dendritic cell or T-cell which acts as Anomaly Detector.
- **Artificial Recognition Ball:** The ARB (Artificial Recognition Ball) which is also known as B Cell in Human Immune System having capable of generating immune response. It consists of Antigen, count of resource hold and current stimulation value.
- **Candidate Agent:** the Candidate Agent is an antibody of ARB of same class as the training antigen, which most stimulated after expose to the given antigen.
- **Clonal rate:** the clonal rate is the number of mutated clones a given ARB is allowed to attempt to produce. It is an integer value to determine (clonal rate * stimulation value) mutated clones after responding to a given antigen.

The Artificial Immune Network [17] in cyber-physical system for resiliency development. Since CPS is represented as MAS layered discussed above section. Each layer works with different type of population of Agent for their Local Decision and Global Performance. We adopted Danger theory concept, such that Danger signal and Danger Zone of an agent, dendritic cell and Artificial Recognition Ball concept for state awareness

TABLE II
COMPARING ABOVE CONCEPT WITH PROPOSED CONCEPT[4]

Artificial Immune Concept	Agent Interaction for state awareness in Cyber-Physical System	Agent State in Cyber-physical System Architecture
PAMPs	Signal from Signature Based	Activate outer Self-healing Module
Danger Signals	Signal from Behavior of other Agent	Activate outer Self-healing Module
Safe Signals	Signal within variable threshold value	Present in Inner State awareness loop
Initialization of Abnormal Agent	Random generation of memory Agent by stimulation threshold of Abnormal Agent	Present in Inner State awareness loop
Clone operation	Memory Agent	Activate outer Self-healing Module
Mutation operation	ARB Agent	Activate outer Self-healing Module

and healing process. So individual Agent population, acts as data fusion and its anomaly detection are identifying depends on danger signal and danger zone for each environment

An abstract view of CPS interaction is Shown Figure 3. The algorithm is based on a multi-agent framework, where each Agent processes its own environmental signals and collects antigens. The diversity is generated within the Agent population through the application of a ‘migration threshold’- this value limits the number of signal instances an individual the agent can process during its lifespan. This creates a variable Time window effect, with different cells processing the signal and antigen input streams over a range of time periods [20]

The combination of signal/antigen correlation and the dynamics of a cell population are responsible for the anomaly detection capabilities of the DCA.

Let Agents in the population is defined as follows, If **S** is the set of Agent with its lifespan, $s(t) = \{ A g_1(t), A g_2(t), \dots, A g_n(t) \in R^n \}$, **Rⁿ** is the decision variable with **n** variable dimension,

Let Antigen set, $A g_1(t) = \{ a_0, a_1, a_2, \dots, a_n \}$ has attribute value in the set, may act as Antigen in the process.

Let, $f(Ag(t))$ be the function of each Agent. Agent population has to normalize as, $\min\{f(Ag_i(t)), Ag_j(t) \in R^n\}$ or $\max\{f(Ag_i(t)), Ag_j(t) \in R^n\}$. The Signal transformation between Agents is represented as, $w_{ij} \in \mathbf{R}$ weight matrix of signal transformation as W in matrix with two rows and three columns used to categories state of the agent.

Let Agents in the population for training to healing process is defined as follows,

If $AnAg_{Ag.c}(t)$ is the set of Abnormal Agent with its lifespan from state awareness module for healing process by training shown in Fig. 3

$$AnAg_{Ag.c}(t) = \{AnAg_1(t), AnAg_2(t), \dots, AnAg_{Ag.cn}(t) \in R^n\}$$

R^n is the decision variable with n variable dimension,

If $MgMg.c(t)$ is the set of memory Agent with its lifespan for the corresponding Abnormal Agent. Since R^n is same, memory cell and Abnormal Antigen should belong to a same class.

$$Mg_{Mg.c}(t) = \{Mg_1(t), Mg_2(t), \dots, Mg_{Mg.cn}(t) \in R^n\}$$

If $ARB_{Agent.c}(t)$ is the set of Artificial Recognition Ball Agent with its lifespan act as healing Agent for the corresponding Abnormal Agent with the help of memory Agent of the same class.

$$ARB_{Agent.c}(t) = \{ARB_1(t), ARB_2(t), \dots, ARB_{Agent.cn}(t) \in AbAg_{Ag.c}\}$$

Let Abnormal Agent Stimulation level represent, $AbAg.stim$ of the ARB $AbAg$.

Let number of resources held by the ARB $AbAg$ represent $AbAg.resources$.

Let $TotalNumResources$ represent the total number of systems wide resources allowed.

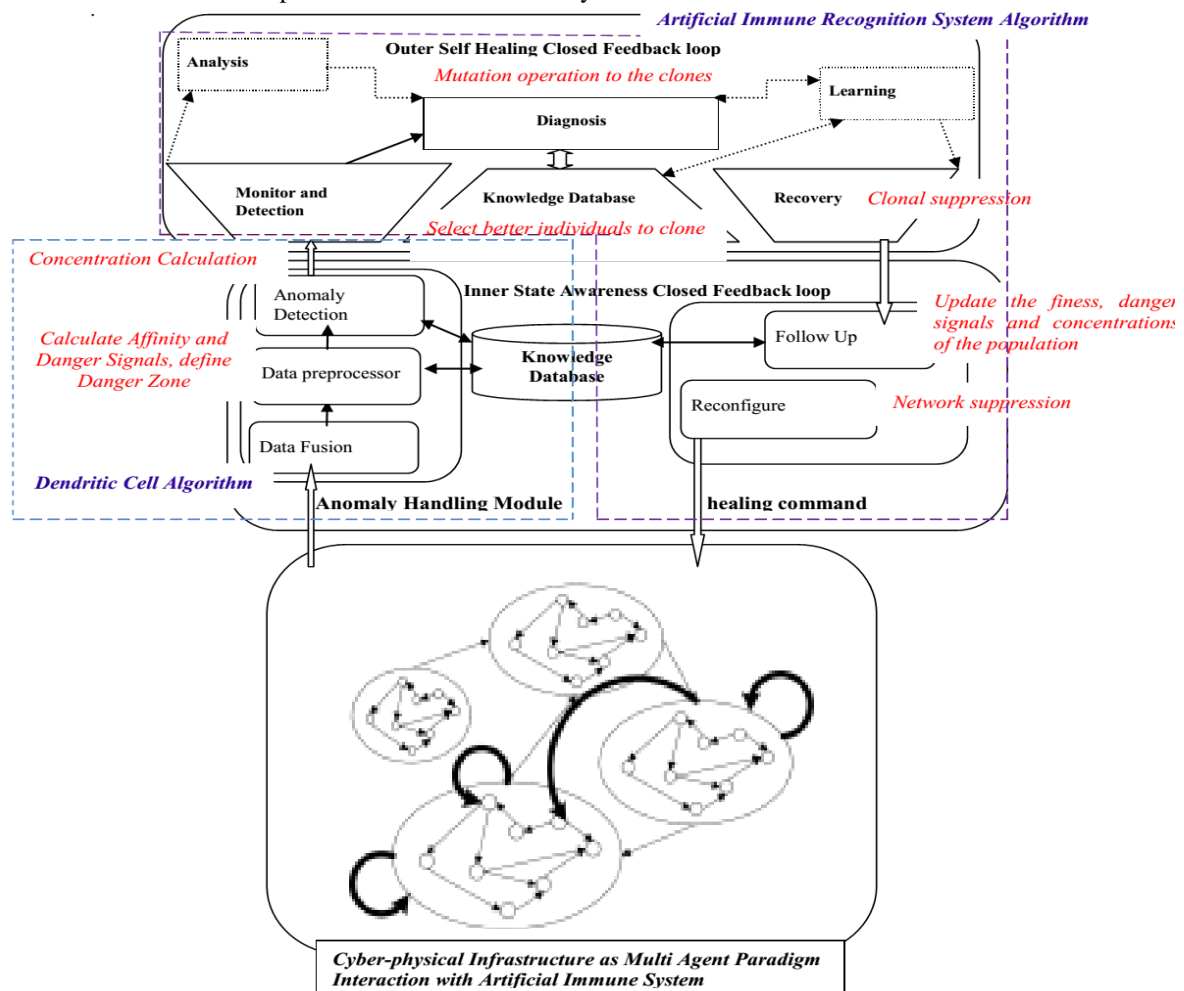


Fig. 3. Agent Population Interaction in each Layer with Danger Theory concept[22]

An Algorithm for resiliency using Artificial Immune Network[4]

Step 1: Initialize, initial network population of Monitored Agent with affinity function, normalization with max and min population. If the same type of Agent Eq(1) will calculate by,

$$affinity(Ag_i(t)) = \begin{cases} \frac{f(Ag_i(t)) - f_{min}}{f_{max} - f_{min}}, P = \max f(x) \\ 1 - \frac{f(Ag_i(t)) - f_{min}}{f_{max} - f_{min}}, P = \min f(x) \end{cases}$$

If the Agent has different type Eq (2) will calculated Euclidean distance by

$$affinity(Ag_i(t), Ag_j(t)) = \frac{1}{\sqrt{\sum_{k=1}^n (Ag_{ik}(t) - Ag_{jk}(t))^2}}$$

Step 2: Each Monitored Agent in the population should calculate its danger zone, which reflects the working environment to maintain local stability in the population.

$$Dz(Ag_i(t)) = \{ Ag_j(t) \mid \frac{1}{\sqrt{\sum_{k=1}^n (Ag_{ik}(t) - Ag_{jk}(t))^2}} < r_{danger}$$

An agent in the Danger zone should maintain its state by interaction with another Agent with its environment state.

Step 3: If the concentration of Agent whose affinity is greater than of another Agent in the danger zone and also distance among them, then danger signal is generated in that Agent.

$$Ds(Ag_i(t)) = \sum_{Ag_j \in Dz(Ag_i(t)) \cap \{affinity(Ag_j(t)) > affinity(Ag_i(t))\}} con(Ag_j) \cdot (r_{danger} - affinity(Ag_i(t), Ag_j(t)))$$

Step 4: Danger Signal depends on the concentration of Agent Population where, concentration of Agent signal for the next time cycle.

If $Ds(Ag_i(t)) > 0$ the Population of Agent concentration is normal and No Danger Signal.

If $Ds(Ag_i(t)) = 0$ $con(Ag_j(t))_{\tau+1} = \{con(Ag(t))_{\tau} (1 + \exp(affinity(Ag_i)^{0.25}))\}$

The Ranges from $Con(Ag_i(t)) \in [0, 1]$, if “0” danger signal high and “1” danger Signal low.

Step 5: If $Con(Ag_i(t)) = 0$, Dendritic Cell Agent are sensitive to signal and collects the signal to its Data Structure. This signal is Per-categorize as PAMP, Danger Signal, Safe Signal along with predefine Safe Signal information and inflammation signal as a threshold define in DC Agent and decide either one of the Agent State as CSM, Semi Mature and Mature State as the output signal of DC.

$$Con(Ag_j(t))_{\tau+1State} = \begin{bmatrix} W_{00} & W_{01} & W_{0n} \\ W_{m0} & & W_{mn} \end{bmatrix}$$

This Signal Category uses approximate theories [26] as step 6-8.

Step 6.If DC Agent output is in CSM state it in **immature State**, if DC Agent input calculation weight is below migration threshold categories as Safe Signal along with danger signal and inflammation signal.

$$Con(Ag_j(t))_{\tau+1immatureState} = \begin{bmatrix} W_{00} & W_{01} & W_{0n} \\ W_{m0} & & W_{mn} \end{bmatrix} * Con(Ag_j(t))_{\tau+1State} (1 - 3I)$$

The weight of the Matrix will update by receiving Danger Signal and compared with Predefined Safe Signal and inflammation signal.

It is initialized once to All the Agent in the population uniformly till the next Danger Signal arrives.

The calculation of Matrix Weight as follows, if signal Weight less than population of agent concentration.

$W_{m \times n InitialThreshold} = Sf(Ag_i(t)) + nxI < Con(Ag_j(t))_{\tau+1}$ Where I is inflammation signal and “n” Natural number depends on the number of Signal. The Predefined Safe Signal and Inflammation signal act as a threshold dynamically in the population.

Step 7 If the agent is *Semi mature state*, if DC Agent input calculation weight is above migration threshold categories as a PAMP Signal along with inflammation signal and calculate severity and sensitivity of abnormal Agent.

$$Con(Ag_j(t))_{\tau+1SemiMatureState} = \begin{bmatrix} W_{00} & W_{01} & W_{0n} \\ W_{m0} & & W_{mn} \end{bmatrix} * Con(Ag_j(t))_{\tau+1State} (1 - 3I)$$

The Weight of this matrix updates if the condition is it satisfy

$$W_{m \times n SemiMature} = Sf(Ag_i(t)) + nxI > Con(Ag_j(t))_{\tau+1}$$

The Final update in this state in the DC Agent acts as threshold for signal categorize to Mature State

$$W_{m \times n SemiMature} = W_{m \times n ThresholdSemiMature} .$$

Step 8: If the agent is mature state, if DC Agent input calculation weight is above semi mature threshold categories as, Danger Signal and along with inflammation signals through weight is calculated in the DC Agent data structure.

$$Con(Ag_j(t))_{\tau+1MatureState} = \begin{bmatrix} W_{00} & W_{01} & W_{0n} \\ W_{m0} & & W_{mn} \end{bmatrix} * Con(Ag_j(t))_{\tau+1State} (1 - 3I)$$

The Weight of the matrix will update if

$$W_{m \times n SemiMature} > W_{m \times n ThresholdSemiMature} .$$

Step 9: Above State of the Agent having similar type of antigen concentration in DC Data structure. Output DC

Agent calculates mature context antigen value as $MCAV_a = \frac{\sum 1_{R^+ .S}(t)}{Ag_n(t)}$

$\sum 1_{R^+ .S}(t)$ is indicate of anomaly collected abnormal Agent otherwise its value is 0.

“a” is the attribute value in the dataset S(t) of attribute set. Similar type of attribute value collected will triggers an alarm to T Agent (healing module) with the causes of abnormal Agent to immune response.

Step 10: If MCAV not “0” that means the value having either one of the threshold value, then Initialize, from state awareness population to healing in the one-shot incremental algorithm. This Abnormal Agent population from state awareness should identify and generation ARB Agent for given specific training Abnormal Agent AnAg_i population, to find memory Agent, Mg_{match} should have following property,

$$Mg_{match} = \arg \max_{mg \in Mg_{AnAg.c}} stimulation(AnAg, mg)$$

where stimulation(x, y) = 1 - affinity(x, y), AnAg.c is class of given Abnormal Agent.

If $Mg_{AnAg.c} \equiv 0$ then $Mg_{match} \leftarrow AnAg$ and $Mg_{AnAg.c} \leftarrow Mg_{AnAg.c} \cup AnAg$.

That is, if the set of memory Agents of the same classification as the Abnormal Agent is empty, then add the Abnormal Agent to the set of memory Agents and denote this newly added memory Agent as the match memory Agent, Mg_{match}.

If the stimulation function for the current work depends on Euclidean distance, then above stimulation is not applicable.

The identified memory Agent Mg_{match}, is used to generate a population of pre exiting ARB Agent for as follows

$$ARB_{generation(x)} = \begin{cases} drandom() & (0 - 1) \\ lrandom() \bmod nc & (0 - nc) \end{cases}$$

The drandom() generation of ARB Agent within mutation rate threshold else lrandom()mod nc is used as above. Step 11: After creating population of ARB Agent, the corresponding candidate Agent should generate to classify a given AnAg. This is done three methods as follows, as the algorithm is one-shot, only one Abnormal Agent goes through the entire process at a time.

First, competition for system wide resources that is allocation of resources to ARB Agent depends on its normalized stimulation value that indicates fitness of Abnormal Agent. Is represented as follow,

$$ARB_{Agent}.resources \leftarrow AnAg.stim * clonal\ rate = \begin{cases} AnAg.stim & \min\ stim < stim > \max\ stim \\ AnAg.stim < - - \frac{AnAg.stim - \min\ stim}{\max\ .stim - \min\ stim} & \text{else} \\ AnAg.stim < - - 1 - \frac{AnAg.stim - \min\ stim}{\max\ .stim - \min\ stim} & \end{cases} \quad ARB_{Agent}.c \equiv AnAg.c$$

Second, use of mutation for diversification and shape-space exploration. If number of class of AnAg, then resource allocation as follow,

$$resAllco = \begin{cases} \sum_{j=1}^{|ARB_i|} AnAg_j.resources & ARB_j.c \in ARB_i \\ \frac{TotalNumResources}{2} & AnAg_j \in ARB_i \\ \text{else} \\ \frac{TotalNumResources}{2 * (\max\ stim - 1)} & \end{cases}$$

Third, are the uses of an average stimulation threshold as a criterion for determining when to stop training on Abnormal Agent.

$$ARB_{remove.resource} = \begin{cases} \arg\ min\ ARB \in ARB_i (AbAg.stim) & NumResAllow < reAlloc > NumResRemove \\ \text{else} \\ ARB_{remove.resource} - NumResRemove & \end{cases}$$

Once candidate memory Agent is generated for addition into set of training set, one Abnormal Agent training is completed and the next Abnormal Agent is selected for the healing process.

Step 12: All the healing process of the individual Abnormal Agent is completed in the ARB population. Fitness, Danger Signal and concentration of population fixed by state awareness that is fitness rechecked with the network by the newly generated Agent are calculated.

$$Resiliency\ rate = \frac{Average\ Cost\ in\ each\ iteration}{rate\ of\ occurrence\ of\ fluctuation}$$

This achieves resiliency.

V.SIMULATION RESULTS

Cyber-Road traffic system infrastructure contains a large number of sensors and actuator device with wireless communication and computation, with limited constrain like battery power, sensitivity, time delay, heterogeneous and federated diversity working environment effect of large scale. The state of these compounds is monitored by deploying large scale Software entity called Multi Agent System and it maintain its state through proposed biological inspire Algorithm.

TABLE IV
SUMMARY OF COMPOUND IN CYBER-ROAD TRAFFIC CONTROL SYSTEM[28]

Communication Mode	Representative Standards	Representative Applications
In-Vehicle	SAE J1760, SAE J2366/x, SAE J2395	Data Collection and Information Display
Vehicle-to-vehicle	IEEE 802.11P, IEEE 1609.x, SAE J2735	Cooperative Collision avoidance
Vehicle to Infrastructure	ASTME2213, IEEE802.11P, IEEE 1609 x, SAE J2735	Road hazard alert Traveler Information
Center-to-Field	NTCIP	Traffic Management
Center-to-center	IEEE 1512.x TMDD	Emergency management, Traffic Management

Test Data Set

The Random number dataset is taken to demonstrate propose an algorithm depends on the general characteristics of cyber-road traffic control infrastructure used in each layer . The dataset contains signal of each layer, is a measure of monitoring system’s status with certain time periods. This is maintained with corresponding Agent. This Agent acts as system state to maintain agent concentration, using the methodology, dendritic cell and if any variation with specified threshold semi-mature and mature state, trigger healing module, this healing module uses Artificial Immune Recognition 2 concept for its process, then it terms Artificial Immune Network which acts as resiliency in cyber-Road Traffic control system.

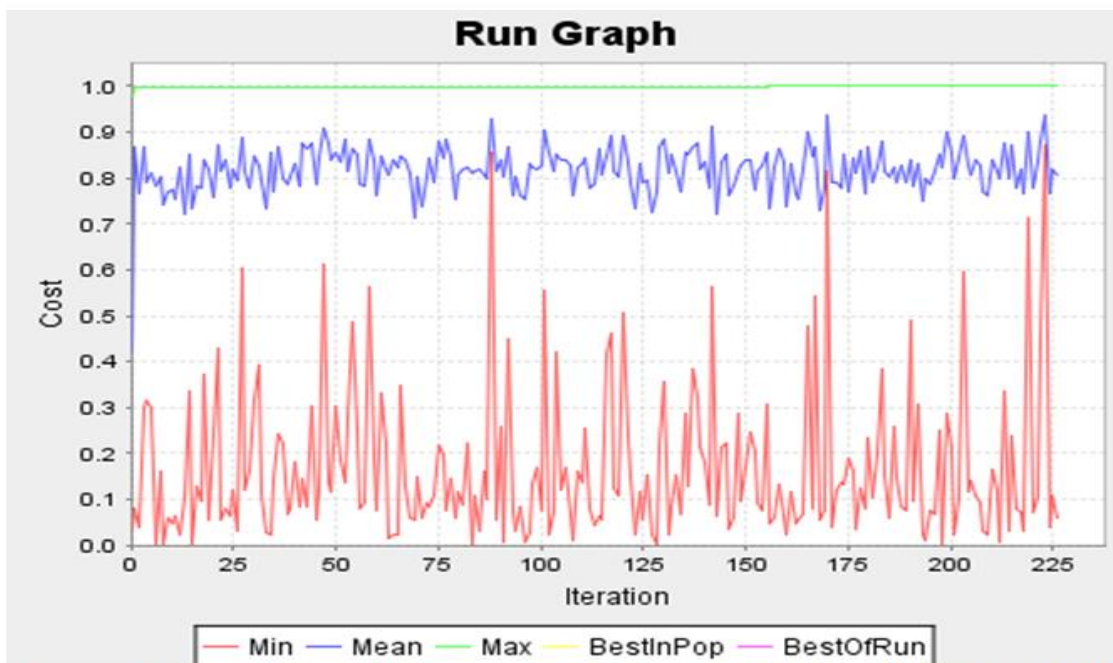


Fig. 5. Shows dynamic threshold change for each state green line indicate threshold of danger state with cost of 12.4. Blue line indicates PAMP signal with its threshold with cost 7.6 and Red line indicate initial danger signal trigger form Safe signal with cost of 2.

The Graph shows iteration 84, 170, 223 triggers healing process. Between this iteration, 19 times cost occurs in 84th iteration defines resiliency rate. Similarly 14 times cost occurs at 170th iteration and 13 times cost occurs at 223rd iteration. That shows that number of iteration at run time reduce occurrence of even is reducing. Indicates the cost of the healing process is less compared to the consequent iteration. This defines the resiliency activity in the Multi Agent system.

Results Discussion

The Table 3 and 4 show results with different population in each layer. Corresponding threshold as 0.34, 0.39, 0.28, 0.32, 0.4, 0.45 shown in table 4 above this threshold is considered as Semi-Mature State. Mature state threshold 0.77, 0.8, 0.69, 0.7, 0.8, 0.89 as an initial threshold to identify abnormal. Healing Participated percentage of agent should create a memory agent for semi mature state as 98, 195, 149, 244, 198, 299 and mature state as 96, 194, 145, 246, 197, 297 similar calculations and analysis for different number of agent population and corresponding results are in the table 5 and table 6 for each state of the population.

TABLE V MATURE STATE AND HEALING PROCESS FOR RESILIENCY IN CYBER-ROAD TRAFFIC AGENT SYSTEM

CPS Layer	Test Case No.	Agent Population	State of Population of Agent		Anomaly MACV	Normal MACV	Memory Agent ARB _{Agent}	State awareness			Healing process			Resiliency rate Avg. cost/ rate of fitness
			Semi Mature State Threshold PAMP Signal	Mature State Threshold				fitness			cost			
Monitor As In-Vehicle and Actuator As Vehicle – Infrastructure	1	100	0.77	0.98	0.9	0.1	96	83	79	50	0.33	0.31	0.24	0.058
	2	200	0.8	0.99	0.93	0.07	194	88	90	57	0.35	0.32	0.25	0.059
Communication As Centre – Field	1	150	0.69	0.82	0.92	0.08	145	87	87	55	0.34	0.31	0.23	0.057
	2	250	0.7	0.89	0.91	0.09	246	89	91	60	0.39	0.35	0.27	0.060
Computation And Control Unit As Centre – Centre	1	200	0.8	0.89	0.92	0.08	197	87	92	60	0.39	0.35	0.27	0.063
	2	300	0.89	0.9	0.94	0.08	297	91	94	64	0.4	0.36	0.28	0.066

TABLE VI SEMI MATURE AND HEALING PROCESS TOWARDS RESILIENCY IN CYBER-ROAD TRAFFIC AGENT SYSTEM

CPS Layer	Test Case No.	Agent Population	State of Population of Agent		Anomaly MACV	Normal MACV	Memory Agent ARB _{Agent}	State awareness			Healing process			Resiliency rate Avg. cost/ rate of fitness
			Initial Threshold Safe Signal	Semi Mature State Threshold PAMP Signal				fitness			cost			
Monitor As In-Vehicle and Actuator As Vehicle – Infrastructure	1	100	0.34	0.76	0.89	0.11	98	84	80	53	0.34	0.32	0.25	0.059
	2	200	0.39	0.79	0.91	0.09	195	89	91	58	0.35	0.33	0.26	0.06
Communication As Centre – Field	1	150	0.28	0.67	0.78	0.22	149	88	89	56	0.33	0.32	0.24	0.058
	2	250	0.32	0.68	0.87	0.13	244	90	92	61	0.38	0.36	0.28	0.061
Computation And Control Unit As Centre – Centre	1	200	0.4	0.78	0.76	0.24	198	88	91	59	0.38	0.36	0.28	0.064
	2	300	0.45	0.8	0.79	0.21	299	92	93	63	0.39	0.37	0.29	0.067

VI. CONCLUSION

The paper objective to show, how biological inspired methodologies are applicable in resiliency development to heterogeneous, federated application. This is modelled with Multi Agent Paradigm and shown in cyber-physical system. Artificial Immune Network is modified with dendritic cell and Artificial Recognition towards state awareness and healing process as resiliency development is shown to algorithmic work. This algorithm is simulated and results are discussed. In this paper the resiliency development is demonstrated on generic algorithm and framework, their is a scope of real world application to further validate, the results discussed in this paper.

REFERENCES

[1] Liviu, Sanislav, T. (2011). About Dependability in Cyber-Physical System. IEEE Conference Publications, 17-21.
 Lee E.(2008). Cyber Physical Systems: Design Challenges. University of California, Berkeley Technical Report. No. UCB/EECS-2008-8.
 [2] Sycara, Katia, et al. "Distributed intelligent agents." IEEE Intelligent Systems 6 (1996): 36-46.
 [3] Lokesh. M. R, Y.S. Kumaraswamy "Modified Danger Theory based Optimized Artificial Immune Network on Resiliency in Cyber-Physical System "IEEE Part Number: CFP15C35-USB IEEE ISBN: 978-1-4673-7909-0, International Conference on Green Computing and Internet of Things (ICGCIoT 2015) 8-10 oct 2015
 [4] Ishida, Yoshiteru. Immunity-based systems: a design perspective. Springer Science & Business Media, 2004.
 [5] Lokesh. M. R, Y.S. Kumaraswamy Nov 2014 "On Autonomic Self Healing Architecture for Resiliency in Cyber Physical System" International Journal of Multimedia and Ubiquitous Engineering ISSN No. 1975-0080 Volume 9, No. 11, Nov 2014
 [6] Work, D., and A. Bayen, 2008, Impacts of the mobile internet on transportation cyberphysical systems: traffic monitoring using smartphones, In National Workshop for Research on High-Confidence Transportation CyberPhysical Systems: Automotive, Aviation, & Rail, pp. 1820.
 [7] F. Y. Wang, "Agent-based control for networked traffic management systems," IEEE Intell. Syst., vol. 20, no. 5, pp. 92–96, Sep./Oct. 2005.
 [8] F. Y. Wang, "Toward a revolution in transportation operations: AI for complex systems," IEEE Intell. Syst., vol. 23, no. 6, pp.

- 8–13, Nov./Dec. 2005
- [9] Shi, J. (2009). "Principles of traffic behavior control". Beijing: China Communications press, 54-58.
- [10] Shi Jianjuna,*, Wu Xub, Guan Jizhenc, Chen Yangzhoua "The analysis of traffic control cyber-physical systems" 13th COTA International Conference of Transportation Professionals (CICTP 2013) pp 1877-0428
- [11] Zhou, Jianhe, Chungui Li, and Zengfang Zhang, 2011, Intelligent transportation system based on SIP/ZigBee architecture." In Image Analysis and Signal Processing (IASP), 2011 IEEE International Conference on, pp. 405409.
- [12] Li, Xu, Wei Shu, Ming-Lu Li, and Min-You Wu, 2008, Vehicle-based Sensor Networks for Traffic Monitoring." In Proc. of 17th IEEE International Conference on Computer Communications and Networks.
- [13] Mundra, Ankit, et al. "Transport Information System using Query Centric Cyber Physical Systems (QCPS)." arXiv preprint arXiv:1401.3623 (2014).
- [14] Q. Zhu, "Game-Theoretic Methods for Security and Resilience in Cyber-Physical Systems", PhD thesis (2013).
- [15] M. Mahmoud Mahmoud Azab, "Cooperative Autonomous Resilient Defense Platform for Cyber-Physical Systems", PhD thesis, (2013) January.
- [16] I. Hong, H. Youn, I. Chun and E. Lee, "Autonomic Computing Framework for Cyber-Physical Systems", Proc. of Int. Conf. on Advances in Computing, Control, and Telecommunication Technologies, (2011).
- [17] A. Jones, M. Merabti and M. Randles "Resilience Framework for Critical Infrastructure Using Autonomics", International Journal of computer Applications, (2012).
- [18] John A. Volpe National Transportation Systems Center "Intelligent Transportation Systems (ITS) Standards Program Strategic Plan for 2011 —2014" Noblis, Inc., with cooperation from the USDOT's
- [19] J. Greensmith, "Dendritic Cell Algorithm", Ph.D. Thesis, The University of Nottingham, (2007).
- [20] Andrew Watkins and Jon Timmis, Lois Boggess" Artificial Immune Recognition System (AIRS): An Immune Inspired Supervised Learning Algorithm" Kluwer Academic Publishers. Printed in the Netherlands 2003
- [22] Lokesh. M. R, Y.S. Kumaraswamy "Demonstration of Inner State Awareness and Outer Self Healing Closed Feedback Loop for Resiliency in Traffic Control Cyber-Physical System", International Journal of Applied Engineering Research (IJAER) Print ISSN 0973-4562 ,2014

BIOMETRICS BASED USER AUTHENTICATION

Tanuj Tiwari¹, Tanya Tiwari² and Sanjay Tiwari³

Maheshwari Public School, Kota (Raj), India

¹Department of Electrical & Electronics Engg, Birla Institute of Science & Technology, Pilani (Raj), India
²S.O.S. in Electronics & Photonics, Pt. Ravishankar Shukla University, Raipur (C.G.), India

Abstract : *Biometrics is automated methods of recognizing a person based on a physiological or behavioral characteristic. Biometrics technologies are base for a plethora of highly secure identification and personal verification solutions. It is measurement of biological characteristics – either physiological or behavioral – that verify the claimed identity of an individual. Physiological biometrics include fingerprints, iris recognition, voice verification, retina recognition, palm vein patterns, finger vein patterns, hand geometry and DNA. But there arises a need for more robust systems in order to tackle the increasing incidents of security breaches and frauds. So there is always a need for fool proof technology that can provide security and safety to individuals and the transactions that the individuals make. Biometrics is increasingly used by organizations to verify identities, but coupled with quantum cryptography it offers a new range of security benefits with quantum cryptography where we form a key when we need it and then destroy it. In this paper, we give a brief overview of the field of biometrics and summarize some of its advantages, disadvantages, strengths, limitations, and related privacy concerns.*

Keywords: *Biometrics, identification, multimodal biometrics, recognition, verification, security*

I. Introduction

Reliable user identification is increasingly becoming important in the Web enabled world today and there has been a significant surge in the use of biometrics for user identification. Many corporate heads use laptops and personal digital assistants (PDAs) loaded with sensitive business and personal information. Over 250,000 mobile gadgets are lost or stolen every year, and only 25-30 per cent of these ever make it back to their rightful owners. Such mishaps have created a dire need to ensure denial of access to classified data by unauthorized persons.

Therefore various aspects of everyday life are gradually being digitized as our life experiences and creative efforts are accumulated in personal computers, digital media devices, and mobile devices. People use passwords and other authentication methods to protect these collections of personal and potentially confidential information. Business organizations have been highlighting the importance of ascertaining a user's identity before permitting access to confidential information. Traditional confidentiality and authentication methods (e.g., personal passwords) are less than secure. In addition to requiring the user to remember a variety of passwords, which can result in user error, passwords can be stolen and pure password authentication is vulnerable to unauthorized breach. In a race to improve security infrastructures faster than hackers and stealers can invent to penetrate passwords and firewalls, new technologies are being evaluated to confirm or deny user authentication.

Given the pervasive use of passwords and identification codes for user authentication across all aspects of our daily life, attackers have developed powerful password cracking codes. However, these problems can be resolved through the use of “physiological passwords” through unique personal biometric identification methods such as recognition of the user's face, fingerprints, personal signature, or iris, which are very difficult to either replicate or steal.

Any human physiological and/or behavioral characteristic can be used as a biometric characteristic as long as it satisfies the following requirements:

- *Universality:* each person should have the characteristic.
- *Distinctiveness:* any two persons should be sufficiently different in terms of the characteristic.

- *Permanence*: the characteristic should be sufficiently invariant (with respect to the matching criterion) over a period of time.
 - *Collectability*: the characteristic can be measured quantitatively.
- A practical biometric system should meet the specified recognition accuracy, speed, and resource requirements, be harmless to the users, be accepted by the intended population, and be sufficiently robust to various fraudulent methods and attacks to the system.

Biometrics modes of identification have been found to be the most compelling and intriguing authentication technique. Biometrics are automated methods of recognizing a person based on his physiological or behavioral characteristics. Tokens can be lost, stolen or duplicated and passwords can be forgotten or shared. However, biometrics can authenticate you as you.

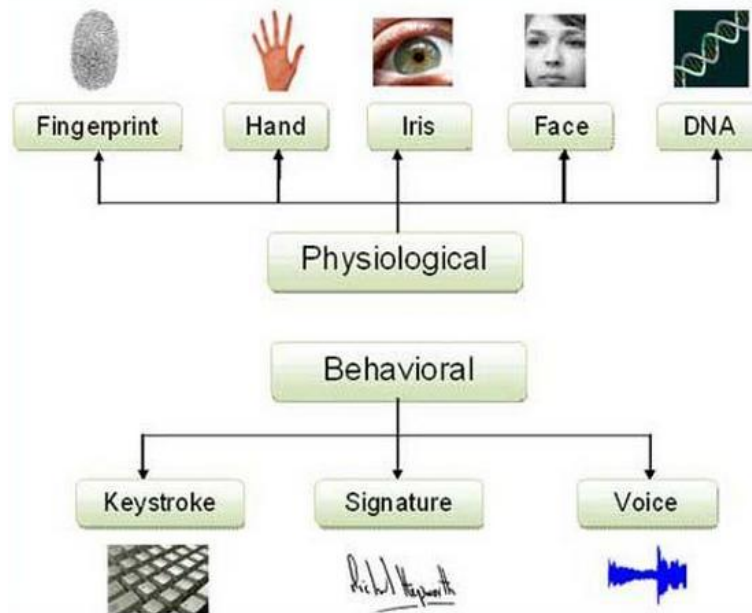


Fig.1 Classification of Biometrics

Biometrics is a means of using parts of the human body as a kind of permanent password. Just as your fingerprints are unlike those of any other person, your eyes, ears, hands, voice, and face are also unique. Technology has advanced to the point where computer systems can record and recognize the patterns, hand shapes, ear lobe contours, and a host of other physical characteristics. Using this biometrics, laptop and other portable devices can be empowered with the ability to instantly verify your identity and deny access to everybody else. It is fundamentally a pattern recognition system that recognizes a person by determining the authentication by using his different biological features i.e. Fingerprint, retina-scan, iris scan, hand geometry, and face recognition are leading physiological biometrics and behavioral characteristic are Voice recognition, keystroke-scan, and signature-scan[1-8].



Year	Biometrics	Description
1960	Face	First semi-automatic system for face recognition.
1965	Signature	First project on automatic signature recognition.
1969	Fingerprint	First proposal for fingerprint automatic identification by the FBI.
1970	Face	Further achievements for automatic face recognition.
1974	Hand Geometry	First commercial hand geometry system becomes available.
1976	Voice	First prototype of a speaker recognition system is released.
1977	Signature	Patent awarded for live signature acquisition.
1985	Hand Geometry	Patent for the proposal of hand-based identification is awarded.
1986	Fingerprint	Standard for the exchange of fingerprint minutiae is released.
1986	Iris	Patent for the proposal of iris-based identification is awarded.
1988	Face	Techniques for automatic face recognition are proposed.
1991	Face	Real-time face recognition becomes feasible.
1994	Iris	First Iris identification system is patented.
1998	DNA	DNA indexing system is released by the FBI.
1999	Fingerprint	FBI released the first automated fingerprint identification system.
2000->	Multibiometrics	New biometric systems have been released and more recent techniques combine different biometric traits.

Fig 2 Biometrics traits and history of biometric technology.

II. Principle of working

Once identified, the physical characteristics can be exactly measured and analysed. The statistical use of the characteristic variations in unique elements of living organisms is known as biometrics. Biometrics data of human beings can be collected and analysed in a number of ways, and has been introduced as a mode of personal identification. Biometric systems automatically verify or recognise the identity of a living person based on physiological or behavioural characteristics. Physiological characteristics pertain to visible parts of the human body. These include fingerprint, retina, palm geometry, iris, facial structure, etc. Behavioural characteristics are based on what a person does. These include voice prints, signatures, typing patterns, key-stroke pattern, gait, and so on. A variety of factors, such as mood, stress, fatigue, and how long ago you woke up, can affect behavioural characteristics.

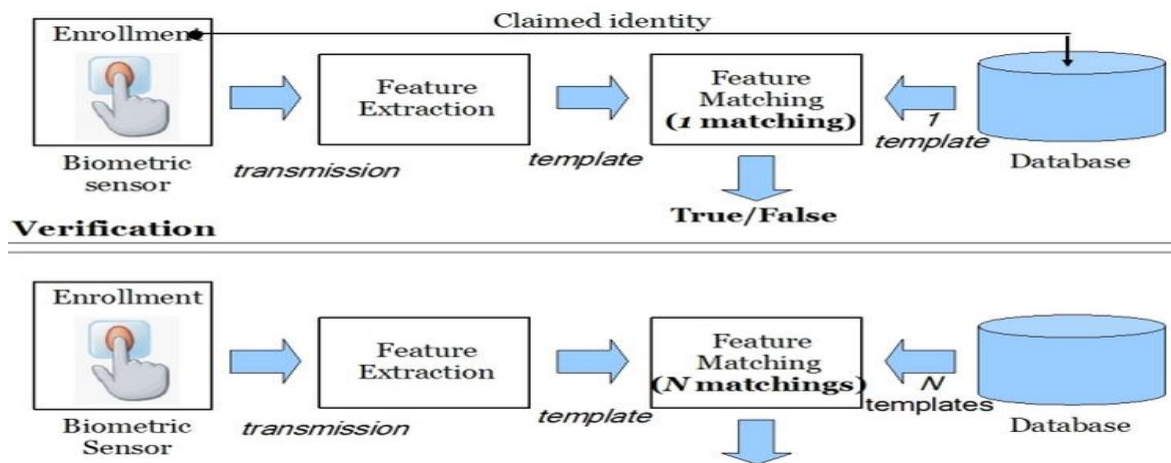
Voice print is a fine series of spectral power density plots that depict how the energy in one's voice at different frequencies varies with time as one vocalises a word or phrase. Voice experts say that sufficient characteristics of one's voice print remain constant under all circumstances, enabling these plots to reliably verify one's identity while physiological traits are usually more stable than behavioural traits, systems incorporating them are typically more intrusive and more expensive to implement

A biometric system can be either an 'identification' system or a 'verification' (authentication) system, which are defined below.

Identification - One to Many: Biometrics can be used to determine a person's identity even without his knowledge or consent. For example, scanning a crowd with a camera and using face recognition technology, one can determine matches against known database.

Verification - One to One: Biometrics can also be used to verify a person's identity. For example, one can grant physical access to a secure area in a building by using finger scans or can grant access to a bank account at an ATM by using retinal scan.

Biometric authentication requires to compare a registered or enrolled biometric sample (biometric template or identifier) against a newly captured biometric sample (for example, the one captured during a login). This is a three-step process (Capture, Process, Enroll) followed by a Verification or Identification process.



Identification

Fig. 3 Block diagrams of enrollment, verification, and identification tasks are shown using the four main modules of a biometric system, i.e., sensor, feature extraction, matcher, and system database.

During Capture process, raw biometric is captured by a sensing device such as a fingerprint scanner or video camera. The second phase of processing is to extract the distinguishing characteristics from the raw biometric sample and convert into a processed biometric identifier record (sometimes called biometric sample or biometric template). Next phase does the process of enrollment. Here the processed sample (a mathematical representation of the biometric - not the original biometric sample) is stored / registered in a storage medium for future comparison during an authentication. In many commercial applications, there is a need to store the processed biometric sample only. The original biometric sample cannot be reconstructed from this identifier.

III. Advantages of Biometric Technology

Using biometrics for identifying and authenticating human beings offers unique advantages over traditional methods. Tokens, such as smart cards, magnetic stripe cards, and physical keys can be lost, stolen, or duplicated. Passwords can be forgotten, shared, or unintentionally observed by a third party. Forgotten passwords and lost smart cards are a nuisance for users and waste the expensive time of system administrators. In biometrics the concerned person himself is the password, as biometrics authentication is based on the identification of an intrinsic part of a human being. The biometrics technique can be integrated into applications that require security, access control, and identification or verification of users. Biometrically secured resources effectively eliminate risks, while at the same time offering a high level of security and convenience to both the users and the administrators.

Methods	Description
Face	This method involves analyzing facial characteristics such as the measure of the overall facial structure, including distances between eyes, nose, mouth, and jaw edges.
Fingerprint	This method looks at the patterns found on a fingertip. Patterns are made by the lines on the tip of the finger.
Hand geometry	This method involves analyzing and measuring the shape of a hand.
Iris	This method involves analyzing features found in the colored ring of tissue surrounded the pupil.
Retina	This method involves analyzing the layer of blood vessels situated at the back of the eye.
Vascular Patterns	Vascular patterns are best described as a picture of the veins in a person's hand or face. The thickness and location of these veins are believed to be unique enough to an individual to be used to verify a person's identity.
Voice	This method does not involve the recognition of the user voice, but to convert the voice of the user to text for authentication purposes.
Signature	This method analyzes the way the user signs his/her name, recording signature characteristics such as stroke order, speed, and pressure.



Fig.4. Pattern matching

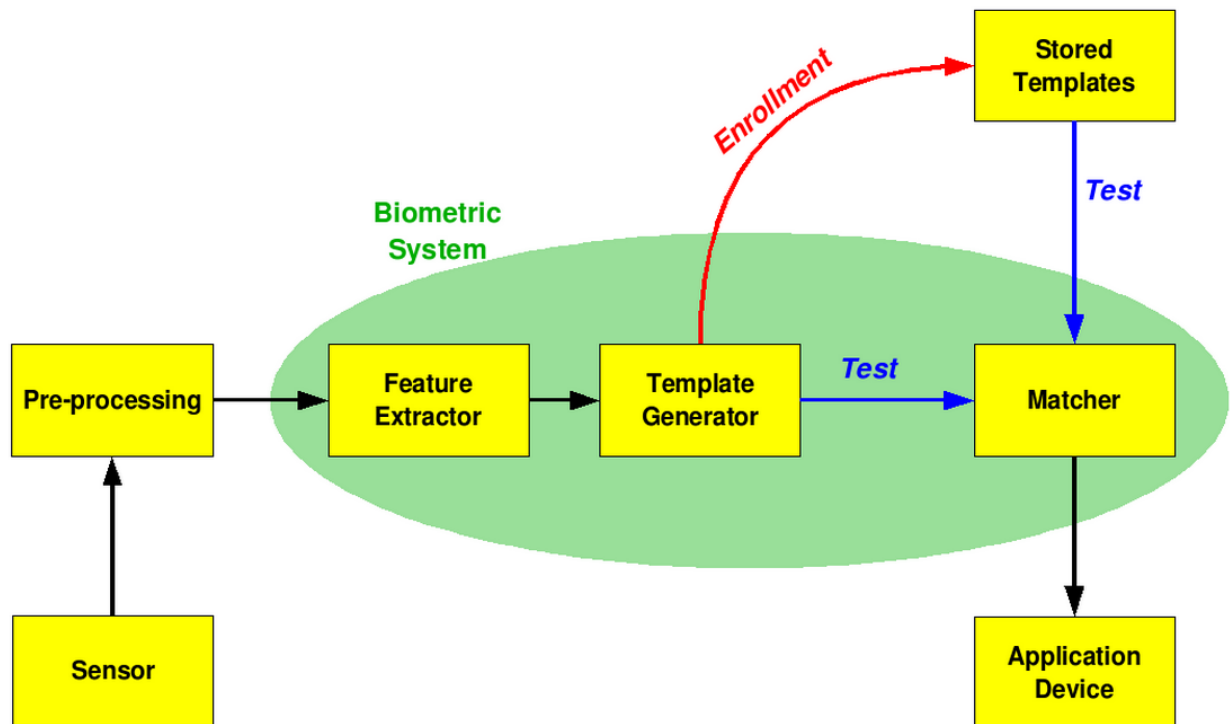


Fig.5 Working of Biometric system

IV. Applications in use

Biometric systems have a powerful potential to provide security for a variety of applications, systems are nowadays being introduced in many applications and have already been deployed to protect personal computers, Banking machines, credit cards, electronic transactions, airports, high security institutions like nuclear facilities, Military Bases and other applications like borders control, access control, sensitive data protection and on-line tracking systems.

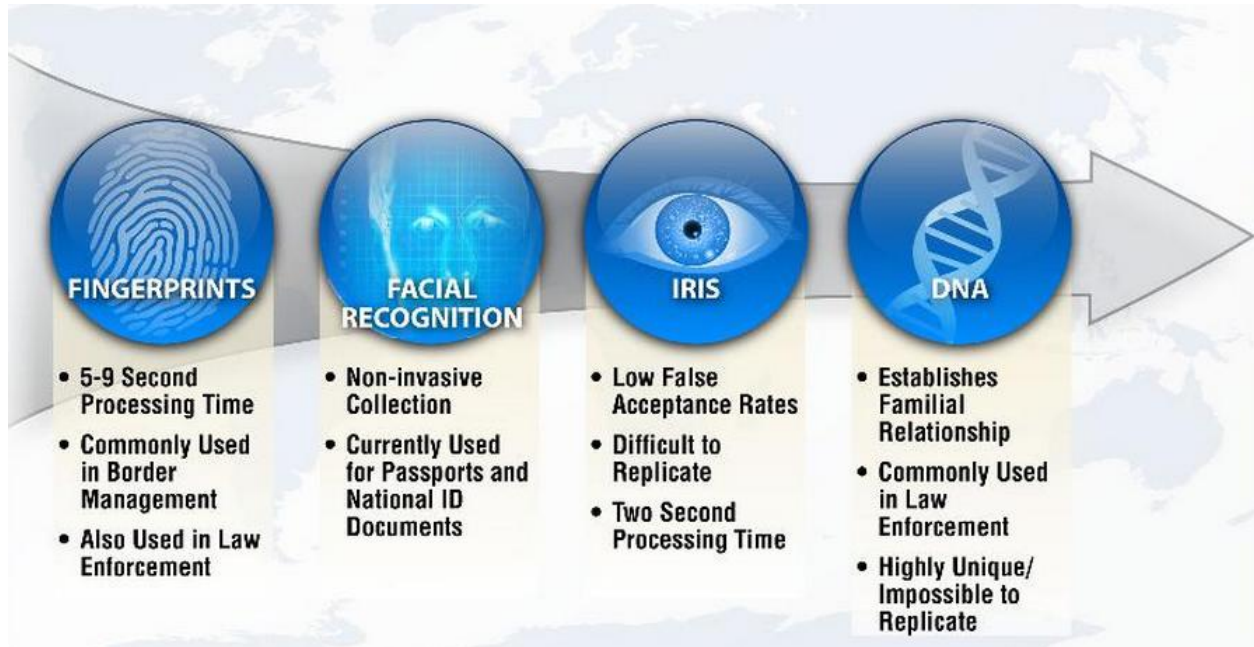


Fig.6 Biometric traits

Nationwide Building Society, the UK, has incorporated an iris recognition system at ATMs. A camera takes a digital record of each user's iris. The iris print is stored in a database to verify personal identity during transactions.

Biometric Comparison Chart						
Sr. No	Characteristics	Fingerprint	Iris	Face	Palm Print	Voice Recognition
1	Speed	Medium/Low	Medium	Medium	Medium	Medium
2	FTE Rate	Medium/Low	Low	Low	Low/Medium	Medium
3	Standards	High	Medium	High	High	Low
4	Uniqueness	High	High	Medium	High	Medium
5	Maturity	High	Medium	Medium	Medium	Low
6	Durability	High	High	Medium	High	Low
7	Invasiveness	High	Medium	Low	High	Low
8	Overtness	High	Medium	High	Low	Low
9	Range	Low	Low	Medium	Low	High
10	Template Size	Medium (250-1,000 bytes) (per finger)	Medium (688 bytes)	High (84-2,000 bytes)	Medium (250-1000 bytes)	High (1,500-3,000 bytes)
11	Age Range	High	High	High	High	Medium
12	Universality	High	Medium	High	High	High
13	Stability	High	High	Medium	High	Low
14	Skill	Medium	Medium	Low	High	Low
15	Accuracy	Medium-High	High	Medium	High	Low
16	Hygienic Level	Low	High	High	Low	High
17	Performance	High	High	Low	High	Low
18	Cost	Low	High	Low	High	Low

Iris recognition subsystem is also being incorporated into ATMs in Japan. Siemens Nixdorf, Germany, is incorporating facial recognition mode into ATM systems. Standard Bank, South Africa, scans the fingerprints of its customers, instead of using a personal identification number (PIN), when they wish to withdraw cash. Basically, the biometrics security technique acts as a front end to a system that requires precise identification before it can be accessed or used. The system could be a sliding door with electronic locking mechanisms, an

operating system (OS), or an application where individual users have their own rights and permissions. Imagine unlocking your house or withdrawing money from your bank with just a blink of an eye, a tap of your finger, or just showing your face. Kelly Gates of Iris Scan is developing an authentication system, wherein users only have to open their eyes and look towards the camera lens for a few seconds to be identified.

Keystroke biometrics provides a foolproof authentication solution. The gap between consecutive keystrokes when typing the access code and typing rhythm are unique to a user, so even if an unauthorized person discovers the access code, he can't access the system unless he knows the user's typing rhythm also.

A multi-application travel card would enable the holders to participate in various frequent flier and border control systems as well as pay for air ticket, hotel room, etc. all with one convenient token.

A biometric chip reader incorporated into a PC can facilitate secure Internet based online transactions. Applications that are being developed to accept biometric data include computer networks, cars, cellular phones, and hoards of other types of embedded systems. Biometrics could authenticate e-mail and other documents transmitted via computer networks.

In hospitals, biometric techniques could replace ID bracelets to establish patients' identities, for instance, during blood administration.

With existing voice-transmission technology, voice recognition biometric techniques can function over long distances using the ordinary telephone. A well conceived and properly implemented voice based security system could provide a greater safety to financial transactions conducted over the telephone.

Biometrics on the move

Immigration and naturalization passenger accelerated service systems (INP ASS) allow international airports to use hand geometry scanners to verify the identity of travelers. Airports are testing face recognition scanners to help weed out terrorists.

One of the most hotly pursued applications of biometrics is handheld. Researchers are working on means to integrate eye scanners, fingerprint readers, and voice recognition systems into mobile phones, PDAs, and laptops. Scanners are getting smaller, cheaper, and more accurate, and can be used in mobile gadgets without sprucing up the size, cost, and power consumption. Not only biometrics renders handheld and laptops worthless to would-be stealers, it could also eliminate fraudulent transactions. Mobile manufacturers and wireless operators are incorporating voice and fingerprint scanning techniques in their devices.

Voice is an obvious preference for mobile phones. Since it doesn't require any extra hardware in the device, it is naturally integrated into the way people use phones. All the processing is done on the mobile phone system that stores the reference voiceprints, which are as unique as a fingerprint, looking for particular patterns of tone, inflection, and behaviour in a voice. This ensures that a real person, not a tape recording, is on the line.

V. Characteristics of Biometric system

A number of biometric characteristics may be captured in the first phase of processing. However, automated capturing and automated comparison with previously stored data requires that the biometric characteristics satisfy the following characteristics:

1. **Universal:** Every person must possess the characteristic/attribute. The attribute must be one that is universal and seldom lost to accident or disease.
2. **Invariance of properties:** They should be constant over a long period of time. The attribute should not be subject to significant differences based on age either episodic or chronic disease.
3. **Measurability:** The properties should be suitable for capture without waiting time and must be easy to gather the attribute data passively.
4. **Singularity:** Each expression of the attribute must be unique to the individual. The characteristics should have sufficient unique properties to distinguish one person from any other. Height, weight, hair and eye color are all attributes that are unique assuming a particularly precise measure, but do not offer enough points of differentiation to be useful for more than categorizing.
5. **Acceptance:** The capturing should be possible in a way acceptable to a large percentage of the population. Excluded are particularly invasive technologies, i.e. technologies which require a part of the human body to be taken or which (apparently) impair the human body.
6. **Reducibility:** The captured data should be capable of being reduced to a file which is easy to handle.
7. **Reliability and tamper-resistance:** The attribute should be impractical to mask or manipulate. The process should ensure high reliability and reproducibility.
8. **Privacy:** The process should not violate the privacy of the person.
9. **Comparable:** Should be able to reduce the attribute to a state that makes it digitally comparable to others. The less probabilistic the matching involved, the more authoritative the identification.
10. **Inimitable:** The attribute must be irreproducible by other means. The less reproducible the attribute, the more likely it will be authoritative.

IV. The biometric model

A generic biometric model consists of five subsystems, namely, data collection, transmission, signal processing, decision making, and data storage. Data collection involves use of sensors to detect and measure an individual's physiological or behavioural characteristics.

The measured biometric must be unique and repeatable over multiple measurements. However, technical parameters of the sensor, as well as the ergonomics of the device and the manner in which the biometric characteristic is presented to effect the measurement, could eventually impact the outcome of the system. For instance, background noise and acoustics of the environment may impact a speech recognition system, while the pressure applied to a fingerprint scanner might also affect the data. The data collection subsystem most directly impacts the user. Sensor specifications determine the intrusiveness of the system. Intrusiveness is the degree to which the user feels that the measurement process violates his personal space, and is often correlated to how close the user has to be near the sensor. For instance, a retinal scan, which requires close proximity to the camera, is considered far more intrusive than a voice recognition system.

Not all biometric systems process and store data on the measuring device. Often measurement is made using a relatively simple device to a computer or server for processing and/or storage. Depending on the system, the data may be relatively large and thus would need to be compressed for quick transfer. The compression algorithm needs to be selected carefully, otherwise it may introduce some artifacts that could impact the decision process

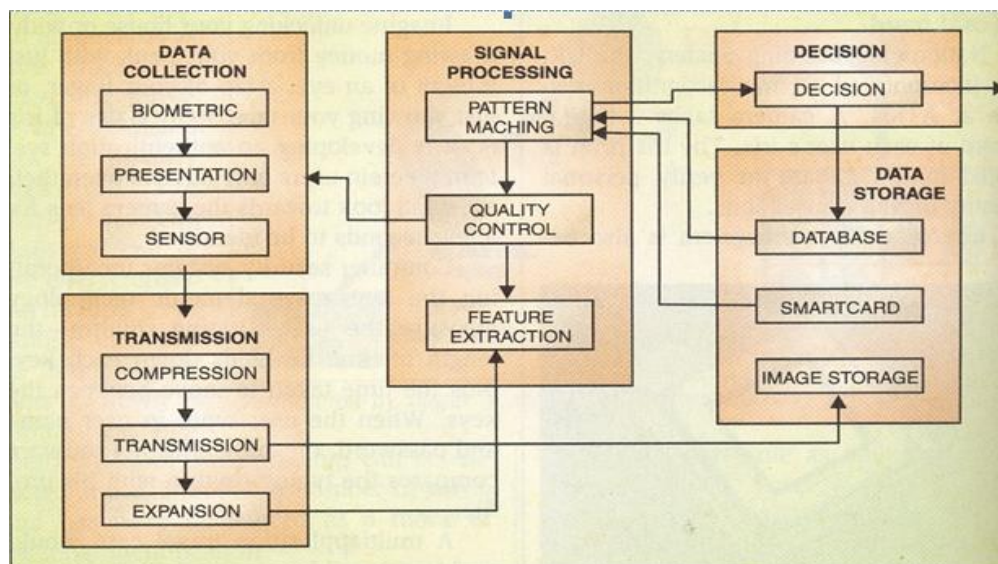


Fig. 7 Block diagram of a biometric model

In fingerprint scanning systems, wavelet scalar quantisation is often preferred to JPEG compression due to the blockings that the latter produces at high compression ratios. The data can also be transmitted to the database for storage as raw data. The signal processing subunit uses feature extraction algorithms to extract true biometric information from the sample in the presence of noise introduced during data collection and transmission. Additional measurements are made if any flaw or corruption is noted, to ensure good quality. Pattern matching involves comparing the feature sample to a stored sample. (Biometric data can be stored locally on the biometric device, some central database/ server, or on a smart card issued to users.) The result of comparison is sent to the decision system to determine the match. The decision subsystem uses statistical methods to confirm authentication if the variance between the sample and template data is within a certain threshold.

System quality The quality of a biometrics authentication algorithm is specified in terms of false rejection rate (FRR) and false acceptance rate (FAR). FRR indicates the percentage of instances an authorized individual is falsely rejected by the system. FAR states the percentage of instances an unauthorized individual is falsely accepted by the system. FRR and FAR are diametrically opposed, therefore increasing the FAR will lower the FRR, and vice-versa. FRRs and FARs can be adjusted according to the needs of a given security system.

The biometric system should be able to account for permanent/semi-permanent changes in authorized / unauthorized users. For instance, a user's biometric characteristics, even if these are physiological, can change over time. People can grow beards, injure their hands, change their accent become better typists, change their hairstyles, and so on. Robust biometric systems are able to meet these contingencies by slightly modifying the template for accepted authentication situations. The user's profile in the database adapts to changes in the user's biometric features.

VII. Vulnerability to attacks

Biometric systems, like all security systems, have vulnerabilities. This entry provides a survey of the many possible points of attack against traditional biometric systems [9-12]. Biometric system security is defined by its absence: a vulnerability in biometric security results in incorrect recognition or failure to correctly recognize individuals. This definition includes methods to falsely accept an individual (spoofing), to decrease overall system performance (denial of service), or to attack another system via leaked data (identity theft)[13-14]. In a biometrics based authentication system, there are five points vulnerable to attacks by invaders as shown in the figure 8.

Bio Enable Technologies, Pune, is a software company that develops biometric products to cater to the tough Indian working conditions and environments. The firm has developed intelligent biometric solutions for physical access control, banking transaction, timing, and attendance applications.

Bio Enable has introduced a fingerprint-based identification terminal for use in factories, defence installations, public Kiosks, offices, retail outlets, etc. The fingerprint system translates illuminated images of fingerprints into digital code. The digital code is subjected to system software code for verification/ authentication of requested users and enrollment/registration of new users' fingerprints.

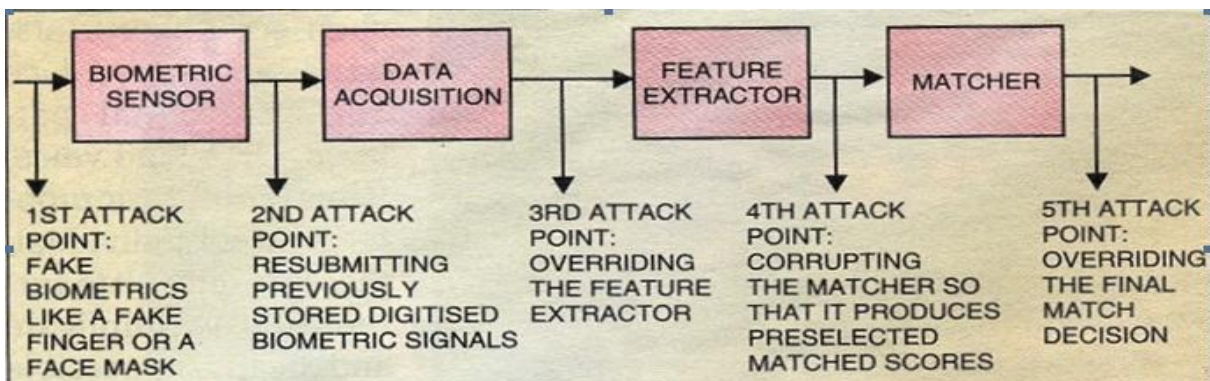


Fig.8 Five point vulnerable to attacks in biometric based authentication system

- > RBI wants multi-factor authentication for card transactions
- > Besides the card's presence and signature/PIN, it wants an additional fraud-proof feature
- > The security feature should be usable by customers who are only numerically literate

WHAT ARE THE CONCERNS?

- > Biometric authentication will push up hardware and telecom costs significantly
- > In fact, bankers say



machines will require 3G speeds to send scanned images for verification

- > Aadhaar itself has not yet been made mandatory

Fig.9 Looking for more security

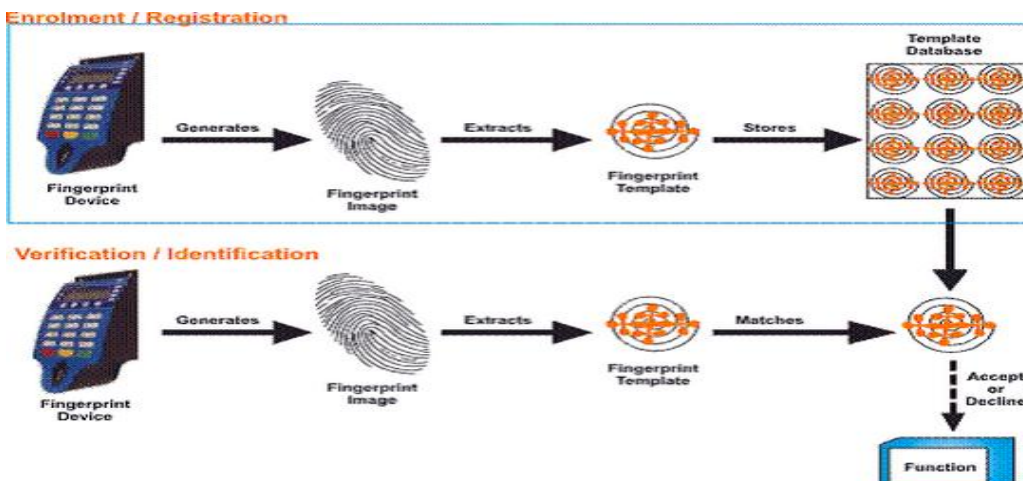


Fig.10 Bio enabled fingerprint recognition system

CMOS image sensors capture high-contrast, high-resolution fingerprint images that are virtually distortion-free. Powerful algorithms developed by Bio enabled extract minutiae data from the images to map the distinguished characteristics of fingerprint ridge ends, bifurcation, loops, splits, and upper and lower cores. The data is then converted into a template and stored in the database. To identify or verify, the algorithm compares the new template with the extracted minutiae points from the stored sample. The entire matching process takes roughly one second.

Siemens Information Systems Ltd (SISL), Bangalore, has developed a text independent autonomous speech recognition system to identify and authorize a speaker by analyzing his voice. Central Forensic Science Laboratories, Chandigarh, uses this system to track down and identify criminals by comparing their voice samples using SISL software.

Other innovations of SISL include fingerprint identification and management system (FIMS), language-independent speech recognition system, and optical character recognition system. SISL is developing low-cost chips that can be fitted into cars and toys. These chips will store fingerprint of the user and allow selective access to devices and homes.

Axis Software, Pune, deals in fingerprint, iris, and face recognition technology and is planning to add voice recognition technology to its range of authentication products and systems. The Axis system stores biometric records in an record by itself is of no use to a stealer and cannot be reconstructed to reveal , person's identity to someone else.

Biometric Society of India (INBIOS), affiliated to the International Society of Computational Biology (ISCB), provides innovative professional solutions and services dedicated to bioinformatics.

Global developments

Internet security. Litronix, USA, a leading provider of public key infrastructure (PKI)based Internet security solutions, has developed biometric identification techniques for use in electronic data applications such as digital networks and smart cards. Apart from iris, voice and handwritten signature recognition can be used for authentication purposes when digitally signing a document or obtaining access to secure WebPages. The smart card, integrating voice and handwritten functions, incorporates the appropriate biometric template to deliver the final match and authorization.

The company plans to incorporate capture, manipulation, enrollment, and extraction features in the smart card reader also.

Biometric smart cards. Polaroid and Atmel have developed secure identity cards that merge ultra-secure smart cards, fingerprint verification, biometric identification, and digital imaging. These cards will be used in e-commerce, online, remote access, and any IT environment where authentication is required.

The information stored in the card is protected by circuits inside the card that perform encryption/decryption of the data in the card. The tiny smart card circuits in these ID cards are actually integrated circuits, called smart card ICs, supplied by Atmel. Atmel's smart card ICs can perform critical encryption; decryption functions within the card and are able to securely identify the person or system reading the card.

Biometrics cellulars. Fujitsu Microelectronics has developed an innovative fingerprint identification system that combines sweep sensor technology with advanced algorithms to provide a powerful, dependable, easy-to-use authentication for PDAs, cell phones, and other mobile devices. The sensor measures just 1.28x0.20 cm and is powered by sophisticated algorithms that generate unique minutiae templates that correspond to specific fingerprint features. A single-fingerprint sweep across the sensor captures fingerprint features to rapidly authenticate users of cell phones and PDAs.

Cyber security. Cyber SIGN, USA, has built-in signature security management features of Adobe Acrobat 4.0 software. This software enables the handwritten signature to be included as an electronic signature in any Acrobat portable document format (PDF) file on the Web. Anyone can online use his handwritten signature to authorize and sign electronic Acrobat documents. Costs involved in businesses are reduced, as signed documents and forms are available online, and productivity and security are increased when vendors and suppliers can quickly access signed, secure, and trusted electronic documents.

8. Challenges for Biometrics

Imagine a world without keys, passwords, pins or passports, where you interact seamlessly with technology, where personalization is ubiquitous and devices recognise who you are in order to make life more convenient. And it is all implemented properly, with due consideration to privacy.

Customer behavior is changing with transactions moving more and more to the digital world. Fraud and cyber-attacks are on the increase which demand more controls to be put in place. User name and password are clearly outdated. Is this the right time to try to invest into making the customer journey more seamless? Where do biometrics fit in the future?

As usernames and passwords are so regularly compromised, we are rapidly moving to a new form of digital identity authentication. Digital signatures and sign-ons, enabled by mobile and biometrics, are becoming standard, but where does this take us in the longer term?

Identity management in government applications remains a popular topic and we will continue the debate from last year looking at different countries and how they address this issue – including an update on the use of biometrics in developing economies such as identity systems and voter registration

Privacy on trial! Customer authentication and identification are on the increase in the cyber world. We are being validated by people connected to us. We even are prepared to give up some privacy to receive certain benefits in return. “Selfies” are being advertised as the password for transactions on mobile devices but while this offers great convenience, are there any risks to be considered?

Biometric vulnerability assessments are now being recognised as an important part of the implementation of biometrics and the international standards community is also addressing presentation attacks. With a high demand of smaller and faster scanners for mobile devices, the question about vulnerability becomes even more important.

IX. Multibiometrics

Multibiometrics is a system, which implements two or more biometric systems and performs the function of verification or identification. For instance, mutibiometrics can combine fingerprint recognition and hand geometry with iris recognition and speaker verification to give foolproof identification. In fact, a multimodal biometric system has been introduced, which integrates face recognition, fingerprint recognition, and speaker verification in making a personal identification.

Multimodal Biometric Systems

Multimodal biometric systems are those that utilize more than one physiological or behavioral characteristic for enrollment, verification, or identification. In applications such as border entry/exit, access control, civil identification, and network security, multi-modal biometric systems are looked to as a means of

1. Reducing false non-match and false match rates,
2. Providing a secondary means of enrollment, verification, and identification if sufficient data cannot be acquired from a given biometric sample, and
3. Combating attempts to fool biometric systems through fraudulent data sources such as fake fingers.

A multimodal biometric verification system can be considered as a classical information fusion problem i.e. can be thought to combine evidence provided by different biometrics to improve the overall decision accuracy. Generally, multiple evidences can be integrated at one of the following three levels.

- Abstract level: The output from each module is only a set of possible labels without any confidence value associated with the labels; in this case a simple majority rule may be used to reach a more reliable decision.
- Rank level: The output from each module is a set of possible labels ranked by decreasing confidence values, but the confidence values themselves are not specified.
- Measurement level: the output from each module is a set of possible labels with associated confidence values; in this case, more accurate decisions can be made by integrating different confidence values.

X. Mobile Biometrics

MOBIO concept is to develop new mobile services secured by biometric authentication means. Scientific and technical objectives include robust-to-illumination face authentication, robust-to-noise speaker authentication, joint bi-modal authentication, model adaptation and scalability.

These days, portable personal devices such as PDAs or mobile phones are indeed widely used. They provide the mobile worker or the customer with portable computing and wireless access to Telecom networks and to the Internet. It is then possible to provide anywhere anytime a natural access to any service, such as PIN code replacement, phone card reloading, remote purchase, telephone banking or voice-mail. Most of these services involve micro payments that can currently be done only using PIN codes or passwords.

Efforts to develop and evaluate bi-modal (face and voice) biometric authentication (BMBA: Bi-modal biometric authentication) technologies in the context of portable and networked devices are in progress. Although biometric authentication is a complex problem, and is still not reliable enough to be widely accepted, it has also been shown that the use of multiple modalities increases the performance of biometric systems. However, most of the current multi-modal biometric systems simply perform fusion and do not actually take advantage of temporal correlations between modalities. As a matter of fact, very little work in the research community has been done on joint multi-modal fusion to perform joint authentication of several modalities (in our case face and voice).

XI. Social, Ethical, and Legal Issues

The success of a biometric-based identification system depends to a large extent on human itself. If a biometric system is able to measure the characteristic of an individual without contact, such as those using face, voice, or iris, it may be perceived to be more user-friendly and hygienic[15]. Biometrics, has various implications that have to be considered. Some of the social issues are that some people are wary of this new technology. The fear of having your personal belongings and data stolen (such as a car, banking accounts, assets, and even social

The improvement of voltage stability and reactive power compensation in the two-area system with PSS and FACTS-devices

Mohammad Niyazi¹, Ashkan Borji², Siroos Hemmati³

¹Tarah Energy Sepanta Consulting Engineering Company, Tehran, Iran

² Department of Electrical Engineering Kermanshah branch, Islamic Azad University, Kermanshah, Iran

³ Department of Electrical Engineering Kermanshah University of Technology, Kermanshah, Iran

ABSTRACT: In fact, The power system stability is the most important feature of the power system. This article discusses about successful application of FACTS-devices and PSS in transmission system. The purpose of using the FACTS-devices and PSS are the regulation of effective voltage and compensation of reactive power in particular system. Power systems are operated near the limits of their stability, for economic reasons. Keeping system stability and safe operation are very important. The shunt FACTS-devices have an important role in the stability, increasing of transmission capacity and damping the low frequency fluctuations. In this article FACTS-devices and PSS, a two-area power system have been used for improving of power system stability. For simulation of systems, MATLAB software, has been used.

Keywords -FACTS-devices , disturbance, power system stabilizer, compensator, two-area system

I. INTRODUCTION

In recent years, there has been a lot of demands on the power transmission network, and these demands are on the rise, because the number of units of generation and competition between them are increased. Also, the electric power systems is changing to reach flexibility, reliability, quick response and accuracy in the fields of generation, transmission, distribution and consumption. Reactive power control is an important factor in the design and operation of electric power systems. Reactive power compensators such (SVC) and (STATCOM) are devices that is used to improve voltage and control reactive power in AC systems. As well as increasing of the transmission capacity is a result of damping of power fluctuations. Power system stability is one of the most important aspects of the performance of electrical systems and should preserved the frequency and voltage under any disturbance including suddenly increment of load [1,2]. On the other hand, power system's stabilizer (additional excitation controller) is an auxiliary controller that, to improve the dynamic performance of power system by adding of auxiliary signals to excitation system. The effectiveness of this control method depend on the optimum point and selected proper signal in the power system[3]. In [4] , is examined the improvement of transient stability of two systems with different loading conditions. Flexible AC transmission power system(FACTS- devices) put in the middle of long transmission lines and designed the power system stabilizer for both generation units. That has an important role in the control of damping and distribution of reactive power in system. The analyzes of the performance of SVC and STATCOM with PSS, for improvement of dynamic behavior of the desired system is purpose in this study.

II. FACTS- DEVICES

The Improvement of power systems stability and also increasing of reliability of system is by the use of FACTS- devices [5]. However, the using of these devices, can improve the capacity of transitional power of lines . The devices used in this study are include SVC and STATCOM.

A) Static Var Compensator (SVC)

SVC can be used for setting of voltage profile and improvement of capacity of transmission line, and as well as setup itself with change of operation conditions of grid [6]. With proper control of equivalent reactance, is possible regulation of voltage amplitude. In simplest form, a TCR is parallel with the capacitor [7,8]. Figure 1 show a diagram of the SVC .

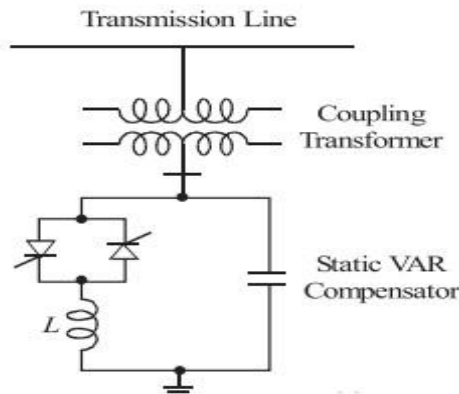


Fig 1.SVC connected to transmission line .

SVC can be operate in following two modes:

1. Voltage regulation mode
2. Reactive power control mode

V-I characteristic in one SVC is shown in figure 2.

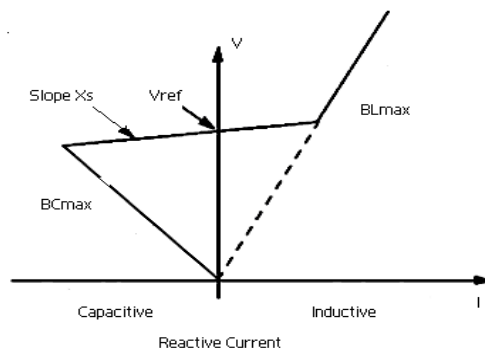


Fig 2. V-I characteristic in SVC

Since ,voltage unstable and even voltage collapse can be occur if reactive power balance are collide in the grid, Connect a SVC in a specific point of grid, to increase transmission capacity and improves dynamic stability of voltage, and preserves the voltage profile in different situations [9].

B) Static Synchronous Compensator (STATCOM)

STATCOM (static synchronous compensator) put on in parallel mode in the grid, and the most application of it is supply of voltage and reactive power. In other words, STATCOM works as a source of variable reactive power in a power system and with injection of reactive power, to prevent from voltage drop and also to increase transitional active power [10]. Figure 3 show v-1 characteristic in the STATCOM compensator [11] , and figure 4 show a schematic base diagram of one STATCOM.

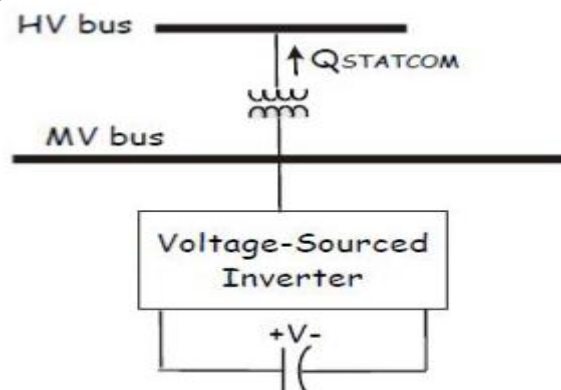


Fig 3.schematic base diagram of one STATCAM.

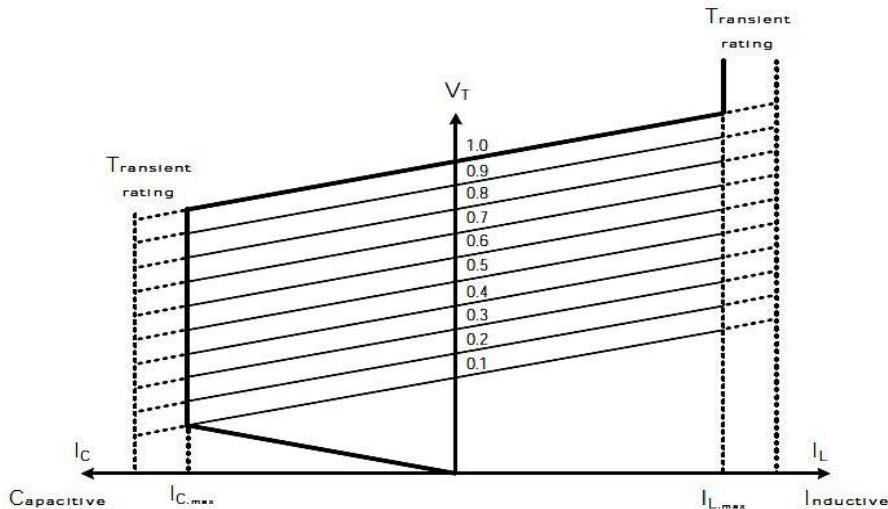


Fig 4. V-I characteristic in STATCOM compensator

In other words because this compensator is an important member of the family of FACTS- devices, has a capabilities such as damping of power fluctuations, improve of transient stability, voltage support and ... [12].

III. POWER SYSTEM STABILIZER (PSS)

Power system stabilizer , is the most economic method for attenuating of electromechanical fluctuations. PSS is the most original and the most widely used damping maker in power systems[13]. This stabilizer normally used from signals such as rotor speed , frequency and power of generator, and with to attenuate low frequency fluctuations puts the desirable impact on the small signal stability of system. PSS with the creation of the synchronizing and damping torque coefficients to improve the digression of rotor rotation. In fact,PSS to regulate and optimize the stimulation voltage with the creation of positive and negative voltage in the time needed [14] .figure 4 show a power system stabilizer model[15].

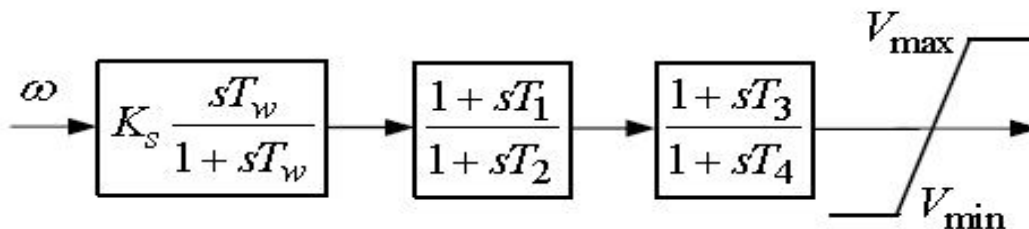


Fig 5. power system stabilizer

To get the proper functioning of stabilizer in a large range of frequencies, has been suggested The use of PSS with several frequency band, [16].

IV. SYSTEM MODELING

To show the improvement of voltage stability and compensation of reaction power by PSS and FACTS- devices that specified in this article, a two-area power system is used [4] . This model that consists of two generation units and a long transmission line, is showed in figure 6.

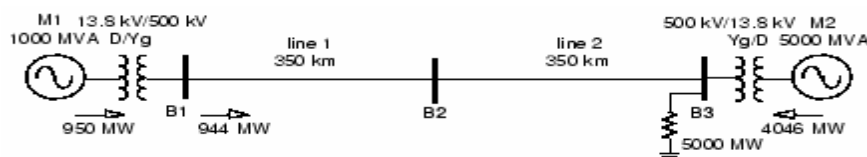


Fig 6. system under study

The second bus is considered as connect point of SVC and STATCOM. And both units to supply load. For both generation units, is designed power system stabilizer. For analyze of performance of these devices, was designed one short circuit disturbance in bus B1.

V. SIMULATION RESULT

According to figure 6, a disturbance occurs on the transmission line in B1. after it, system suffers of fluctuation and instability, and because of flowing of high current, the voltage of this bus is dropped, and also decrease reactive power, meanwhile, the instability to occur quickly. Figure7 show the effect of disturbance on the dynamic stability

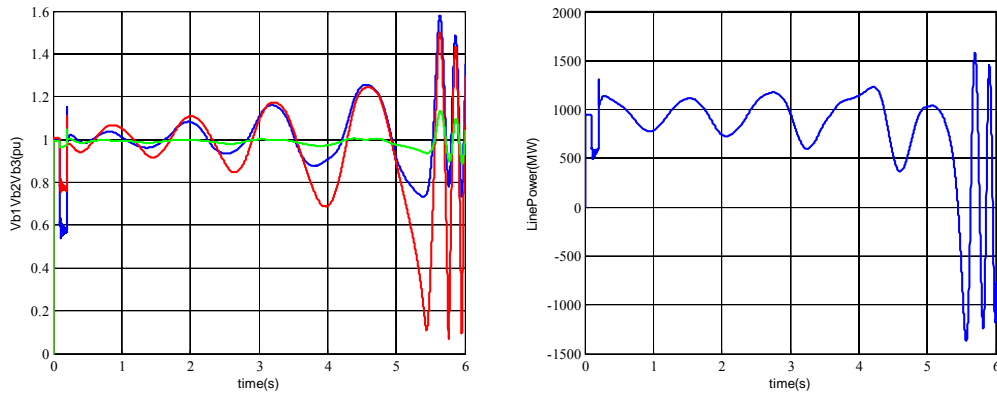


Fig 7.A: the effect of the disturbance on the system

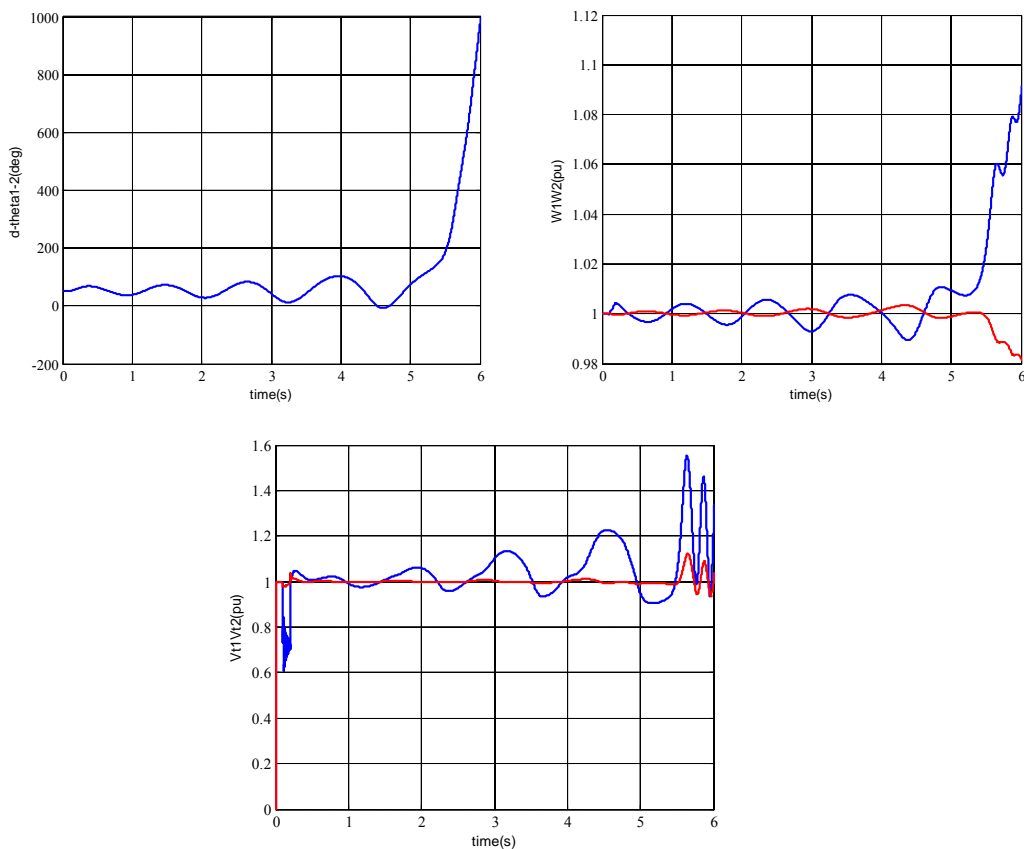


Fig 7.B:the effect of the disturbance on the machines

after analyze of grid with simultaneous placing of SVC in B2 and designing of PSS and simulation of this system, improvement of damping of voltage power fluctuations and also stability are observed. The results are in figure 8.

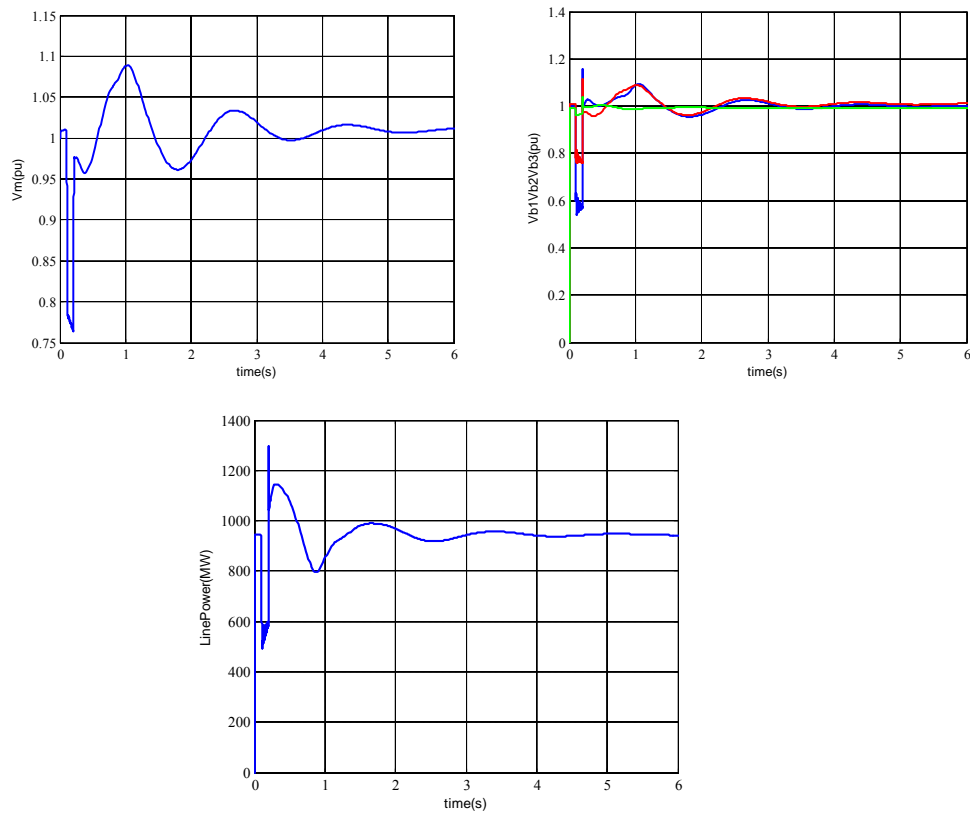


Fig 8.A:synchronous effect of PSS and SVC after disturbance,SVC compensator

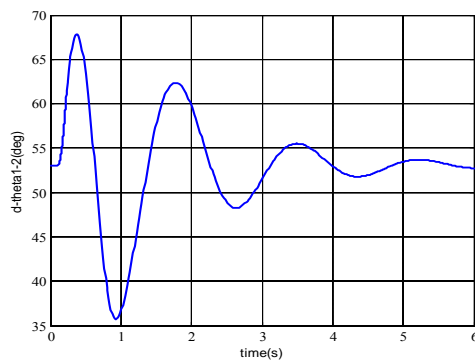


Fig 8.B:synchronous effect of PSS and SVC after disturbance,system

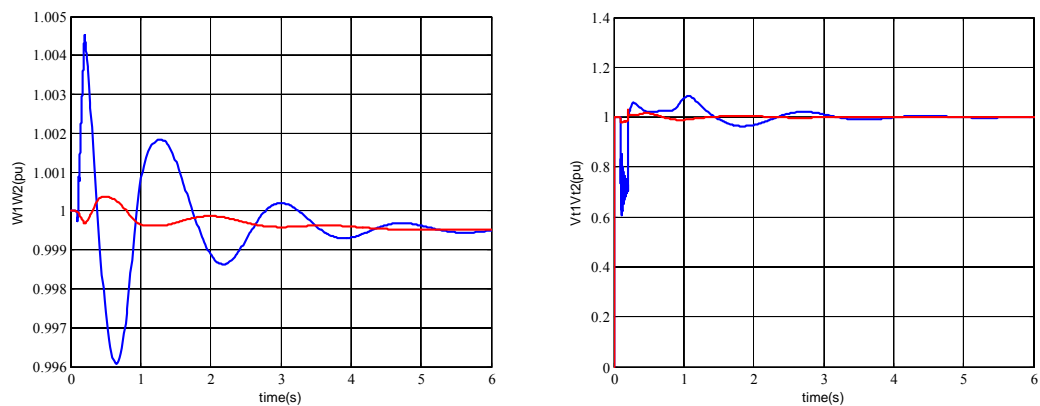


Fig 8.C:synchronous effect of PSS and SVC after disturbance,machines

Now, placing of STATCOM compensator instead of SVC in B2 and synchronous design of PSS, the results reviews after simulation; figure 9 show these results.

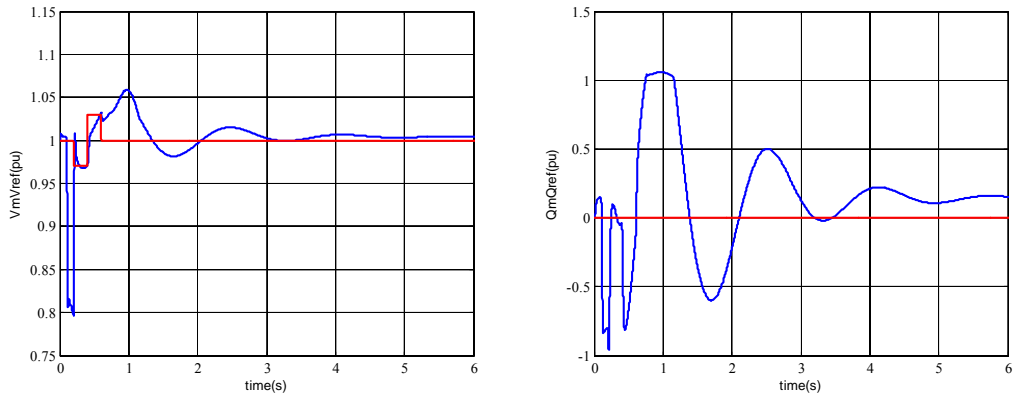


Fig 9.A:synchronous effect of PSS and STATCOM ,STATCOM compensator

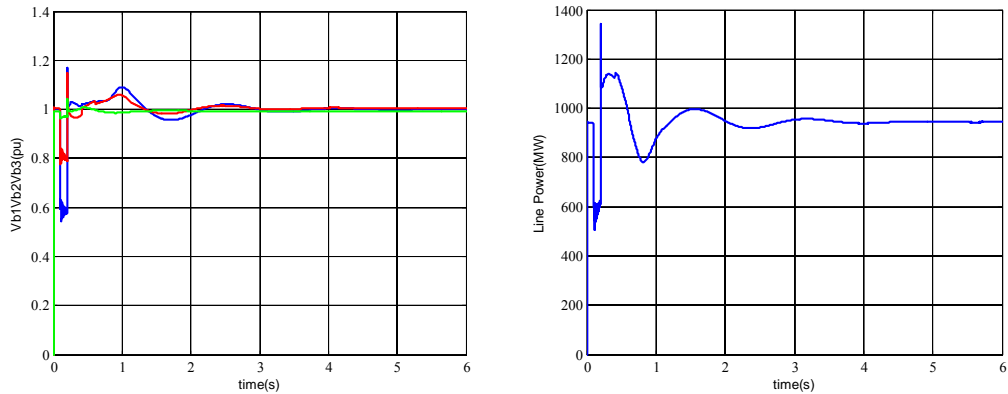


Fig 9.B:synchronous effect of PSS and STATCOM ,system

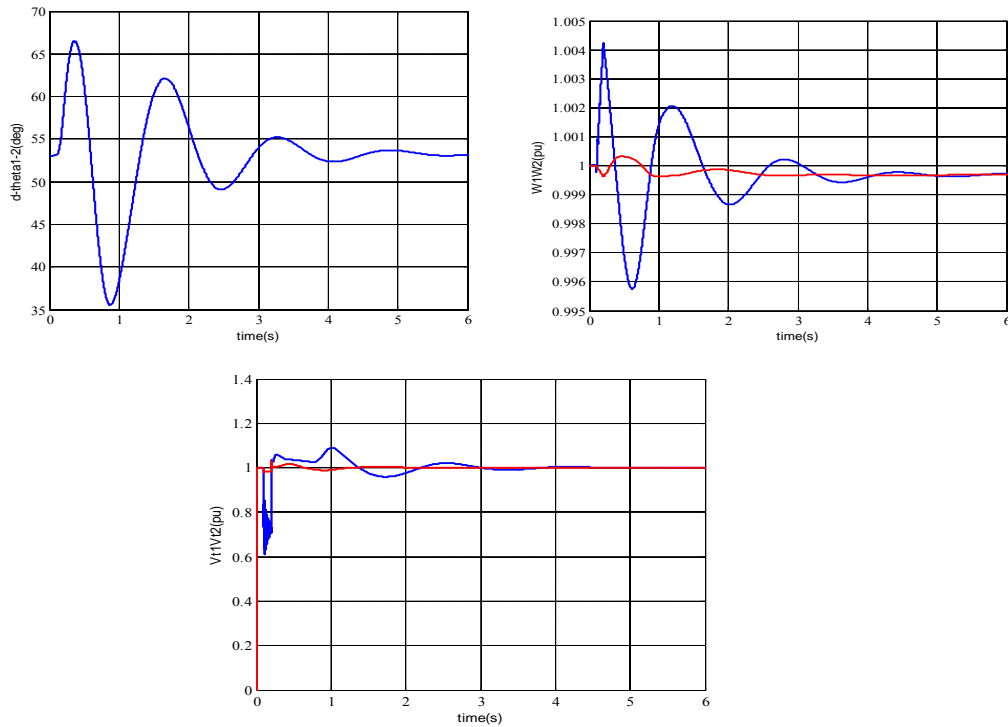


Fig 9.C:synchronous effect of PSS and STATCOM ,machines

VI. Conclusion

In this article, discussed the main of performance of svc and STATCOM to voltage control and design the PSS in particular system. That show PSS and FACTS-devices improve voltage stability and reactive power in power systems. In this study, a first state, synchronous effect PSS and svc and second state, synchronous effect PSS and STATCOM is analyzed and compared. The result of simulation show effective performance synchronous effect PSS and STATCOM to improve damping fluctuations and dynamic stability of the systems.

REFERENCES

- [1]. Al-Awami A. T. , Abdel-Magid Y. L. , Abido M. A. , 2007, "A particle-swarm-based approach of power system stability enhancement with unified power flow controller", Electric Power and Energy Systems, Vol. 29, pp. 251 – 259.
- [2]. Anderson P. M. , Fouad A. A. , 1977, "Power System Control and Stability", Ames, IA: Iowa State University . Press
- [3]. Atef Aly El-Emary, "Effect of static VAR compensator upon synchronizing Torque coefficient. " Electric Machines and Power Systems 25:371-386, 1977
- [4]. Virk, Pardeep Singh, and Vijay Kumar Garg. "Power System Stability Improvement of Long Transmission Line System by Using Static Var Compensator (SVC). "
- [5]. N. G. Hingorani and L. Gyugyi, "Understanding FACTS: Concepts and Technology of Flexible AC Transmission Systems", IEEE Press, New York, 1999.
- [6]. IEEE TASK FORCE: " Proposed Terms and Definitions for Flexible AC Transmission Systems (FACTS)", IEEE Trans. On Power Delivery, vol. 12, No. 4, 2005.
- [7]. N. Hingorani, —FACTS — Flexible ac transmission systems, I in Proc. IEE5th Int. Conf. AC DC Transmission, London, U. K. , 1991, Conf. Pub.345, pp.1–7.
- [8]. N. G. Hingorani and L. Gyugyi, *Understanding FACTS: Concepts and Technology of Flexible AC Transmission Systems*. New York: Wiley, 2000, vol. 1
- [9]. Dr. Tarlochan Kaur and Sandeep Kakran, Transient Stability Improvement of long transmission line using SVC, *International Journal of Advanced research in Electrical, Electronics and Instrumentation Engineering, Oct 2012, Vol. 1, Issue 4*
- [10]. A. Kazemi H. A. Shayanfar M. A. Rafiee, "Impact of STATCOM and OPF on Power System Voltage Stability Using Modal Analysis and Quadratic Programming", Department of Electrical Engineering Iran University of Science and Technology. 2004.
- [11]. Kazemi, A. , S. Jamali, and H. Shateri. "Effects of STATCOM on distance relay tripping characteristic. " *Transmission and Distribution Conference and Exhibition: Asia and Pacific, 2005 IEEE/PES*. IEEE, 2005.
- [12]. C. A. Canizares, M. Pozzi, and E. Uzunovic, "STATCOM modeling for voltage and angle stability studies," *International Journal of Electrical Power & Energy Systems*, vol.25, no.6, pp. 431–441, June . 2003.
- [13]. S. M. Abd-Elazim, E. S. Ali, "Coordinated design of PSSs and SVC via bacteria foraging optimization algorithm in a multimachine power system" ELSEVIER. 2013.
- [14]. P. Kundur, M. Klein, G. J. Rogers, and M. S. Zywno, "Application of Power System Stabilizers for Enhancement of Overall System Stability", *IEEE Transactions on Power Systems*, Vol. 4, 1989, pp. 614-626.
- [15]. P. Kundur, "Power System Stability and Control", Mc-Grall Hill, New York, 1994.
- [16]. I. Kamwa, R. Grondin, G. Trudel, "IEEE PSS2B versus PSS4B: the limits of performance of modern power system stabilizers ", *IEEE Trans on Power Systems*, Vol. 20, No.2, pp. 903-915, May 2005.

Modeling and Characterization of Next Generation Network in a Developing Economy: From Data Collection to Estimation of Traffic Parameters

Nathaniel S. Tarkaa¹, Cosmas I. Ani²

¹Department of Electrical and Electronics Engineering, University of Agriculture, Makurdi, Nigeria

²Department of Electronic Engineering, University of Nigeria, Nsukka, Nigeria

ABSTRACT: The accurate estimation of the traffic parameters, especially traffic intensity that the network must support is a key criterion in the development of an effective Next Generation Network (NGN) model. In this paper, starting from data collection involving users of telecommunication services in Benue State, Nigeria, the call rate, data transaction rate, call holding times/data transaction time and traffic intensity have been estimated at the 23 local government headquarters of the State. The existing network in Benue State is GSM based and the services provided are Voice, SMS and Internet. A marketing research was first conducted to determine the level of services usage by the amount of money spent by the high, middle and low income earners. Then using the prevailing tariff rates, the amount of data transferred in bits for the three classes of services were determined. The traffic model used is based on a probabilistic model of events initiated by calls and transactions of NGN services. The model is used to estimate the symmetrical and asymmetrical traffic intensities separately at each of the 23 headquarters representing the network nodes. Generally, the results of the study show that a developing country is characterized by a prevalence of voice and SMS services, and limited Internet services; large number of low income earners; and low rates of call/data transactions and traffic intensities. The study demonstrates a method to estimate traffic parameters at different network nodes starting from subscriber field studies. The use of the method will facilitate the preparation of both business and technical plans for effective and efficient planning and dimensioning of NGN networks in a developing economy.

Keywords - Developing Economy, Gini Coefficients, Next Generation Network, Probabilistic Model, Symmetrical and Asymmetrical Traffic Intensity

I. INTRODUCTION

The aim of telecom operators (fixed and mobile) around the world is to migrate their networks to NGN in order to benefit from the NGN features as well as to avoid the drawbacks coming from their legacy networks, beside the financial factors such as reducing the capital expenditure (CAPEX) and the operation expenditure (OPEX) [1], [2], [3], [4]. The reduction of CAPEX and OPEX together with the guarantee for delivery of high quality of services can be achieved by careful data collection and estimation of traffic parameters [3], [5], [6]. Network dimensioning entails the estimation of the needed resources and requirements such as traffic intensity, bandwidth, number of links, number of interfaces (E1s), e.t.c., which help to determine the needed quantities of equipment for the network [3], [5]. Especially, the accurate estimation of the traffic intensity that the network must support is quintessential for efficient network modeling and dimensioning [7], [8].

Under the cap-and-replace scenario, for the migration of PSTN to NGN, when NGN equipment coexists with PSTN equipment, traffic measurements are usually made of the existing network and the values obtained may be used for dimensioning purposes. This cannot be the case in a replace-and-grow scenario which characterizes the design of the NGN architecture of a typical developing economy, whereby the existing PSTN is completely dispensed with [9]. Ostensibly, this situation requires the application of traffic modeling methods for which there are no historical data. Some of the commonly employed techniques for forecasting of telecommunications services for which there are no historical data are market research, expert opinion and sectorial econometrics [8], [10]. One traffic modeling methodology that incorporates the above-mentioned techniques is the probabilistic model of events initiated by calls of NGN services [11].

In this paper, starting from data collection involving users of telecommunication services in Benue State, Nigeria, the rate of calls and data transactions, call holding times, and traffic intensities have been estimated at the 23 local government headquarters of the State. A marketing research was first conducted to determine the level of services usage by amount of money spent by the high, middle and low income earners. Then using the prevailing tariff rates, the amount of data transferred in bits for the different services were determined.

In the classic work of A. Krendzel et al [11], symmetrical and asymmetrical subsets of services could be decomposed into as much as three classes each, including voice, data, video and multimedia services. However, the existing network in Benue State is GSM based and the NGN services provided are mainly voice, and data services comprised mainly of text messages and internet browsing. Hence the Benue State NGN is modeled with voice based services (belonging to symmetrical subset) and designated as class 1, and SMS and Internet services (belonging to asymmetrical subset) and designated as class 1 and class 2 respectively. Then, using the procedures of the probabilistic model, the symmetrical and asymmetrical traffic intensities are estimated separately at each of the 23 headquarters representing the network nodes. The values of the traffic intensities are significant for the capacity planning and dimensioning of NGN network in a developing economy.

The rest of the paper is organized as follows: Section 2 describes the decomposition of NGN services. This is followed by a discussion in section 3 about the distribution of NGN users. Section 4 is about the estimation of the rate of calls and data transactions. In section 5, the procedure for the estimation of the traffic intensity is outlined; while section 6 presents data collection and analysis. Lastly, in section 7, is the conclusion.

II. DECOMPOSITION OF NGN SERVICES

The probabilistic model enables estimating the main parameters for symmetrical and asymmetrical traffic separately depending on the NGN services generating the traffic. In this case, NGN services are decomposed into some classes, and the potential users distributed into some subgroups.

Firstly, a set of NGN services is divided into two subsets with each of the subset divided into different classes in accordance with features of the generated traffic intensity. The subsets and classes of services are as follows.

2.1 First Subset

These are services concerning the real-time establishment of connectivity between endpoints. These are characterized by the transfer of the symmetrical traffic and the strict control of Quality of Service (QoS). This subset is made up of the following classes of services [11]:

2.1.1 Traditional Telephony

On the provision of such services, network equipment should support the transfer of the bidirectional flow with the rate of 64 kbit/s.

2.1.2 Video Telephony

On the provision of video telephony, it is necessary to support the transfer of bidirectional E1 flow from network equipment with a throughput of 2048kbit/s.

2.1.3 Other Services

These are other services that require support of the transfer of some bidirectional E1 flows from network equipment.

2.2 Second Subset

These are services that generate the asymmetrical traffic. This subset is made up of the following classes of services:

2.2.1 E-mails, Web-pages, etc

These are services that deal with the transfer of a small amount of information about 1 kbit/transaction on average.

2.2.2 Texts, Small Amount of Audio and Visual Information

This class is characterized by the transfer of information of about 100 kbits per transaction on average.

2.3 Multimedia Services

These are services that deal with the transfer of information of about 10 Mbit/transaction on average.

In the classic work of A. Krendzel et al [11], symmetrical and asymmetrical subsets could be decomposed into as much as three classes each, including video and multimedia services. However, in the Benue State situation, the NGN services used as shown by the marketing research are voice calls, SMS and Internet. Hence the voice based services will be designated as class 1 belonging to the symmetrical subset, SMS services as class 1 belonging to the asymmetrical subset and Internet as class 2 also belonging to the asymmetrical subset.

III. DISTRIBUTION OF NGN USERS

The demand for NGN services depends on both the solvency of users and tariffs on the services. Since it is supposed that the tariffs on the aforementioned different classes of services will be unequal, then a non-uniformity of distribution of services between users will exist for each class. In order to take into account this fact when estimating parameters of data traffic, it is worthwhile to distribute all NGN users into some subgroups in accordance with their demand for NGN services from the different classes. Parameters of the non-uniformity of the distribution of NGN services for each class may be considered as the input data. Usually the non-uniform distribution of incomes between inhabitants is characterized by the Gini coefficients in statistics [11]. Values of the Gini coefficients may be defined on a basis of statistical information regarding the demand for NGN services [11].

Given the values of Gini coefficients, users may be distributed in accordance with their demand for NGN services [11]. In this case, the users are distributed into three subgroups and considering that only two classes of services are used and designated as class 1 and class 2 as stated earlier, the procedures are as follows:

Let the income group, $F_i (i=1, 2, 3)$ produce the highest say A% of demand for NGN services from the second class of services. The relative number of users, say in the high income group, is determined as follows:

$$F_3 = (A\%)^{\left(\frac{\alpha_2}{\alpha_2-1}\right)} \quad (1)$$

Where $\alpha_i (i = 1, 2, 3)$ are parameters of Pareto distribution derived from the Gini coefficients.

Then let users of a second subgroup create the highest B% and the above-considered subgroup (i.e. the high income group) create C% of demand for NGN services from the first class. Then the users from these two subgroups will create (B+C)% of demand for NGN services from the first class. Then the relative number of users in the second subgroup is determined as:

$$F_2 = [(C + B)\%]^{\left(\frac{\alpha_1}{\alpha_1-1}\right)} - F_3 \quad (2)$$

Finally, the relative number of users in the remaining subgroup may be found as:

$$F_1 = 1 - F_2 - F_3 \quad (3)$$

In Benue State, majority of the local areas use only one class of services for each of the symmetrical and asymmetrical subsets so the application of the above procedure in such cases involve only one class separately.

IV. ESTIMATION OF THE RATE OF CALLS AND DATA TRANSACTIONS

The decomposition of NGN services and the distribution of NGN users give the possibility to form the probabilistic model of the initiation of the calls and data transactions based on the intersection of events from two statistically independent exhaustive groups.

Let the events included in the first group be denoted by $i = 1, 2, 3$; they correspond with demand for services from the first, second, and third classes respectively. And the events included in the second group are denoted $j = 1, 2, 3$; they correspond with demands initiated by users from the low income, middle income and high income subgroups respectively. Since these groups of events are independent, the probability of an intersection of the events is equal to the product of probabilities of each of the events [11].

The procedure for the calculation of the specific rate of calls and data transactions (λ_{ij}) per user between nodes of an NGN network subsystem in busy hour for the nine ($i, j = 1, 2, 3$) intersections of events from the two above-mentioned groups of events is outlined by the following equations [11]. It is based on the solution of three systems of equations that are formed for each of the classes of NGN services.

The solution will yield the values for λ_{ij} when $i = 1$, and $j = 1, 2, 3$ as follows:

$$\lambda_{12} = \frac{\lambda_{11} Q_{12} F_1}{Q_{11} F_2} \quad (4)$$

$$\lambda_{13} = \frac{\lambda_{11} Q_{13} F_1}{Q_{11} F_3}$$

Where Q_{ij} ($i, j = 1, 2, 3$) represents the share of calls and transactions in busy hour, relating to users of low income, middle income and high income subgroups respectively when services from first and second classes respectively are initiated; where the value, λ_{11} is included in the input data.

It can be readily seen that (4) apply ideally to our case study, since $i = 1$ in majority of the local government areas, and the different income groups are also three.

In order to find the family of solutions when $i = 2, 3$ and $j = 1, 2, 3$, the input data defined in (5) is used.

$$\gamma_i, \quad i = 1, 2, 3, \quad \gamma_1 + \gamma_2 + \gamma_3 = 1, \quad (5)$$

where γ_i is the distribution of total amount of transaction in busy hour amongst the different classes i .

The solutions are given as follows:

$$\lambda_{ij} = \frac{\gamma_i \sum_j \lambda_{1j} F_j}{\gamma_i F_j}; \quad i = 2, 3; \quad j = 1, 2, 3 \quad (6)$$

It is also easy to apply (6) to suit our case study by simply setting $i = 2; j = 1, 2, 3$ since, in this case, there are only up to two classes of services.

V. ESTIMATION OF THE TRAFFIC INTENSITY

In order to calculate the traffic intensity in Erlangs generated on network nodes in Benue State, it is necessary to determine the average call holding time and the average transaction time T_i ($i = 1, 2$) corresponding to procedures of NGN services supported by the above-mentioned classes of symmetrical and asymmetrical services. This is also an application of the probabilistic model in line with our case study.

For the symmetrical subset of services, that is, voice calls, characterized by strict control of Quality of Service (QoS), the values of T_i ($i = 1, 2$) are assigned on the basis of statistical information.

The traffic intensity per user generated by calls of NGN services belonging to the i th class if they are initiated by users from the j th subgroup is obtained as follows [11]:

$$A_{ij} = \frac{\lambda_{ij} T_i}{3600} \quad i = 1; \quad j = 1, 2, 3 \quad (7)$$

Therefore, the traffic intensity, from all the users may be determined as:

$$A_i = \frac{T_i \sum_j F_j \lambda_{ij}}{3600}; \quad i = 1; \quad j = 1, 2, 3 \quad (8)$$

Therefore, the total traffic intensity created by NGN services on channels with the throughput c_i , from the first subset may be found as:

$$A_s = \frac{\sum c_i A_i}{c_2} \quad i = 1 \quad (9)$$

The average transaction time corresponding to procedures of NGN services from the asymmetrical subset is:

$$T_i = \frac{w_i}{c_i}, \text{ sec/trans} \quad i = 1, 2 \quad (10)$$

Where w_i is the average amount information transferred during a transaction to be assigned on the basis of statistical data.

The value of c_2 in (9) is chosen as 2048 kbits/s for the basic channel, E1, with regard to the level of demand for NGN services. The values of $c_i(i = 1, 2)$ are chosen as $c_1 = 64$ kbits/s for voice calls and text messages (SMS), and $c_2 = 2048$ kbits/s for Internet.

The traffic intensity generated per user by NGN services belonging to the i th class, if they are initiated by users from the j th subgroup is obtained as follows:

$$A_{ij} = \frac{\lambda_{ij}T_i}{3600} \quad i = 1, 2; \quad j = 1, 2, 3 \quad (11)$$

The traffic intensity created by transactions from the asymmetrical subset of NGN services that are initiated by all users may be found as:

$$A_i = \frac{T_i \sum_j F_j \lambda_{ij}}{3600}; \quad i = 1, 2; \quad j = 1, 2, 3 \quad (12)$$

Therefore, the expression for the estimation of the total traffic intensity created by NGN services from the second subset (the asymmetrical load) on channels with the throughput c_i , is:

$$A_a = \frac{\sum c_i A_i}{2048} \quad i = 1, 2 \quad (13)$$

Finally, the total traffic intensity generated by NGN services on some E1 channels is:

$$A_T = A_s + A_a \quad (14)$$

VI. DATA COLLECTION AND ANALYSIS

The data collection methodology was a marketing research carried out in the 23 local government headquarters of Benue State, conducted with oral interviews and filling of questionnaires. The result of the survey gave the distribution of the demand for NGN services into symmetrical (voice) and asymmetrical (SMS and Internet) services, and users into high, medium and low income groups. A total number of one hundred inhabitants were involved in each local government area. The results are shown in Table 1 and graphically in Fig. 1. The results show the preponderance of voice and SMS services in the State. It can be seen that 100 % of the inhabitants use Voice and SMS services in the 23 and 6 local government areas respectively. The Internet services are used in only 5 local government areas each having less than 100 % of users as depicted in Table 1 and Fig. 1. Also notice that the low income users are more in number followed by the middle income users for all the three classes of services, except Internet which has the highest number of users in the middle income group. This shows that the high income group has the least number of users of NGN services in Benue State.

For the purpose of this analysis, voice based services will be designated as class 1 belonging to the symmetrical subset, SMS services as class 1 belonging to the asymmetrical subset and Internet services as class 2 also belonging to the asymmetrical subset.

Table 2 shows the distribution of demand for NGN services by total amount of data in megabits transferred in busy hour for each class of services. The calculation of the values was based on the cost of 1 kilobit of data at the rate of 5 Kobo (approximately 0.05 Cents) charged by GSM operators in Benue State. The demand trend is shown graphically in Fig. 2. It is clear that the demand for voice services is somewhat the highest throughout the State with Internet services having the highest demand in Makurdi, the State capital, followed by the main cities of Otukpo, Gboko, Oju and Katsina-Ala. The SMS services generally have the least demand.

Table I: Distribution of Demand for Each Class of NGN Services by Number of Inhabitants into High, Medium and Low Income Groups

S/ N	LOCAL GOVERNMENT T	SYMMETRICAL SERVICES: VOICE	ASYMMETRICAL SERVICES: SMS	ASYMMETRICAL SERVICES: INTERNET
---------	--------------------------	-----------------------------------	----------------------------------	---------------------------------------

	HEADQUARTERS	High Income Group %	Midle Income Group %	Low Income Group %	Total %	High Income Group %	Midle Income Group %	Low Income Group %	Total %	High Income Group %	Midle Income Group %	Low Income Group %	Total %
1	Igumale	11	41	48	100	11	38	30	79	0	0	0	0
2	Obagaji	9	36	55	100	9	36	45	90	0	0	0	0
3	Ugbokpo	8	34	58	100	8	34	44	86	0	0	0	0
4	Buruku	8	38	54	100	8	37	44	89	0	0	0	0
5	Gboko	20	37	43	100	20	37	38	95	20	31	26	77
6	Gbajimba	8	30	62	100	8	30	45	83	0	0	0	0
7	Aliade	12	37	51	100	12	37	39	88	0	0	0	0
8	Naka	9	29	62	100	9	29	47	85	0	0	0	0
9	Katsina-Ala	14	38	48	100	14	38	48	100	13	37	18	68
10	Tse-Agberagba	10	33	57	100	10	33	57	100	0	0	0	0
11	Adikpo	12	33	55	100	12	33	55	100	0	0	0	0
12	Ugba	11	40	49	100	11	40	31	82	0	0	0	0
13	Makurdi	26	38	36	100	26	38	36	100	26	37	29	92
14	Obarike-Ito	10	34	56	100	10	34	45	89	0	0	0	0
15	Otukpa	13	30	57	100	13	30	38	81	0	0	0	0
16	Idekpa	10	35	55	100	10	34	41	85	0	0	0	0
17	Oju	13	40	47	100	13	40	38	91	13	33	16	62
18	Okpoga	12	33	55	100	12	29	33	74	0	0	0	0
19	Otukpo	19	41	40	100	19	41	40	100	17	39	19	75
20	Wannune	9	28	63	100	9	28	56	93	0	0	0	0
21	Sankera	10	30	60	100	10	30	38	78	0	0	0	0
22	Lessel	8	25	67	100	8	24	48	80	0	0	0	0
23	Vandeikya	14	35	51	100	14	35	51	100	0	0	0	0
	Mean	12	35	53	100	12	34	43	89	18	35	22	75

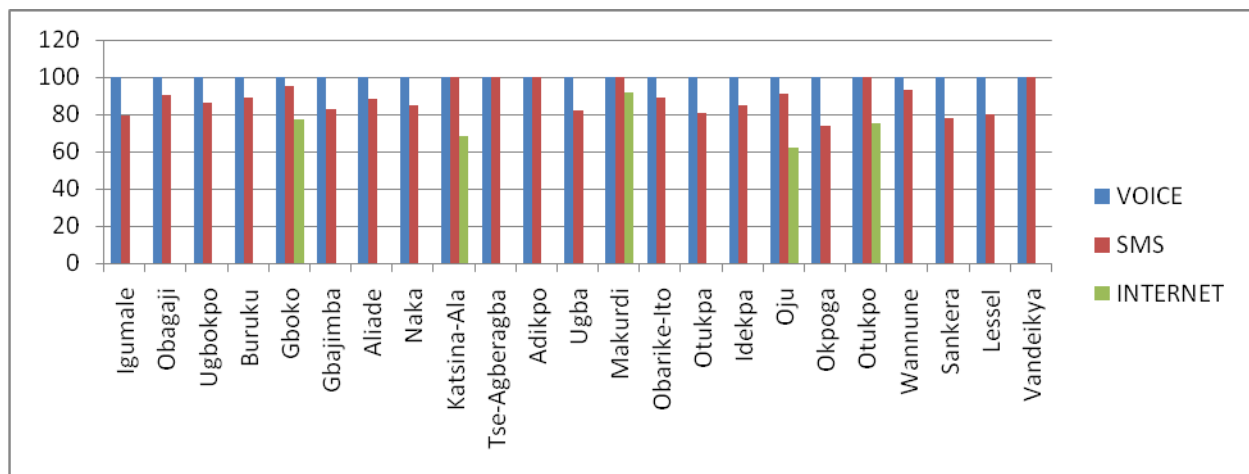


Figure 1: distribution of demand for each class of NGN services by the total number of inhabitants in the high, medium and low income groups

Table II: Distribution of Demand for Each Class of NGN Services by Total Amount of Data Transferred in Busy by the High, Medium and Low Income Groups

S/N	LOCAL GOVERNMENT	VOICE Megabits	SMS Megabits	INTERNET Megabits
-----	------------------	----------------	--------------	-------------------

	<i>T HEADQUARTERS</i>	<i>Hig h Inco me Gro up</i>	<i>Mid dle Inco me Gro up</i>	<i>Lo w Inco me Gro up</i>	<i>Tot al</i>	<i>Hig h Inco me Gro up</i>	<i>Midd le Inco me Gro up</i>	<i>Low Inco me Gro up</i>	<i>Tota l</i>	<i>Hig h Inco me Gro up</i>	<i>Mid dle Inco me Gro up</i>	<i>Lo w Inco me Gro up</i>	<i>Tota l</i>
1	Igumale	132	160	71	363	6.4	22.32	11.40	40	0	0	0	0
2	Obagaji	160	199	73	432	14	34.40	22.40	70	0	0	0	0
3	Ugbokpo	150	219	88	457	13	21.60	26.80	61	0	0	0	0
4	Buruku	94	153	82	329	6.4	23.20	26.52	56	0	0	0	0
5	Gboko	392	334	127	853	39	45.80	38.00	123	388	264	93	745
6	Gbajimba	150	216	84	450	10	28.00	22.76	61	0	0	0	0
7	Aliade	208	241	81	530	18	33.60	26.40	78	0	0	0	0
8	Naka	180	170	83	433	6.6	31.00	27.28	65	0	0	0	0
9	Katsina-Ala	248	222	102	572	23	45.60	41.80	110	102	327	52	482
10	Tse-Agberagba	110	157	69	336	11	14.40	10.40	36	0	0	0	0
11	Adikpo	99	133	64	296	7.0	16.04	24.32	48	0	0	0	0
12	Ugba	240	317	80	637	22	45.20	19.20	86	0	0	0	0
13	Makurdi	330	296	91	717	50	43.38	55.16	148	718	619	290	1626
14	Obarike-Ito	190	219	79	488	16	31.40	27.00	74	0	0	0	0
15	Otukpa	260	204	78	542	24	33.20	22.00	79	0	0	0	0
16	Idekpa	136	151	62	349	4.4	18.00	15.80	38	0	0	0	0
17	Oju	226	355	104	685	18	54.40	37.20	109	164	280	77	521
18	Okpoga	174	149	78	401	6.4	14.00	6.52	27	0	0	0	0
19	Otukpo	356	334	133	823	34	65.80	59.80	160	282	435	103	820
20	Wannune	92	159	70	321	6.4	17.20	22.04	46	0	0	0	0
21	Sankera	200	186	83	469	20	26.00	22.40	69	0	0	0	0
22	Lessel	123	104	91	318	5.2	16.00	27.00	48	0	0	0	0
23	Vandeikya	92	155	58	305	14	29.20	23.16	66	0	0	0	0
	Mean	189	210	84	483	16	31	27	74	331	385	123	839

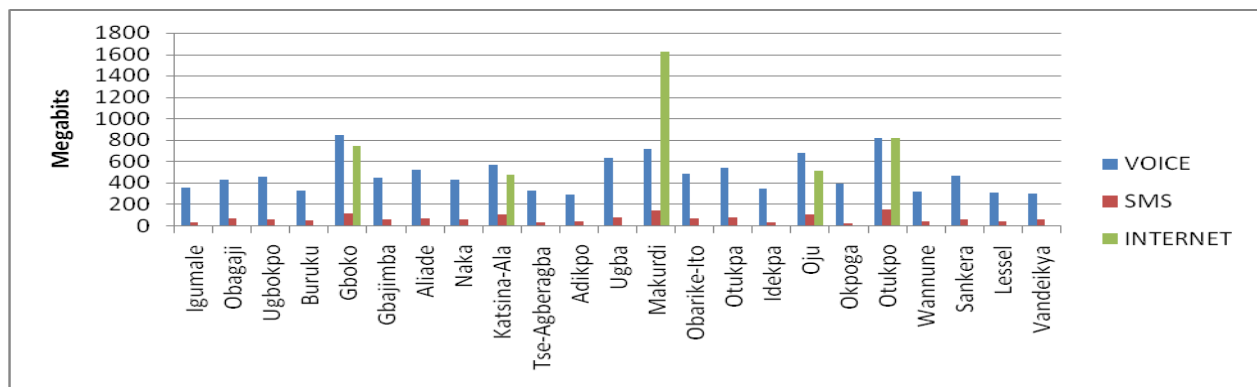


Figure 2: total amount of data transferred in busy hour for each class of services

Other important data collected were call number, number of text messages, call holding time and number of Internet transactions.

Using the initial data shown in Table 2, other model input parameters were calculated using (1), (2), (3) and (5). They include the following.

- i. Criteria for decomposition of services (γ_1, γ_2);
- ii. Relative number of users in the High, Middle and Low Income subgroups F_3, F_2 , and F_1 respectively.
- iii. Share of calls and transactions in busy hour, Q_{11}, Q_{12}, Q_{13} ; and Q_{21}, Q_{22}, Q_{23} relating to users of low income, middle income and high income subgroups respectively when services from first and second classes respectively are initiated.

Given these input parameters, the main traffic parameters, that is, rate of voice calls and rate of data transactions, call holding time and data transaction time, and traffic intensity were estimated using (4) to (14) and the results are as shown in Tables 3, 4 and 5 respectively. Also, the results are shown graphically in Figs. 3, 4 and 5 respectively.

Table III: Rate of Calls and Data Transactions in Busy Hour per User

S/N	LOCAL GOVERNMENT HEADQUARTERS	VOICE				SMS				INTERNET			
		HIGH INCOME λ_{13}	MIDDLE INCOME λ_{12}	LOW INCOME λ_{11}	TOTAL	HIGH INCOME λ_{13}	MIDDLE INCOME λ_{12}	LOW INCOME λ_{11}	TOTAL	HIGH INCOME λ_{23}	MIDDLE INCOME λ_{22}	LOW INCOME λ_{21}	TOTAL
1	Igumale	2.32	5.10	4.5	11.9	3.93	9.66	5.0	18.6	0	0	0	0
2	Obagaji	1.80	5.05	4.3	11.2	5.18	10.3	6.2	21.7	0	0	0	0
3	Ugbokpo	1.95	5.36	4.5	11.8	4.43	4.99	7.6	17.0	0	0	0	0
4	Buruku	2.50	5.55	4.9	13	3.30	3.95	8.0	15.3	0	0	0	0
5	Gboko	7.67	5.62	7.2	20.5	12.9	14.5	12.5	39.9	72	96.2	77	245
6	Gbajimba	1.92	4.29	4.4	10.6	4.97	11.7	6.3	22.3	0	0	0	0
7	Aliade	2.08	6.06	4.8	12.9	7.54	12.4	8.5	28.4	0	0	0	0
8	Naka	2.58	2.72	4.3	9.60	5.98	15.8	7.3	29.1	0	0	0	0
9	Katsina-Ala	4.02	4.64	5.6	14.3	6.98	8.76	11.0	26.7	28	55.6	26	110
10	Tse-Agberagba	1.69	4.27	4.4	10.4	2.45	5.49	2.0	9.94	0	0	0	0
11	Adikpo	2.25	3.43	4.6	10.3	2.53	3.00	6.0	11.5	0	0	0	0
12	Ugba	2.09	6.06	4.4	12.6	8.37	14.2	7.7	30.3	0	0	0	0
13	Makurdi	6.30	4.30	6.0	16.6	36.3	42.2	20.0	98.6	370	486	270	1126
14	Obarike-Ito	1.84	3.61	4.6	10.1	6.46	10.9	7.5	24.9	0	0	0	0
15	Otukpa	3.33	2.69	4.3	10.3	7.96	10.2	7.2	25.3	0	0	0	0
16	Idekpa	1.66	3.72	4.4	9.78	4.01	10.3	5.0	19.3	0	0	0	0
17	Oju	2.77	7.29	5.6	15.7	7.61	20.9	12.0	40.5	69	116	29	213
18	Okpoga	2.84	2.56	4.6	10.0	1.92	3.64	6.0	11.6	0	0	0	0
19	Otukpo	4.74	4.55	6.7	16	23.8	26	19.0	68.7	112	171	72	355
20	Wannune	1.81	3.88	4.6	10.3	2.15	2.56	5.0	9.71	0	0	0	0
21	Sankera	2.63	2.69	4.2	9.52	6.94	8.53	7.4	22.9	0	0	0	0
22	Lessel	1.31	3.06	4.7	9.07	2.68	3.00	7.0	12.7	0	0	0	0
23	Vandeikya	2.17	4.05	4.7	10.9	5.01	8.91	6.0	19.9	0	0	0	0
	Mean	2.8	4.4	4.9	12.1	7.5	11.4	8.3	27.2	130	924	185	410

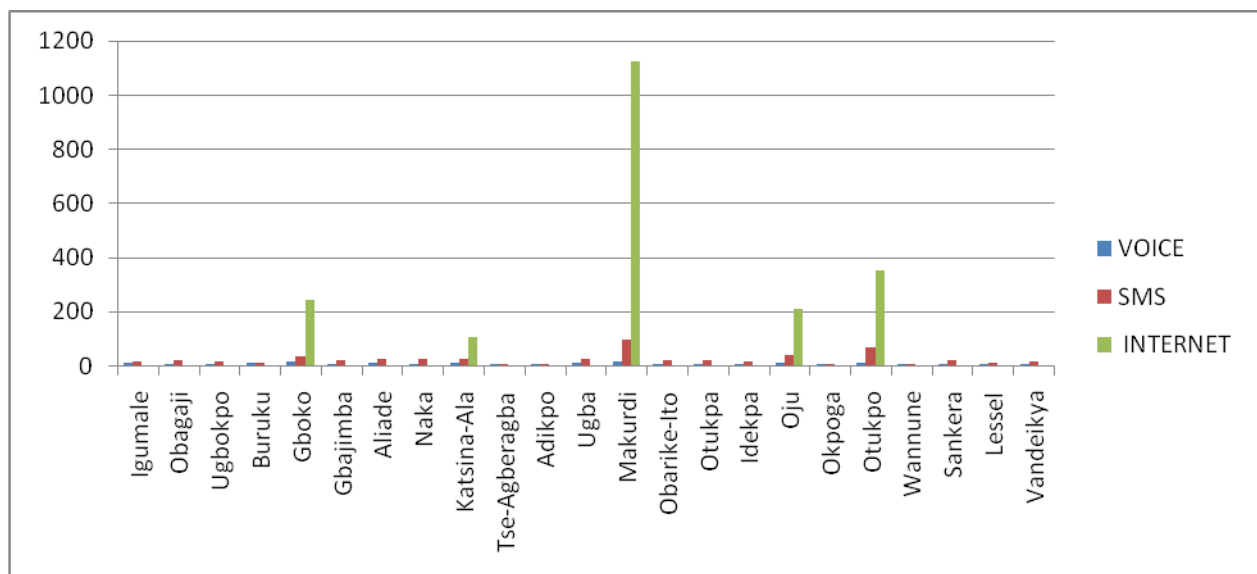


Figure 3: rate of calls and data transactions in busy hour per user

Table IV: Average Call Holding Time and Data Transaction Time per User

S/N	LOCAL GOVERNMENT HEADQUARTERS	VOICE	SMS	INTERNET
		Average Call Holding Time, T_1 Secs	Average Transaction Time, T_1 Secs	Average Transaction Time, T_2 Secs
1	Igumale	135	1.25	0
2	Obagaji	168	1.25	0
3	Ugbokpo	174	1.25	0
4	Buruku	113	1.25	0
5	Gboko	192	1.25	6
6	Gbajimba	168	1.25	0
7	Aliade	174	1.25	0
8	Naka	174	1.25	0
9	Katsina-Ala	153	1.25	4
10	Tse-Agberagba	109	1.25	0
11	Adikpo	115	1.25	0
12	Ugba	186	1.25	0
13	Makurdi	194	1.25	10
14	Obarike-Ito	174	1.25	0
15	Otukpa	174	1.25	0
16	Idekpa	121	1.25	0
17	Oju	192	1.25	5
18	Okpoga	146	1.25	0
19	Otukpo	205	1.25	6
20	Wannune	103	1.25	0
21	Sankera	180	1.25	0
22	Lessel	79	1.25	0
23	Vandeikya	107	1.25	0
	Mean	154	1.25	6.2

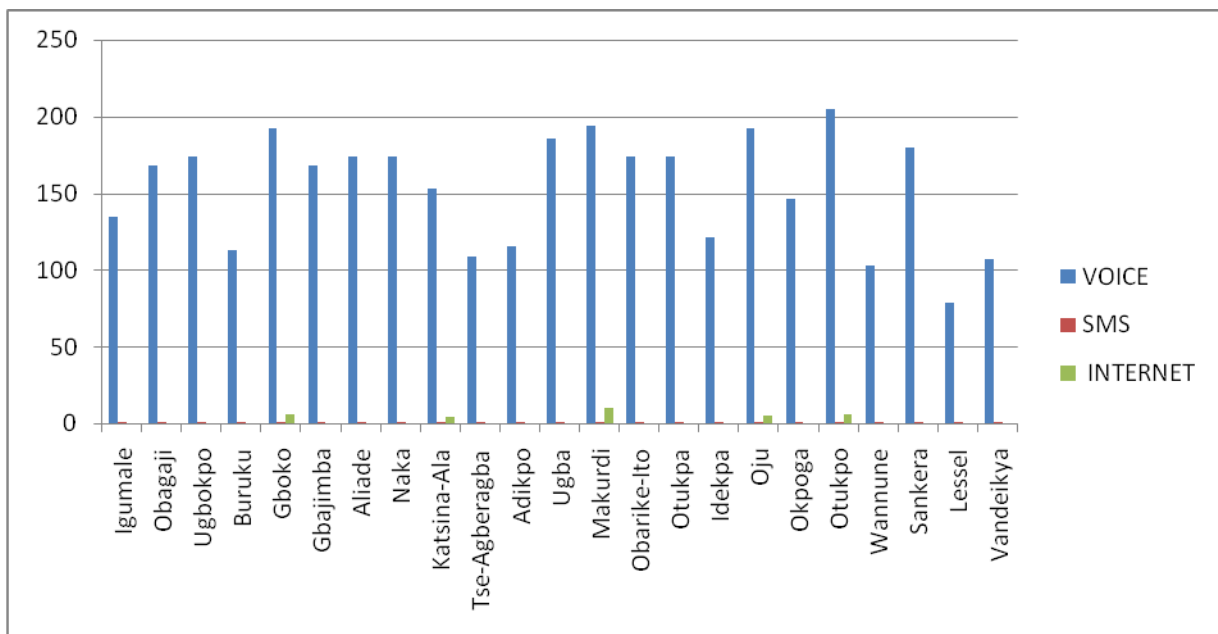


Figure 4: average call holding time and data transaction time per user

Table V: Traffic Intensity per User at the Network Nodes

S/N	LOCAL GOVERNMENT HEADQUARTERS	SYMMETRICAL SERVICES	ASYMMETRICAL SERVICES			TOTAL TRAFFIC INTENSITY PER USER $A_T = (A_s + A_a)$ ERLANGS
		VOICE Erlangs A_s	SMS Erlangs	INTERN ET Erlangs	TOTAL Erlangs A_a	
1	Igumale	0.0044	0.000069	0	0.000069	0.0045
2	Obagaji	0.0050	0.000080	0	0.000080	0.0051
3	Ugbokpo	0.0057	0.000062	0	0.000062	0.0058
4	Buruku	0.0056	0.000056	0	0.000056	0.0057
5	Gboko	0.011	0.0046	0.14	0.14	0.15
6	Gbajimba	0.0050	0.000081	0	0.000081	0.0051
7	Aliade	0.0059	0.00010	0	0.00010	0.0060
8	Naka	0.0046	0.00010	0	0.00010	0.0047
9	Katsina-Ala	0.0062	0.0031	0.043	0.043	0.049
10	Tse-Agberagba	0.0031	0.000038	0	0.000038	0.0031
11	Adikpo	0.0034	0.000044	0	0.000044	0.0034
12	Ugba	0.0061	0.00011	0	0.00011	0.0062
13	Makurdi	0.0088	0.011	1.030	1.030	1.040
14	Obarike-Ito	0.0046	0.00009	0	0.00009	0.0047
15	Otukpa	0.0049	0.000092	0	0.000092	0.0050
16	Idekpa	0.0031	0.000069	0	0.000069	0.0032
17	Oju	0.0083	0.0049	0.095	0.095	0.10
18	Okpoga	0.0041	0.000041	0	0.000041	0.0041
19	Otukpo	0.0090	0.0080	0.20	0.20	0.21
20	Wannune	0.0030	0.000035	0	0.000035	0.0030
21	Sankera	0.0047	0.000083	0	0.000083	0.0048
22	Lessel	0.0021	0.000047	0	0.000047	0.0022
23	Vandeikya	0.0033	0.000073	0	0.000073	0.0034
	Mean	0.005	0.001	0.07	0.07	0.07

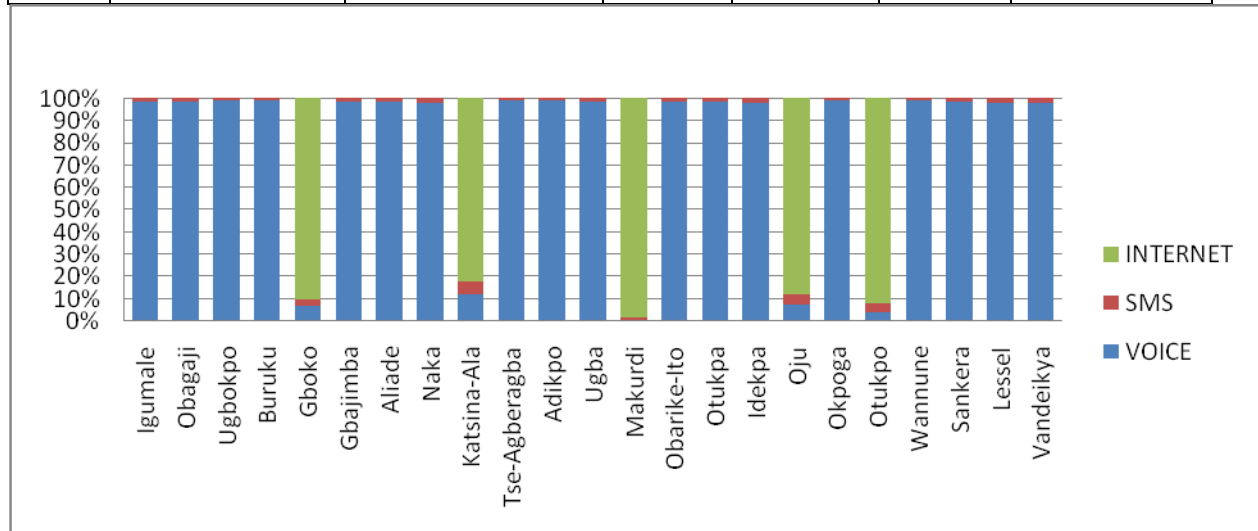


Figure 5: traffic intensity per user at the network nodes

Fig. 5 shows that the symmetrical voice services and asymmetrical SMS services constitute the predominance of NGN traffic in Benue State occurring at all the 23 network nodes; the asymmetrical Internet traffic occurs at only 5 network nodes. Notice the huge dominance of voice traffic (with a contribution of more than 95%) over SMS traffic in all the 18 towns covered by only these two services. Also notice that Internet traffic similarly dominates the voice and SMS services in the 5 areas covered by all the three classes of services.

Generally speaking, the average values of traffic intensity per user in Erlangs are 0.005 for voice services; 0.001 for SMS; and 0.07 for Internet. This typifies the traffic pattern for a developing economy since the existing telecommunications infrastructure are still largely legacy and not encouraging for widespread Internet services. Also the low solvency of majority of the users owing to the fledgling economy is a major factor for the generally low values of rate of calls/data transactions, and traffic intensities. Thus, it is instructive to dimension the NGN taking this traffic pattern into consideration. Fig. 5 succinctly illustrates this traffic pattern.

VII. CONCLUSION

In this paper, the probabilistic traffic model has been used for the estimation of traffic parameters for an NGN in a developing society. Such model input parameters as Gini coefficients defining the non-uniformity of demand for NGN services; relative number of subscribers in the low, medium and high income subgroups; the distribution of the total amount of calls and transactions in busy hour for each class of service; the distribution of the total amount of data transferred; and the share of calls and transactions in busy hour relating to users of each of the sub-groups were obtained either directly or derived from statistical data obtained from a marketing research conducted on the 23 local government headquarters of Benue State. The research primarily sourced information on the level of usage of various NGN services by the high, middle, and low income groups in the State. This consequently showed the main services used in the State as voice calls, text messages and Internet. Then using the prevailing tariff at the rate 5 Kobo (approximately 0.05 Cents) per 1 kilobit, the amount of data transferred, in bits, was estimated for each class of service and used to derive the various model input parameters. Then, using the procedures of the probabilistic model, the symmetrical and asymmetrical traffic intensities were estimated separately at each of the 23 headquarters representing the various network nodes of the NGN. Other key traffic parameters that were got from this method include rate of voice calls and rate of data transactions, call holding time and data transaction time. For instance, the average values of traffic intensity per user in Erlangs are 0.005 for voice services; 0.001 for SMS; and 0.07 for Internet.

Generally, the results of the study show that a developing country is characterized by a prevalence of voice and SMS services and limited Internet services; high number of low income earners; and low rates of call/data transactions, and traffic intensities.

This study demonstrates a method to estimate traffic parameters at different network nodes starting from subscriber field studies. The use of the method will facilitate the preparation of both business and technical plans for effective and efficient planning and dimensioning of NGN networks in a developing economy.

REFERENCES

- [1] The International Engineering Consortium, www.iec.org, Local-Exchange Softswitch System: Softswitch and Packet voice, *Web Proforum Tutorials*, 2002.
- [2] J.C. Crimi, Next Generation Network (NGN) Services, *Telcordia Technologies*, 2002.
- [3] Ahmad A. Almughales and Ali M. Alsaih, Next Generation Network Design, Dimensioning & Services Innovation, *International Journal of Computer Science and Network Security*, 10 (6), June 2010.
- [4] Mustafa Shakir, Mahmood Ashraf Khan, Shahzad A. Malik and Izharul Hak, Performance and Capacity Planning of NGN, *International Journal of Communications, Network and System Sciences*, 4, 2011, 756-760.
- [5] Cherif Ghazel and Leila Saidane, Dimensioning of NGN Main Components with Improved and Guaranteed Quality of service, *Journal of Networks*, Vol. 5, July 2010.
- [6] Cherif Ghazel, and Leila Saïdane, Dimensioning of Next Generation Networks Signaling Gateway for Improving a Quality of Service Target, *International Journal of Hybrid Information Technology*, 2 (2), 2009.
- [7] Villy B. Iversen, *Teletraffic Engineering Handbook*, (ITU-D SG 2/16 & ITC Draft 2001-06-20).
- [8] Network Planning and Design, "http://en.wikipedia.org/w/index.php?title=Network_planning_and_design&oldid=525267992" *Categories*:
- [9] Nathaniel S. Tarkaa, and Cosmas I. Ani, On the Design of Next Generation Network Architecture for a Developing Economy, *American Journal of Engineering Research (AJER)*, 03 (05), 2014, 193-202.
- [10] Manuel Villen – Altamirano Telefonica I + D. Spain, Chairman of the ITU-T Working Party 3/2 on Traffic Engineering, *Overview of ITU Recommendations on Traffic Engineering*, 2012.
- [11] A. Krendzel, V. Derjavina, and S. Lopatin, Method for Estimating Parameters of NGN Traffic: *Proc. International Conf. on Next Generation Teletraffic and Wired/Wireless Advanced networking (NEW2AN)*, St. Petersburg, Russia, 2004, 50 – 54

Modal analysis of cantilever beam Structure Using Finite Element analysis and Experimental Analysis

S. P. Chaphalkar¹, Subhash. N. Khetre², Arun M. Meshram³

¹Head of Department, Department of Automobile Engineering, Pimpri Chinchwad, Polytechnic, Pune

²Assistant professor, Department of Mechanical Engineering, RSCOE, Tathawade, Pune

³Assistant professor, Department of Mechanical Engineering, RSCOE, Tathawade, Pune

ABSTRACT: The modal analysis is presented in this paper some basic concepts of modal analysis of transverse vibration of fixed free beam. It is described an experimental apparatus and the associated theory which allows to obtain the natural frequencies and modes of vibration of a cantilever beam. The concept of modal analysis plays an important role in the design of practical mechanical system. So it becomes important to study its effects on mechanical system for different frequency domain i.e. low, medium and high frequency. This paper focuses on the numerical analysis and experimental analysis of transverse vibration of fixed free beam and investigates the mode shape frequency. All the frequency values are analyzed with the numerical approach method by using ANSYS finite element package has been used. The numerical results are in good agreement with the experimental tests results.

Keywords - Finite Element analysis, Modal analysis, Fixed Free Beam, Experimental Analysis, Free vibration.

I. INTRODUCTION

In the past two decades, modal analysis has become a major technology in the quest for determining, improving and optimizing dynamic characteristics of engineering structures. Not only has it been recognized in mechanical and aeronautical engineering, but modal analysis has also discovered profound applications for civil and building structures, biomechanical problems, space structures, acoustical instruments, transportation and nuclear plants. The Free vibration takes place when a system oscillates under the action of forces integral in the system itself due to initial deflection, and under the absence of externally applied forces. The system will vibrate at one or more of its natural frequencies, which are properties of the system dynamics, established by its stiffness and mass distribution. In case of continuous system the system properties are functions of spatial coordinates. The system possesses infinite number of degrees of freedom and infinite number of natural frequencies. Vibration analysis of fixed free Beam like components has been an active research subject and numerous technical papers have been published. For to calculating the natural frequencies and mode shapes of a structure modal analysis method is used. This method determined the dynamic response of complicated structural dynamic problems.

In general, applications of modal analysis today cover a broad range of objectives identification and evaluation of vibration phenomena, validation, structural integrity assessment, structural modification, and damage detection. In engineering design, it is important to calculate the response quantities such as the displacement, stress, vibration frequencies, and mode shapes of given set of design parameters. The study of mathematical models which involve physical and geometric parameters such as mass density ρ , elastic modulus E , Poisson's ratio ν , lengths, and cross-section shape characteristics. In many practical engineering applications, these parameters frequently do not have well-defined values due to non-homogeneity of the mass distribution geometric properties or physical errors, as well as variation arising from the assembly and manufacturing processes.

II. MAIN OBJECTIVES:

All the Vehicles, aircraft and home appliances structures are made up of fixed beam with one end free or combination of fixed beams so it becomes necessary to study fixed beam vibration. The following are main objective of yoke design.

1. A detailed understanding of function and configuration of fixed beam with one end free
2. To Analysis of fixed beam with one end free using FEA Method.
3. To Analysis of fixed beam with one end free using Experimental method.

III. NUMERICAL ANALYSIS BY USING ANSYS:

3.1 Basic steps of finite element analysis:

There are three basic steps involved in this procedure,

1. Pre Processor (Building the model (or) Modeling)
2. Solution (Applying loads and solving)
3. Post Processor (Reviewing the results)

3.2. Numerical Approach for Transverse Vibration of Fixed Free Beam:

We shall now investigate the free vibration of fixed free beam using the ANSYS program, a comprehensive finite element package. We use the ANSYS structural package to analyse the vibration of fixed free beam. Finite element procedures at present very widely used in engineering analysis. The procedures are employed extensively in the analysis of solid and structures and of heat transfer and fluids and indeed, finite element methods are useful in virtually every field of engineering analysis.

3.3. Description of the finite element method:

The physical problem typically involves an actual structure or structural component subject to certain loads. The idealization of the physical problem to a mathematical model requires certain assumptions that together lead to differential equations governing the mathematical model. Since the finite element solution technique is a numerical procedure, it is necessary to access the solution accuracy. If the accuracy criteria are not met, the numerical solution has to be repeated with refined solution parameters until a sufficient accuracy is reached.

3.4. Important features of finite element method

The following are the basic features of the finite element method: Division of whole in to parts, which allows representation of geometrically complex domains as collection of simple domains that, enables a systematic derivation of the approximation functions. Derivation of approximation functions over each element the approximation functions are algebraic polynomials that are derived using interpolation theory.

3.5. Boundary Conditions:

The meshed model is then analyzed (static) and the boundary conditions are:

- One end is fixed (All DOF).

3.6. Numerical (FEA) Results:

The dimensions and the material constant for a uniform fixed free beam (cantilever beam) studied in this paper are: Material of beam = mild steel, Total length (L) = 0.8 m , width (B) = 0.050 m, height (H) = 0.006 m, Young's Modulus (E) = 210×10^9 , mass density = 7856 kg/ m^3 . Poisson Ratio= 0.3. The numerical results were found out by using the ANSYS program as shown in Table 3. The Numerical (FEA) values obtained are 7.67 Hz and 688.89 Hz for first and last modes respectively.

Table 1: Numerical frequency from ANSYS

Mode	Numerical frequency from ANSYS program in Hz
1	7.6769
2	48.1
3	63.585
4	134.69
5	229.16
6	264.01
7	391.46
8	436.63
9	652.62
10	688.89

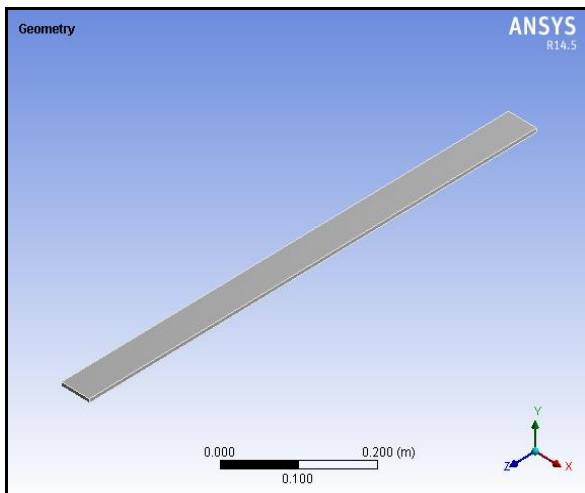


Fig. 1 : Geometry of fixed beam at one end

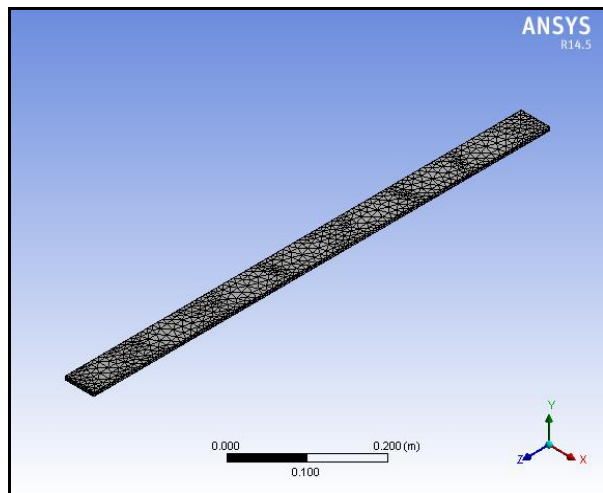


Fig. 2 : Meshing of fixed beam at one end

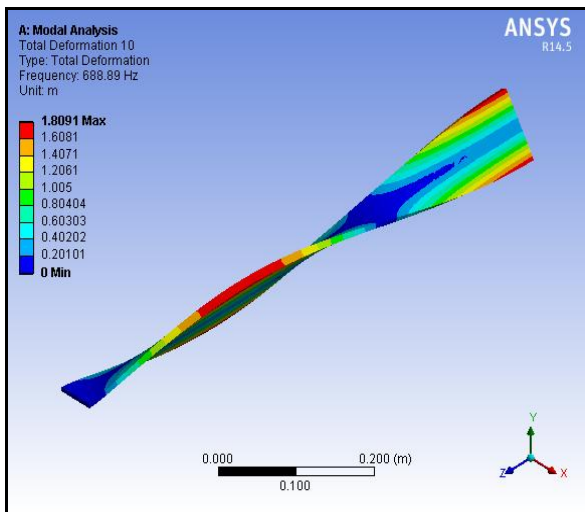


Fig. 3 : Total Deformation-10

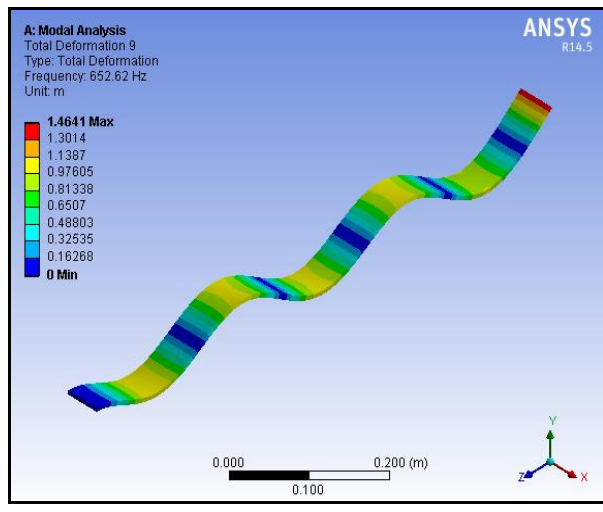


Fig. 4 : Total Deformation-9

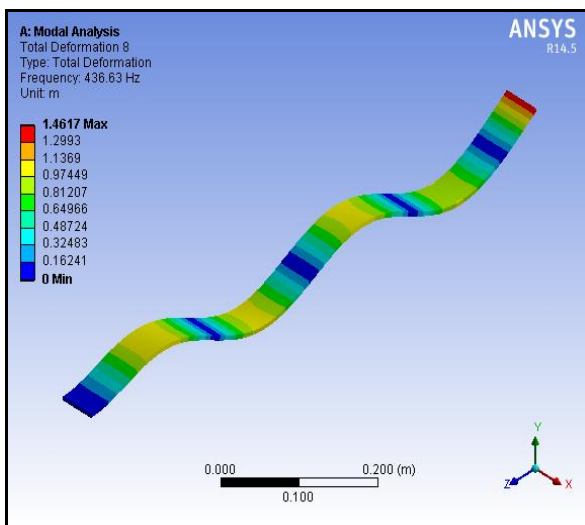


Fig. 5 : Total Deformation-8

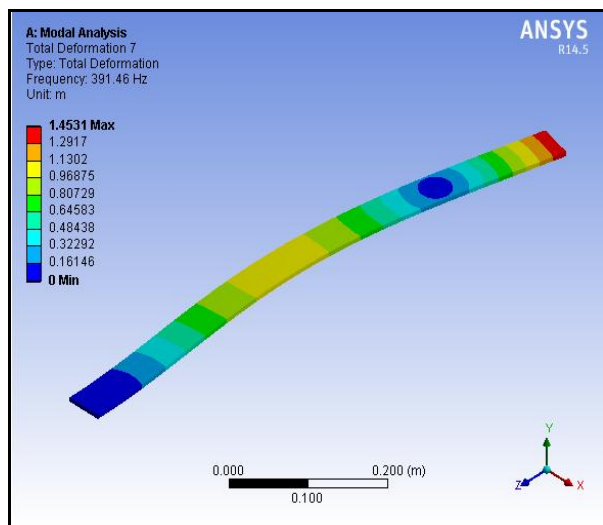


Fig. 6 : Total Deformation-7

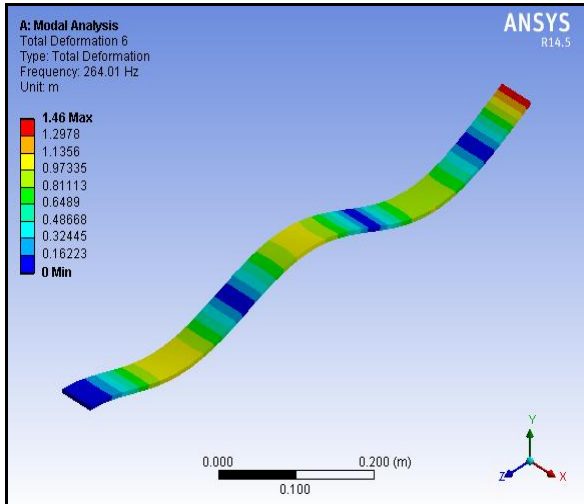


Fig. 7 : Total Deformation-6

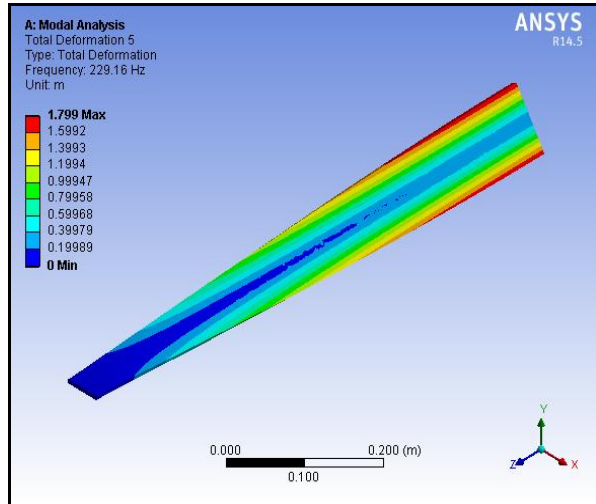


Fig. 8 : Total Deformation-5

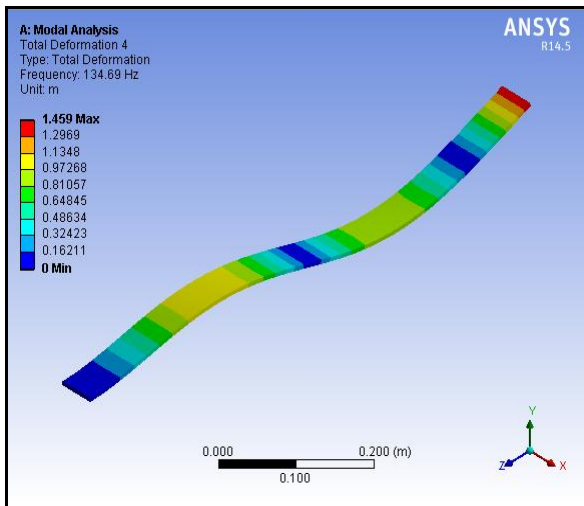


Fig. 9 : Total Deformation-4

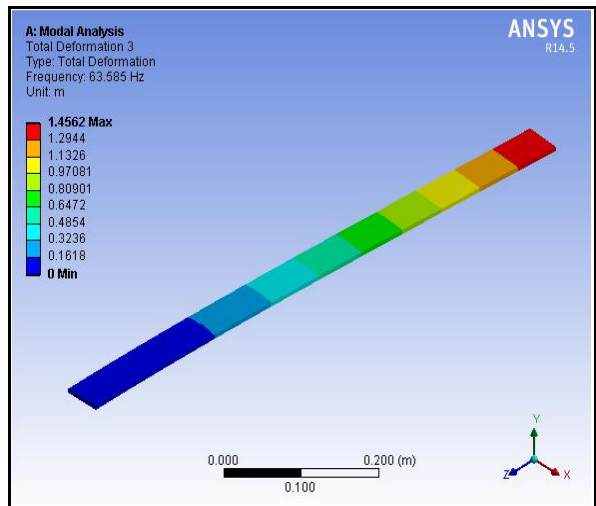


Fig. 10 : Total Deformation-3

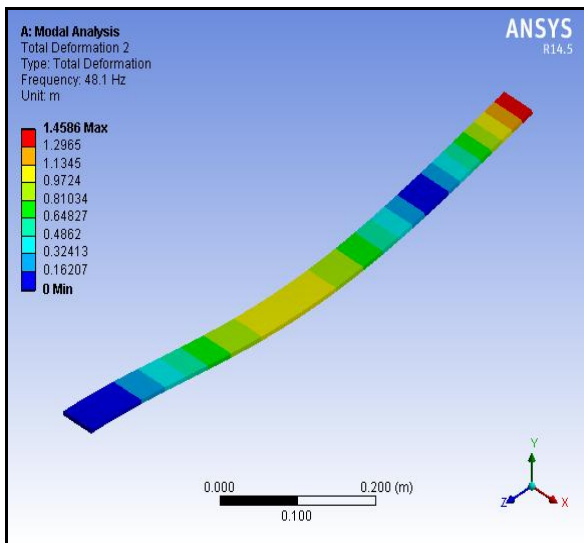


Fig. 11 : Total Deformation-2

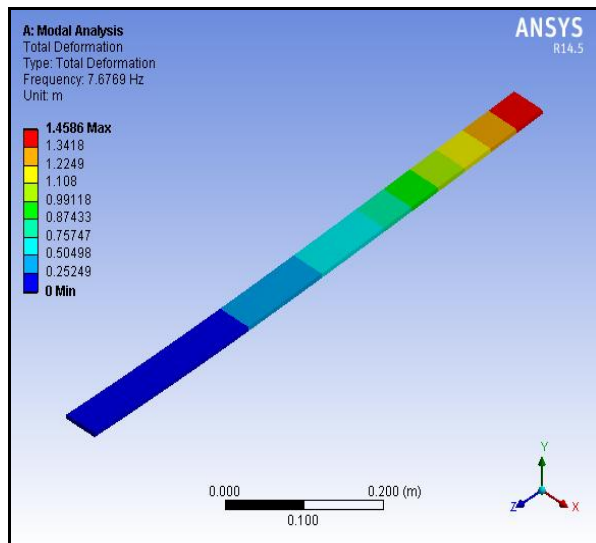
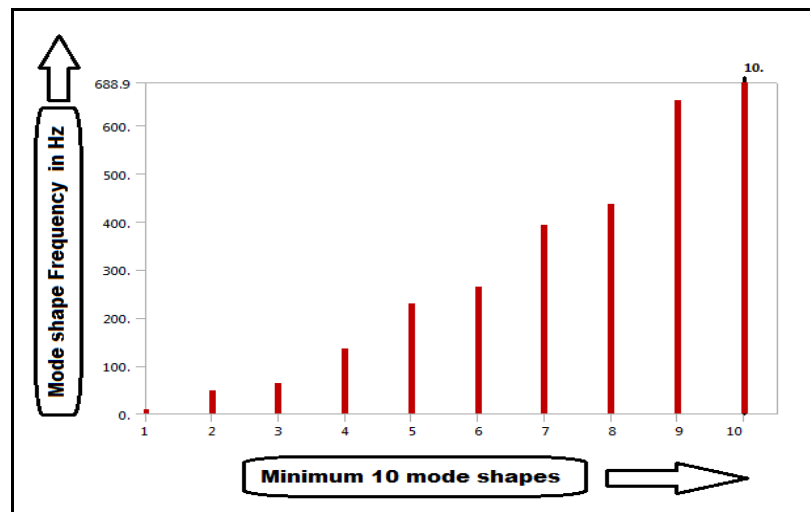


Fig. 12 : Total Deformation-1



Graph. 1 : Graphical representation of the modal frequencies

IV. EXPERIMENTAL ANALYSIS OF TRANSVERSE VIBRATION OF FIXED FREE BEAM:

4.1 Experimental Setup:

The dimensions and the material constant for a uniform fixed free beam (cantilever beam) studied in this paper are: Material of beam = mild steel, Total length (L) = 0.8 m , width (B) = 0.050 m, height (H) = 0.006 m, Young's Modulus (E) = 210×10^9 , mass density = 7856 kg/m^3 . Poisson Ratio= 0.3

A beam which is fixed at one end and free at other end is known as cantilever beam. From elementary theory of bending of beams also known as Euler-Bernoulli. In experiment we will use digital phosphor oscilloscope (Model DPO 4035) for data acquisition.

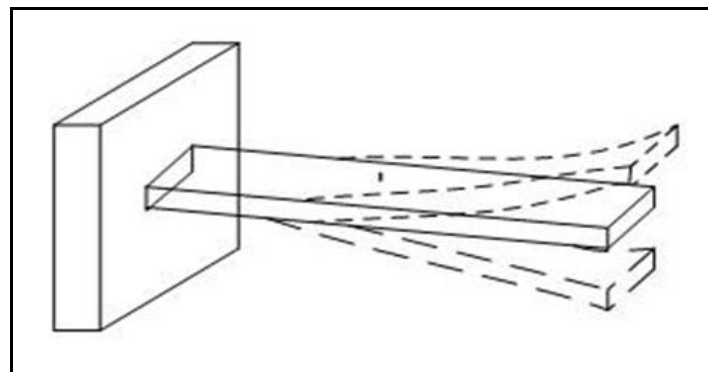


Fig. 13. Free vibration for cantilever

Accelerometer is a kind of transducer to measure the vibration response (i.e., acceleration, velocity and displacement). Data acquisition system acquires vibration signal from the accelerometer, and encrypts it in digital form. Oscilloscope acts as a data storage device and system analyzer. It takes encrypted data from the data acquisition system and after processing (e.g., FFT), it displays on the oscilloscope screen by using analysis software. Fig. shows an experimental setup of the cantilever beam.

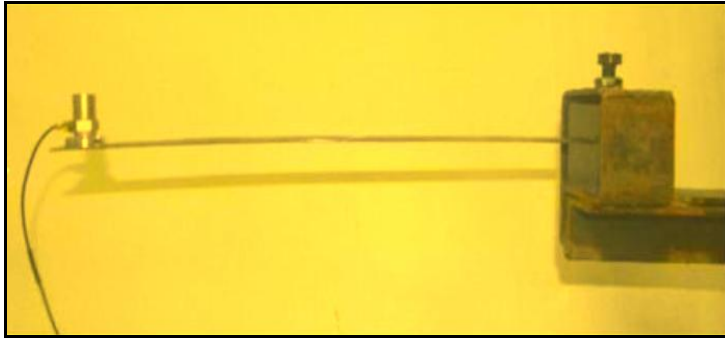


Fig. 14. Experimental setup

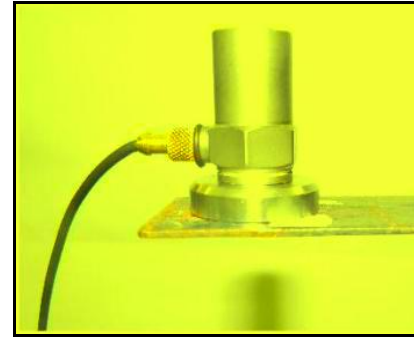


Fig. 15. Closed View of Accelerometer

It includes a beam specimen of particular dimensions with a fixed end and at the free end an accelerometer is clamped to measure the free vibration response. The fixed end of the beam is gripped with the help of clamp. For getting defined free vibration cantilever beam data, it is very important to confirm that clamp is tightened properly; otherwise it may not give fixed end conditions in the free vibration data.

4.2 Experimental Procedure:

- [1] A beam of a particular material (steel, aluminum), dimensions (L, w, d) and transducer (i.e., measuring device, e.g. strain gauge, accelerometer, laser vibrato meter) was chosen.
- [2] One end of the beam was clamped as the cantilever beam support.
- [3] An accelerometer (with magnetic base) was placed at the free end of the cantilever beam, to observe the free vibration response (acceleration).
- [4] An initial deflection was given to the cantilever beam and allowed to oscillate on its own. To get the higher frequency it is recommended to give initial displacement at an arbitrary position apart from the free end of the beam (e.g. at the mid span).
- [5] This could be done by bending the beam from its fixed equilibrium position by application of a small static force at the free end of the beam and suddenly releasing it, so that the beam oscillates on its own without any external force applied during the oscillation.
- [6] The free oscillation could also be started by giving a small initial tap at the free end of the beam.
- [7] The data obtained from the chosen transducer was recorded in the form of graph (variation of the vibration response with time).
- [8] The procedure was repeated for 5 to 10 times to check the repeatability of the experimentation.
- [9] The whole experiment was repeated for same material, dimensions, and measuring devices.
- [10] The whole set of data was recorded in a data base.

4.3 Experimental Results:

To observe the natural frequencies of the cantilever beam subjected to small initial disturbance experimentally up to third mode, the experiment was conducted with the specified cantilever beam specimen. The data of time history (Displacement-Time), and FFT plot was recorded. The natural frequencies of the system can be obtained directly by observing the FFT plot. The location of peak values relates to the natural frequencies of the system. Fig. below shows a typical FFT plot.

Table 2: Mode shape frequency by Using Experimental Method

Mode	Experimental frequency in Hz
1	7.6769
2	48.1001
3	63.5854
4	134.6906
5	229.1626
6	264.0133
7	391.4638
8	436.6341
9	652.6247
10	688.8954

The present experimental results are based on the assumption that one end of the cantilever beam is properly fixed. However, in actual practice it may not be always the case because of flexibility in support. The experimental values obtained are 7.6769 Hz and 688.8954Hz for first and last modes respectively.

V. SUMMARY OF RESULT

The numerical (FEA) calculated natural frequency and the experimental are found good agreement. The correction for the mass of the sensor will improve the correlation better. The present numerical (FEA) results and experimental results is based on the assumption that one end of the cantilever beam is properly fixed. However, in actual practice it may not be always the case because of flexibility in support. The summary of analysis of result summarized as show in table 3.

Table 3: Summary of result in Percentage error

Mode	Numerical (FEA) frequency in Hz	Experimental frequency in Hz	Percentage Error %
1	7.6769	7.6769	0
2	48.1	48.1001	0.0001
3	63.585	63.5854	0.0004
4	134.69	134.6906	0.0006
5	229.16	229.1626	0.0026
6	264.01	264.0133	0.0033
7	391.46	391.4638	0.0038
8	436.63	436.6341	0.0041
9	652.62	652.6247	0.0047
10	688.89	688.8954	0.0054

VI. CONCLUSION

We have studied the free vibration of fixed free beam by using experimental approach and the numerical (FEA) approach using the ANSYS program, it has been found that the relative error between these two approaches are very minute. The percentage error between the numerical (FEA) approach and the experimental approach are allowed up to 5% to 7%. Firstly we obtained the results for mode shape frequency numerically (FEA) and analyzing this mode shape frequency by experimental on the fixed free beam which we were used in this paper. The numerical study using the ANSYS program allows investigates the free vibration of fixed free beam to find out mode shape and their frequencies with high accuracy. The experimental mode shape frequency values are also compared with the numerical (FEA) results that are obtained from the ANSYS software. It is observed that the numerical (FEA) results values are in-tuned with the experimental values. The procedure and experimental models that are used in this paper are very useful to researchers who willing to work experimental analysis.

VII. ACKNOWLEDGEMENTS

We gratefully acknowledge department of mechanical engineering of **Rajarshri College of Engineering, Tathawade, Pune (India)**, for technical support and providing the research facilities. Their help and dedication toward our work and related research, also their library staff and expert for their directly & indirectly help, support and excellent co-operation.

REFERENCES

Journal Papers:

- [1] Thin-Lin Horng, "Analytical Solution of Vibration Analysis on Fixed-Free Single-Walled Carbon Nanotube-Based Mass Sensor", Journal of Surface Engineered Materials and Advanced Technology, 2012; 2(1): PP 47-52.
- [2] J S Wu And H-M Chou, "Free Vibration Analysis Of A Cantilever Beam Carrying Any Number Of Elastically Mounted Point Masses With The Analytical-And-Numerical-Combined Method", Journal of Sound and Vibration, 1998, 213(2): PP 317-332.
- [3] Tarsicio Belezandez, Cristian Neipp, "Numerical and Experimental Analysis of a Cantilever Beam: a Laboratory Project to Introduce Geometric Nonlinearity in Mechanics of Materials", Int. J. Engng Ed., 2003;19(6): PP 885 -892.

- [4] J. J. Wu and A. R. Whittaker, "The Natural Frequencies and Mode Shapes Of A Uniform Cantilever Beam With Multiple Two-DOF Spring Mass Systems", Journal of Sound and Vibration, 1999; 227 (2): PP 361-381.
- [5] S.S Queini, A.H Nayfeh, single mode control of a cantilever beam under principal parametric excitation, journal of sound and vibration 224 (1999) 3347.
- [6] M.MKannel, Y.A.Amer, response of parametrically excited one degree of freedom system with non linear damping and stiffness, Physica Scripta 66 (2002) 410-416.
- [7] C.Chin, A.H.Nayfeh, W. Lacarbonara, two-to-one internal resonance in parametrically excited buckled beam, AIAA , 1997; 97 : 1081
- [8] Haxton RS, Barr ADS. The auto parametric vibration absorber, ASME J.Eng Industry 1972; 94:119-25.
- [9] Brian J. Schwarz & Mark H. Richardson, " EXPERIMENTAL MODAL ANALYSIS", CSI Reliability Week, Orlando, FL, Oct-1999.
- [10] D. Ravi Prasad and D.R. Seshu "A STUDY OF DYNAMIC CHARACTERISTIC OF STRUCTURAL MATERIALS USING MODAL ANALYSIS" Asian journal of civil engineering.
- [11] D.Y. Zheng. Free Vibration Analysis Of A Cracked Beam By finite Element Method. Journal of Sound and Vibration, 2004: 457-475.
- [12] Huszar, Zsolt. Vibration of cracked reinforced and prestressed concrete beams Architecture and Civil Engineering, Vol. 6, 2008: 155-164
- [13] G.M.Owolabi, Swamidias, Seshadri Crack detection in beams using changes in frequencies and amplitudes of frequency response functions. Journal of Sound and Vibration, 265(2004) 1-22
- [14] M.Behzad, Ebrahimi, A.Meghdari. A continuous vibration theory for beams with a vertical edge crack. Mechanical Engineering, Vol. 17, 2010: 194-204.
- [15] E. I. Shifrin. "Natural Frequencies Of A Beam With An Arbitrary Number Of Cracks." Journal of Sound and Vibration, 222(3), 1999: 409-423

AUTHOR'S BIOGRAPHY:



Mr. S. P. Chaphalkar:

Currently working as Head of Department, in *Automobile Engineering Department* at Pimpri Chinchwad, Polytechnic, Pune (India) Total experience in teaching 20 Years.

Email: chaphalkar77@gmail.com



Mr. Subhash N. Khetre:

Currently working as a Lecturer, in *Mechanical Engineering Department* at Rajarshri Shahu College of Engineering, Tathawade, Pune (India) Total experience in teaching 3.5 Years.

Email: subhash2010khetre@gmail.com



Mr. Arun M. Meshram:

Currently working as a Lecturer, in *Mechanical Engineering Department* at Rajarshri Shahu College of Engineering, Tathawade, Pune (India) Total experience in teaching 6 Years.

Email: arunmeshram82@gmail.com

Unsteady Similarity Solution of Free convective boundary layer flow over porous plate with variable properties considering viscous dissipation and Slip Effect

Md.Jashim Uddin

(Electrical & Electronic Engineering, International Islamic University Chittagong, Bangladesh)

Abstract: The combined effects of viscous dissipation and slip effect on the momentum and thermal transport for the unsteady boundary layer flow over porous plate have been carried out. We have applied free parameter method to solve governing partial differential equations. The governing non-linear partial differential equations are transformed into a system of coupled non-linear ordinary differential equations using similarity transformations and then solved numerically using the Runge–Kutta method with shooting technique for better accuracy. The flow and temperature fields as well as the free convective parameter and heat transfer coefficient are determined and displayed graphically involved in the similarity transformation. Effects of the slip parameter, free convection parameter, Prandtl number and unsteadiness parameter on the flow and heat transfer are examined and analyzed.

Keywords: Free convection, Partial Slip, Similarity solution, Unsteady, Viscous dissipation

I. INTRODUCTION

In the recent years free convective boundary layer flows have a great interest from both theoretical and practical point of views because of its vast and significant applications in cosmic fluid dynamics, solar physics, geophysics, electronics, paper production, wire and fiber coating, composite processing and storage system of agricultural product etc.

The study of boundary layer flow over porous surface moving with constant velocity in an ambient fluid was initiated by Sakiadis [1]. Erickson et al. [2] extended Sakiadis [1] problem to include blowing or suction at the moving porous surface. Subsequently Tsou et al. [3] presented a combined analytical and experimental study of the flow and temperature fields in the boundary layer on a continuous moving surface. R. Ellahi et al. [4] investigated numerical analysis of unsteady flows with viscous dissipation and nonlinear slip effects. Excellent reviews on this topic are provided in the literature by Nield and Bejan [5], Vafai [6], Ingham and Pop [7] and Vadasz [8]. Recently, Cheng and Lin [9] examined the melting effect on mixed convective heat transfer from a permeable over a continuous Surface embedded in a liquid saturated porous medium with aiding and opposing external flows. The unsteady boundary layer flow over a stretching sheet has been studied by Devi et al. [10], Elbashaeshy and Bazid [11], Tsai et al. [12] and Ishak [13].

Andersson et al. [14] investigated using a similarity transformation the flow of a thin liquid film of a power-law fluid by unsteady slip surface. Ellahi et al. [15] discussed Analysis of steady flows in viscous fluid with heat/mass transfer and slip effects. Zeeshan and Ellahi [16] studied Series solutions for nonlinear partial differential equations with slip boundary conditions for non-Newtonian MHD fluid in porous space. Williams *et al.*, [17] studied the unsteady free convection flow over a vertical flat plate under the assumption of variations of the wall temperature with time and distance. They found possible semi-similar solutions for a variety of classes of wall temperature distributions. Kumari *et al.*, [18] observed that the unsteadiness in the flow field was caused by the time dependent velocity of the moving sheet. Hong et al. [19], Chen and Lin [20] and Jaisawal and Soundalgekar [21] studied the free convection in a porous medium with high porosity. After a pioneering work of Sakiadis [22,23] the study of flow and heat transfer characteristics past continuous stretching surfaces has drawn considerable attention, and a good amount of the literature has been generated on this problem for instance [24]. The effects of slip boundary condition on the flow of Newtonian fluid due to a stretching sheet were explained by Andersson [25] and Wang [26]. Although various aspects of this class of boundary layer

problems have been tackled, the effect of buoyancy force was ignored. It will be demonstrated that the system of time-dependent governing equations can be reduced to a Some parameter problem by introducing a suitable transformation variables. Accurate numerical solutions are generated by applying shooting method. A comprehensive parametric study is conducted and a representative set of graphical results for the velocity slip and thermal slip parameter are reported and discussed. The analysis showed that the unsteadiness parameter, buoyancy force, free convection parameter and viscous dissipation have significant influence on the flow and thermal fields.

II. MATHEMATICAL ANALYSIS

Consider the unsteady-two-dimensional free convection boundary layer flow of viscous dissipating incompressible fluid embedded in a porous medium and moving with variable velocity. Under the usual boundary-layer approximation, the governing equations for the flow and heat and mass transfer have the form:

$$\frac{\partial u}{\partial x} + \frac{\partial v}{\partial y} = 0 \quad (1)$$

$$\frac{\partial u}{\partial t} + u \frac{\partial u}{\partial x} + v \frac{\partial v}{\partial y} = \nu \frac{\partial^2 u}{\partial y^2} + g\beta^*(T - T_\infty) \quad (2)$$

$$\frac{\partial T}{\partial t} + u \frac{\partial T}{\partial x} + v \frac{\partial T}{\partial y} = \frac{k}{\rho c_p} \frac{\partial^2 T}{\partial y^2} \quad (3)$$

where x and y are axes along and perpendicular to the plate respectively, u and v are velocity components in x - and y -directions respectively, ρ is the fluid density, μ is the coefficient of fluid viscosity, ν is the kinematic fluid viscosity, β is the volumetric coefficient of thermal expansion, g is the acceleration due to gravity, T is the temperature, T_∞ is the free stream temperature, k is the thermal conductivity of the fluid and c_p is the specific heat and the other symbols have their usual meanings.

The corresponding boundary conditions are:

$$u = L_1 \left(\frac{\partial u}{\partial y} \right), v = 0 \text{ at } y = 0; u \rightarrow U_\infty \text{ as } y \rightarrow \infty \quad (4)$$

$$\text{and } T = T_w + D_1 \left(\frac{\partial T}{\partial y} \right) \text{ at } y = 0; T \rightarrow T_\infty \text{ as } y \rightarrow \infty \quad (5)$$

Here L_1 and D_1 is the velocity slip factor and thermal slip factor respectively.

The continuity equation (1) is satisfied by introducing the stream function $\psi(x, y)$, such that $u = \frac{\partial \psi}{\partial y}$, $v = -\frac{\partial \psi}{\partial x}$

The momentum and energy equations (2) and (3) can be transformed to the corresponding ordinary differential equations by introducing the following similarity transformations:

$$\psi = \sqrt{U_\infty x \nu t} f(\eta) \quad \eta = y \sqrt{\frac{U_\infty}{\nu x t}}, \theta(\eta) = \frac{(T - T_\infty)}{(T_w - T_\infty)} \quad (6)$$

where ν_∞ is a reference kinematic viscosity.

If $U = U_\infty = ax$, $x = \delta$, $t = \mu$ then the momentum and energy equations (2) – (3) after some simplifications, reduce to the following forms:

$$f''' + \frac{1}{2} A f f'' + A_1 \eta f'' + \lambda \theta = 0 \quad (7)$$

where $\lambda = \frac{g\beta^*(T_w - T_\infty)\delta\mu}{U_\infty^2}$ (Free convection parameter), $A = \mu$ (Unsteadiness parameter) and $A_1 = \frac{1}{a}$

$$\theta'' + A_1 P_r \eta \theta' + A P_r f \theta' = 0 \quad (8)$$

where $P_r = \frac{\rho c_p \nu}{2k}$ (Prandtl number) .

The corresponding boundary conditions are:

$$f = 0; f' = \xi f''; \text{ at } \eta = 0; f' \rightarrow 1 \text{ as } \eta = \infty \quad (9)$$

$$\text{and } \theta = 1 + \tau \theta' \text{ at } \eta = 0; \theta \rightarrow 0 \text{ as } \eta = \infty \quad (10)$$

Where the prime ($'$) denotes differentiation with respect to η and ξ is the velocity slip parameter, τ is the thermal slip parameter.

It is important to note that for liquids ($Pr > 1.0$) and for gases ($Pr < 1.0$).

The equations (8) and (9) constitute a non-linear coupled boundary value problem prescribed at two boundaries, the analytical solution of which is not feasible. Therefore, these equations have been solved numerically on computer using Newton's shooting techniques with the Runge-kutta Gill method with a step size of 0.01. The corresponding velocity and temperature profiles are shown in figure.

III. RESULT AND DISCUSSION

In order to get clear insight into the physics of the problem, a parametric study is performed and the obtained numerical results are displayed with the help of graphical illustrations. The profiles for velocity and temperature are shown in fig.1 to fig.6.

3.1 Effect of initial boundary condition:

It is seen from fig.1 that the velocity and shear stress profiles for free convection flow for no-slip condition at the boundary $\lambda = 0, \tau = 0, \xi = 0$

3.2 Effect of free convection parameter:

In the fig.2(a), the buoyancy aiding flow ($\lambda > 0$), increase in free convection parameter will increase the velocity inside the boundary layer due to favourable buoyancy effects in both slip and no-slip cases and consequently heat transfer rate from the plate will increase. In the fig.2(b), the shear stress profile $f''(\eta)$ though initially increases with λ but it decreases for large η . From the fig.2(c) it is found that for the increase of λ the temperature distribution is suppressed in case of slip as well as no-slip condition and consequently the thermal boundary layer thickness becomes thinner. Physically $\lambda > 0$ means heating of the fluid or cooling of the surface of the plate (assisting flow).

3.3 Effect of the velocity slip parameter:

In Fig.3(a)-3(b) the velocity $f'(\eta)$ and shear stress $f''(\eta)$ profiles exhibit opposite character before and after some points. With increasing values of ξ , the velocity increases up to $\eta \approx 2.72$ and then decreases. Also, the dimensionless shear stress decreases up to $\eta \approx 3.52$ and after that it increases. In fig.3(c) it is observed that the temperature decreases significantly with the increase in slip parameter ξ and also the thickness of the thermal boundary layer reduces.

3.4 Effect of the Prandtl number:

From the fig.4(a)-4(c) it is observed that The velocity $f'(\eta)$ along the plate decreases with increase in Pr for both slip and no-slip cases and the profile $f''(\eta)$ decreases up to a point, then increases.

In both cases, as Prandtl number increases, the temperature at every location in the thermal boundary layer decreases. The thickness of the boundary layer decreases as Prandtl number increases which is usual case of an isothermal flat plate with no-slip.

3.5 Effect of the thermal slip parameter:

Variations of velocity, shear stress and temperature due to thermal slip parameter are presented in fig.5(a)-5(c).

As the thermal slip parameter increases, the velocity increases and the shear stress at first increases and then after a point

($\eta \approx 1.26$) it decreases. This happens due to the combined

effects of free convection and velocity slip. From fig.5(c) we observed that with the increasing thermal slip, the temperature rises above the plate temperature T_w before it decays to the ambient temperature T_∞ .

3.6 Effect of the Skin-friction coefficient and Temperature gradient:

It is seen from the fig.6(a)-6(b) that it indicates the effects of velocity slip and thermal slip on skin friction coefficient and temperature gradient at the plate. Although the skin friction coefficient increases with increasing thermal slip parameter but it decreases with increasing velocity slip. Plate temperature gradient is found to increase with the increasing thermal slip parameter as well as with the increasing velocity slip parameter.

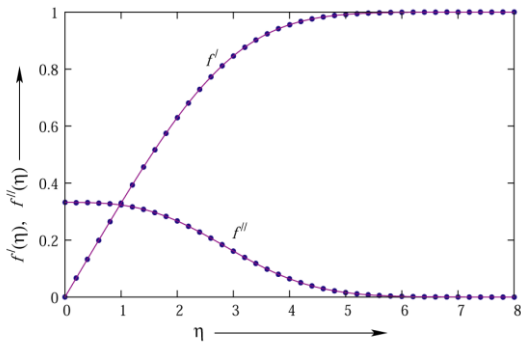


Fig. 1 Velocity profile $f'(\eta)$, and shear stress profiles $f''(\eta)$ for $\lambda = 0, \xi = 0, \tau = 0$.

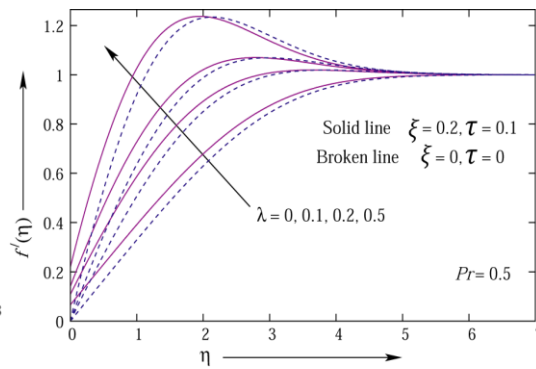


Fig. 2a Velocity profiles $f'(\eta)$ for several values of λ

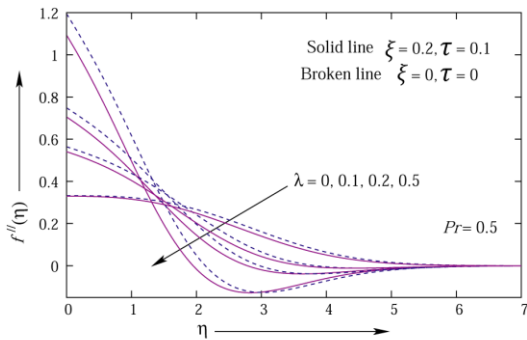


Fig. 2b Shear stress profiles $f''(\eta)$ for several values of λ

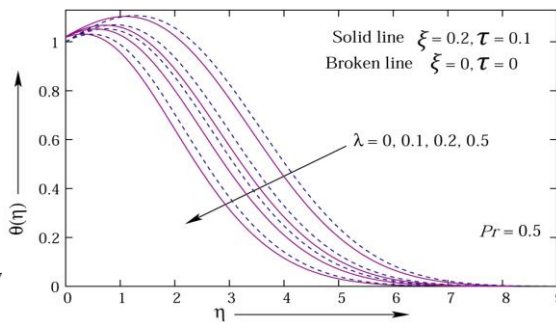


Fig. 2c Temperature profiles $\theta(\eta)$ for several values of λ

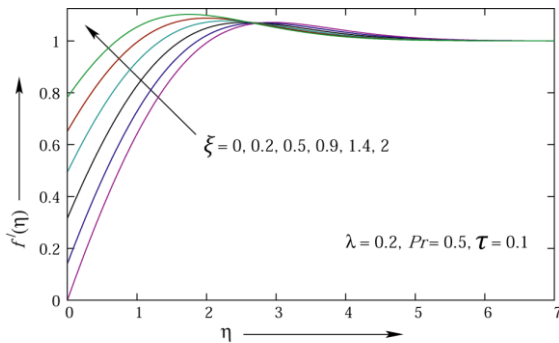


Fig. 3a Velocity profiles $f'(\eta)$ for several values of ξ

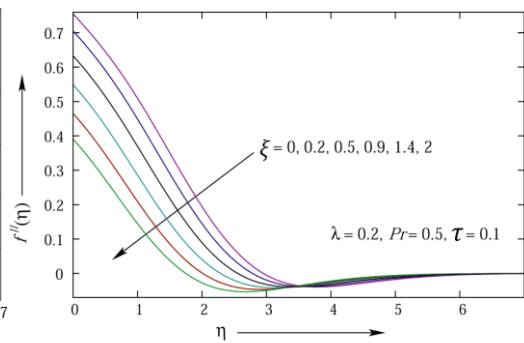


Fig. 3b Shear stress profiles $f''(\eta)$ for several values of ξ

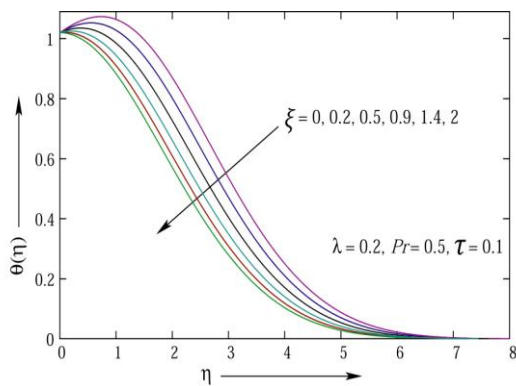


Fig. 3c Temperature profiles $\theta(\eta)$ for several values of ξ

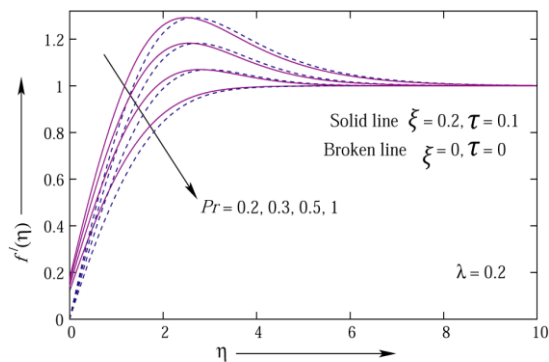


Fig. 4a Velocity profiles $f'(\eta)$ for several values of Pr

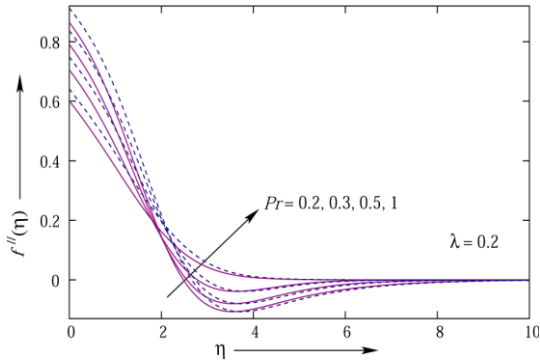


Fig. 4b Shear stress profiles $f''(\eta)$ for several values of Pr

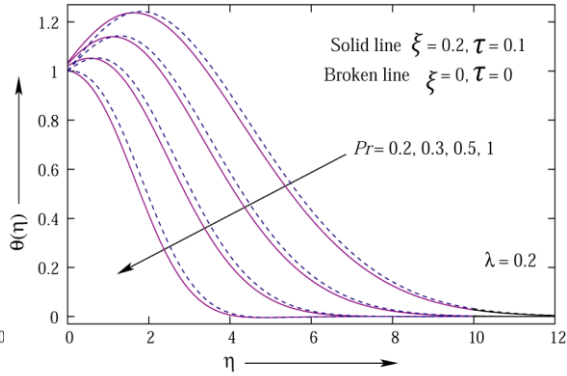


Fig. 4c Temperature profiles $\theta(\eta)$ for several values of Pr

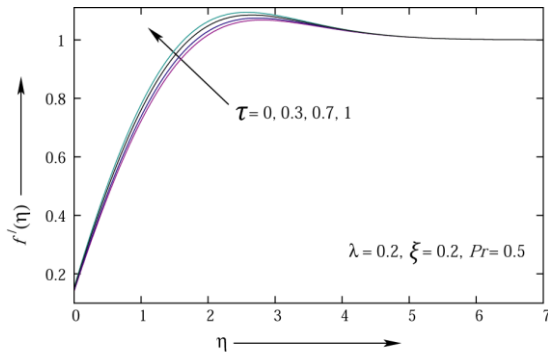


Fig. 5a Velocity profiles $f'(\eta)$ for several values of τ

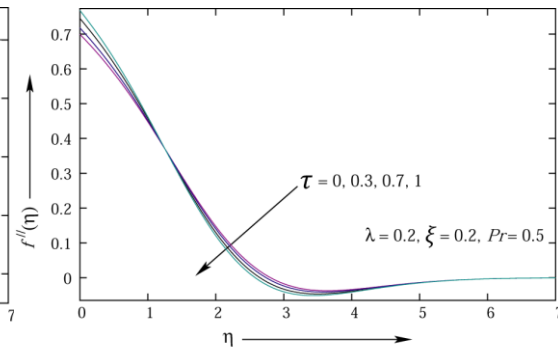


Fig. 5b Shear stress profiles $f''(\eta)$ for several values of τ

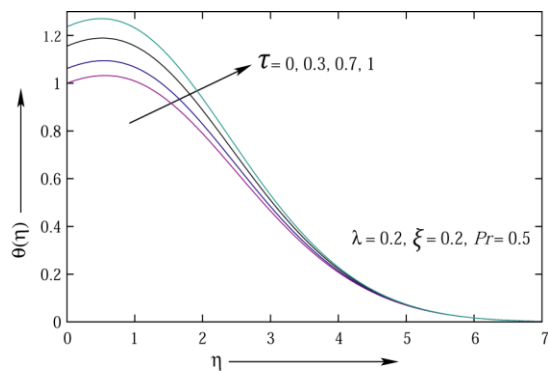


Fig. 5c Temperature profiles $\theta(\eta)$ for several values of τ

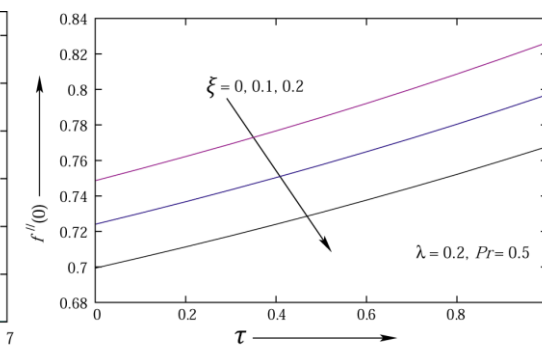


Fig. 6a Skin-friction coefficient $f''(0)$ against τ for various values of ξ

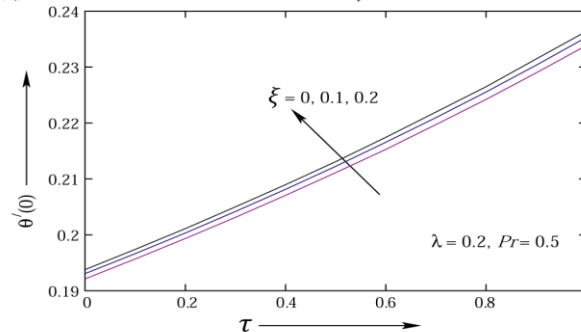


Fig. 6b Temperature gradient at the plate $\theta'(0)$ against τ for various values of ξ

IV. CONCLUSION

From the present study, we have derived a new set of non-linear ordinary differential equations (7) to (8) with boundary conditions (9) and (10) of the unsteady boundary layer free convection flow over porous plate and slip effect. In this paper we have discussed the effects of velocity and thermal slip parameter on an unsteady two dimensional free convective boundary layer flow. The numerical results have been presented in the form of graphs. From the present numerical investigations the following major conclusions may be drawn:

- (i) Velocity and temperature in the unsteady case is observed to be lesser than those of the steady case.
- (ii) It is observed that an increase the free convection parameter, the velocity increases and the temperature decreases.
- (iii) With increasing the values of velocity slip, the velocity increases at a fixed point and then it decreases.
- (iv) The increase of Prandtl number reduces the velocity along the plate as well as the temperature.
- (v) Increasing the thermal slip parameter both velocity and temperature be increased.

References

- [1]. Sakkiadis BC. Boundary layer behaviors on continuous surface. *AIChE*. 1961;7(2):221-225.
- [2]. Erikson LE, Fan LT., Fox VG. Heat and mass transfer on a moving continuous porous plate with suction and injection. *Ind. Eng. Chem. Fundamental*.1966;5:19-25.
- [3]. Tsou FK , Sparrow FM, Goldstien RJ. Flow and heat transfer in the boundary layer in continuous moving surface. *Int. J. Heat Mass transfer*. 1967;10:219-235.
- [4]. Ellahi R, Hameed M. Numerical analysis of steady flows with heat transfer, MHD and Nonlinear slip effects. *International Journal for Numerical Methods for Heat and Fluid Flow*. 2012;22(1):24-38
- [5]. Nield, D.A. and A. Bejan, 2006. *Convection in Porous Media* (3rd Edn.). Springer, New York.
- [6]. Vafai, K. 2005. *Handbook of Porous Media* (2nd Edn.). Taylor & Francis, New York.
- [7]. Ingham, D.B. and I. Pop, 2005. *Transport Phenomena in Porous Media III*. Elsevier, Oxford.
- [8]. Vadasz, P., 2008. *Emerging Topics in Heat and Mass Transfer in Porous Media*. Springer, New York
- [9]. Cheng, W.T. and C.H. Lin, 2007. Melting effect on mixed convective heat transfer with aiding and opposing external flows from the vertical plate in a liquid saturated porous medium. *Int. J. Heat Mass Transfer* 50: 3026-3034.
- [10]. C. D. S. Devi, H. S. Takhar, G. Nath, "Unsteady mixed convection flow in stagnation region adjacent to a vertical surface," *Heat Mass Transfer*, 26(1991) 71-79.
- [11]. E. M. A. Elbasheshy, M. A. A. Bazid, "Heat transfer over an unsteady stretching surface," *Heat Mass Transfer*, 41(2004) 1-4.
- [12]. R. Tsai, K. H. Huang, J. S. Huang, "Flow and heat transfer over an unsteady stretching surface with non-uniform heat source," *Int. Commun. Heat Mass Transfer*, 35(2008) 1340-1343.
- [13]. A. Ishak, Unsteady, "MHD flow and heat transfer over a stretching plate," *J. Applied Sci.* 10(18)(2010) 2127-2131.
- [14]. Andersson, H.I. Aarseth, J.B. and Dandapat, B.S.: Heat transfer in a liquid film on unsteady slip stretching surface. *International Journal of Heat and Mass Transfer*. 43(1), 69–74, (2000).
- [15]. Ellahi, R., Shivanian, E., Abbasbandy, S., Rahman, S. U., and Hayat, T.: Analysis of steady flows in viscous fluid with heat/mass transfer and slip effects. *International Journal of Heat and Mass Transfer*. 55, 6384-6390, (2012).
- [16]. Zeeshan, A. and Ellahi, R.: Series solutions for nonlinear partial differential equations with slip boundary conditions for non-Newtonian MHD fluid in porous space. *Applied Mathematics & Information Sciences*. 7 (1), 253-261, (2013).
- [17]. Williams J. C., Mulligan J. C. and Rhyne T. B. 1987. Semi-similar solutions for unsteady free convection boundary Layer flow on a vertical flat plate. 175: 309-332.
- [18]. Kumari M., Slaouti A., Nakamura S., Takhar H. S. and Nath G. 1986. Unsteady free convection flow over a continuous moving vertical surface. *Acta Mechanica*. 116: 75-82.
- [19]. Hong .J.T., Tien, C.L. and Kaviany, M (1985), Non-Darcian effects on vertical-plate natural convection in porous media with high porosities, *Int. J. Heat Mass Transfer* Vol.28, pp. 2149-2175.
- [20]. Chen.C.K. and Lin, C.R. (1995), Natural convection from an isothermal vertical surface embedded in a thermally stratified high-porosity medium, *Int. J. Engg. Sci.*, Vol.33, pp.131-138. [21] Jaisawal, B.S. and Soundalgekar, V.M. (2001), Oscillating plate temperature effects on a flow past an infinite vertical porous plate with constant suction and embedded in a porous medium, *Heat Mass Transfer* ,Vol.37, pp.125-131.
- [22]. B.C. Sakiadis, Flow and heat transfer in the boundary layer on a continuous moving surface, *AIChE J.* 7 (1) (1961) 26–28.
- [23]. B.C.Sakiadis, Boundary layer behavior on continuous solid surface, II. The boundary layer on a continuous flat surface, *AIChE J.*7 (1) (1961) 221–225.
- [24]. F.K. Tsou, E.M. Sparrow, R.J. Goldstein, Flow and heat transfer in the boundary layer on a continuous moving surface, *Int. J. Heat Mass Transfer* 10 (1967) 219–235.
- [25]. Andersson HI. Slip flow past a stretching surface. *Acta Mech* 2002;158:121–5.
- [26]. Wang CY. Flow due to a stretching boundary with partial slip –an exact solution of the Navier-Stokes equations. *Chem Eng Sci* 2002;57:3745–7.

Causes of Borehole Failure in Complex Basement Terrains: ABUAD Case Study, Southwestern Nigeria

^{1*} Ogundana, A.K , ² Aladesanmi A. O., ³ Okunade A., ⁴ Olutomilola O.O

Department of Geology, Afe Babalola University, Ado-Ekiti.

ABSTRACT : *A preliminary assessment of primary causes of borehole failure has been conducted using Afe Babalola University as a case study. A total of fourteen boreholes (namely borehole 1-14) were studied, vertical electrical soundings, depth sounding, flushing and pump testing were conducted on each of the boreholes to establish their status at the time of the study and possible evaluation of the groundwater potential of the wells. Four out of the fourteen boreholes (borehole 1-4) are productive and in-use, while the remaining ten (borehole 5-14) are out-of-use and abandoned for various. The productive holes were able to support continuous flow of water for over 3 hours without drop in volume of water flow. Seven of the holes (boreholes 5, 6, 8, 9, 11, 12 & 14) failed and were abandoned because of low yield (could not flow beyond 5 minutes), while the remaining three (boreholes 7, 10 & 13) failed and were abandoned due to wrong location and improper completion, caving/formation problems, and wrong installation/completion respectively. Proper well completion is essential in areas prone to caving and other formation related problems. Air drilling should be avoided in areas with thick and loose overburden. Right mixture of drilling mud should be applied to secure the hole wall while flushing should be continuous throughout drilling in such formation. Casing should be done immediately and such holes should be lined and grouted. Timers should be installed on low yield wells and regulated/programmed for 5 or 10 minutes flow depending on the recharge rate. Pump rating for installation should be strictly based on well recharge rate. Productive wells should be properly maintained and monitored for optimal performance.*

KEYWORDS: *Caving, Loose overburden, Improper completion, Grouting, Optimal performance.*

I. INTRODUCTION

The rate of borehole failure has been alarming in recent time. High expectations from borehole yield and the huge amount of resources involved in sinking a borehole are making such failures unbearable and unacceptable. The unprofessional approach of many drillers are partly responsible for the failure while the role of poor maintenance culture and practices are also hindering optimal well performance. The need for careful, detailed geophysical study in citing borehole location and appropriate completion design cannot be overemphasized. Groundwater exploration reports around Ado-Ekiti suggest low fracture in most part of this state capital. This results in low yield in most of the boreholes own by private individual and public.

Several workers such as Dutcher and Garret (1965), Clerk (1985), Olorunfemi and Olorunniwo (1985), Olorunfemi (1990), Olayinka and Olorunfemi (1992) Olorunfemi and Olayinka (1992), Olorunfemi and Fasuyi (1993), Oladipo et al, (2005) Olayinka and Weller (1993), Rehil and Birk (2010), Ojo et al, (2011), Talabi (2013) have carried research in various aspect of groundwater exploration/investigation, evaluation and structural delineation using geophysical methods in several location within the basement complex terrain around the world.

Groundwater exploration in the basement aquifers posed a serious challenge resulting from complexity of rocks and minerals and their attendant heterogeneous grain size distribution. Olayinka and Olorunfemi (1992) emphasized the need to conduct a surface geophysical survey such as Vertical Electrical Resistivity Sounding in identifying the localized aquiferous zones before siting boreholes. Electrical resistivity method has been used extensively in groundwater investigation especially in the basement complex terrains (Grant and West, 1965, Olorunfemi and Olorunniwo, 1985. Olorunfemi, 1990. Olorunfemi and Olayinka, 1992). Recently, Ademiluwa and Eluwole 2013 evaluated groundwater potential of some part of the university and concluded that weathered basement and fractured basement constitute the main aquifer types within the study area based on their layer thicknesses and resistivity.

Afe Babalola University (ABUAD) has a total of 30 boreholes to cater for the daily water requirement of the University; however, some of the boreholes have failed due to various reasons. This study therefore aims at assessing the primary causes of borehole failure in basement complex using ABUAD as a case study

II. LOCATION AND GEOLOGY OF THE STUDY AREA

2.1 Location

Afe Babalola University is located in Ado-Ekiti along Ijan road, opposite The Federal Polytechnics. The study area is randomly selected within the university campus. The terrain is gently undulating, with topographic elevation ranging from 345m to 370m above sea level. Ado Ekiti is underlain by crystalline rocks made of Older granite, Migmatite and Charnockites, with little or no fracture in most location and shallow overburden.

2.2 Climate, Geology and Hydrogeology of The Area

The area is situated within the tropical rain forest region, with a climate characterized by dry and wet seasons. Average annual rainfall in this area is 1300 mm, with average wet days of about 100. The annual temperature varies between 18°C to 34°C. The study area lies within the basement complex of south-western Nigeria and is made up of; older granite, Migmatite and Charnockites. The overburden is relatively shallow within the study area with average of 9.6m. The groundwater is found within the overburden and fractured basement while the area is drained by the river Ogbese which flow SW-NE direction. The basement complex rocks are poor aquifers as they are characterized by low porosity and negligible permeability, resulting from their crystalline nature.

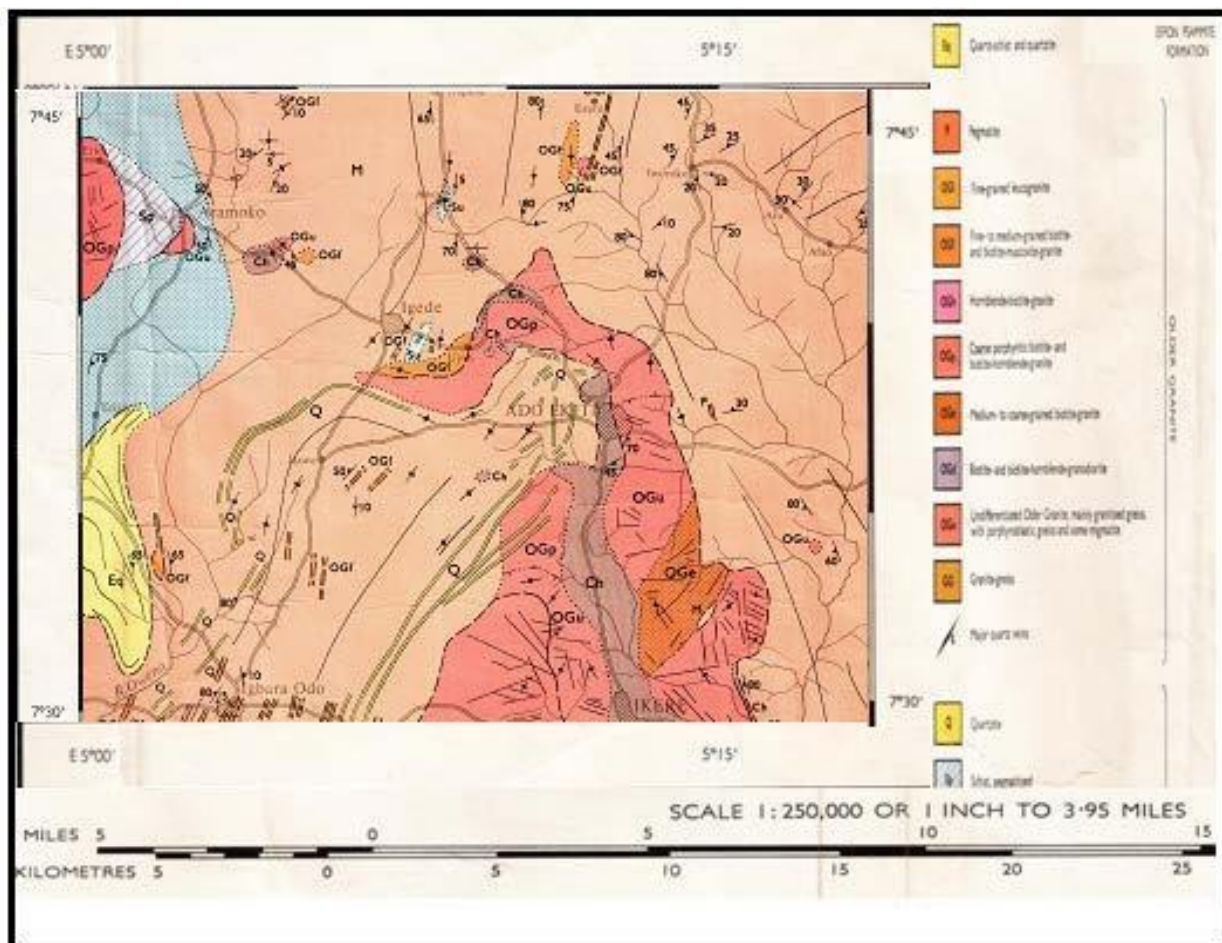


Fig. 1. Geological Map of the study area (Adapted from NGSA)

III. Methodology, Data acquisition and Interpretation

A reconnaissance survey of study area was carried out for site familiarization, planning and selection of the wells for the study. This was followed with geophysical investigation of the wells, flushing, depth sounding and pump testing. Resistivity sounding was adopted in resolving resistivity variation with depth, thus sounding helped in delineating the various subsurface lithological units, aquiferous layers and their hydrogeological significance.

IV. RESULTS AND DISCUSSIONS

4.1 Vertical Electrical Sounding

A total of 14 selected boreholes across the study area were sounded. The processed data were interpreted, resulting curve types were assessed, existing subsurface lithologic units were established, and the geoelectric properties of the various subsurface layers were used in delineating the aquiferous units in the study area. Field observations were made, flushing and pump testing were conducted on the boreholes. Status of each of the boreholes at the time of the study were established. The results are presented in the form of table (Table 1), geoelectric curves (Figure 2a, b, c & d) and sections (Figure; 3a, b, c & d).

Two curve types were obtained from the study area namely; HA and HK. Five geo-electric layers were delineated from the sounding curves namely; top soil, sandy clay, weathered basement, fractured basement and basement. A correlation table was generated by comparing different geo-electric layers revealed by the sounding curves (Table 1). The top soil, sandy clay and weathered basement layers constitute the overburden. Basement is relatively shallow in this area with an average depth-to-basement of 10.8m.

A summary of the results of interpretation, on which the findings were hinged, is shown in figure 2 below.

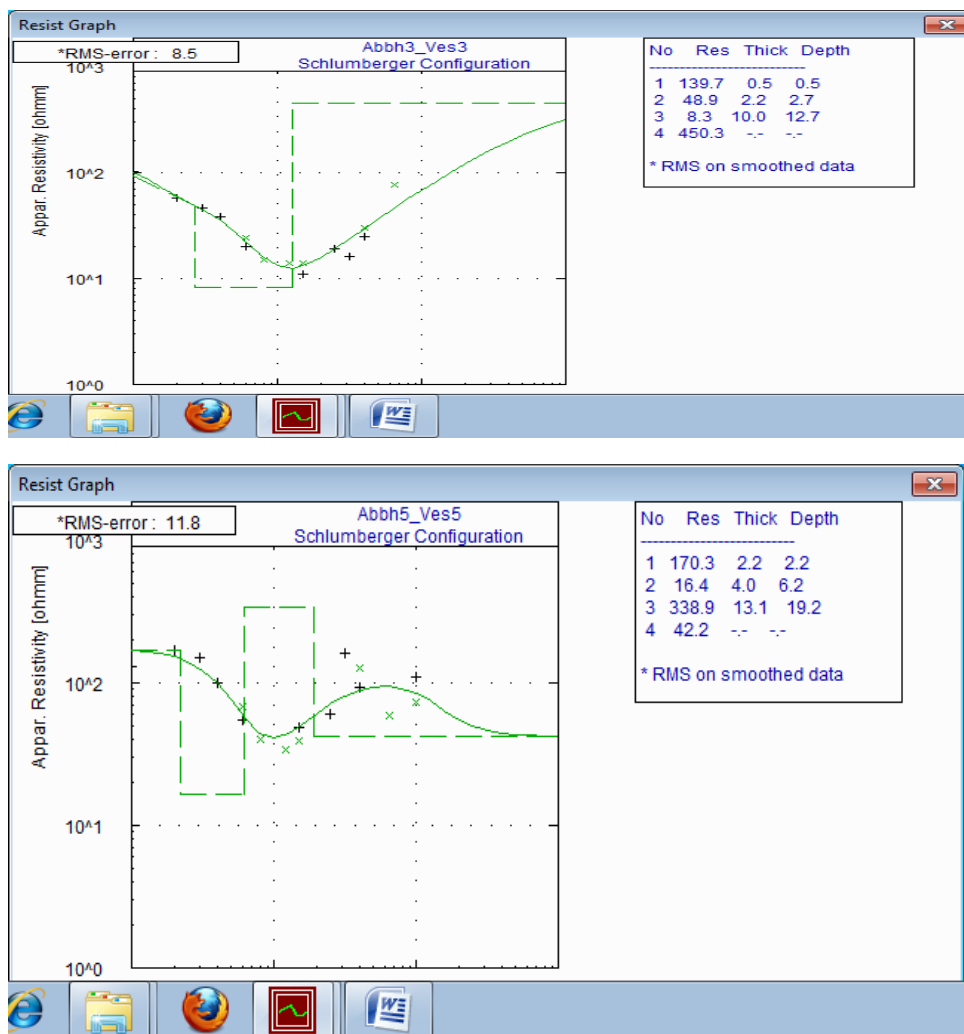


Fig. 2. Typical Geoelectric curves from the study area

Table 1a: Correlation Table

VES POINT		1	2	3	4	5	6	7
CURVE TYPE		HA	HA	HA	HK	HA	HA	HA
LITHOLOGY								
TOP SOIL	TOP	0.0	0.0	0.0	0.0	0.0	0.0	0.0
	BASE	1.0	1.0	3.0	2.0	1.0	1.0	1.0
	THICKNESS	1.0	1.0	3.0	2.0	1.0	1.0	1.0
	Ω_m	123	140	70	170	95	80	110
CLAYEY SAND	TOP	1.0	1.0	3.0	2.0	1.0	1.0	1.0
	BASE	16.0	13.0	11.0	6.0	17.0	16.0	20.0
	THICKNESS	15.0	12.0	8.0	4.0	16.0	15.0	19.0
	Ω_m	49	49	65	16	85	90	60
WEATHERED BASEMENT	TOP	-	-	-	6.0	-	-	-
	BASE	-	-	-	19.0	-	-	-
	THICKNESS	-	-	-	13.0	-	-	-
	Ω_m	-	-	-	339	-	-	-
FRACTURED BASEMENT	TOP	-	-	-	19.0	-	-	-
	BASE	-	-	-	-	-	-	-
	THICKNESS	-	-	-	-	-	-	-
	Ω_m	-	-	-	42	-	-	-
BASEMENT	TOP	16.0	13.0	11.0	-	17.0	16.0	20.0
	Ω_m	256	450	1042	-	397	312	374

Table 1b: Correlation Table

VES POINT		8	9	10	11	12	13	14
CURVE TYPE		HA						
LITHOLOGY								
TOP SOIL	TOP	0.0	0.0	0.0	0.0	0.0	0.0	0.0
	BASE	1.0	3.0	1.0	1.0	1.0	1.0	1.0
	THICKNESS	1.0	3.0	1.0	1.0	1.0	1.0	1.0
	Ω_m	173	152	39	42	78	47	33

CLAYEY SAND	TOP	1.0	3.0	1.0	1.0	1.0	1.0	1.0
	BASE	10.0	15.0	12.0	7.0	7.0	13.0	14.0
	THICKNESS	9.0	12.0	11.0	6.0	6.0	12.0	13.0
	Ωm	30	79	44	54	37	35	14
WEATHERED BASEMENT	TOP	-	-	12.0	-	-	13.0	14.0
	BASE	-	-	-	-	-	-	-
	THICKNESS	-	-	-	-	-	-	-
	Ωm	-	-	183	-	-	163	120
FRACTURED BASEMENT	TOP	-	-	-	-	-	-	-
	BASE	-	-	-	-	-	-	-
	THICKNESS	-	-	-	-	-	-	-
	Ωm	-	-	-	-	-	-	-
BASEMENT	TOP	10.0	15.0	-	7.0	7.0	-	-
	Ωm	274	505	-	349	794	-	-

The correlation tables presents the summary of the different inferred subsurface layers as revealed by the sounding curves.

4.1.1 Geoelectric Units

The geoelectric sections (Figures 3a, b, c & d) show the variations of resistivity and thickness values of layers within the depth penetrated in the study area. Five subsurface layers were revealed: Lateritic Topsoil, Clayey-sand, weathered Basement, Fractured Basement and presumed Fresh basement.

Topsoil

The topsoil is relatively thin across the study area with an average resistivity and thickness values of 97 Ω m and 1.1m respectively.

Clayey-sand

Clayey-sand was encountered across the area with average resistivity and thickness values of 51 Ω m and 13.5m respectively.

Weathered Basement

The weathered basement was encountered in only four of the locations with average resistivity value of 201 Ω m.

Fractured Basement

The fractured basement was encountered in only one of the locations and the resistivity value is 42 Ω m.

Basement

The basement is the fresh bedrock and is the last layer. It is relatively shallow in the study area, it was encountered in ten locations and the average resistivity and depth values to the top of basement are 475 Ω m and 13.2m respectively.

Overburden

The overburden is assumed to include all materials above the presumably fresh basement and they constitute the aquiferous units within the study area.

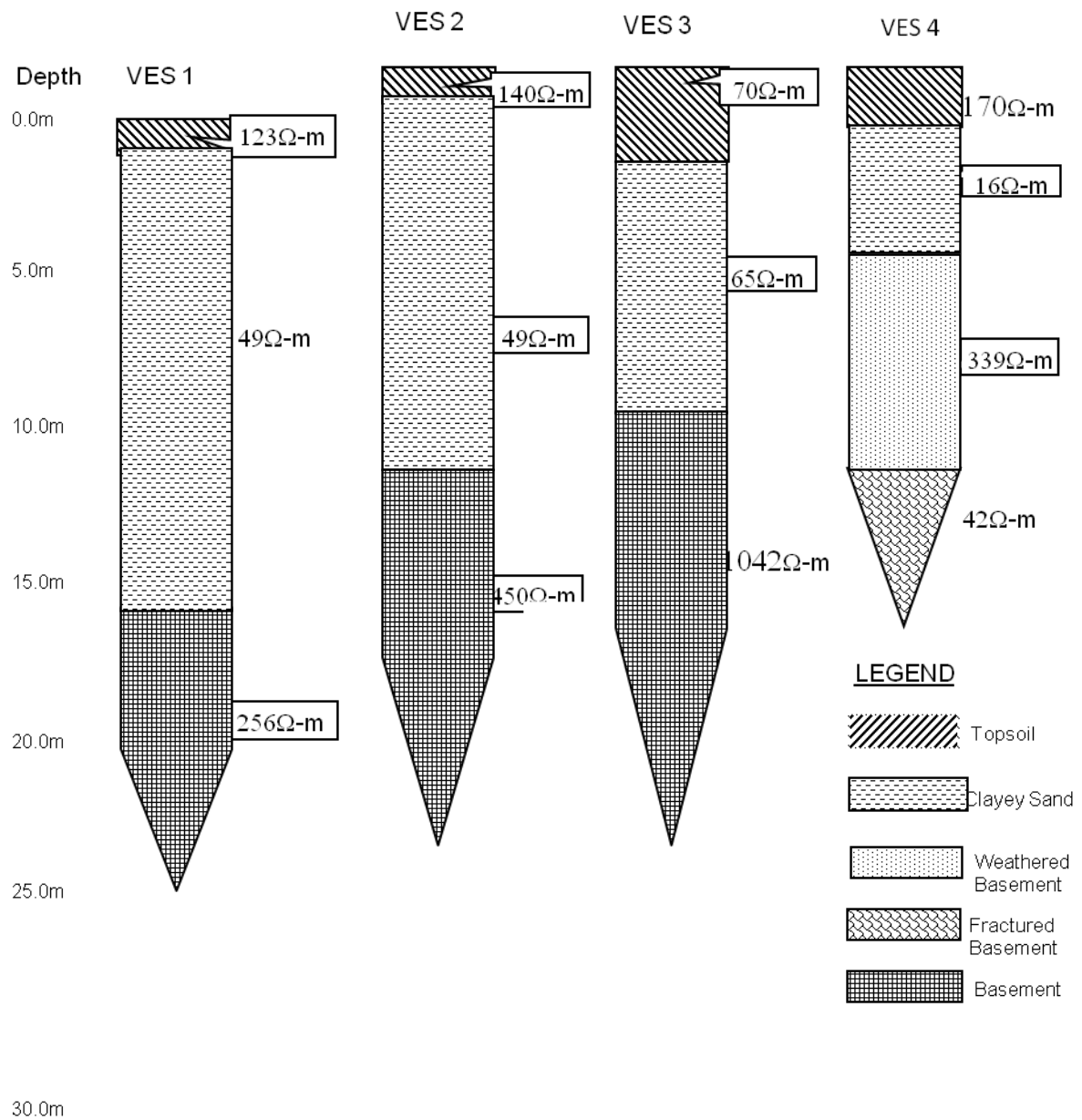


Fig. 3a: Geoelectric Section of VES 1 – 4.

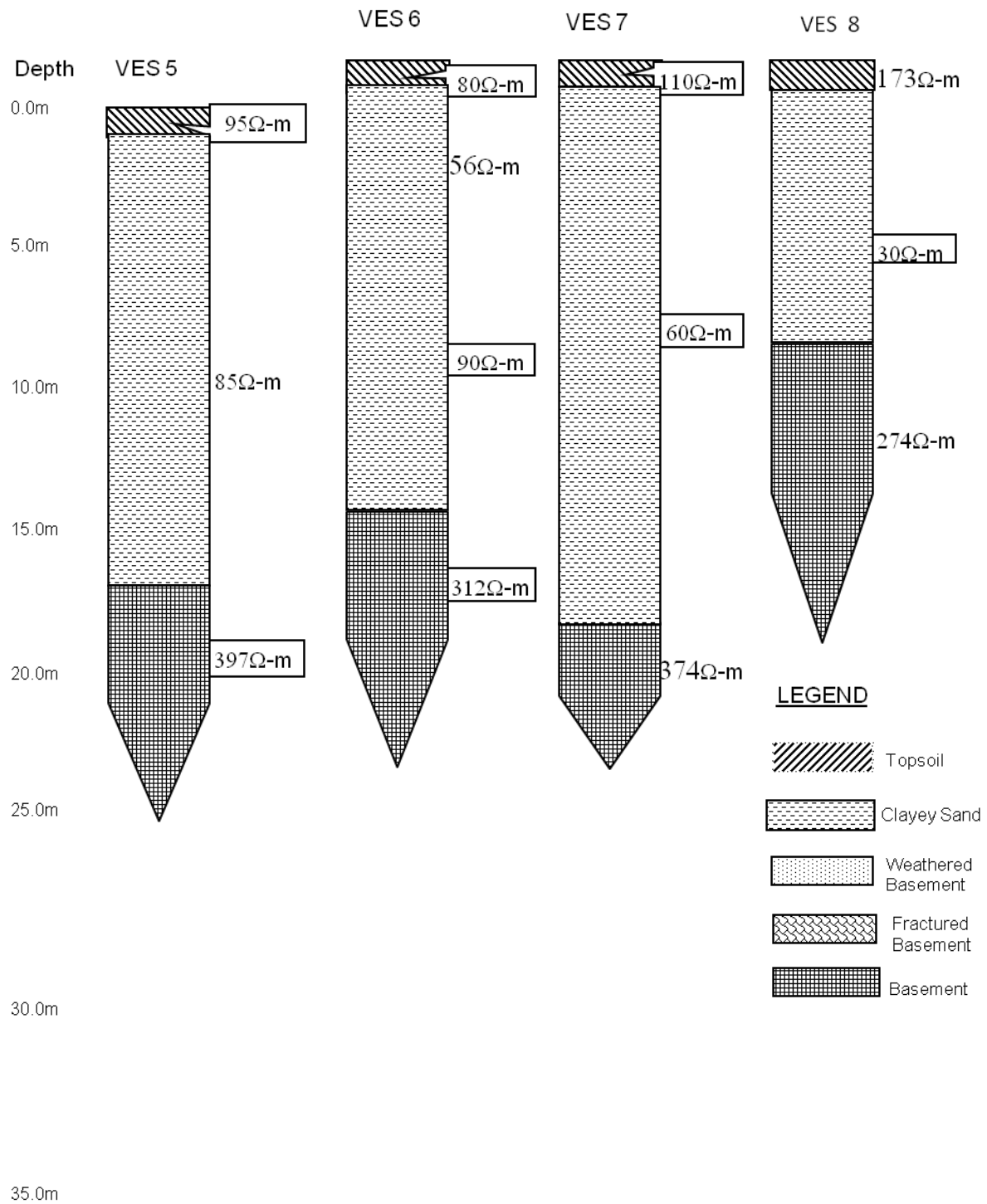


Fig. 3b: Geoelectric Section of VES 5 - 8.

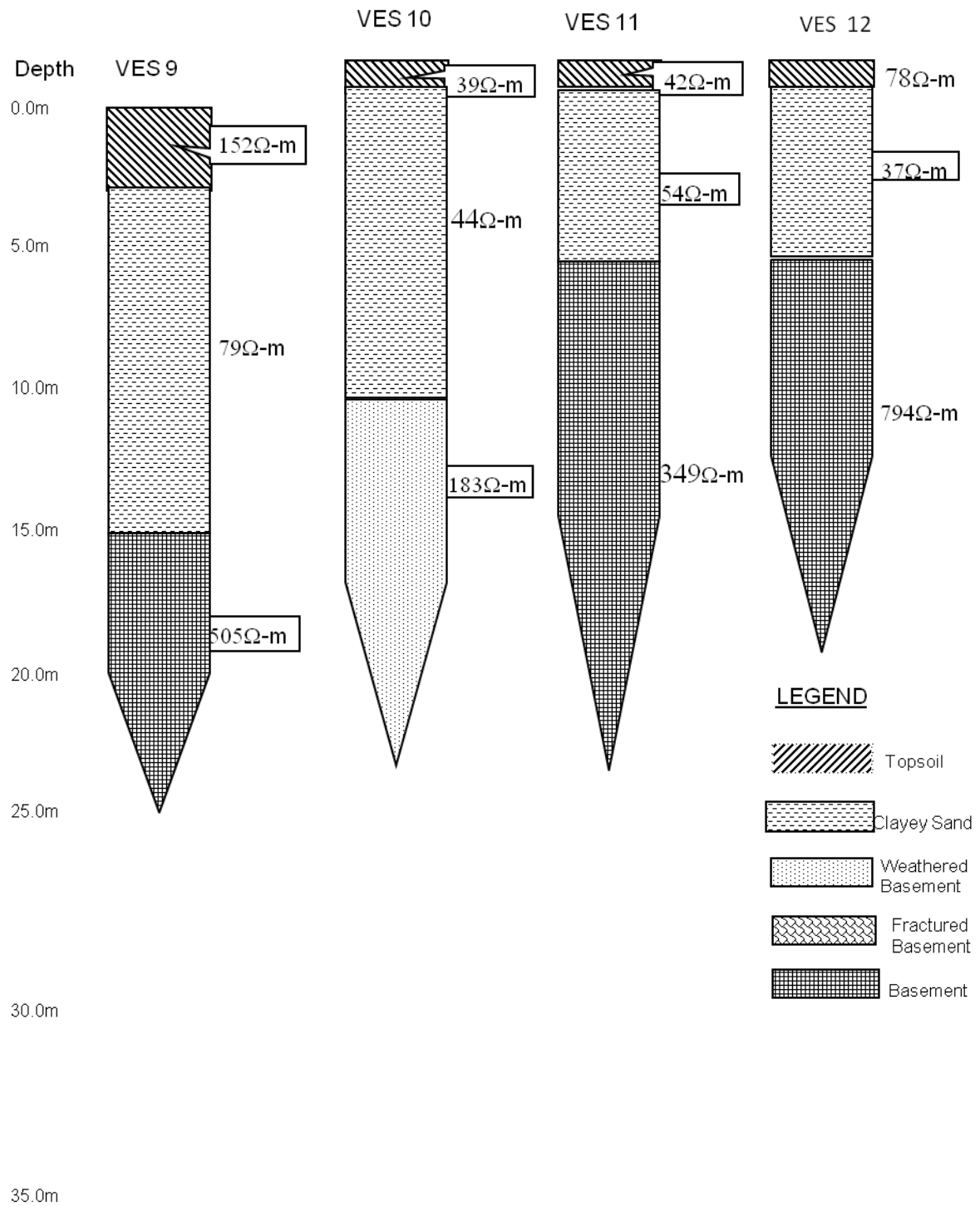


Fig. 3c: Geoelectric Section of VES 8 - 12.

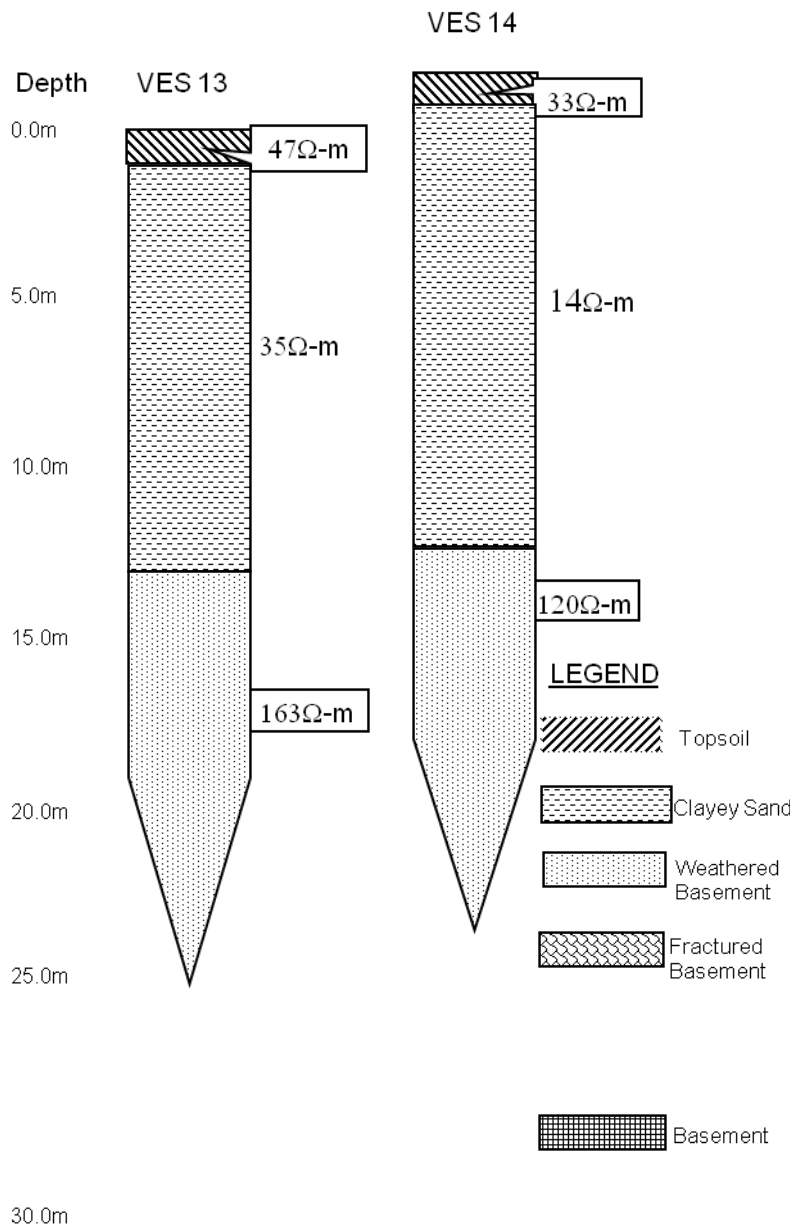


Fig. 3d: Geoelectric Section of VES 11 & 12.

The geoelectric sections correlate the various vertical subsurface layers revealed by the sounding curves of the study area.

4.2 DISCUSSION

Fourteen boreholes were investigate The top soils are generally thin (within 0.5 – 2.5 m, with the average of 1.1m) in most parts and the average apparent resistivity value is 97Ω-m while the sandy clay layers are relatively thick (within 4.0 – 18.7 m, with an average of 11.5m). The sandy clay average apparent resistivity value is very low (51Ω-m) across the study area. The combination of the top soil, sandy clay and weathered basement zones constitute the overburden units within the study area with an average thickness of 13.5m.

The overburden materials and the fractured basement constitute the aquiferous units within the study area with low to medium groundwater potential (sandy clay units have low water yield and prone to caving, while fractured basement zones have medium groundwater potential).

Four out of the fourteen boreholes (boreholes 1 – 4) are productive and in-use, while the remaining ten boreholes (boreholes 5 – 14) are out-of-use and abandoned for various reasons. The four productive boreholes

were able to support continuous flow of water for 1 hour. Seven of the boreholes (boreholes 5, 6, 8, 9, 11, 12 and 14) failed and were abandoned because of low yield (could not flow beyond 5 minutes), while the remaining three (boreholes 7, 10 and 13) failed and were abandoned due to wrong location and completion, caving/formation/completion problem, and wrong installation/completion respectively.

4.3 RECOMMENDATIONS

Detail and extensive geophysical studies are prerequisite for citing borehole locations. Proper completion should be ensured in areas prone to caving and other formation problems. Air drilling should be avoided in areas with thick and loose overburden, right mixture of drilling mud should be applied to secure the hole wall while flushing should be continuous throughout drilling in such formation. Casing should be done immediately and such holes should be lined and properly grouted. Timers should be installed on low yield wells and regulated/programmed for 5 minutes flow and 10 minutes recharge. The productive wells should be properly maintained and monitored for optimal performance.

4.4 CONCLUSION

The failed boreholes were partly due to low groundwater potential of the area, wrong location of some of the boreholes (boreholes 5, 6, 8, 9, 11, 12 and 14), improper installation, completion and formation problem (boreholes 13 and 10) and poor maintenance culture (borehole 7). With proper maintenance and monitoring of the productive wells and reactivation of the abandoned ones, there will be improved performance from the existing wells.

References

- [1] Ademilwa OL and Eluwole AB (2013) Hydrogeophysical Evaluation of the Groundwater Potential of Afe Babalola University Ado Ekiti, South-western Nigeria. *Journal of Emerging trends in Engineering and Applied Sciences*, Vol 4 Issue 1 p77
- [2] Clerk L (1985). Groundwater Abstraction from Basement Complex Areas of Africa. *J. Eng. Geol.*, London 18: 25-34.
- [3] Dutcher, L.C. and Garrett. A.A., 1963, Geologic and hydrologic features of the San Bernardino area, California: U.S. Geological Survey Water-Supply Paper 1419, 114p.
- [4] Oladipo, A. A., Oluyemi, E. A., Tubosun, I. A., Fasisi, M. K. and Ibitoye, F. I. Chemical Examination of Ikogosi Warm Spring in South Western Nigeria. *Journal of Applied Sciences*, 2005, 5 (1): 75-79
- [5] Olayinka A. I. and Weller A. 1997. The inversion of geoelectrical data for hydrogeological applications in crystalline basement areas of Nigeria. *Journ. of Applied Geosciences*, Vol. 37, Issue 2, June 1997, pp 103 – 105.
- [6] Olayinka AI, Olorunfemi MO (1992). Determination of geoelectrical Characteristic in Okene Area and implication for boreholes setting. *J. Min. Geol.*, 28: 403 - 412.
- [7] Ojo, J.S., Olorunfemi, M.O. and Falebita, D.E, An Appraisal of the Geologic Structure beneath the Ikogosi Warm Spring in South- Western Nigeria Using Integrated Surface Geophysical Methods. *Earth Sciences Research Journal*. 2011, 15(1):27-34.
- [8] Olorunfemi MO, Fasuyi SA (1993). Aquifer types and geoelectric/hydrogeologic characteristics of part of central basement terrain of Nigeria (Niger State). *J. Africa Earth Sci.*, 16(3): 309-317.
- [9] Olorunfemi M. D. & Olayinka A. I. (1992): Alteration of Geoelectric in Okene are and Implication for Borehole Sitting. *Journal of Mining and Geology*, pp. 403-411.
- [10] Olorunfemi M. O. (1990): The Hydrogeological Implication of Topographic Variation with Overburden Thickness in Basement Complex. Area of South Western Nigeria. *Journal of Mining and Geology*. Vol 26, No. 1.
- [11] Olorunfemi M. O. & Oloruniwo M. A. (1985): Geoelectric Parameters and Aquifer Characteristics of Some Part of South Western Nigeria. *Journal of Mining and Geology*.
- [12] Olorunfemi MO, Olorunniwo MA (1985). Parameters and aquifer characteristics of some parts of SW. Nigeria *Geologic Applica E. Hydrogeological*, XX Part 1, pp. 99-109.
- [13] Rehr, C. and Birk, S. 2010, Hydrogeological Characterisation and Modelling of Spring Catchments in a Changing Environment. *Austrian Journal of Earth Sciences* Volume 103 Issue 2, p106-117 Vienna.
- [14] Talabi, A. O., 2013, Hydrogeochemistry and Stable Isotopes ($\delta^{18}O$ and δ^2H) Assessment of Ikogosi Spring Waters. *American Journal of Water Resources*, 2013, Vol. 1, No. 3, 25-33.